

**Impact of Cardiac Autonomic Neuropathy on
Diabetic Kidney Disease: Assessment by
Magnetic Resonance Imaging**

Kywe Kywe Soe

Submitted in accordance with the requirements for the degree of
Doctor of Philosophy



The University of Sheffield
Division of Clinical Medicine
School of Medicine and Population Health

October 2024

This thesis has been completed with funding support from the BEAt-DKD project. The candidate, Kywe Kywe Soe, was responsible for participants screening, recruitment, and conducting baseline and follow-up study visits at the Royal Hallamshire Hospital. She also processed biofluid samples in the University laboratory and performed MRI images analysis. The candidate collaborated closely with the iBEAt centre in Leeds before establishing the recruitment process in Sheffield, under the guidance of Professor Steven Sourbron and Dr. Dinesh Selvarajah.

The candidate confirms that the work presented in this thesis is her own, except where contributions have been made as part of jointly submitted abstracts, which have been appropriately acknowledged. The specific contributions of the candidate and other authors are detailed on the following page. Furthermore, appropriate credit has been given throughout the thesis for any referenced work of others.

This copy is supplied with the understanding that it is copyright material and that no part of this thesis may be quoted or published without proper acknowledgement.

The right of Kywe Kywe Soe to be identified as the author of this work has been asserted in accordance with the Copyright, Designs and Patents Act 1988.

© 2024 The University of Sheffield and Kywe Kywe Soe

Conference abstracts

International presentations

1. Kywe Kywe Soe, Kanishka Sharma, Joao Periquito, Jonathan Fulford, Michael Mansfield, Nicolas Grenier, Angela Shore, Kim Gooding, Dinesh Selvarajah, Maria Gomez, Steven Sourbron. Kidney shape in magnetic resonance imaging: A possible novel biomarker for diabetic kidney disease. American Diabetes Association Conference, Orlando, Florida, June 2024.
2. Kywe Kywe Soe, Emma Robinson, Misbah Oleolo, Solomon Tesfaye, Jefferson Marques, Kanishka Sharma, Joao Periquito, Steven Sourbron, Maria Gomez, Dinesh Selvarajah. Cardiac autonomic neuropathy: An independent risk factor for renal decline in diabetic kidney disease. European Renal Association- European Dialysis and Transplantation Association (ERA-EDTA), Stockholm, Sweden, May 2024.

National presentations

1. Kywe Kywe Soe, Emma Robinson, Misbah Oleolo, Solomon Tesfaye, Jefferson Marques, Steven Sourbron, Maria Gomez, Dinesh Selvarajah. Impact of cardiac autonomic neuropathy on diabetic kidney disease. Royal College of Physician regional poster presentation, London, October 2023
-Awarded 'Highly commended abstract award'
2. Kywe Kywe Soe, Emma Robinson, Misbah Oleolo, Solomon Tesfaye, Jefferson Marques, Steven Sourbron, Dinesh Selvarajah. The correlation between cardiac autonomic neuropathy and diabetic kidney disease in Type 1 diabetes population; 15 year follow up study. UK Kidney week, Wales, UK, June 2023.
3. Kywe Kywe Soe, Emma Robinson, Misbah Oleolo, Solomon Tesfaye, Jefferson Marques, Steven Sourbron, Dinesh Selvarajah. The impact of cardiac autonomic neuropathy on diabetic kidney disease: 15 years follow up study. Diabetes UK conference, Liverpool, UK, April 2023.

Acknowledgements

I would like to express my deepest gratitude to my supervisors, Professor Steven Sourbron and Dr. Dinesh Selvarajah, for their unwavering patience, guidance, and dedication throughout this journey. Their incredible support, despite my initial struggles with academic writing and inexperience, has been invaluable. Special thanks to Professor Steven Sourbron, whose development of the MRI image analysis software was fundamental to the success of this PhD. I am deeply grateful to Dr. Dinesh Selvarajah for his dedication, extra hours reviewing my work, and kindness which have been instrumental in helping me complete this 3.5-year journey.

I am also deeply grateful to Dr. Kanishka Sharma and Dr. Joao Periquito for their generosity in sharing their expertise and for their hands-on training and guidance in MRI analysis. Their willingness to teach me, despite my novice level, has greatly enhanced my skills and knowledge in this field.

A special thanks to Sue Smith, Senior Laboratory Technician at the University of Sheffield, and Jo Brown, Senior Technical Manager from Leeds, for their vital roles in establishing the recruitment process in Sheffield, which was essential to the progress of this PhD.

I am profoundly grateful to the BEAt-DKD consortium for their generous funding, without which this PhD would not have been possible. I would also like to thank Dr. Sharon Caunt, Research Co-ordinator, for her ongoing support and help throughout the 3.5 years of this research project.

To my family—my father, mother, brother, and sister—thank you for being my unwavering foundation and supporting me in pursuing my dreams and career here in the UK. Lastly, I am

indebted to my friends, loved ones, and everyone who has been an emotional pillar of support during this journey. Your belief in me has been a constant source of strength.

Abstract

Background and motivation

Diabetic kidney disease (DKD) constitutes a major global health burden, significantly contributing to chronic kidney disease (CKD) and end-stage renal failure (ESRF). Due to the incurable nature of DKD, its management remains largely conservative, emphasising glycaemic and blood pressure control, alongside lifestyle modifications. Although the emergence of sodium–glucose cotransporter 2 inhibitors (SGLT2i), glucagon-like peptide 1 receptor agonists (GLP1RAs), and non-steroidal mineralocorticoid receptor antagonists (nsMRAs) has shown particular benefit in type 2 diabetes mellitus (T2DM), the prevalence of DKD has remained relatively unchanged over the past three decades. The pathophysiology of DKD is closely linked to other diabetes-related microvascular and macrovascular complications, including neuropathy, retinopathy, and peripheral vascular disease. One such complication is diabetic autonomic neuropathy (DAN), often presenting as cardiac autonomic neuropathy (CAN), which is diagnosed using cardiovascular autonomic reflex tests (CARTs).

Aims of the PhD

The overall aim is to investigate whether magnetic resonance imaging (MRI) biomarkers can enhance our understanding of the association between CAN and DKD. The specific objectives are: (1) to review the current literature on the relationship between CAN and DKD; (2) to test these hypotheses in a longitudinal cohort study of individuals with type 1 diabetes mellitus (T1DM); (3) to evaluate whether simple shape metrics derived from MRI can detect early changes in DKD that are not identified through routine blood and urine analyses; and (4) to determine whether MRI-based perfusion metrics can elucidate a direct mechanistic link between CAN and DKD.

Results

A comprehensive literature review identified 27 studies (17 in T2DM) published over the past 30 years, demonstrating a clear association between CAN and DKD progression, including in patients without microalbuminuria. Ten prospective studies highlighted the predictive value of CAN for future declines in estimated glomerular filtration rate (eGFR). The review offers evidence-based recommendations for future research aimed at revealing the mechanisms of autonomic renal regulation, which are essential for understanding CAN's contribution to DKD progression and for guiding the development of targeted therapeutic interventions.

A 15-year longitudinal study in T1DM showed that CAN severity was significantly associated with eGFR decline and increased urinary albumin creatinine ratio (UACR). CAN was linked to a higher baseline Kidney Disease: Improving Global Outcomes (KDIGO) CKD risk category and strongly predicted adverse renal outcomes, including macroalbuminuria, progression in KDIGO risk, doubling of serum creatinine, $\geq 30\%$ eGFR decline, kidney replacement therapy initiation, or kidney disease-related death.

An investigation using MRI to assess three-dimensional shape of the kidneys identified potential biomarkers for DKD progression. Reduced kidney compactness correlated with irregular shape, despite similar eGFR values, suggesting subclinical early DKD changes, such as hyperfiltration, in structurally deformed kidneys. These findings indicate that MRI-based structural assessments may detect disease progression that routine biomarkers overlook, offering potential for improved DKD risk stratification and management.

Further research using dynamic contrast-enhanced MRI (DCE-MRI) assessed the impact of CAN on renal perfusion. No significant differences in MRI-derived renal blood flow were found between participants with and without CAN, consistent across T1 and T2DM, eGFR grades, and CAN severity. These findings suggest that CAN may not directly influence renal perfusion in these populations.

Overall conclusion

This research investigated the role of MRI biomarkers to improve the understanding of the relationship between CAN and DKD progression. By exploring renal structural changes and perfusion metrics, the studies seek to identify early subclinical DKD changes that may be overlooked by conventional biomarkers. Ultimately, these findings could contribute to more precise risk stratification and better management strategies for DKD, particularly in patients with coexisting CAN.

Outlook

The work presented in this thesis contributes evidence regarding the impact of CAN on DKD, the potential utility of renal imaging in DKD research and clinical practice and generates future research directions to investigate renal perfusion in populations with CAN and DKD. These insights may enhance the understanding of the interplay between CAN and renal function decline, ultimately advancing DKD management strategies.

Table of Contents

| | |
|--|-----------|
| Conference presentations | 3 |
| Acknowledgements | 4 |
| Abstract | 5 |
| Table of Contents..... | 8 |
| List of Tables..... | 10 |
| List of Figures..... | 12 |
| List of Abbreviation..... | 15 |
| Chapter 1 Introduction | 23 |
| 1.1 Context and motivation..... | 23 |
| 1.2 Research aims and hypotheses..... | 23 |
| 1.3 Thesis overview | 25 |
| Chapter 2 Background on diabetes mellitus, diabetes kidney disease and diabetic autonomic neuropathy..... | 27 |
| 2.1 Diabetes mellitus | 27 |
| 2.2 Diabetic kidney disease..... | 29 |
| 2.3 Diabetic autonomic neuropathy..... | 48 |
| 2.4 Cardiac autonomic neuropathy..... | 50 |
| Chapter 3 Background on magnetic resonance imaging of renal perfusion | 55 |
| 3.1 Anatomy, function and blood supply of kidneys..... | 55 |
| 3.2 Factors affecting renal blood flow..... | 60 |
| 3.3 MRI methods for measurements of renal blood flow..... | 68 |
| 3.4 Imaging biomarkers in diabetic kidney disease | 77 |
| 3.5 MRI of kidneys as novel biomarker for diabetic kidney disease | 79 |
| 3.6 Summary..... | 92 |
| Chapter 4 A review on impact of cardiac autonomic neuropathy on diabetic kidney disease..... | 93 |
| 4.1 Introduction..... | 94 |
| 4.2 Search strategy..... | 99 |
| 4.3 Relationship between cardiac autonomic neuropathy and diabetic kidney disease..... | 100 |

| | |
|--|------------|
| 4.4 Potential mechanisms for impact of cardiac autonomic neuropathy on progressive renal function decline in diabetic kidney disease | 108 |
| 4.5 Summary | 110 |
| Chapter 5 Cardiac autonomic neuropathy severity and its impact on renal decline in type 1 diabetes mellitus: A 15-year follow up study | 112 |
| 5.1 Introduction..... | 113 |
| 5.2 Materials and methods..... | 114 |
| 5.3 Results | 120 |
| 5.4 Discussion..... | 126 |
| 5.5 Conclusion..... | 129 |
| Chapter 6 Kidney shape: A potential novel magnetic resonance imaging biomarker for diabetic kidney disease..... | 131 |
| 6.1 Introduction..... | 132 |
| 6.2 Materials and methods..... | 133 |
| 6.3 Results | 137 |
| 6.4 Discussion..... | 150 |
| 6.5 Conclusion | 153 |
| Chapter 7 Renal perfusion assessment by dynamic contrast enhanced magnetic resonance imaging in patients with cardiac autonomic neuropathy..... | 155 |
| 7.1 Introduction | 157 |
| 7.2 Materials and methods..... | 157 |
| 7.3 Results | 170 |
| 7.4 Discussion..... | 196 |
| 7.5 Conclusion | 200 |
| Chapter 8 Conclusion of future work..... | 201 |
| 8.1 Overview and summary of findings | 201 |
| 8.2 Implications of research findings | 201 |
| 8.3 Limitations and future work | 204 |
| 8.4 Overall conclusion..... | 205 |
| Appendices..... | 207 |
| References..... | 226 |

List of Tables

| | |
|---|-----|
| Table 2.1 Microvascular complications of diabetes mellitus | 29 |
| Table 2.2 Macrovascular complications of diabetes mellitus | 29 |
| Table 2.3 The evolution and progression of diabetic kidney disease..... | 39 |
| Table 2.4 Classification of diabetic kidney disease..... | 40 |
| Table 2.5 Clinical presentations of diabetic autonomic neuropathy..... | 49 |
| Table 2.6 Structural and functional changes in cardiac autonomic neuropathy..... | 52 |
| Table 3.1 Different MRI techniques and measured parameters in kidneys..... | 80 |
| Table 3.2 Recent MRI studies in diabetic kidney disease..... | 85 |
| Table 4.1 Different tests for diagnosis of cardiac autonomic neuropathy..... | 95 |
| Table 4.2 Studies describing association between cardiac autonomic neuropathy and diabetic kidney disease..... | 101 |
| Table 5.1 Evaluation of cardiovascular reflex tests by O'Brien protocol..... | 117 |
| Table 5.2 Baseline demographic data of participants with different CAN stages..... | 121 |
| Table 5.3 Multiple regression analysis of CAN and its association with eGFR decline and UACR increase across adjusted models | 123 |
| Table 5.4 Comparison of eGFR and UACR changes in CAN and no CAN in participants with normal eGFR and normoalbuminuria..... | 124 |
| Table 5.5 Summary of follow up eGFR and UAR changes in different KDIGO risk groups | 126 |
| Table 6.1 Baseline characteristics/ demographics of participants..... | 138 |
| Table 6.2 Summary statistics for 15 kidney shape factors..... | 139 |
| Table 6.3 Multiple regression analysis of compactness and its association with eGFR and UACR across adjusted models | 146 |
| Table 7.1 Inclusion criteria for type 1 and type 2 DM | 158 |
| Table 7.2 Exclusion criteria for type 1 and type 2 DM..... | 159 |
| Table 7.3 Standard MRI exclusion criteria | 159 |
| Table 7.4 Outline of data collection, biofluid and clinical examination..... | 162 |
| Table 7.5 Blood tests and urine tests data collected..... | 163 |
| Table 7.6 Evaluation of cardiovascular reflex tests by Ewing's method..... | 164 |
| Table 7.7 MRI sequences for iBEAt..... | 165 |

| | |
|--|-----|
| Table 7.8 Baseline demographics of overall, type 1 and type 2 diabetes mellitus participants..... | 171 |
| Table 7.9 Summary values of renal blood flow parameters measured by DCE-MRI..... | 173 |
| Table 7.10 Comparison of participants characteristics between no CAN and CAN group (overall data) | 177 |
| Table 7.11 Comparison of characteristics between no CAN and CAN group (Type 1 diabetes mellitus)..... | 179 |
| Table 7.12 Comparison of characteristics between no CAN and CAN group (Type 2 diabetes mellitus) | 180 |

List of Figures

| | |
|---|-----|
| Figure 2.1 Estimated number of adults with diabetes mellitus (in millions) | 28 |
| Figure 2.2 Multifactorial pathogenesis of diabetic kidney disease..... | 35 |
| Figure 2.3 Normal kidney morphology and structural changes in diabetes mellitus..... | 37 |
| Figure 2.4 KDIGO 2022 guidelines for diabetes management in chronic kidney disease..... | 42 |
| Figure 3.1 Cross-sectional anatomy of kidney..... | 55 |
| Figure 3.2 Functional unit of kidney, nephron, and its microcirculation..... | 56 |
| Figure 3.3 Blood flow in the kidney..... | 58 |
| Figure 3.4 Cross section of glomerulus | 61 |
| Figure 3.5 DCE MRI images of right kidney acquired at different time points before and after administration of contrast agent..... | 69 |
| Figure 3.6 An example of signal intensity time curve obtained from DCE-MRI for renal perfusion (contrast agent concentration time curve) | 70 |
| Figure 3.7 Example of parameters estimated from DCE-MRI in kidneys..... | 71 |
| Figure 3.8 The basic principle of ASL..... | 74 |
| Figure 3.9 Schematic representation of phase-contrast magnetic resonance imaging acquisition and processing..... | 76 |
| Figure 4.1 Kidney nerve supply..... | 99 |
| Figure 4.2 PRISMA flow diagram for screening of articles..... | 100 |
| Figure 4.3 Potential mechanisms for the impact of cardiac autonomic neuropathy on incidence and progression of diabetic kidney disease..... | 109 |
| Figure 5.1 CONSORT diagram of participant data collection..... | 115 |
| Figure 5.2 KDIGO CKD prognostic risk classification..... | 118 |
| Figure 5.3 The numbers of participants with different KDIGO risk classification in each stage of CAN..... | 125 |
| Figure 6.1 Clustered correlation heatmap with dendrogram of different kidney shape factors..... | 141 |
| Figure 6.2 Correlation between 2 different kidney volume (unadjusted and BSA adjusted) with different demographics parameters..... | 142 |

| | |
|---|-----|
| Figure 6.3 Correlation between 15 kidney shape parameters and eGFR, UACR..... | 144 |
| Figure 6.4 Correlation between compactness/ extent and different baseline demographics | 145 |
| Figure 6.5 Correlation between shape factors (compactness and extent) and kidney volume | 147 |
| Figure 6.6 Different compactness and kidney shape in similar BSA adjusted kidney volume..... | 148 |
| Figure 6.7 Similar compactness and kidney shape in different ages of participants..... | 149 |
| Figure 6.8 Similar compactness and kidney shape in different eGFR..... | 150 |
| Figure 7.1 Participant recruitment flow chart for type 1 and type 2 DM..... | 160 |
| Figure 7.2 A Segmentation of aorta n DCE-derived map of maximal signal enhancement and derived concentration-time curve..... | 167 |
| Figure 7.2 B Segmentation of left renal parenchyma on DCE-derived map and derived concentration-time curve..... | 167 |
| Figure 7.3 CONSORT diagram of participants and MRI data..... | 170 |
| Figure 7.4 Correlation heatmap demonstrating the correlation between renal perfusion parameters with different demographic data..... | 176 |
| Figure 7.5 Comparison of parameters between no CAN and CAN group (Overall cohort) | 182 |
| Figure 7.6 Comparison of parameters between no CAN and CAN group (G1, eGFR $\geq 90\text{ml/min/1.93m}^2$) | 183 |
| Figure 7.7 Comparison of parameters between no CAN and CAN group (G2, eGFR 60-89ml/min/1.73m ²) | 184 |
| Figure 7.8 Comparison of parameters between no CAN and CAN group (Type 1 diabetes mellitus cohort) | 186 |
| Figure 7.9 Comparison of parameters between no CAN and CAN group (Type 2 diabetes mellitus cohort) | 187 |
| Figure 7.10 Comparison of parameters between no CAN and CAN group (G2, Type 1 diabetes mellitus cohort) | 188 |
| Figure 7.11 Comparison of parameters between no CAN and CAN group (G2, Type 2 diabetes mellitus cohort) | 189 |

| | |
|--|-----|
| Figure 7.12 Comparison of renal parameters among different stages of CAN (Overall cohort) | 190 |
| Figure 7.13 Comparison of renal parameters among different stages of CAN (Type 1 diabetes mellitus) | 192 |
| Figure 7.14 Comparison of renal parameters among different stages of CAN (Type 2 diabetes mellitus) | 193 |
| Figure 7.15 Comparison of renal parameters between G1 and G2 (Overall cohort) | 194 |
| Figure 7.16 Comparison of renal parameters between G1 and G2 (No CAN group) | 195 |
| Figure 7.17 Comparison of renal parameters between G1 and G2 (CAN group) | 196 |

List of Abbreviation

| Abbreviation | Full Term |
|--------------|---|
| ABPM | Ambulatory Blood Pressure Monitoring |
| ACCORD | Action to Control Cardiovascular Risk in Diabetes Study Group |
| ACE | Angiotensin Converting Enzyme |
| ACEi | Angiotensin Converting Enzyme inhibitor |
| ACP | Average Cortical Perfusion |
| ADA | American Diabetes Association |
| ADC | Apparent Diffusion Coefficient |
| ADDITION | The Anglo-Danish Dutch Study of Intensive Treatment In People with Screen Detected Diabetes in Primary Care |
| ADH | Antidiuretic Hormone |
| ADPKD | Autosomal Dominant Polycystic Kidney Disease |
| ADVANCE | The Action in Diabetes and Vascular Disease-PreterAx and DiamicroN Controlled Evaluation |
| AGE | Advanced Glycation End products |
| AIF | Arterial Input Function |
| AKEF | Average Kidney Extraction Fraction |
| AKI | Acute Kidney Injury |
| AKMTT | Average Kidney Mean Transit Time |
| AKP | Average Kidney Perfusion |
| ALA | Alpha Lipoic Acid |
| ALC | Acetyl L-Carnitine |
| AMP | Adenosine Monophosphate |
| ANP | Atrial Natriuretic Peptide |
| ANS | Autonomic Nervous System |
| APOE | Apolipoprotein E |
| ARB | Angiotensin II Receptor Blocker |
| ASL | Arterial Spin Labelling |

| | |
|----------|---|
| ATF | Average Tubular Flow |
| ATP | Adenosine Triphosphate |
| BEAt-DKA | Biomarker Enterprise to Attack Diabetic Kidney Disease |
| BMI | Body Mass Index |
| BOLD-MRI | Blood Oxygen Level Dependent MRI |
| BP | Blood Pressure |
| BSA | Body Surface Area |
| CAN | Cardiac Autonomic Neuropathy |
| CARTs | Cardiovascular Autonomic Reflex Tests |
| CASL | Continuous Arterial Spin Labelling |
| CCB | Calcium Channel Blocker |
| CHMP | Committee for Medicinal Products for Human Use |
| CKD | Chronic Kidney Disease |
| CKD-EPI | Chronic Kidney Disease Epidemiology Collaboration |
| CREDENCE | Canagliflozin and Renal Events in Diabetes with Established Nephropathy Clinical Evaluation |
| CT | Computed Tomography |
| CVD | Cardiovascular Disease |
| CVRR | Coefficient of Variation of the R-R interval |
| DAN | Diabetic Autonomic Neuropathy |
| DAPA-CKD | Dapagliflozin and Prevention of Adverse Outcomes in Chronic Kidney Disease trial |
| DB | Deep Breathing |
| DBP | Diastolic Blood Pressure |
| DCCT | The Diabetes Control and Complications Trial |
| DCE-MRI | Dynamic Contrast-Enhanced Magnetic Resonance Imaging |
| DCT | Distal Convoluted Tubule |
| DKA | Diabetic Ketoacidosis |
| DKD | Diabetic Kidney Disease |
| DKI | Diffusion Kurtosis Imaging |
| DM | Diabetes Mellitus |
| DN | Diabetic Nephropathy |

| | |
|-------------|---|
| DTI | Diffusion Tensor Imaging |
| DWI | Diffusion Weighted Imaging |
| EASD | European Association for the Study of Diabetes |
| EFPIA | European Federation of Pharmaceutical Industries and Association |
| eGFR | Estimated Glomerular Filtration Rate |
| ELIXA | The Evaluation of Lixisenatide in Acute Coronary Syndrome |
| EMA | European Medicines Agency |
| EMPA-Kidney | The Study of Heart and Kidney Protection with Empagliflozin |
| ESRD | End Stage Renal Disease |
| ESRF | End Stage Renal Failure |
| EXSCEL | Exenatide Study of Cardiovascular Event Lowering |
| FA | Fractional Anisotrophy |
| FDA | Food and Drug Administration |
| FF | Fat Fraction |
| FIDELIO-DKD | Finerenone in Reducing Kidney Failure and Disease Progression in Diabetic Kidney Disease |
| FIGARO-DKD | Finerenone in Reducing Cardiovascular Mortality and Morbidity in Diabetic Kidney Disease |
| FLOW | Evaluate Renal Function with Semaglutide Once Weekly trial |
| FP | Plasma Flow |
| FSGS | Focal Segmental Glomerular Sclerosis |
| GBCA | Gadolinium-Based Contrast Agent |
| GBM | Glomerular Basement Membrane |
| Gd-BOPTA | Gadobenate Dimeglumine |
| Gd-DTPA | Gadopentetate Dimeglumine |
| GFR | Glomerular Filtration Rate |
| GLP-1RA | Glucagon-Like Peptide 1 Receptor Agonist |
| HARMONY | Albiglutide and cardiovascular outcomes in patients with type 2 diabetes and cardiovascular disease |
| HbA1C | Glycosylated Haemoglobin A1C |
| HDAC4 | Histone Deacetylase 4 |
| HF | High Frequency |

| | |
|--------|---|
| HHS | Hyperosmolar Hyperglycaemic State |
| HRV | Heart Rate Variation |
| HTN | Hypertension |
| IDNT | Irbesartan Diabetic Nephropathy Trial |
| IGT | Impaired Glucose Tolerance |
| IL-6 | Interleukin – 6 |
| IRMA | Irbesartan Microalbuminuria Study |
| JAK | Janus Kinase |
| JDRF | Juvenile Diabetes Research Foundation |
| KDIGO | Kidney Disease: Improving Global Outcomes |
| KV | Kidney volume |
| LEADER | Liraglutide Effect and Action in Diabetes: Evaluation of Cardiovascular Outcome Results |
| LF | Low Frequency |
| LK | Left Kidney |
| LS | Lying and Standing |
| MAF | Mean Arterial Flow |
| MAPK | Mitogen-Activated Protein Kinase |
| MARVAL | Microalbuminuria Reduction with Valsartan Study |
| MCP-1 | Monocyte Chemoattractant Protein -1 |
| MCR | Mean Circular Resultant |
| MIBG | Meta-iodobenzylguanidine |
| MIR99A | microRNA 499a |
| MODY | Maturity-Onset Diabetes of the Young |
| MRE | Magnetic Resonance Elastography |
| MRI | Magnetic Resonance Imaging |
| MTT | Mean Transit Time |
| NF-KB | Nuclear Factor – Kappa B |
| NGT | Normal Glucose Tolerance |
| NICE | National Institute for Health and Care Excellence |
| NOX | Nicotinamide adenine dinucleotide phosphate Oxidase |
| Ns MRA | Nonsteroidal Mineralocorticoid Receptor Antagonist |

| | |
|-----------|---|
| NSAID | Non-Steroidal Anti-Inflammatory Drug |
| NSF | Nephrogenic Systemic Fibrosis |
| OCP | Oral Contraceptive Pills |
| OH | Orthostatic Hypotension |
| PASL | Pulsed Arterial Spin Labelling |
| PC-MRI | Phase Contrast MRI |
| pCASL | Pseudo Continuous Arterial Spin Labelling |
| PCT | Proximal Convoluted Tubule |
| PIONEER 6 | Peptide Innovation for Early Diabetes Treatment 6 |
| PKC | Protein Kinase C |
| PLD | Post Labelling Delay time |
| PMI | Platform for research in Medical Imaging |
| PMTT | Plasma Mean Transit Time |
| pNN50 | The Proportion of NN50 divided by the total number of NN (R-R) intervals. |
| PS | Permeable Surface Area Product |
| PUFA | Polyunsaturated Fatty Acid |
| PVD | Peripheral Vascular Disease |
| PWI | Perfusion Weighted Image |
| QSART | Quantitative Sudomotor Axon Reflex Test |
| RAAS | Renin-Angiotensin-Aldosterone System |
| RABF | Renal Artery Blood Flow |
| RBF | Renal Blood Flow |
| RCT | Randomised Control Trial |
| RENAAL | Angiotensin II Antagonist Losartan |
| REWIND | Dulaglutide and cardiovascular outcomes in type 2 diabetes |
| RK | Right Kidney |
| RMSSD | Root Mean Squared Difference of Successive RR Intervals |
| ROI | Region Of Interest |
| ROS | Reactive Oxygen Species |
| RPF | Renal Plasma Flow |
| RSF | Renal Sinus Fat |

| | |
|------------|--|
| SBP | Systolic Blood Pressure |
| SDANN | Standard Deviation of the Averaged Normal RR intervals for all 5-minute segments |
| SDNN | Standard Deviation of the R-R Interval |
| SDNNi | Standard Deviation of the R-R Interval index |
| SGLT2 | Sodium-Glucose co-Transporter 2 |
| SGLT2i | Sodium-Glucose co-Transporter 2 Inhibitor |
| SOD | Superoxide Dismutase |
| SSR | Sympathetic Skin Response |
| STAT | Signal Transducers and Activators of Transcription |
| SUSTAIN -6 | Evaluate Cardiovascular and Other Long-term Outcomes With Semaglutide in Subjects With Type 2 Diabetes |
| T1DM | Type 1 Diabetes Mellitus |
| T2DM | Type 2 Diabetes Mellitus |
| TCF7L2 | Transcription Factor 7 Like 2 |
| TE | Echo Time |
| TGF | Transforming Growth Factor |
| TGF | Tubuloglomerular Feedback |
| TI | Inversion Time |
| TMMT | Tubular Mean Transit Time |
| TNF | Tumour Necrosis Factor |
| TR | Repetition Time |
| TST | Thermoregulatory Sweat Testing |
| UACR | Urinary Albumin Creatinine Ratio |
| UAE | Urinary Albumin Excretion |
| UKPDS | The United Kingdom Prospective Diabetes Study |
| US | Ultrasound |
| VAT | Visceral Adipose Tissue |
| VEGF | Vascular Endothelial Growth Factor |
| VLF | Very Low Frequency |
| VM | Valsalva Manoeuvre |
| VNS | Vagal Nerve Stimulation |

| | |
|-----|---------------------------|
| VP | Plasma Volume |
| WHO | World Health Organisation |

Chapter 1

Introduction

1.1 Context and motivation

Diabetic kidney disease (DKD) is a major contributor to chronic kidney disease (CKD) and end-stage renal failure (ESRF), with about one-third of diabetic patients developing kidney disease (1). Even mild DKD increases morbidity and mortality (2–4). DKD pathophysiology is closely linked with other diabetic complications, including neuropathy and peripheral vascular disease. One such complication is diabetic autonomic neuropathy (DAN) which can result in reduced vagal tone, increased sympathetic activity, and impaired renal perfusion.

Research has explored the role of autonomic neuropathy in DKD progression, with sympathetic dominance causing renal vasoconstriction and reduced renal blood flow. However, imaging-based studies investigating this mechanism are limited. Given recent advancements in magnetic resonance imaging (MRI), assessing renal blood flow via MRI could provide valuable insights, forming the basis of this research.

1.2 Research aims and hypotheses

The overall aim of this research is to determine if MRI biomarkers can improve our understanding of the link between CAN and DKD. The specific aims, hypotheses and methods are outlined as follows.

Study Aim 1:

To assess the current understanding of the association between CAN and DKD through a literature review.

Hypothesis:

CAN contributes to DKD pathogenesis and progression, leading to renal function decline.

Methods:

A literature review was conducted, analysing studies on type 1 and type 2 diabetes mellitus (T1 and T2DM) over the past 30 years to explore the association between CAN and DKD.

Study Aim 2:

To test hypotheses from the literature review by conducting a longitudinal study in a T1DM cohort.

Hypothesis:

CAN is associated with renal function decline in T1DM and correlates with higher KDIGO CKD prognostic risk.

Methods:

The association between CAN, diagnosed via cardiovascular autonomic reflex tests (CARTs), and DKD, stratified by KDIGO CKD risk categories, was evaluated using data from a 15-year longitudinal follow-up study.

Study Aim 3:

To explore whether MRI-derived shape metrics can identify subclinical DKD changes undetected by routine tests.

Hypothesis:

Three-dimensional MRI shape metrics serve as novel biomarkers for monitoring DKD progression.

Methods:

MRI-derived shape parameters were correlated with kidney function indices to evaluate their potential in detecting subclinical DKD and monitoring disease progression.

Study Aim 4:

To investigate whether MRI-based renal perfusion metrics reveal a mechanistic link between CAN and DKD.

Hypothesis:

CAN contributes to DKD pathogenesis via a vascular mechanism, where increased sympathetic tone reduces renal blood flow, leading to renal function decline.

Methods:

Renal perfusion and blood flow, measured using dynamic contrast-enhanced MRI (DCE-MRI), were compared between participants with and without CAN. Image analysis was performed using PMI software after specialised training.

1.3 Thesis overview

Chapter 2: Background on diabetes mellitus, diabetic kidney disease and diabetic autonomic neuropathy

This chapter provides the foundational background for the research studies presented in this thesis. It begins with an overview of diabetes mellitus, followed by an exploration of DAN, with a particular focus on CAN, and concludes with a general overview of DKD.

Chapter 3: Background on magnetic resonance imaging of renal perfusion

This chapter outlines methods for assessing renal perfusion using MRI, beginning with the basic principles of each technique. The first section covers renal anatomy, including arteries, veins, and microcirculation, while the second focuses on factors affecting renal blood flow, providing context for the application of MRI techniques in evaluating renal perfusion and role of MRI biomarkers in DKD.

Chapter 4: A review on impact of cardiac autonomic neuropathy on diabetic kidney disease

This literature review explores the relationship between DKD and CAN by analysing evidence from studies on T1 and T2DM over the past three decades. The review synthesizes various hypotheses and research findings to evaluate whether CAN plays a causal role in the development of DKD or whether both conditions are parallel complications of diabetes. Through this analysis, the review seeks to clarify the underlying mechanisms and potential clinical implications of the CAN-DKD relationship.

Chapter 5: Cardiac autonomic neuropathy severity and its impact on renal decline in type 1 diabetes mellitus: A 15-year follow up study

This chapter explores the relationship between CAN, diagnosed using the gold-standard cardiovascular autonomic reflex tests (CARTs), and DKD, classified according to KDIGO prognostic risk categories. The analysis is based on data from a 15-year longitudinal follow-up study, offering insights into the progression of DKD in relation to CAN over an extended period.

Chapter 6: Kidney shape: a potential novel magnetic resonance imaging biomarker for diabetic kidney disease

This chapter evaluates the potential of three-dimensional kidney shape metrics, obtained through MRI, as biomarkers for the progression of DKD. By correlating these imaging-derived parameters with kidney function indices, the study aims to assess their utility in monitoring DKD progression. Additionally, reference values for kidney shape factors are established, providing a foundation for comparison in future research.

Chapter 7: Renal perfusion assessment by dynamic contrast enhanced magnetic resonance imaging in patients with cardiac autonomic neuropathy.

This chapter investigates the effects of CAN on renal perfusion using dynamic contrast-enhanced (DCE) MRI. The analysis focuses on comparing MRI-derived renal blood flow parameters between participants with and without CAN, offering insights into how CAN influences renal perfusion dynamics.

Chapter 8: Conclusions and future work

This chapter presents a general discussion and conclusion of the key findings from the research studies conducted in this thesis. It evaluates the implications of the results within the broader context of existing literature, highlighting significant contributions to the field. Additionally, it identifies directions for future research, outlining areas where further investigation could enhance understanding and advance the field.

Chapter 2

Background on diabetes mellitus, diabetic kidney disease and diabetic autonomic neuropathy

This chapter provides essential background information for the research studies presented in this thesis. It begins with an overview of diabetes mellitus (DM), DKD, and DAN, with a particular focus on CAN.

2.1 Diabetes mellitus

Diabetes mellitus (DM), a chronic metabolic disorder characterised by hyperglycaemia, encompasses two primary types: type 1 and type 2DM (T1 and T2DM). T1DM is marked by autoimmune-mediated destruction of pancreatic beta cells, resulting in absent or extremely low insulin levels (5). T2DM, a disease of insidious onset, is characterised by insulin resistance, hyper-insulinaemia, and eventual beta cell failure. It is more common in older adults, with both genetic and lifestyle factors playing crucial roles in its pathogenesis and progression (5).

Other subtypes of DM include maturity-onset diabetes of the young (MODY), gestational diabetes, neonatal diabetes, and secondary causes (e.g., endocrinopathies, steroid use). These subtypes account for less than 10% of all DM cases and often require specialist, personalised management to improve clinical outcomes(6). The focus of this thesis will be on the two major types of diabetes: T1 and T2DM.

The global prevalence of DM, primarily T2DM, has surged over the past three decades, with approximately 537 million individuals affected worldwide (Figure 2.1)(7). The majority reside in low- and middle-income nations. According to World Health Organisation (WHO) data, diabetes is responsible for 1.5 million deaths annually (8). In the UK, over 5 million people have DM, with around 90% of cases being T2DM. Approximately 850,000 individuals

are living with undiagnosed T2DM, and an additional 2.4 million are at increased risk of developing the condition (9).

Given this escalating trend, the burden of DM on individuals and society is expected to rise, primarily due to the associated long-term complications (10). DM significantly increases the risk of microvascular complications, such as retinopathy, nephropathy, and neuropathy, as well as macrovascular complications, including cardiovascular disease, cerebrovascular disease, and peripheral vascular disease (10,11).

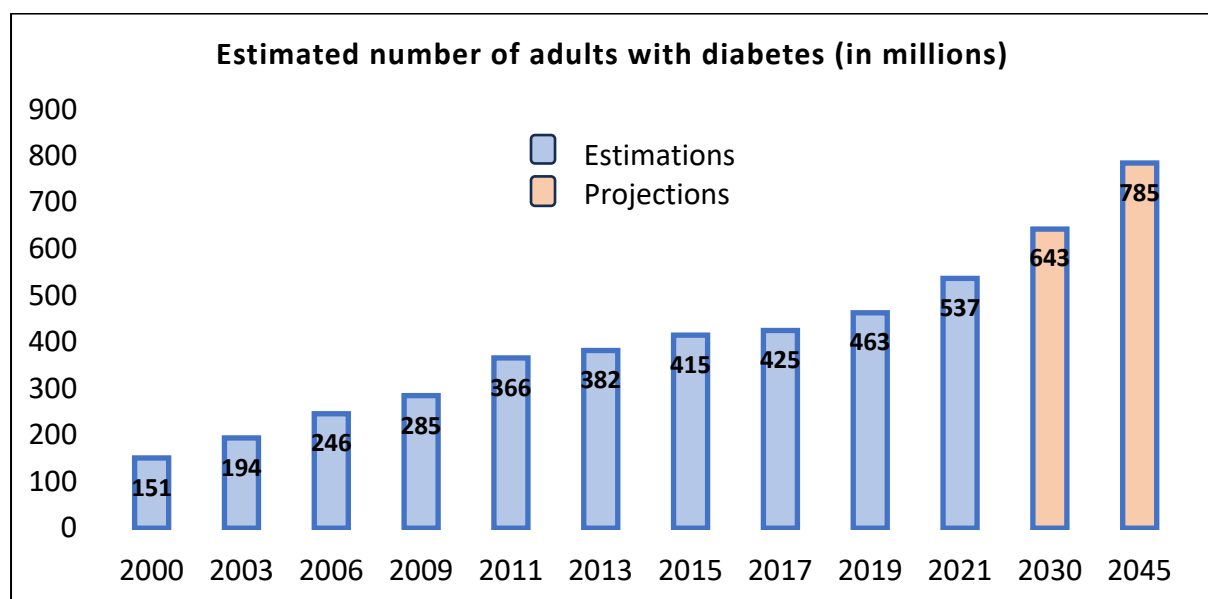


Figure 2.1: Estimated number of adults with diabetes mellitus (in millions) (adapted from International Diabetes Federation Atlas) (7)

2.1.1 Complications of diabetes mellitus

Poorly controlled DM can result in both acute and chronic complications. Acute complications include hypoglycaemia, diabetic ketoacidosis (DKA) and hyperosmolar hyperglycaemic state (HHS). Prolonged exposure to hyperglycaemia can lead to chronic complications which include microvascular (Table 2.1) and macrovascular diseases (Table 2.2) (10).

DM complications impose substantial physical and psychological burdens on patients and contribute to absenteeism, early retirement, and increased social benefits costs. The financial impact on the NHS exceeds £1.5 million per hour, constituting 10% of the NHS budget for England and Wales, with a significant portion allocated to managing complications (12).

Table 2.1: Microvascular complications of diabetes mellitus (13)

| Organs | Complications |
|------------|--|
| 1. Eyes | Nonproliferative retinopathy – microaneurysms, venous loops, retinal haemorrhage, hard exudates, and soft exudates Proliferative retinopathy – new blood vessels with or without vitreous haemorrhage. (Progression of non-proliferative retinopathy) |
| 2. Kidneys | Nephropathy – progressive decline in renal function with albuminuria leading to end stage renal failure |
| 3. Neurons | Neuropathy – Focal, diffuse, sensory, motor, and autonomic neuropathy |

Table 2.2: Macrovascular complications of diabetes mellitus

| Organs/ systems | Complications |
|---|---|
| 1. Heart (Cardiovascular) | Hypertension Coronary heart disease such as myocardial infarction, ischaemic heart disease |
| 2. Brain (Cerebrovascular) | Stroke, transient ischaemic attack, cognitive impairment, and dementia |
| 3. Extremities (Peripheral vascular) | Intermittent claudication, lower limb critical ischaemia/ necrosis |

2.2 Diabetic kidney disease

The terms ‘diabetic kidney disease (DKD)’ and ‘diabetic nephropathy (DN)’ are often used interchangeably in the medical literature to describe kidney disease resulting from DM. DKD is clinically diagnosed by the presence of either albuminuria, a reduced glomerular filtration

rate (GFR), or both (14,15). Albuminuria is defined as an elevated spot urinary albumin-to-creatinine ratio (UACR) of >30 mg/g (>3 mg/mmol), which must be present on at least 2 out of 3 occasions over a period of 3 to 6 months. This approach helps minimise false positives caused by transient increases in UACR due to factors such as exercise, fever, haematuria, urinary tract infection, and congestive heart failure (15,16).

DKD is one of the most prevalent complications of DM and the leading cause of ESRF in the UK. One-third of patients with DM develop DKD during their lifetime, accounting for nearly 15% of all ESRF cases in the UK (and nearly 40% in the US) (1). Affected individuals often experience increased frailty and reduced quality of life. As the disease progresses to ESRF, it leads to widespread end-organ damage and premature mortality (14). Even a mild degree of DKD significantly increases morbidity and mortality (17).

In addition to hyperglycaemia, various other pertinent risk factors contribute to both the onset and progression of DKD in both T1 and T2DM. These include onset of T1DM before the age of 20, hypertension, smoking, male gender, familial tendency, socio-economic factors especially poverty and ethnicity (e.g., Indo-Asian, African American, Pima Indians in the US) (18). The factors such as hypertension, poor glycaemic control and degree of proteinuria play as fuelling conditions for progression of DKD to ESRF once DKD is established (18,19).

Most clinical guidelines, including those issued by the American Diabetes Association (ADA), the National Institute for Health and Care Excellence (NICE) and the European Association for the Study of Diabetes (EASD) recommend annual screening of DKD with UACR (e.g., spot urinary albumin-to-creatinine ratio) and estimated glomerular filtration rate (eGFR) for all patients with diabetes, with a requirement for repeat testing to confirm elevated results (20–22). Specifically, screening is advised for individuals with T1DM duration of ≥ 5 years and for all patients with T2DM regardless of treatment duration. Furthermore, patients presenting with DM and exhibiting UACR exceeding 300 mg/g creatinine (30mg/mmol) and/or an eGFR within the range of 30–60 mL/min/1.73 m² warrant biannual monitoring to inform therapeutic strategies (15,20).

The DKD should also be suspected if there is decline in renal function (eGFR) in T1DM patients with proteinuria, retinopathy, and diabetes duration of more than 10 years. The diagnosis of DKD in T2DM can be more challenging and uncertain disease duration often complicates diagnosis. Additionally, concurrent comorbidities further obscure the clinical picture. Non-specific renal injuries such as arteriolar damage, interstitial fibrosis, and secondary focal segmental glomerular sclerosis (FSGS) are possible differential diagnosis of DKD in T2DM and may be indistinguishable in terms of clinical presentation (19,23,24).

While presence of albuminuria and decline in renal function indicates DKD in majority of cases (25), this is not universally observed. A study examining 52 patients with T2DM and clinical features suggestive of DKD (urine protein excretion 900-9200 mg/24 h, serum creatinine 80-796 micromol/L [0.9-9 mg/dL]), revealed diverse renal biopsy findings, including classical diabetic glomerulopathy (36.5%), predominantly ischaemic changes (30.8%) and another glomerular disease superimposed on DKD (32.7%) (26). Similarly, another investigation involving 34 individuals with T2DM and moderate (A2) albuminuria (urine ACR 3-30mg/mmol) revealed a spectrum of renal pathology ranging from diabetic changes in 10 biopsies (29.4%), ischaemic/fibrotic changes in 14 (41.2%) and minimal pathology in the remaining 10 (29.4%) (23,27). These findings underscore the inherent complexity in diagnosing DKD and emphasise the necessity for thorough evaluation to distinguish among various aetiologies, comorbidities such as hypertension and underlying renal dysfunction, in patients with T2DM.

In clinical practice, the diagnosis of DKD predominantly relies on clinical evaluation, and renal biopsy is reserved for instances where alternative renal pathologies are suspected (23) or in the event of rapid decline in renal function. Although kidney biopsy is the gold standard for diagnostic and prognostic purpose in various renal disorders, its routine utilisation for DKD diagnosis remains the most debated and a personalised decision in many specialist centres (28).

2.2.1 Multifactorial pathogenesis of diabetic kidney disease

Understanding the pathogenesis and risk factors of DKD is essential for both primary prevention and clinical management strategies. Notably, early histopathological changes in the renal microcirculation precede the clinical onset of significant albuminuria and eGFR decline, which eventually progresses to ESRF (29). As with other diabetic complications, chronic hyperglycaemia is a pivotal contributor to the development of DKD (Figure 2.2). Elevated glucose levels affect haemodynamics, hormone production, metabolic pathways, oxidative stress, and inflammatory responses (30,31). DKD causes damage to podocytes, glomeruli, and renal tubules, while also inducing cellular alterations such as mitochondrial injury and epigenetic modifications.

Hyperglycaemia and hyperfiltration

Hyperglycaemia affects the kidneys by disrupting osmotic forces, increasing osmolality in the glomerular capillaries, and elevating glomerular pressures (31). This leads to hyperfiltration, initially causing falsely high to normal eGFR due to increased creatinine filtration (32). The process of hyperfiltration is largely mediated by the tubuloglomerular feedback as larger amounts of filtered glucose leads to higher sodium resorption in the proximal convoluted tubule (PCT) via sodium-glucose co-transporter 2 (SGLT2) (33). SGLT2 upregulation and maximal reabsorption of sodium and glucose in PCT due to supraphysiological level of blood glucose cause decreased tubular pressure, reduced distal sodium delivery, and lead to activation of the renin–angiotensin–aldosterone system (RAAS) (34). This process is exacerbated by increased intraglomerular pressure influenced by systemic hypertension, and other factors such as obesity, which promotes renal enlargement, hyperglycaemia, and increased intra-abdominal pressure (35). This hyper-flow state leads to proteinuria, causing structural nephron alterations and mesangial hypertrophy in diabetic kidneys (31).

Haemodynamic effects and endothelial injury

RAAS activation caused by hyperglycaemia and SGLT2 upregulation leads to efferent arteriolar vasoconstriction, afferent vasodilation, and increased intraglomerular

hypertension (30,34). It also exacerbates systemic hypertension and triggers the mitogen-activated protein kinase (MAPK) signalling pathway by renin (31). Angiotensin II promotes fibrosis by increasing transforming growth factor (TGF)- β (36), vascular endothelial growth factor (VEGF), cell adhesion molecules, and nuclear factor-kappa B (NF- κ B) pathway activation (37). TGF- β regulates fibrosis and inflammation, angiotensin II induces reactive oxygen species (ROS) production and inflammatory responses, and aldosterone stimulates fibroblast production, epithelial-mesenchymal transition, and a hypercoagulable state (31,38). Angiotensin and hyperglycaemia increase endothelin production, exacerbating vasoconstriction, inflammation, podocyte injury, nephrin shedding (a crucial protein located in the slit diaphragm of podocytes, cells that play a key role in the kidney's filtration barrier), and interstitial fibrosis (39).

Metabolic changes

DM is associated with the dysregulation of multiple metabolic pathways. Hyperglycaemia activates pathways such as hexosamine, polyol, advanced glycation end products (AGE), and protein kinase C (PKC), leading to increased reactive oxygen species (ROS) and elevated levels of MAPK, Janus kinase/signal transducers and activators of transcription (JAK/STAT), and NF- κ B (30). These pathways contribute to inflammation and fibrosis. MAPK is linked to extracellular matrix production and podocyte injury (40), while NF- κ B promotes adhesion molecules and cytokines like monocyte chemoattractant protein (MCP-1), Interleukin- 6 (IL-6), and tumour necrosis factor alpha (TNF- α) (41). ROS causes cellular damage by oxidising lipids, nucleic acids, and proteins(42).

Hypoxia and oxidative stress

Renal hypoxia, the inability of oxygen supply to meet renal demands, correlates with blood supply and tubular metabolic activity. Hyperglycaemia induces oxidative stress and hypoxia via several mechanisms: RAAS-mediated vasoconstriction causing ischemic injury, hyperfiltration and tubular hypertrophy, overactivation of SGLT2 channels, depleting adenosine triphosphate (ATP) and oxygen (31). An imbalance between antioxidants and ROS accelerates tissue damage. Chronic hyperglycaemia overexpresses nicotinamide adenine dinucleotide phosphate oxidases (NOX) enzymes, increasing ROS levels and leading to

podocyte injury, apoptosis, mesangial expansion, and vasoconstriction (41). Hypoxia also induces hypoxia-inducible factor, which becomes unstable under hyperglycaemic conditions, promoting fibrosis and perpetuating a cycle of inflammation, vascular injury, and further hypoxia (43).

Individually, these factors do not cause DKD but together with increased levels of growth factors, vasoactive hormones, cytokines and chemokines in the kidney, glucose-induced endothelial dysfunction amplifies the kidney's vulnerability to shear stress, oxidative stress, and other vascular stressors. These alterations concomitantly diminish renal blood flow while augmenting oxygen consumption, thereby fostering a hypoxic microenvironment conducive to glomerular neoangiogenesis (44).

Inflammation and complement system activation

DKD involves multiple intertwined pathways, with inflammation playing a pivotal role in its development. Inflammation leads to the production of inflammatory molecules and activation of the complement system, contributing to disease progression (45). DM triggers inflammatory cascades through oxidative stress, advanced glycation end products (AGEs), obesity, ischemia, and cellular damage, producing molecules like NF- κ B, IL-1 β , IL-6, and IL-18 (30,45). Increased AGEs are directly associated with activation of mesangial cells and ongoing Inflammation also leads to amyloid A protein deposition which can be used as a disease progression marker (14). Furthermore, the complement system activation has a huge impact on DKD progression. DKD progression has been linked to complement activation through mannose-binding lectins and ficolin-associated activation of the lectin pathway in the complement cascade (46).

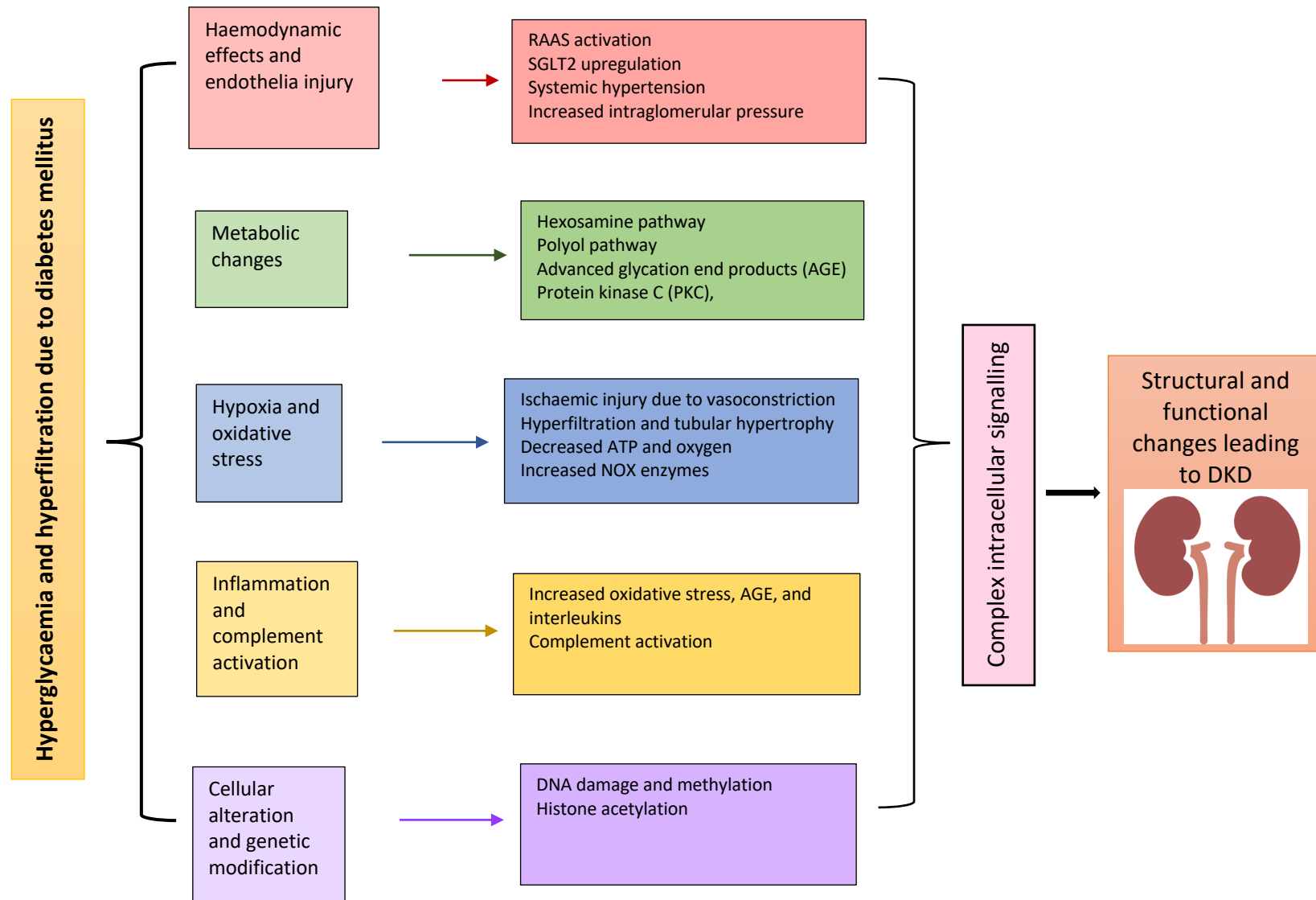


Figure 2.2: Multifactorial pathogenesis of diabetic kidney disease

Cellular alteration and genetic modification

Studies have shown familial clustering of DKD across diverse ethnic groups, indicating a genetic component in its development (47). Furthermore, genetic risk factors in DKD interact with environmental factors such as lifestyle, diet, and medication (47–49). Hyperglycaemia causes DNA damage and accelerates ageing in patients with DM by shortening chromosomal telomeres, leading to proteinuria and DKD progression (50,51). Epigenetic changes involve alterations in genome function that occur without modifications to the DNA sequence and directly associated with lifestyle factors and environmental exposures in the initiation and progression of DKD (31). Hyperglycaemia induces the activity of histone deacetylase 4 (HDAC4), which deacetylates signal transducers and activators of transcription 1 (STAT1), thereby inhibiting autophagic processes in podocytes (52). Studies have linked histone acetylation and methylation to the dysregulation of genes involved in inflammation, fibrosis, and oxidative stress (53–57). These modifications promote pro-inflammatory and pro-fibrotic pathways, leading to structural and functional changes in diabetic kidneys (30).

Structural changes in kidneys: Glomerular changes

The earliest changes in DKD are attributed to glomerular hyperfiltration, resulting in glomerular basement membrane (GBM) thickening, stiffness, and extracellular matrix deposition (Figure 3). This phenomenon is pervasive, manifesting in nearly all individuals diagnosed with diabetes within a few years of onset, with more pronounced changes typically observed in the context of DKD (58). These modifications in the composition and architecture of the GBM contribute to development of albuminuria (58). Furthermore, stiffening of the GBM might also reduce distensibility of the pericapillary wall and compromise the sub-podocyte space, facilitating glomerular injury through haemodynamic mechanisms (59).

Hyperglycaemia also stimulates mesangial cells to undergo proliferation and hypertrophy while increasing their production of matrix proteins (19). This leads to an expansion in the fractional volume of the glomerulus occupied by the mesangium (mesangial expansion), focal degeneration of mesangial cells and the mesangial matrix (mesangiolysis), and

ultimately glomerulosclerosis with the formation of Kimmelstiel-Wilson nodules (60). The resulting reduction in capillary surface area due to the expansion of the mesangium contributes to the development of glomerular hypertension, proteinuria and reduced glomerular filtration (61).

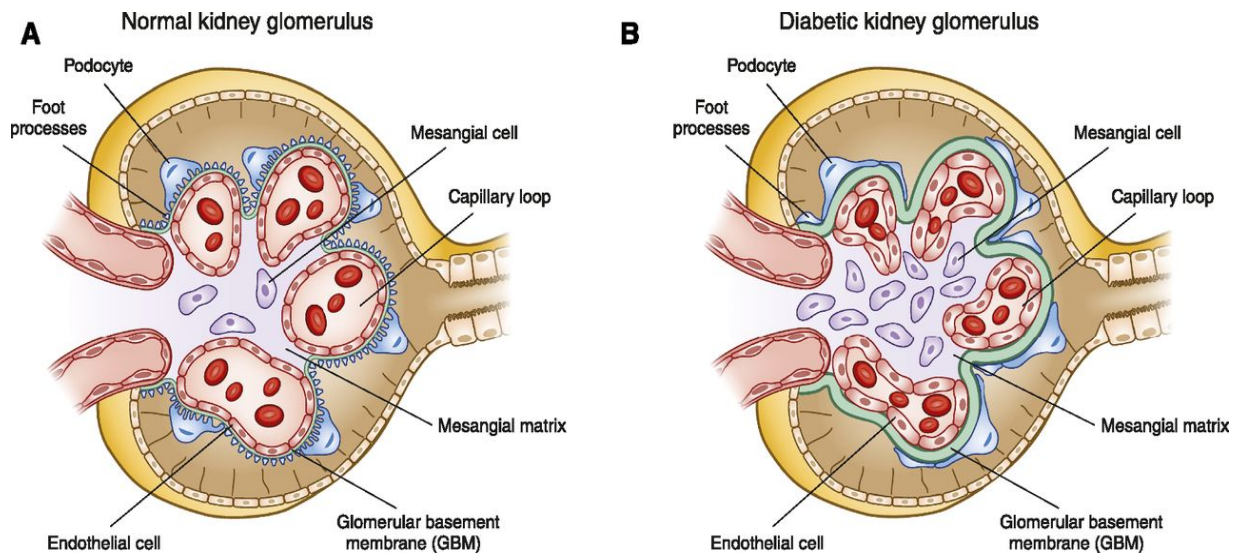


Figure 2.3: Normal kidney morphology and structural changes in diabetes mellitus

(thickening of the glomerular basement membrane, fusion of foot processes, loss of podocytes with denuding of the glomerular basement membrane, and mesangial matrix expansion) (29)

Structural changes in kidneys: Podocytes changes

In normal kidneys, together with glomerular endothelial cells, podocytes play crucial roles in maintaining the structural integrity of the GBM, preserving its charge barrier, and ensuring the shape and integrity of the glomerular capillary loop (62). All these functions are compromised in patients with DM (14), precipitating the development of glomerulosclerosis and subsequent nephron loss. Hyperglycaemia, oxidative stress, and inflammation induce a spectrum of 'patho-adaptive' changes in podocytes, including cytoskeletal rearrangement such as tight junction and slit diaphragm abnormalities, apoptosis, and autophagy which manifest morphologically as widening, retraction and flattening (known as effacement) (31). These alterations further entail reduced motility, increased formation of intercellular tight junctions, reduction in slit diaphragm length, glomerular hypertrophy, podocyte

detachment and dropout (63,64). Consequently, compromised podocyte function leads to altered glomerular permeability and proteinuria, which, in turn, exacerbates renal tubular injury and interstitial fibrosis (19) (Figure 2.3).

Structural changes in kidneys: Tubular changes

Renal tubules, with their high metabolic demand, are rich in mitochondria. In diabetes, mitochondrial abnormalities, such as fragmentation, decreased ATP, increased permeability, and uncoupling, occur early (31). Hyperglycaemia-induced oxidative stress damages electron transport chain subunits, impairing mitochondrial functions and shifting glycolytic pathways to polyol and hexosamine pathways (31). This oxidative stress reduces adenosine monophosphate (AMP)-activated protein kinase activity, leading to NF- κ B-mediated inflammation and cellular injury in tubules (32).

Ultimately, the convergence of these mechanisms culminates in fibrosis and renal tubular atrophy, leading to DKD progression (30,31). Notably, the extent of tubulointerstitial fibrosis may surpass glomerular lesions in determining overall renal function (65). Given the complex and multifaceted pathogenesis of DKD, it is crucial to manage risk factors proactively, as once DKD is established, it is exceedingly difficult to reverse.

2.2.2 Natural history and progression of DKD

The evolution and progression of DKD can be described in five stages (66) (Table 2.3), applicable to both T1 and T2DM, although a less predictable course observed in the latter (19). It may take years for the effects of diabetes on kidneys to become clinically detectable. Due to initial hyperfiltration, increase in kidney size can start within 5 years of diagnosis with GBM expansion and mesangial thickening will take about 10–15 years to develop from onset of diabetes (31). Overt fibrosis occurs after approximately 20 years of T1DM (32).

Although it is mostly silent in initial phase of hyperfiltration with increased eGFR and histological changes, the earliest clinical sign of diabetic nephropathy is microalbuminuria. Within ten years, 20-40% of patients with microalbuminuria progress to overt nephropathy,

and about 20% of these develop ESRF (67,68). In T1DM, 50% of patients with overt nephropathy reach ESRF within ten years, and over 75% do so within twenty years without treatment. Patients with T2DM often exhibit microalbuminuria and overt nephropathy shortly after diagnosis and rate of progression tends to vary considerably between individuals (69).

Table 2.3: The evolution and progression of diabetic kidney disease (66)

| Stage | Duration | Clinical and pathological correlation |
|-------|--------------|---|
| 1 | At diagnosis | Hyper filtration with renal hypertrophy and increased eGFR. |
| 2 | <5 years | Early histological changes though clinically silent. |
| 3 | 5-15 years | Microalbuminuria. Blood pressure starts to rise. |
| 4 | 15-25 years | Overt diabetic nephropathy with declining eGFR. |
| 5 | >25 years | Advanced CKD/ ESRF. |

Alternative DKD progression was described in 2014 (Table 2.4) by the Joint Committee on Diabetic Nephropathy in Japan by updating its 'Classification of Diabetic Nephropathy' to incorporate widely used concepts such as eGFR and CKD (70). The classification includes five stages of DKD including pre-nephropathy with normoalbuminuria, incipient nephropathy with microalbuminuria, overt nephropathy with macroalbuminuria, kidney failure with any level of albuminuria and eGFR < 30ml/min/1.73m² followed by dialysis therapy. Compared to Mogensen DKD classification (66) in table 2.3, the new classification encompasses all kidney diseases affecting diabetic patients, and the Committee emphasised the importance of differential diagnosis between diabetic nephropathy and non-diabetic kidney disease at all stages (70) although the duration of progression was not mentioned.

Table 2.4: Classification of diabetic kidney disease 2014 (70)

| Stage | Urinary albumin (mg/g Cr) or urinary protein (g/g Cr) | eGFR (mL/min/1.73 m ²) |
|------------------------------------|--|---------------------------------------|
| Stage 1 (pre-nephropathy) | Normoalbuminuria (<30) (< 3mg/mmol) | ≥ 30 |
| Stage 2 (incipient nephropathy) | Microalbuminuria (30–299) (3-29.9 mg/mmol) | ≥ 30 |
| Stage 3 (overt nephropathy) | Macroalbuminuria (≥300) (≥ 30mg/mmol) or persistent proteinuria (≥0.5) | ≥ 30 |
| Stage 4 (kidney failure) | Any albuminuria/proteinuria status | < 30 |
| Stage 5 (dialysis therapy) | Any status on continued dialysis therapy | |

With advancing stages of DKD, the risk of mortality escalates as indicated by the United Kingdom Prospective Diabetes Study (UKPDS). This landmark investigation showed that annual mortality risks corresponded to 1.4% (no microalbuminuria), 4.6% (microalbuminuria), and 19.2% (CKD and ESRF) (71). Beyond mortality risks, intensive monitoring and therapeutic interventions exert a pivotal influence on the natural trajectory of DKD by forestalling the progression from incipient DKD to overt nephropathy.

2.2.3 Management of DKD

Being an incurable disease, primary prevention remains the most vital part in the comprehensive management strategy for DKD. The goals for primary prevention include optimising glycaemic control with target HbA1C of less than 7% (53 mmol/mol), attaining target blood pressure below 130/80 mmHg, smoking cessation, weight reduction and regular physical exercise (72,73). Annual screening for DKD is a corner stone for the management of DKD and is recommended to start after 5 years of T1DM and promptly upon diagnosis in T2DM. Timely detection affords the opportunity to delay or prevent the

progression of DKD to ESRF (19,20). Figure 2.4 summarises the treatment approaches to DKD in more details.

Treatment goals for DKD are individualised and dependent on each stage with overall aim to prevent progression from microalbuminuria (incipient DKD) to macroalbuminuria (overt DKD) and preventing progressive decline in renal function in patients with macroalbuminuria. Central to this therapeutic approach is the effective management of modifiable risk factors to prevent cardiovascular events which represent the foremost cause of mortality in patients with DKD.

Lifestyle measures

Non-pharmacological measures remain the vital component of managing any chronic illness including DKD. Imbalanced lifestyle factors such as unhealthy diet, poor physical activity, smoking including second hand smoke exposure and obesity exert significant influence on the risk profile for CKD (74). They are the most challenging aspects because of reliance on the patients' willingness and motivation to participate to achieve the desired goals. Moreover, health inequalities and socio-economic determinants of health present significant challenges. The efficacy of such interventions lies in healthcare providers' ability to educate patients and effective utilisation of locally available resources (75). It is essential that patients occupy a central role in the formulation of lifestyle intervention strategies to achieve the mutually agreed targets and follow up (23).

Key components of lifestyle modification encompass adherence to a balanced diet characterised by a protein intake of 0.8 grams per kilogram of body weight per day for individuals with diabetes and CKD not undergoing dialysis, alongside sodium restriction to less than 2 grams per day (or < 90 mmol of sodium per day, or < 5 grams of sodium chloride per day in individuals with diabetes and CKD). Engaging in moderate physical activity for a minimum of 20 minutes per day or a cumulative duration of 150 minutes per week, smoking cessation, and weight reduction are underscored as integral components of lifestyle interventions, yielding favourable impacts on both diabetes and DKD management (72).

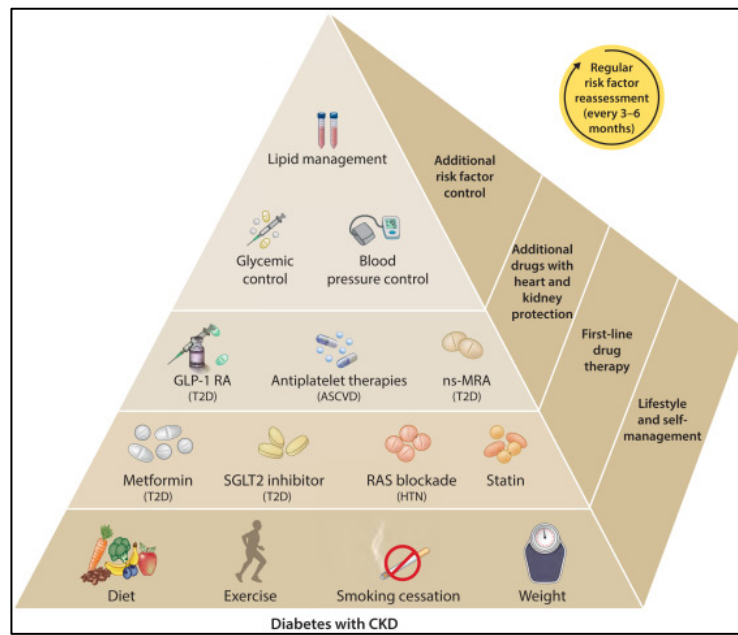


Figure 2.4: KDIGO 2022 guidelines for diabetes management in CKD (Kidney heart risk factors management) (76)

Glycaemic control

Hyperglycaemia is a critical factor in the pathogenesis of DKD. Several key studies in both T1 and T2DM have demonstrated significant benefits from managing hyperglycaemia.

The Diabetes Control and Complications Trial (DCCT) randomized 1,441 people with T1DM to intensive insulin therapy (target HbA1c <6.05%, achieved 7.3%) or standard therapy (achieved HbA1c 9.1%) (77). After a mean follow-up of 6.5 years, there was a significant reduction in the development of moderate (UACR 3-30mg/mmol) and severe (UACR >30mg/mmol) albuminuria in the intensive arm, as well benefits for other microvascular complications (23,77). Long-term assessment revealed that intensive insulin treatment slowed eGFR decline and reduced the proportion of people who developed a persistent reduction in eGFR to < 60 mL/min/1.73 m² (50% risk reduction with intensive therapy) (78). The United Kingdom Prospective Diabetes Study (UKPDS) also clearly demonstrated the benefits of good glycaemic control in impeding DKD progression in T2DM. The study showed that there was 33% reduction in relative risk of developing microalbuminuria or clinical grade proteinuria over a 12-year period, and a significant reduction in the proportion of individuals experiencing doubling of their plasma creatinine levels (19,71).

The Action in Diabetes and Vascular Disease-PreterAx and DiamicroN Controlled Evaluation (ADVANCE) trial involved 11,140 participants with T2DM to intensive (HbA1c 6.5%) or standard (HbA1c 7.3%) glycaemic control (79). Intensive glycaemic control yielded reductions in combined macrovascular and microvascular complications, particularly a decrease in the incidence or exacerbation of DKD (4.1% vs 5.2%; hazard ratio 0.79; 95% CI 0.66-0.930). In contrast, the Action to Control Cardiovascular Risk in Diabetes Study Group (ACCORD) trial, involving 10,251 participants to randomised intensive or standard glycaemic control, was discontinued early due to higher mortality in the intensive therapy arm and no evidence of benefit on DKD (80).

The latest Kidney Disease Improving Global Outcomes (KDIGO) 2022 guidelines for diabetes management in CKD recommend glycaemic monitoring (individualised HbA1c target ranging from < 6.5% to < 8.0% in patients with DM and CKD not treated with dialysis) in addition to monitoring long-term glycaemic control by HbA1c twice per year (76). HbA1c may be measured as often as 4 times per year if the glycaemic target is not met or after a change in antihyperglycaemic therapy. The National Institute for Health and Care Excellence (NICE) guidelines advocate for the target HbA1C < 7.0% if high risk of hypoglycaemia such as severe frailty and multiple comorbidities and to aim for < 6.5% if low risk of hypoglycaemia (11). A review of the evidence for each class of hyperglycaemic treatment for DKD is beyond the scope of this thesis.

For patients with T2DM, CKD, and an eGFR more than 30 mL/min per 1.73 m², KDIGO suggests initiating treatment with metformin and to add Sodium-glucose cotransporter-2 inhibitors (SGLT2i) if the glycaemic target is not met. Glucagon-like peptide-1 receptor agonists (GLP-1 RA) are to be considered if the patients are not achieving the target despite the combined use of metformin and SGLT2i (72). Over the last few years, the use of SGLT2i has increased in the T2DM population due to the evidence showing a reduction in the risk of ESRF, doubling of serum creatinine or death from renal or cardiovascular causes in patients with albuminuric diabetic nephropathy (eGFR 30-90 mL/min/1.73 m² and severe albuminuria) and receiving RAAS inhibitors (81). Intense glycaemic control can minimise the

risk of development and progression of DKD but target for HbA1C will need to be tailored to individual patient profiles and comorbidities.

Cardiovascular risk reduction

In addition to lifestyle modifications and glycaemic control, several other modifiable cardiovascular risk factors have been implicated in the development and progression of DKD. Hyperlipidaemia has been posited as a potential contributory factor in the pathogenesis of glomerulosclerosis (82). Individuals with DM are susceptible to concurrent hyperlipidaemia and significant disruptions in lipid metabolism. This includes elevated levels of circulating free fatty acids, cholesterol, and triglycerides, as well as excessive fat deposition in various tissues, including the liver, kidneys, and muscles (83). While some clinical data and meta-analysis suggest a correlation between dyslipidaemia treatment and improved renal outcomes (84), some trials have not substantiated this hypothesis (85,86).

Similarly, there is ongoing debate regarding the potential role of lipid lowering agents such as statins in prevention and progression of DKD (23). Several studies have suggested that statin therapy may help to preserve eGFR or reduce albuminuria although more definitive studies are required (23,82,87,88). As per KDIGO 2013 guidelines for lipid management in CKD, the principal justification for pharmacological cholesterol-lowering therapy is to decrease cardiovascular morbidity and mortality (89) rather than to improve renal outcomes. While statin therapy does not markedly influence the progression of DKD, it effectively reduces cardiac events and mortality in patients with non-dialysis-dependent renal disease, regardless of the presence of DM (90,91). Since many statins are metabolised by the kidneys, dosage adjustments are necessary for patients with significantly reduced eGFR.

RAAS blockade and renal protection

One of the most important steps in management of DKD in both T1 and T2DM is inhibition of Renin- Angiotensin- Aldosterone System (RAAS). The Microalbuminuria Captopril Study Group randomised 235 normotensive patients with T1DM and moderate albuminuria (UACR 3-30mg/mmol) to captopril or placebo. Active treatment with captopril reduced the risk of

progression to severe albuminuria (>30mg/mmol) over 24 months with risk reduction of > 60% and smaller increases in albumin excretion rate (92). Other similar trials (93)(94) have also confirmed that captopril therapy significantly impeded progression to clinical proteinuria and prevented the increase in UACR.

For T2DM, the evidence for RAAS inhibition comes from the trials such as the Irbesartan Diabetic Nephropathy Trial (IDNT) and the Angiotensin II Antagonist Losartan (RENAAL) study. In IDNT, 1,715 people with T2DM, reduced eGFR and severe albuminuria were randomised to irbesartan, amlodipine or placebo. Irbesartan resulted in 20% risk reduction in doubling of serum creatinine, ESRF or death from any cause versus either of the other two study arms. Those effects were independent of blood pressure (95). Losartan was compared with placebo in 1,513 people with T2DM and DKD in the RENAAL study and losartan group is shown to reduce the composite endpoint of a doubling of serum creatinine, ESRF or death by 16% (96). Two other studies -The Irbesartan Microalbuminuria Study (IRMA) and the Microalbuminuria Reduction with Valsartan study (MARVAL) were conducted in T2DM with microalbuminuria and shown to have similar positive impact of RAAS inhibition for renal protection in DKD (97–99).

The KDIGO guidelines recommend that RAAS blockade (an angiotensin-converting enzyme inhibitor (ACEi) or an angiotensin II receptor blocker (ARB) must be initiated in patients with DM, hypertension, and albuminuria, and be titrated to the highest approved dose that is tolerated (72). The reno-protective effects of RAAS blockers extend beyond their impact on systemic blood pressure by also lowering the intraglomerular pressure (100).

It is also essential to be aware that maintaining good blood pressure is fundamental in reducing the cardiovascular risk as well as reducing progression of CKD. It is reported in a meta-analysis that included 40 RCTs with over 100 000 participants (101) that for each 10mmHg lowering of systolic BP, there was a 17% lower risk of mortality, 11% reduction in cardiovascular events and 17% reduction in the development of albuminuria. In general, the target BP is <130/80 mmHg if 10-year CV risk \geq 15% in DM population (20), but the latest KDIGO guideline mentioned to aim for systolic BP < 120mmHg in patients with CKD and albuminuria if there is no contraindication (102). Apart from different target of BP for DKD

population, management of hypertension remains the same with different groups of anti-hypertensives such as calcium channel blockers, diuretics, beta blockers and alpha blockers. However, details of each classification will not be discussed here.

Newer drugs in type 2 diabetes mellitus

In addition to the aforementioned interventions, recent pharmacological advancements in T2DM management extend beyond glycaemic control. Several new drugs have demonstrated positive effects on both cardiovascular and renal outcomes, as evidenced by various studies conducted over the years.

SGLT2 inhibitors have emerged as a significant advancement in the management of DKD over the past decade. Studies such as CREDENCE (81), DAPA-CKD (103) and EMPA-Kidney (104) trials have demonstrated their efficacy in reducing cardiac mortality, decreasing proteinuria, and slowing disease progression. In addition to reducing fasting and postprandial plasma glucose concentrations (105), SGLT2 inhibitors decrease the renal threshold for glucose excretion, increase urinary glucose excretion and consequently reduce the plasma glucose concentration (106).

Additionally, anti-hypertensive effect of SGLT2 inhibitors have also been described in literature (107–109) and possible mechanisms include natriuresis, osmotic diuresis, decreased body weight, reduction of sympathetic nervous system activation, reduced arterial stiffness and improved endothelial function (109). Recommendations for the use of SGLT2 inhibitors are expanding rapidly due to its benefits on DKD in T2DM, CKD and heart failure. The mechanisms underlying enhanced renal and hepatic erythropoietin synthesis by SGLT2 inhibitors was also described in literature (110). Although the exact pathway for blood pressure lowering effect is not known, SGLT2 inhibitors are now well-placed as a valuable drug in DKD management in T2DM population.

Glucagon-like peptide 1 receptor agonists (GLP-1RAs) increase insulin secretion by pancreatic beta cells in the presence of hyperglycaemia, delay gastric emptying and promote weight loss (111). A 2021 meta-analysis encompassing eight trials of GLP-1RAs (ELIXA, LEADER, SUSTAIN-6, EXSCEL, HARMONY, REWIND, PIONEER 6, and AMPLITUDE-O)

evaluated pooled cardiovascular and kidney outcome data in total of 60,080 participants with T2DM, including those with CKD (112). Compared to placebo, GLP-1RA treatment resulted in a significant reduction in cardiovascular death (HR: 0.87; 95% CI: 0.80–0.94), stroke (HR: 0.83; 95% CI: 0.76–0.92), myocardial infarction (HR: 0.90; 95% CI: 0.83–0.98), all-cause mortality (HR: 0.88; 95% CI: 0.82–0.94), and hospitalisation for heart failure (HR: 0.90; 95% CI: 0.83–0.98). For kidney outcomes in these studies, GLP-1RA treatment reduces risk for development of new severely increased albuminuria, decline in eGFR, or rise in serum creatinine, progression to kidney failure, or death from kidney disease cause; HR: 0.79; 95% CI: 0.73–0.87 compared to placebo in populations with T2DM.

These findings were also established by the latest randomised controlled trial, known as the FLOW (Evaluate Renal Function with Semaglutide Once Weekly) (113), which primarily focused on renal outcomes. The study (113) included participants with T2DM and CKD (n= 3,533), characterised by eGFR ranging from 25 to 75 ml/min/1.73 m², and the presence of either microalbuminuria or macroalbuminuria. Following early cessation of the trial, with a median follow-up of 3.4 years, the study demonstrated that the risk of primary outcome events—such as renal failure, a decline in eGFR of 50% or more, reduction in eGFR to less than 15 ml/min/1.73 m², and death from renal or cardiovascular causes—was 24% lower in the semaglutide group compared to the placebo group (331 vs. 410 first events; hazard ratio, 0.76; 95% confidence interval [CI], 0.66 to 0.88; P = 0.0003).

Additionally, all confirmatory secondary outcomes were favourable in the treatment group. The mean annual eGFR slope was significantly less steep (P < 0.001), the incidence of major cardiovascular events was 18% lower (hazard ratio, 0.82; 95% CI, 0.68 to 0.98; P = 0.029), and the risk of death from any cause was 20% lower (hazard ratio, 0.80; 95% CI, 0.67 to 0.95; P = 0.01) (113). Although the precise mechanisms underlying the renal protective effects of GLP-1RAs remain unclear and are often described as multifactorial (113), it is highly probable that the utilisation of GLP-1RAs will become more widespread in the near future among the T2DM population.

Novel nonsteroidal mineralocorticoid receptor antagonists (Ns MRAs), including finerenone and esaxerenone, are more selective for mineralocorticoid receptors and are shown to

provide reductions in albuminuria with a lower risk of hyperkalaemia (114). The efficiency of finerenone, a third-generation Ns MRA, in improving kidney and cardiovascular outcomes was revealed in FIDELIO-DKD (115) and FIGARO-DKD(116) studies which included participants with T2DM and albuminuria.

The FIDELIO-DKD trial found that finerenone resulted in an 18% lower incidence of the primary composite outcome, which included kidney failure, a sustained 40% decline in eGFR, or death from kidney causes. In the FIGARO-DKD trial, there was a 13% lower risk of the primary cardiovascular composite outcome, including death from cardiovascular causes, nonfatal myocardial infarction, nonfatal stroke, or hospitalisation for heart failure. However, the secondary composite kidney outcome did not differ significantly between finerenone and placebo (HR 0.87, 95% CI 0.76–1.01). Like finerenone, the Ns MRA, esaxerenone, has been shown to lower albumin excretion (117,118) . However, its long-term kidney and cardiovascular benefits remain unestablished, and it lacks widespread regulatory approval.

The development of these new pharmacological agents signifies improved management and survival rates, enhanced quality of life, and increased longevity for the diabetic population, with a concomitant reduction in cardiovascular and renal complications. Due to the multisystem involvement of diabetes, management of DKD will still require a holistic, multidisciplinary, and individualised approach for each patient in clinical practice.

2.3 Diabetic autonomic neuropathy (DAN)

Diabetic autonomic neuropathy (DAN) is a microvascular complication of DM, characterised by autonomic nervous system dysfunction associated with DM or pre-DM metabolic derangements, excluding other causes (119). DAN affects multiple organ systems, most notably the cardiovascular, gastrointestinal, urogenital, and sudomotor functions. Clinical signs and symptoms of DAN typically emerge once the disease is well established. These include orthostatic hypotension, post-prandial nausea and vomiting, constipation or nocturnal diarrhoea, incontinence, and erectile dysfunction (120). Managing these symptoms is challenging and necessitates coordinated care across multiple medical

specialties (121). Table 2.5 summarises the different clinical presentation of DAN in different body systems.

Table 2.5: Clinical presentations of diabetic autonomic neuropathy (DAN)(119) (120) (122)

| System affected | Signs and symptoms |
|-------------------------|---|
| Cardiovascular system | <ol style="list-style-type: none"> 1. Resting tachycardia 2. Exercise intolerance 3. Orthostatic hypotension 4. Silent myocardial ischemia |
| Gastrointestinal system | <ol style="list-style-type: none"> 1. Oesophageal dysmotility 2. Gastroparesis diabeticorum 3. Constipation 4. Diarrhoea 5. Faecal incontinence |
| Genitourinary system | <ol style="list-style-type: none"> 1. Neurogenic bladder (diabetic cystopathy) 2. Erectile dysfunction 3. Retrograde ejaculation 4. Female sexual dysfunction (e.g., loss of vaginal lubrication) |
| Metabolic | <ol style="list-style-type: none"> 1. Hypoglycaemia unawareness 2. Hypoglycaemia-associated autonomic failure |
| Sudomotor | <ol style="list-style-type: none"> 1. Anhidrosis 2. Heat intolerance 3. Gustatory sweating 4. Dry skin |
| Pupillary | <ol style="list-style-type: none"> 1. Pupillomotor function impairment (e.g., decreased diameter of dark-adapted pupil) 2. Argyll-Robertson pupil |

2.4 Cardiac autonomic neuropathy (CAN)

Cardiac autonomic neuropathy (CAN) is a specific subset of DAN that involves damage to the autonomic nerves regulating cardiac function. The prevalence of DAN in diabetic populations ranges from approximately 20% to 65% in individuals with longstanding DM (123). Moreover, patients with CAN face a higher risk of mortality (2,122) commonly attributed to sudden cardiac death, possibly related to abnormal lengthening of QT intervals (124). Like other diabetic microvascular complications, the risk factors for DAN include poor glycaemic control, hypertension, dyslipidaemia, and obesity, although poor glycaemic control is thought to play a greater role in the pathogenesis of CAN in T1DM (123).

2.4.1 Pathophysiology of CAN

The pathogenesis of CAN is complex and involves a cascade of pathways activated by hyperglycaemia resulting in neuronal ischaemia and cellular death(125). Hyperglycaemia is the main factor in development of CAN in T1DM, compared to multifactorial pathogenesis in T2DM (126).

Hyperglycaemia

Hyperglycaemia is central to the development of CAN through toxic glycosylation products and oxidative stress, leading to microvascular endothelial damage, cell stress and apoptosis in the autonomic nervous system (125). Hyperglycaemia disrupts the Krebs cycle, resulting in excessive production of nicotinamide adenine dinucleotide and reactive oxygen species, causing mitochondrial dysfunction and further oxidative stress (127,128). These reactive species damage cellular DNA, leading to the formation of advanced glycation end products (AGE), which harm the microcapillaries supplying neurons (129). This damage alters microvascular morphology, causing vascular occlusion, endothelial leakage, inflammation, neuronal ischemia, and apoptosis (130,131).

Inflammation

Both T2DM and metabolic syndrome create a proinflammatory state, increasing the risk of vascular complications and neuronal ischemia, leading to CAN (132,133). CAN is linked with higher levels of inflammatory markers like C-reactive protein, interleukin-6, and tumour necrosis factor α , as well as adipose tissue inflammation (125). The exact nature of this relationship is unclear and yet to be confirmed (134).

Genetic factors

Genetic factors, including specific genes like ACE, APOE, and TCF7L2, and single-nucleotide polymorphisms, may influence susceptibility to CAN (135). A study in T2DM (n = 150) found that the GG phenotype of the MIR499A gene is linked to a more severe CAN phenotype, along with longer diabetes duration (125,136). However, a twin study (101 pairs) showed no significant genetic effect on cardiovascular autonomic function, with lifestyle and other unshared environmental influences accounting for 85% to 96% of the impact (137). Thus, genetic susceptibility may contribute to CAN only when combined with risk factors such as obesity, insulin resistance, hyperglycaemia, hyperlipidaemia, hypertension, and metabolic syndrome (138).

2.4.2 Natural History of CAN

CAN progresses in an ascending length-dependent manner. The vagus nerve, which is anatomically the longest autonomic nerve and physiologically mediates 75% of overall parasympathetic activity, is affected early in the natural history of CAN. In early stage of CAN, there is an initial reduction in parasympathetic activity, resulting in relative sympathetic overactivity (125). This increase in sympathetic tone continues until the later stages of CAN, when sympathetic denervation ensues (139,140). Sympathetic predominance or overdrive results in many clinical manifestations of CAN (125). Although the timescale for the progression of CAN is unclear, the stage of sympathetic denervation correlates clinically with postural hypotension (141). Table 2.6 summarises the structural and functional changes in different stages of CAN.

Table 2.6: Structural and functional changes in CAN (134)

| Structural changes in CAN | Functional changes in CAN |
|---|--|
| Progressive length–dependent neuropathy predominantly affecting the vagal nerve initially | Sympathetic predominance in early DAN with parasympathetic neuropathy |
| Full length of vagal nerve affected | Loss of blood pressure circadian rhythm leading to nocturnal hypertension |
| CAN progresses to sympathetic plexus of autonomic nervous system | Unopposed sympathetic tone with resting tachycardia and postural BP drop in advanced CAN |
| Both parasympathetic and sympathetic neuropathy with fibrosis | Sympathetic and parasympathetic neuropathy with denervated heart and fixed HR |

2.4.3 Management of CAN

Effective clinical management of CAN primarily focuses on symptomatic control and preventing disease progression.

Glycaemic control and lifestyle modification

Although no cure exists, glucose control is essential for preventing neuropathy in both T1 and T2DM (119). The 2017 ADA recommendations emphasise early glucose optimisation to prevent or delay CAN in T1DM, and a multifactorial approach, including lifestyle modifications such as weight loss, healthy diet, and exercise, to prevent CAN in T2DM and pre-DM (142).

Measures for postural hypotension

For symptomatic postural hypotension, first-line non-pharmacological measures include patient education, optimised salt and fluid intake, compression stockings, abdominal binders, lower body strength training, moderate recumbent exercise, and physical manoeuvres (143). Currently, the two drugs primarily used to treat postural hypotension are midodrine and droxidopa, followed by fludrocortisone in non-responders (144). A key challenge is treating supine hypertension without worsening postural hypotension.

ACEIs and ARBs

By reducing heart rate and blood pressure through blocking the RAAS, ACEIs/ ARBs have shown improvements in heart rate (145) , heart rate variability parameters (146) (HF, LF/HF, TP, SDNN, RMSSD) and significant dipping (2.4%) in nocturnal systolic blood pressure (147).

Beta-blockers

A study by Ebbehøj et al (148) showed the effects of metoprolol in patients with T1DM and abnormal albuminuria. The study concluded that the improvement in 24-hr ambulatory HRV parameters reflected the impact on vagal tone, although there was no impact on diurnal variation, blood pressure, or albuminuria.

Vitamin E

Manzella et al (149) studied vitamin E for treating CAN in T2DM. Fifty participants received either 600 mg of vitamin E daily or a placebo for four months. The vitamin E group showed significant improvement in autonomic indices and a negative correlation between the LF/HF ratio and plasma vitamin E concentration ($r = -0.43$, $p < 0.04$), though there was no effect on mean arterial blood pressure.

Omega – 3 polyunsaturated fatty acid (PUFAs)

Serhiyenko et al. demonstrated the role of omega-3 PUFA in treating CAN in T2DM in two studies (150,151). Participants received either a 1g omega-3 PUFA capsule with hypoglycaemic treatment or hypoglycaemic treatment alone for three months. Significant improvements in HRV ($p < 0.05$ for SDNN, SDANNi, pNN50, RMSSD, HF, LF/HF; $p < 0.01$ for LF) and nocturnal DBP parameters ($p < 0.05$ for load of DBP; $p < 0.001$ for DBP, time index of DBP, standard deviation of DBP) were observed in the omega-3 PUFA group, with no significant changes in nocturnal SBP in either group ($p \geq 0.05$).

Other emerging pharmacological interventions

Due to its beneficial effects on glucose homeostasis parameters and lipid profiles (152), alpha lipoic acid (ALA) used as monotherapy (153) or in combination with other antioxidants

such as acetyl L-carnitine (ALC), superoxide dismutase (SOD), and vitamin B12 (154) was shown to improve autonomic results such as Valsalva manoeuvre, deep breathing test, and orthostatic hypotension.

Vagal nerve stimulation

Preclinical studies suggest vagal nerve stimulation (VNS) might help manage CAN by addressing reduced parasympathetic drive and dominant sympathetic activity. VNS has shown benefits in resuscitating animals in cardiac arrest, improving recovery after myocardial infarction, alleviating heart failure and stroke symptoms, and modulating arrhythmias (155). However, VNS can also cause serious cardiovascular side effects such as bradycardia and cardiac standstill (156–158). More progressive human studies and clinical trials are needed to determine the efficiency and safety of VNS in the near future.

Despite no specific cure for the symptoms, a patient-centred approach including thorough history taking, physical examination, and review of the medication list of all symptomatic patients remains the mainstay of management for both DAN and CAN.

2.5 Summary

This chapter presented a comprehensive overview of DM, DKD and DAN, addressing their pathophysiology, clinical features, diagnostic approaches, and management strategies. A detailed discussion of current treatments and emerging therapeutic interventions was included, supported by evidence from previous studies. The subsequent chapter will delve into the fundamental principles of renal anatomy and explore various magnetic resonance imaging (MRI) techniques employed for the assessment of renal perfusion.

Chapter 3

Background on magnetic resonance imaging of renal perfusion

This chapter will explore the methods of assessment for renal perfusion using magnetic resonance imaging, describing basic principles for each method. Accurate evaluation of renal blood flow (RBF) through MRI necessitates a comprehensive understanding of kidney anatomy, blood supply, and the physiological factors influencing RBF. The chapter's first section will focus on the structural anatomy of the kidneys, detailing the renal arteries, veins, and microcirculation, followed by second section about the factors affecting RBF. This anatomical perspective will provide context for subsequent discussions on MRI techniques and their application in assessing RBF.

3.1 Anatomy, function, and blood supply of kidneys

3.1.1 Renal structure and anatomy

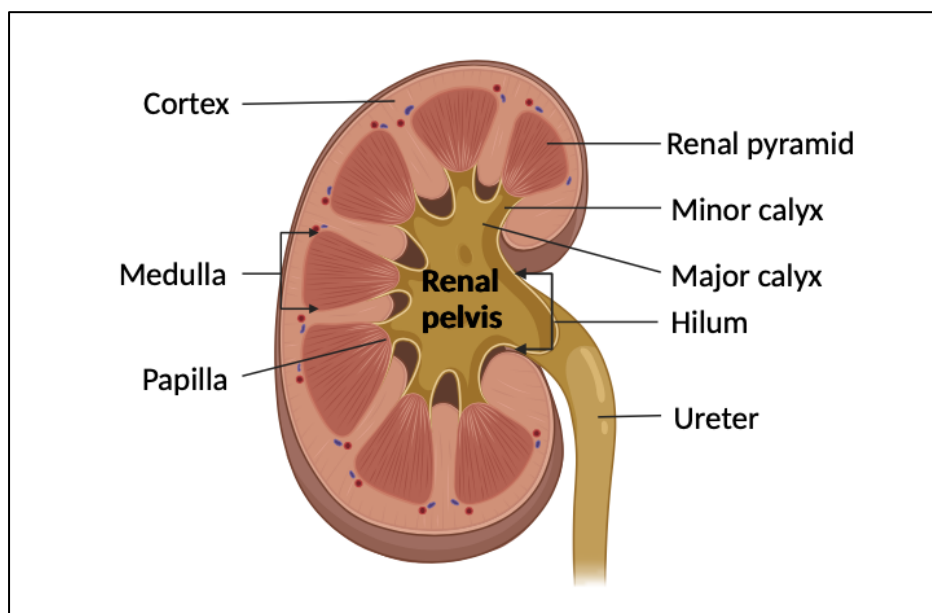


Figure 3.1: Cross-sectional anatomy of kidney

The human kidneys are a pair of bean-shaped organs located retroperitoneally in the abdomen, one on each side of the spine. Each kidney typically measures about 11-14 cm in length, 6 cm in width, and 4 cm in thickness. They are situated at the level of the T12 (thoracic) to L3 (lumbar) vertebrae, with the right kidney positioned slightly lower than the left to accommodate the liver (159). The kidneys are encased in a tough, fibrous capsule surrounded by perirenal fat, which provides protection and support. This is further encased by the renal fascia, a layer of connective tissue.

The hilum, a central fissure on the medial border of each kidney, serves as the entry and exit point for the renal artery, renal vein, and ureter. Internally, the kidney is divided into two main regions: the cortex and the medulla (Figure 3.1). The cortex is the outer layer that houses the glomeruli, the initial filtering units of the kidney. The medulla, located deeper within the kidney, consists of 8-18 conical masses called renal pyramids. The apex of each pyramid, known as the renal papilla, projects into a minor calyx. Multiple minor calyces converge to form major calyces, which in turn drain into the renal pelvis, a funnel-shaped structure that continues as the ureter (159,160).

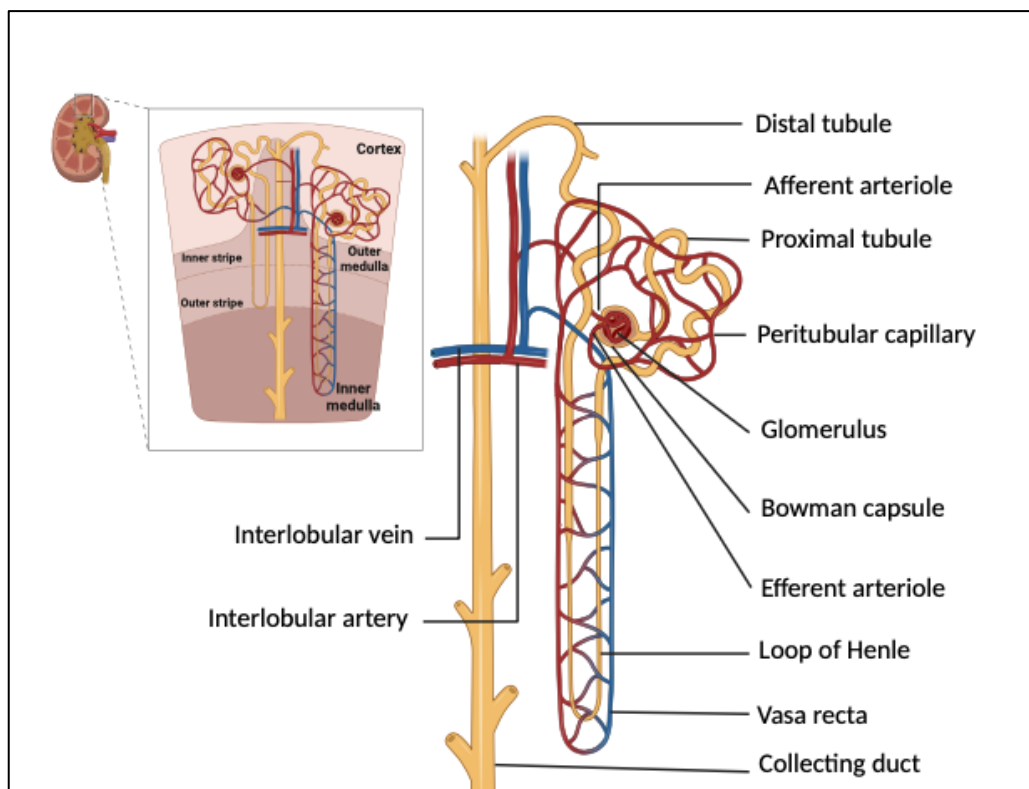


Figure 3.2: Functional unit of kidney, Nephron, and its microcirculation

At the microscopic level, the kidney's functional unit is the nephron (Figure 3.2). Each kidney contains approximately one million nephrons, which are responsible for filtering blood and forming urine. A nephron consists of two main parts: the renal corpuscle and the renal tubule. The renal corpuscle includes the glomerulus, a network of capillaries, and Bowman's capsule, a cup-like sac that encases the glomerulus. This is the site where blood filtration begins (161).

The renal tubule is a long, coiled tube divided into several segments: the proximal convoluted tubule (PCT), the loop of Henle, the distal convoluted tubule (DCT), and the collecting duct. The PCT, lined with microvilli to increase surface area for reabsorption, reabsorbs water, ions, and nutrients back into the bloodstream. The loop of Henle, which extends into the medulla, establishes a concentration gradient that allows the kidney to produce urine of varying concentrations. The DCT further fine-tunes the reabsorption and secretion of ions. Finally, the collecting duct receives urine from multiple nephrons, leading it to the renal pelvis (162).

3.1.2 Function of kidneys

The primary function of the kidneys is to maintain homeostasis by regulating the composition and volume of blood. This involves the excretion of waste products, maintenance of electrolyte balance, and regulation of blood pressure. Filtration occurs in the glomeruli, where blood plasma is filtered under pressure, and large molecules like proteins and blood cells are retained in the bloodstream. The filtrate, containing water, ions, glucose, and other small molecules, enters the renal tubules (162).

Through selective reabsorption and secretion along the tubules, the kidneys adjust the filtrate composition. Essential nutrients, water, and electrolytes are reabsorbed into the blood, while waste products like urea and creatinine are excreted. The kidneys also play a crucial role in regulating blood pH by excreting hydrogen ions and reabsorbing bicarbonate (163).

In addition to their excretory function, the kidneys secrete hormones that are vital for systemic regulation. Erythropoietin stimulates red blood cell production in response to hypoxia. Renin, released in response to low blood pressure, initiates the RAAS to increase blood pressure and sodium reabsorption. The kidneys also convert vitamin D to its active form, calcitriol, which is essential for calcium homeostasis and bone health (163).

Overall, the kidneys' complex structure and multifaceted functions are essential for maintaining the body's internal environment, ensuring the stability necessary for all physiological processes.

3.1.3 Blood supply of kidneys

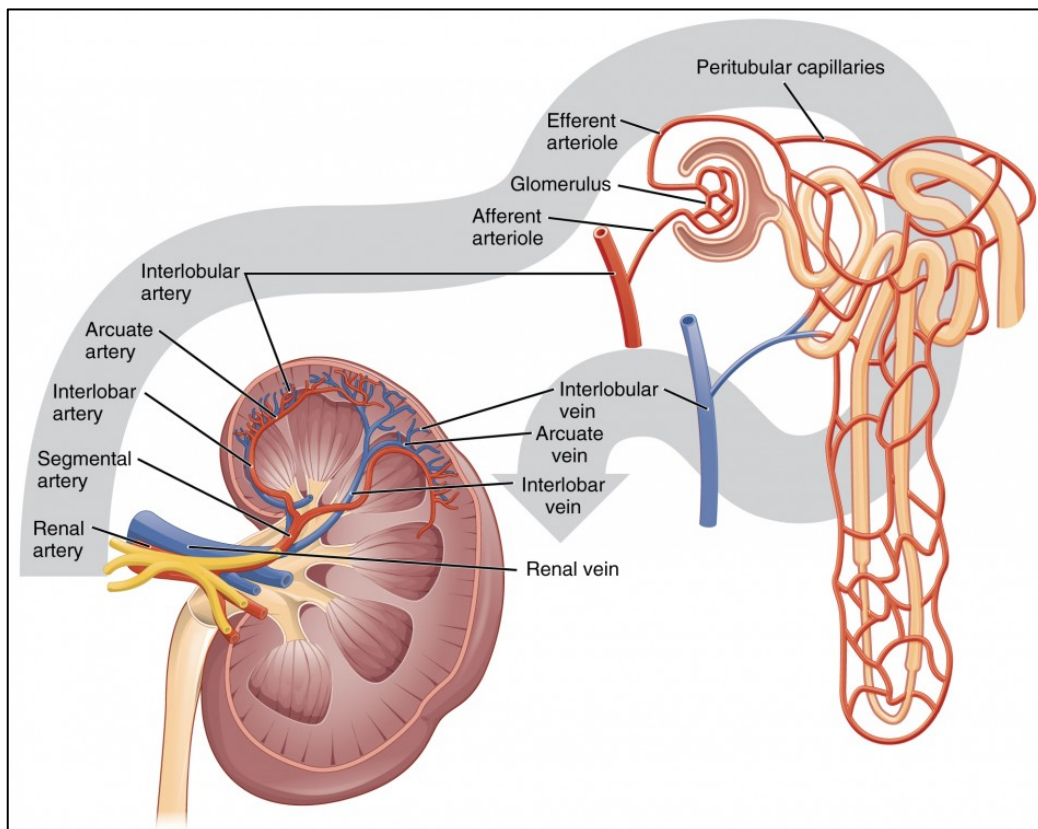


Figure 3.3: Blood flow in the kidney (164)

The blood supply to the kidneys is crucial for their function of filtering blood and maintaining homeostasis. Each kidney receives blood through the renal artery, a direct branch of the abdominal aorta. The renal artery enters the kidney at the hilum and subsequently divides into several segmental arteries, each supplying different regions of the kidney (Figure 3.3). These segmental arteries further branch into interlobar arteries, which ascend within the renal columns located between the renal pyramids and extending along the renal cortex (163). These arteries become arcuate arteries at the corticomedullary junction and again branch into radial cortical arteries and later branch into afferent arterioles to provide blood supply to the glomeruli (165)(166). These glomeruli are, in turn, drained by the efferent arterioles which supply the renal medulla in their juxtamedullary portion through the capillaries of vasa recta.

The deoxygenated blood from the peritubular capillaries and vasa recta is collected by interlobular veins, which drain into arcuate veins, and subsequently into interlobar veins. The interlobar veins converge to form the renal vein, which exits the kidney at the hilum and drains into the inferior vena cava (163). Under physiological conditions, renal artery blood flow (RABF) or renal blood flow (RBF) is the volume of blood delivered to the kidneys per unit time. In human beings, the kidneys receive roughly 20-25% of cardiac output i.e., 1.2 – 1.3 L/min in a 70-kg adult male. Renal blood flow is directly proportional to the difference in pressures between the renal artery and vein, but inversely proportional to the vasculature resistance (167).

RBF is crucial for to the delivery of oxygen and nutrients to the renal tissue. A measure of this process i.e., tissue perfusion at the cellular level is expressed in ml/min/100g or ml/min/100ml. In normal healthy individuals, bilateral renal perfusion is estimated at 1000-1200ml/min or 400ml/min/100g (168). Both RABF and perfusion provide valuable information in assessing acute and chronic kidney disease including DKD.

3.2 Factors affecting renal blood flow

Renal blood flow (RBF) is a critical determinant of kidney function, influencing the filtration rate, urine formation, and overall homeostasis. However, RBF is not constant and can be affected by several factors, including systemic blood pressure, autoregulation mechanisms, neural and hormonal influences, various pathological conditions, and other variations that can arise from difference in physiological status such as dehydration or low blood pressure (169). Understanding these factors is essential for comprehending how kidneys maintain their vital functions under different physiological and pathological states.

3.2.1 Systemic Blood Pressure

Systemic blood pressure is one of the crucial determinants of RBF (170,171). The kidneys receive approximately 20-25% of the cardiac output, which amounts to about 1.2 litres of blood per minute in a healthy adult. Changes in systemic blood pressure can significantly affect this flow. An increase in blood pressure typically increases RBF and glomerular filtration rate (GFR), while a decrease has the opposite effect (172). However, the kidneys have intrinsic mechanisms to maintain relatively stable blood flow despite fluctuations in systemic pressure.

3.2.2 Autoregulation Mechanisms

Autoregulation is a key feature of renal blood flow, allowing the kidneys to maintain a constant RBF and GFR across a wide range of systemic blood pressures (approximately 80-180 mmHg). This is due to two internal autoregulatory mechanisms that operate without outside influence: the myogenic mechanism and the tubuloglomerular feedback mechanism (19)(173).

Myogenic Response: This mechanism involves the smooth muscle cells in the walls of the afferent arterioles. In kidneys, afferent and arteriolar tone controls intra-glomerular

pressure and flow. Increased afferent arteriolar tone leads to vasoconstriction which causes reduced renal blood flow and reduced pressure within the glomerulus while decreased afferent arteriolar tone leads to opposite effects. Meanwhile, increased efferent arteriolar tone (vasoconstriction) leads to reduced renal blood flow and increased pressure within the glomerulus (19,167,173). When vascular pressure increases, these cells stretch and respond by contracting, which reduces the diameter of the arteriole and decreases blood flow. Conversely, a decrease in pressure causes these muscles to relax, increasing the arteriole diameter and maintaining blood flow (174).

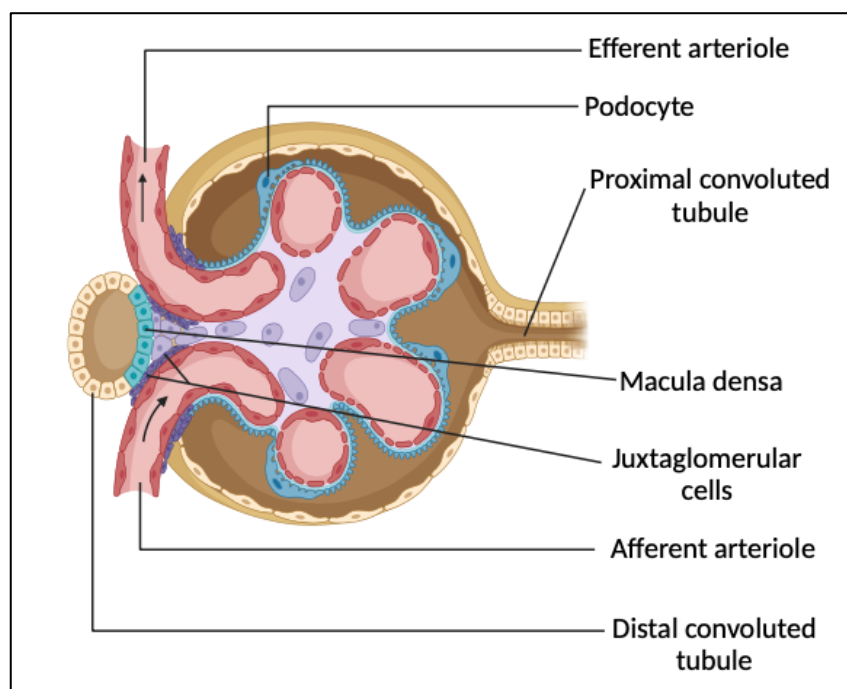


Figure 3.4: Cross section of a glomerulus

Tubuloglomerular Feedback: The TGF mechanism involves the macula densa cells of the distal convoluted tubule (Figure 3.4). These cells sense the concentration of sodium chloride in the tubular fluid. An increase in GFR leads to higher sodium chloride concentration, which the macula densa cells detect and respond to by signalling the afferent arteriole to constrict, thus reducing RBF and GFR. Conversely, a decrease in GFR results in lower sodium chloride concentration, leading to afferent arteriole dilation and increased RBF. Through TGF, reduced renal blood flow leads to reduced GFR which acts as safeguarding action against profound diuresis and volume depletion (19,167,173,175).

3.2.3 Neural Regulation

The kidneys are innervated by the sympathetic neurons of the autonomic nervous system via the coeliac plexus and splanchnic nerves (176) and they play a significant role in regulating RBF. Sympathetic nerve fibres innervate the renal blood vessels, and activation of these nerves causes vasoconstriction and decreased blood flow through the kidneys. In situations such as stress, exercise, or blood loss, increased sympathetic activity can reduce RBF to divert blood to vital organs like the heart and brain especially in systemic hypotension (167,173,176–178). This response is mediated through the release of noradrenaline (norepinephrine), which acts on alpha-adrenergic receptors on the renal vasculature. It causes vasoconstriction of afferent arteriole as well as stimulation of the adrenal medulla which, in turn, induces a generalised vasoconstriction through the release of epinephrine (adrenaline) (179).

3.2.4 Hormonal Regulation

Several hormones influence RBF, including:

Renin-Angiotensin-Aldosterone System (RAAS): Renin is released by the juxtaglomerular cells in response to low blood pressure, low sodium chloride, or sympathetic activation. Renin converts angiotensinogen to angiotensin I, which is further converted to angiotensin II by angiotensin-converting enzyme (ACE) (180). Angiotensin II is a potent vasoconstrictor that reduces RBF and stimulates aldosterone release, promoting sodium and water retention to increase blood volume and pressure.

Antidiuretic Hormone (ADH): ADH, also known as vasopressin, is released from the posterior pituitary in response to high plasma osmolality or low blood volume. It causes vasoconstriction and promotes water reabsorption in the kidneys, indirectly affecting RBF by altering blood volume and pressure (181).

Atrial Natriuretic Peptide (ANP): ANP is released from the atria of the heart in response to increased blood volume and pressure. It promotes vasodilation of the afferent arterioles and constriction of the efferent arterioles, increasing RBF and GFR to facilitate sodium and water excretion, thus reducing blood volume and pressure (182).

3.2.5 Medications

Non-steroidal anti-inflammatory drugs (NSAID): NSAIDs are known to cause changes in the renal blood flow by reducing the formation of prostaglandins which are vasodilators (183). Some studies have shown a decrease in renal perfusion with NSAIDs use compared to baseline in healthy volunteers (184,185).

RAAS inhibitors such as ACEI and ARB: ACEI and ARBs reduce the formation of angiotensin II which decreases GFR, by preventing the constriction of efferent arterioles. By inactivating bradykinin, a potent vasodilator, ACEIs are known to cause two main side effects: angioedema and cough from increased bradykinin levels (167). Although chronic use of RAAS inhibitors improves renal function by maintaining GFR in the long term (23)(186), the initial effect (short-term effect) of those medications can lead to reduction of RBF depending on the dose (187).

Beta blockers: Beta blockers impact renal blood flow by reducing cardiac output and inhibiting the release of renin from the juxtaglomerular cells in the kidneys. This reduction in renin leads to decreased angiotensin II production, a potent vasoconstrictor, thereby promoting vasodilation of renal arteries. However, due to variable cardioselectivity and intrinsic sympathomimetic activity among different beta blockers, they can produce different effects, with cardio selective ones not producing significant reductions in GFR or effective renal plasma flow (188,189).

Calcium channel blockers (CCBs): CCBs inhibit the influx of calcium ions into vascular smooth muscle cells, reducing vascular resistance and increasing renal perfusion. This enhanced blood flow can improve GFR and overall kidney function. In patients with hypertension or

CKD, CCBs can decrease renal vascular resistance, thus preserving renal function (190,191). Additionally, CCBs have been shown to protect against ischemic renal damage by maintaining adequate blood flow and reducing the risk of renal injury associated with prolonged hypertension or other vascular conditions (192).

Diuretics: Diuretics enhance urine production through the promotion of diuresis, achieved by modifying the renal handling of sodium. This process, known as natriuresis, facilitates the excretion of sodium and water. The majority of diuretics induce diuresis by inhibiting sodium reabsorption at various segments of the renal tubular system. By affecting sodium and water balance, diuretics effectively reduce blood volume and venous pressure, which subsequently leads to a decrease in RBF (19,193).

Inotropes: A substantial increase in RBF, reaching up to 26%, has been documented following the infusion of two distinct classes of inotropic agents (levosimendan and dobutamine) in patients with heart failure (194).

Oral contraceptive pills: Oral contraceptive pills (OCP) are associated with increased RAAS activity (195), but their impact on renal haemodynamic is controversial. A study reported a 25% reduction in renal perfusion in normotensive women using combined oestrogen-progestogen OCPs for over six months (196). Similar, though minor, differences in baseline RBF were noted between OCP users and non-users in some studies (197,198). Discontinuation of OCPs for six months showed no effect on baseline RBF in another study (199), attracting attention to the importance of documenting OCP use when measuring RBF in women.

3.2.6 Hydration status and food intake

Food and fluid intake significantly impact RBF through short-term physiological fluctuations.

Hydration status: Dehydration with low blood pressure reduces RBF, while overhydration increases it until euvoemia is achieved (200,201).

Food intake: During digestion and absorption, the mesenteric artery dilates, and renal arteries constrict to direct blood flow to the gastrointestinal tract (202). It was also previously reported that reduced RBF occurs in healthy volunteers shortly after meals, lasting up to four hours (203).

Types of food: In addition, different RBF responses were reported according to the type of consumed food. Some studies demonstrated an increase in RBF from baseline after ingestion of high protein meal in healthy individuals (204,205) and 23% rise in RBF was seen 20 mins after ingestion of high-energy fatty meal (206). Glucose ingestion, salt-rich and zinc-excess diet were reported to cause reduction in RBF (207–209).

3.2.7 Exercise and body temperature

Exercise: Physical exercise significantly alters renal haemodynamic, electrolyte, and protein excretion (200). The reduction in effective renal plasma flow (RPF) is proportional to exercise intensity and is influenced by sympathetic nervous activity and catecholamine release (210). Studies have shown that in both healthy volunteers and CKD patients, RBF can decrease by up to 52% at maximum exercise levels (211,212). This reduction in RBF during exercise also affects the GFR, though GFR decreases to a lesser extent. Hydration status significantly impacts GFR, and intense exercise increases plasma antidiuretic hormone levels, leading to an antidiuretic effect (210,211,213).

High body temperature: Elevated body temperature or heat stress induces peripheral vasodilation to dissipate heat, redirecting blood away from the kidneys to the skin. This leads to a reduction in RBF. Additionally, heat stress activates the sympathetic nervous system and the RAAS, further constricting renal blood vessels and reducing RBF. Chronic exposure to heat stress may exacerbate renal dysfunction, especially in individuals with pre-existing kidney conditions (214–216).

3.2.8 Other factors

Age: Age significantly affects RBF, with a gradual decline observed as individuals age. This reduction in RBF is due to decreased cardiac output, vascular stiffness, and loss of renal mass. Consequently, aging can impair kidney function, affecting the body's ability to maintain fluid and electrolyte balance. RBF was found to decrease after the age of 40 by – 10% each decade (217–219).

Sex: Gender influences RBF, with men typically exhibiting higher RBF than women (220). Hormonal differences, such as the effects of oestrogen and testosterone, play a role in this variation. Oestrogen tends to reduce RBF, while testosterone may increase it (220,221). These differences can impact renal function and disease susceptibility between genders. The total RBF in women was found to be – 20% (range – 16 to – 23%) lower than men by an average of – 243 mL/min (range – 187 to – 385 mL/min) (222,223).

Body mass index: Higher BMI is often associated with increased RBF due to greater metabolic demands and higher cardiac output (224). However, obesity can lead to renal hyperfiltration, increasing the risk of kidney damage over time (225). Conversely, lower BMI may be associated with reduced RBF, potentially impairing kidney function (226). Maintaining a healthy BMI is crucial for optimal renal health.

Pregnancy: In the early weeks of pregnancy, RBF begins to increase due to the vasodilatory effects of hormones such as progesterone and relaxin (227), along with increased cardiac output. This enhancement in RBF supports the growing metabolic demands of the mother and the developing embryo (228,229). As pregnancy progresses to the later stages, RBF can further increase but may plateau or even slightly decrease near term. The expanding uterus can compress the renal veins and inferior vena cava, potentially reducing venous return and slightly affecting RBF (230). Despite these changes, the kidneys maintain an elevated level of function throughout pregnancy to support the heightened needs of both the mother and foetus (228,230).

Menstrual cycle: The menstrual cycle influences RBF through hormonal fluctuations. During the follicular phase, oestrogen levels rise, which may slightly reduce RBF due to its vasoconstrictive properties. In the luteal phase, increased progesterone levels cause vasodilation, potentially enhancing RBF (231). Interestingly, a doppler study in 2005 (232) showed no significant differences in RBF, which was contrary to the earlier study in 1987 (233) showing small range of 7–10% increase in RBF during luteal phase.

Circadian rhythm: RBF typically follows a diurnal pattern, being higher during the day and lower at night. This fluctuation is regulated by the body's internal clock, influencing kidney function and urine production. During the daytime, increased RBF supports higher metabolic activity and waste filtration, while at night, reduced RBF aligns with decreased metabolic demands and a focus on conservation and repair(234–236) . Disruptions in circadian rhythm, such as from shift work or sleep disorders, can impact renal function and overall health.

Mental stress: Mental stress impacts RBF through the activation of the sympathetic nervous system and the release of stress hormones such as adrenaline and cortisol (237). These responses cause vasoconstriction of renal blood vessels, reducing RBF. Chronic mental stress can lead to sustained reductions in RBF, potentially impairing kidney function and exacerbating conditions like hypertension (238). In the elderly, mental stress results in more pronounced and prolonged reduction in RBF (239) .

Smoking: Nicotine and other harmful substances in tobacco smoke cause vasoconstriction, reducing RBF and impairing kidney function (240). Chronic smoking can lead to long-term damage, including increased risk of CKD and hypertension. The use of nicotine gum (4 mg) was found to acutely reduce RPF by 15% in non-smokers. Conversely, habitual smokers demonstrated an impaired renal response after active smoking (2–3 mg nicotine) (241–243). This suggests that habitual smokers may develop nicotine tolerance, which differs from the renal response observed in non-smokers.

High altitude: At high altitudes, reduced oxygen availability (hypoxia) triggers increased sympathetic nervous activity and the release of vasoconstrictive substances like endothelin,

reducing RBF (244). Additionally, hypoxia can stimulate the production of erythropoietin (245), increasing red blood cell production to improve oxygen transport but also increasing blood viscosity, which can further reduce RBF. These changes can impact kidney function and fluid balance, highlighting the importance of acclimatisation when moving to high altitudes.

3.2.9 Pathological Conditions

Various pathological conditions can affect RBF. Hypertension can lead to CKD through sustained high pressure damaging the renal vasculature. DM can cause diabetic nephropathy, characterised by altered RBF and glomerular hyperfiltration (246). Inflammatory diseases such as glomerulonephritis and conditions such as atherosclerosis or renal artery stenosis can significantly reduce RBF, impairing kidney function.

In conclusion, various physiological factors affect RBF through different mechanisms, such as hormonal changes, sympathetic nervous activity, and vasoconstriction or vasodilatation. Understanding these influences is crucial for assessing renal function and health. The next section will describe the different methods of measuring RBF using MRI techniques, providing insights into non-invasive imaging approaches that enhance our ability to monitor and evaluate renal perfusion in both clinical and research settings.

3.3 MRI methods for measurements of renal blood flow

This section introduces various MRI methods for measuring RBF, highlighting the basic principles and applications of non-invasive imaging techniques in nephrology. MRI offers a detailed assessment and valuable insights into renal haemodynamic and structure by techniques such as phase-contrast MRI (PC), arterial spin labelling (ASL), and dynamic contrast-enhanced MRI (DCE-MRI).

3.3.1 Dynamic contrast enhanced imaging (DCE)

DCE-MRI assesses renal perfusion by using a paramagnetic contrast agent, typically gadolinium-based, and capturing a series of rapid sequential images over a specified period, typically spanning several minutes (247). DCE-MRI analyses the signal dynamics before, during and after the administration of contrast agents and assess the tissue enhancement by monitoring the transit of contrast agents. The agent passes through the intrarenal regions, the renal cortex, the medulla, and the collecting system. In this way, DCE-MRI reveals the renal uptake and excretion of the contrast agent (247) (Figure 3.5).

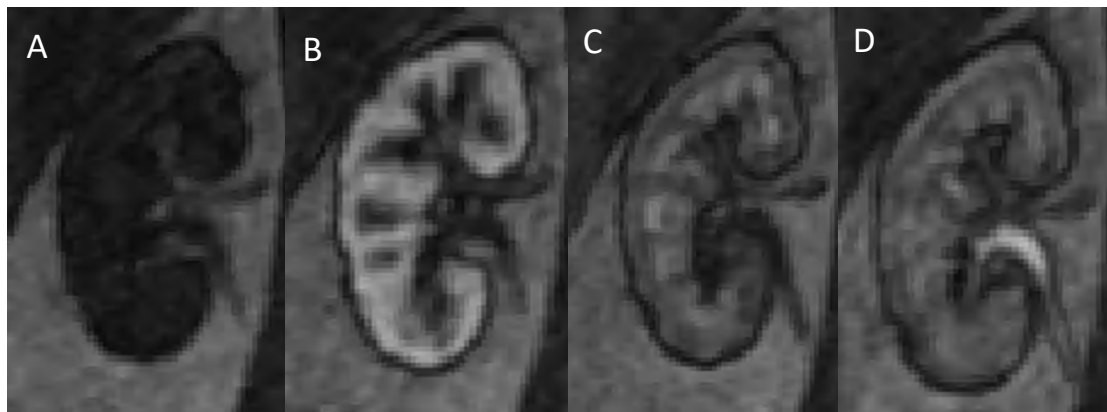


Figure 3.5: DCE MRI images of right kidney acquired at different time points before and after administration of contrast agent

(A= before contrast, B= contrast in renal cortex, C= contrast in renal medulla, D= contrast in ureter)

The dynamic nature of the imaging allows for the creation of signal-intensity time curves (Figure 3.6), which can be generated assuming a linear relationship between MR signal intensity and contrast concentration (248). By analysing the enhancement of the renal tissues over time, one can determine indirect measurement of essential single-kidney functional parameters such as RBF, volume, GFR, intra-renal blood volume and mean transit time (MTT) (247) (249) (Figure 3.7).

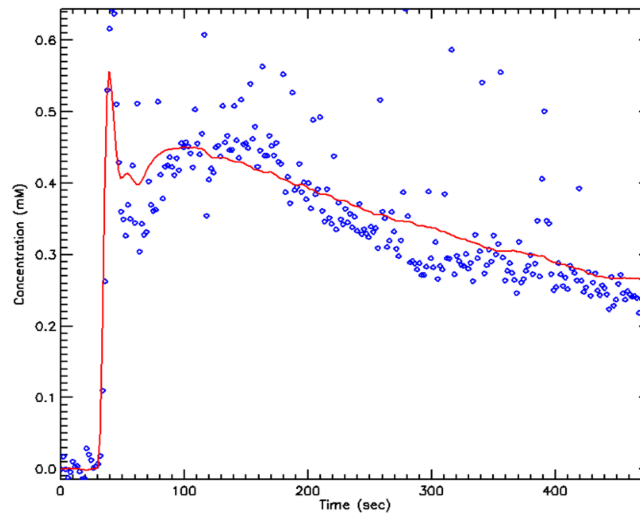


Figure 3.6: An example of signal intensity time curve obtained from DCE-MRI for renal perfusion (Contrast agent concentration over time)

Full quantitative analysis of DCE requires relatively prolonged acquisition period after the bolus administration of the contrast agent (approximately 10 minutes) in order to capture filtration and tubular parameters. However, the accuracy of perfusion measurements can be significantly compromised by motion artifacts, particularly breathing movements. Therefore, a crucial preliminary step in the analysis is the co-registration of images to correct for these motion-induced distortions (250). In the literature, various methodologies have been proposed to address the alignment of dynamic images post-reconstruction. One common approach involves the identification of anatomical landmarks to facilitate rigid transformation (251). Another method incorporates registration during the image reconstruction process itself (252). This motion correction is paramount for ensuring the integrity of the quantitative data derived from these imaging studies, ultimately leading to more precise and clinically relevant assessments of tissue perfusion and function.

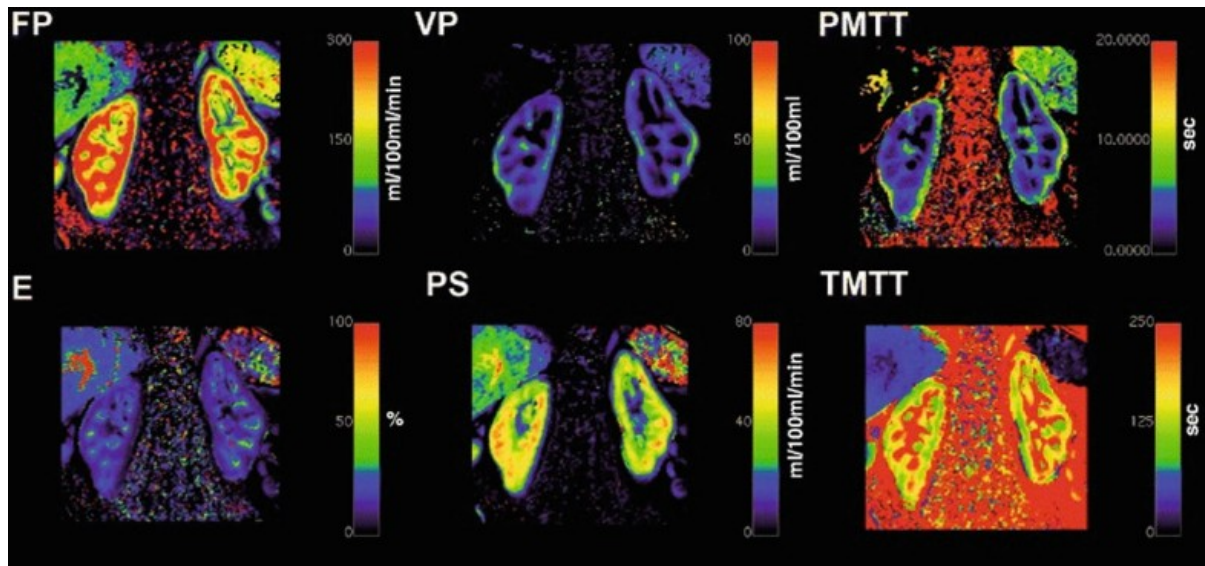


Figure 3.7: Example of parameters estimated from DCE-MRI in kidneys.

Top row from left to right: plasma flow (FP), plasma volume (VP), plasma mean transit time (PMTT).

Lower row from left to right: extraction fraction including, permeable surface area product (PS), and tubular mean transit time (TMMT)(247,253)

Contrast agents for DCE-MRI

Gadolinium-based contrast agents (GBCAs) with low molecular weight are frequently employed in DCE-MRI due to their ability to be excreted without undergoing tubular secretion or reabsorption. This property is particularly advantageous as it permits accurate measurements of GFR (254). GBCAs are generally considered safe, with a lower incidence of allergic reactions and nephrotoxicity compared to iodine-based contrast media (255), and a very low rate of immediate adverse events, ranging from 0.06% to 0.09% (256,257). Major life-threatening reactions to GBCAs are also exceedingly rare, with the incidence of acute, severe reactions estimated at 0.0025% to 0.005% (256,257).

Despite the relatively low doses of contrast material utilised in DCE-MRI, it remains crucial to exercise caution, especially in patients with compromised renal function ($\text{eGFR} < 30\text{ml/min/1.73m}^2$) or severe renal impairment such as end stage failure (258). These patients are at an elevated risk of nephrotoxicity and the development of nephrogenic

systemic fibrosis (NSF) which is characterised by hardening of skin and connective tissue (259).

Certain GBCAs have been more strongly associated with the development of NSF than others. In 2017, the Committee for Medicinal Products for Human Use (CHMP) of the European Medicines Agency (EMA) suspended the use of linear chelates (e.g. gadopentetate dimeglumine (Gd-DTPA), gadobenate dimeglumine (Gd-BOPTA)) deemed to carry the highest risk from intravascular use (255,260). Prior to this, the EMA's Scientific Advisory Group on Diagnostics had concluded that cyclic GBCAs, such as gadobutrol (Gadovist), gadoteridol (ProHance), and gadoterate meglumine (Dotarem), are known for their enhanced stability (255,260) and associated with a lower risk of gadolinium dissociation, making them safer options, especially in patients with compromised renal function.

NSF is a rare but serious and potentially life-threatening condition, characterised by excessive collagen deposition in the skin, resulting in thickening, coarseness, and hardening, which may lead to joint contractures and immobility. NSF can also involve systemic fibrosis of other organs, including the lungs, liver, muscles, and heart. While the exact pathophysiology of NSF remains unclear, diagnosis is based on a combination of clinical and pathological criteria (261,262). The initial clinical presentation of NSF typically includes pain, pruritus, swelling, and erythema, with symptoms most commonly beginning in the lower extremities (262). As the condition progresses, patients develop thickened skin and subcutaneous tissues, often described as having a "woody" texture, along with brawny plaques. In more advanced stages, fibrosis may affect internal organs, including the muscles, diaphragm, heart, liver, and lungs. Other serious manifestations include joint contractures, cachexia, and, in some cases, death (255,262). Although most cases of NSF present within two to three months following gadolinium exposure, there are instances where symptoms manifest years later, with the mechanisms for this delayed onset not yet fully understood (263)(261).

Unfortunately, there is currently no treatment for NSF that can stop its progression or reverse its effects and management remains conservative (264), although renal transplantation has been shown to help with symptoms (265). To decrease the risk of NSF,

the use of GBCAs is contraindicated (mainly in research) in patients who have undergone hepatic or renal transplantation with GFR of less than 60 mL/min/1.73 m², in patients with a GFR of less than 30 mL/min/1.73 m², and in those experiencing acute renal failure (266).

Besides this, DCE-MRI is used in research and has also been demonstrated as the potential method to measure RBF particularly in pathological disorders such as renal carcinoma to assess tumour vascularity (267,268), renal artery stenosis (269,270), renal transplant dysfunction (271,272) and assessment of obstructive uropathy (273).

3.3.2 Arterial spin labelling (ASL)

Arterial spin labelling (ASL) is a non-invasive MRI technique that measures renal perfusion by magnetically labelling the arterial blood water protons proximal to the kidneys. The fundamental principle of ASL involves the use of radiofrequency pulses to invert the longitudinal magnetisation of arterial blood water protons before they enter the tissue of interest (274,275). This labelled blood serves as an endogenous tracer, allowing the measurement of blood flow without the need for exogenous contrast agents. This is a non-invasive and non-ionising MRI technique which is very suitable to use in patients with impaired renal function as there is no concern of developing NSF (276).

ASL can be broadly categorised into continuous ASL (CASL), pulsed ASL (PASL), and pseudo continuous ASL (pCASL) (274,277). CASL involves the continuous application of a labelling radiofrequency pulse, typically over several seconds, to a slab of arterial blood, creating a steady-state magnetisation. PASL, on the other hand, utilises short, high intensity labelling pulses to invert the magnetisation of blood within a specific region. pCASL combines elements of both CASL and PASL, using a train of short pulses to achieve efficient and consistent labelling, which improves signal-to-noise ratio and reduces magnetisation transfer effects (277) .

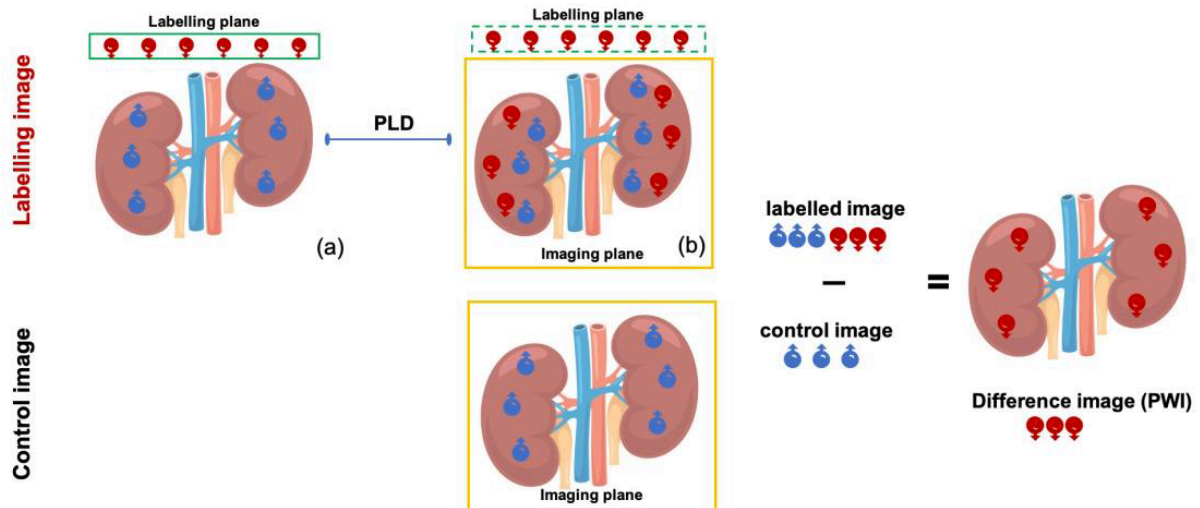


Figure 3.8: The basic principle of ASL

(a) incoming blood water is labelled (red spins) before entering the targeted region,
(b) post labelling delay time (PLD) allows labelled blood to leave labelling plane and disperse in renal tissue where acquisition takes place.

Control image is acquired without prior labelling, where only spins of static tissue (blue spins) are obtained.

A difference image is then obtained containing only spins of labelled blood.

Source: Image from transfer report of Dr Bashair Alhummiyany, Biomedical imaging sciences department, Faculty of medicine and health, The University of Leeds.

In ASL method, blood protons are magnetically labelled by applying radiofrequency pulse followed by labelled image acquisition after delay time. The delay period (post-labelling delay, or PLD) allows the labelled blood to travel to the kidney. Following this, images are acquired with and without labelling (control images). The difference between these images reflects the perfusion signal, which can be quantified to determine blood flow, known as a perfusion weighted image (PWI) whereby fitting a proper kinetic model, a perfusion map will be produced (250,278,279) (Figure 3.8).

One of the major challenges in ASL MRI is optimising the balance between signal strength and imaging duration (275). The PLD must be carefully chosen to ensure adequate delivery of labelled blood while minimising signal loss due to T1 relaxation. Additionally, motion

artifacts, such as those from patient movement or physiological processes like respiration, can affect image quality (280). Advanced image processing techniques, including motion correction and sophisticated modelling of the arterial input function, are employed to enhance the accuracy and reliability of ASL measurements (275,280,281).

The ASL MRI technique offers a powerful tool for assessing renal blood flow, with applications extending to the study of reduced RBF in CKD population (169,282), acute kidney injury patients (283), and lupus nephritis (284) compared to healthy subjects. Moreover, changes in cortical perfusion in different stages of CKD in correlation with eGFR were also reported in literature (285,286). Although it remains largely restricted to research settings in general (104), its non-invasive nature and the absence of exogenous contrast agents will make it particularly advantageous for repeated measures and longitudinal studies in future clinical studies.

3.3.3 Phase contrast MRI (PC-MRI)

Phase-contrast magnetic resonance imaging (PC-MRI) is a non-invasive method used to measure the velocity of moving fluids, such as blood flow, by exploiting the phase shifts of spins induced by motion. In clinical research, PC-MRI is utilised to compute blood flow velocity and volume in a specific vessel during the cardiac cycle and standard MRI technique for measuring blood flow in major vessels (287–289). PC-MRI is already used in mainstream clinical practice in cardiology and has been extensively validated (290). In renal studies, PC-MRI is particularly valuable for assessing blood flow and quantifying renal haemodynamics. Without the need for contrast agents which could potentially be associated with high risks for renal patients, PC-MRI provides a non-invasive alternative to quantitative assessment of RBF, blood velocity and volume (288).

The fundamental principle of PC-MRI involves the application of bipolar gradient pulses along specific directions during the MRI sequence (288). These gradient pulses induce a phase shift in the MR signal that is directly proportional to the velocity of moving spins (in this case, blood) (250). Stationary spins do not experience a net phase shift, allowing for the

differentiation between moving and stationary tissues. To acquire phase-contrast images, two sets of images are typically obtained: one with the velocity-encoding gradients applied (velocity-encoded image) and one without (reference image). By subtracting the reference image from the velocity-encoded image, the phase shifts caused by blood flow can be isolated. The resulting phase difference is proportional to the velocity of the blood flow, which can then be quantified (288).

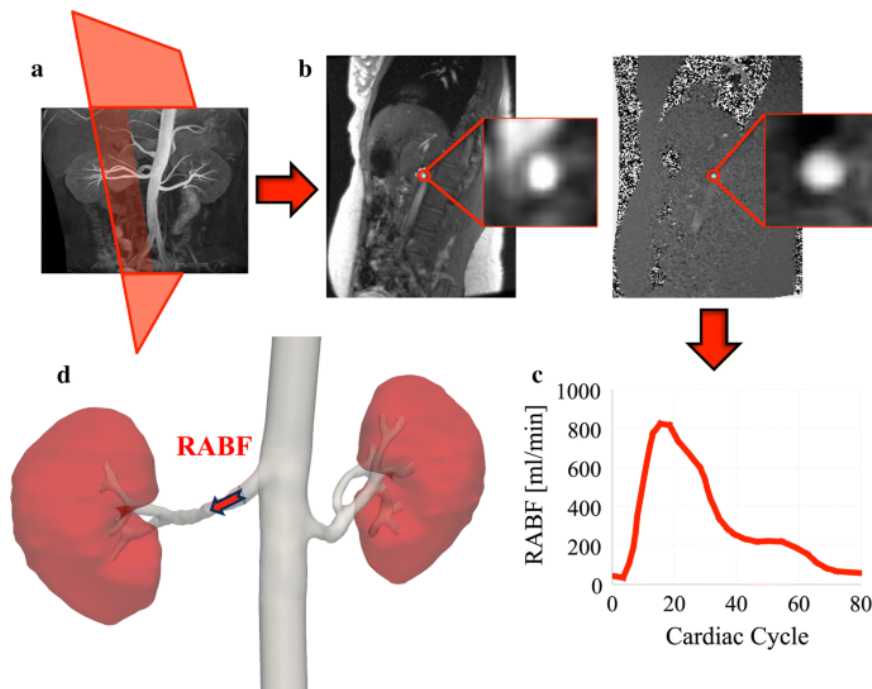


Figure 3.9: Schematic representation of phase-contrast magnetic resonance imaging (PC-MRI) acquisition and processing (287)

a Prescription of PC-MRI of the right renal artery with acquisition plane perpendicular to the vessel direction.

b Acquired coronal oblique magnitude (left) and velocity (right) images, with renal artery highlighted.

c Profile of renal artery blood flow (RABF) in the acquisition plane defined in a.

d 3D reconstruction showing average RABF computed in the right renal artery

The acquisition of diagnostic-quality images necessitates the careful selection of the appropriate imaging plane to ensure accurate measurements and the proper choice of encoding velocity. This prevents aliasing and achieves the highest signal-to-noise ratio (288,289) (Figure 3.9). For reliable blood flow measurement, the scanning orientation of PC-MRI must be perpendicular to the renal artery. Misalignment of the velocity encoding plane can lead to partial volume effects (250). Given that renal arteries typically measure approximately 5 mm in diameter, obtaining a high-quality survey image, such as an angiography scan, is strongly recommended. This approach ensures clear depiction of the arteries and proper positioning of the imaging plane prior to any bifurcations of the artery (287).

Overall, PC-MRI is a powerful, non-invasive tool that provides quantitative information about renal blood flow dynamics although not widely used in clinical practice. Several studies demonstrated the value of PC-MRI in different renal diseases such as reduced RBF in CKD patients compared to healthy volunteers (291–293) and decreased RABF in patients with septic acute kidney injury (AKI) in intensive care setting (294,295). It was also successfully used for detecting and assessing the patients with renal artery stenosis (296). Its application in renal studies enhances the understanding of renal physiology, aids in the diagnosis of renal vascular conditions, and supports the evaluation of therapeutic outcomes, thereby contributing significantly to both clinical and research advancements in nephrology.

3.4 Imaging biomarkers in diabetic kidney disease

With the advancement in imaging technology, researchers are now exploring the role of medical imaging as a source of new biomarkers. Ultrasound (US) and Doppler imaging are non-invasive modalities for evaluating renal diseases. It is a non-invasive, readily available, and cost-effective imaging technique that helps in assessing the kidneys' structure and function. US can detect morphological changes in early stage of DKD such as increased in size due to hyperfiltration (297) and late stage of DKD such as poor corticomedullary differentiation, reduction in length of kidney and decreased parenchymal thickness (298).

Doppler imaging is used to assess blood flow in renal artery and vein as well as renal vascular resistance via indices such as the resistive index in diseases like diabetes mellitus and systemic hypertension (299–302). Recently, one study used US renal score to predict DKD prognosis by measuring parameters such as renal parenchymal echogenicity, shape of cortical margin, mean cortical thickness/renal length/height and cortical thickness/parenchymal thickness (303). The study found that high renal scores were significantly associated with renal disease progression ($p = 0.031$). Additionally, the radiomics nomogram based on two-dimensional ultrasound model has also been proven to have good predictive performance with potential in risk assessment of DKD in T2DM study (304).

Computed tomography (CT) is another imaging modality which plays a valuable role in the evaluation and management of DKD. While not typically the first-line imaging modality due to concerns over radiation exposure and potential nephrotoxicity of contrast agents (305), CT can provide detailed anatomical information and is particularly useful for identifying and characterising renal masses, detecting renal stones, and assessing the extent of renal parenchymal damage. Additionally, CT angiography offers a detailed view of the renal vasculature, which can be instrumental in diagnosing renal artery stenosis and other vascular abnormalities (306). In patients with DKD, CT imaging can complement other diagnostic modalities by providing comprehensive information on the structural features of the kidney (307) and vascular aspects of the kidneys, thus aiding in the formulation of a more precise and tailored therapeutic approach.

The limited ability to detect early morphological changes in DKD often means significant damage has already occurred by the time these changes are identified in USG or CT, reducing opportunities for effective intervention or prevention. Therefore, the adoption of advanced imaging technologies, such as MRI, may be essential for the early detection of DKD changes.

3.5 MRI of kidneys as novel biomarker for DKD

MRI of the kidney is a non-invasive imaging technique used to obtain detailed images of the kidneys and surrounding structures. MRI utilises strong magnetic fields and radiofrequency pulses without using ionising radiation to generate high-resolution images, providing valuable information about the anatomy and function of the kidneys. MRI is superior to CT due to its avoidance of ionising radiation, thereby reducing potential radiation-related risks and provides easier repeatability in research studies. Additionally, MRI surpasses ultrasound by providing higher image quality and eliminating operator dependency, ensuring more consistent and reliable diagnostic outcomes. Being able to differentiate between different types of tissues in the body, MRI is a very useful imaging in the diagnosis of various medical conditions in clinical practice.

With advancements in MRI technology, there has been a growing interest in utilising MRI as biomarker for clinical and research purposes in kidney diseases. Advanced MRI techniques are sensitive to various structural and functional tissue characteristics, including perfusion, oxygenation, blood flow, glomerular filtration, tubular flow, fibrosis, inflammation, metabolism, and tissue composition. Moreover, these characteristics can be independently measured for the left and right kidneys as well as for the cortex and medulla, allowing for detailed characterisation of functional and structural heterogeneity within these regions (308). It is well known that total kidney volume measured by MRI is recognised as a prognostic biomarker for adult polycystic kidney disease progression and is utilised in clinical practice (309,310). Role of MRI as biomarker in CKD, by assessing structural, functional, and pathophysiological changes, will potentially improve the management of CKD (311–313).

For DKD, renal MRI can complement or replace biopsies, evaluating both kidneys entirely and avoiding sampling bias because its high spatial resolution allows detailed visualisation of the renal cortex and medulla. Table 3.1 summarises the different MRI methods used currently and their potential as renal MRI biomarker for DKD.

Table 3.1: Different MRI techniques and measured parameters in kidneys

| | MRI methods | Measured parameters | Significance in DKD as potential biomarker |
|---|--|---|---|
| 1 | Kidney macrostructure | 1. Kidney parenchyma volume, bipolar length 2. Cortical thickness | 1. Increased kidney volume in early stage of DKD due to hyperfiltration and found to have poorer renal outcomes (66,314,315). 2. Cortical thickness correlates positively with eGFR and better predictor of kidney function than bipolar length (316). |
| 2 | Kidney microstructure 1. T1 relaxation time 2. Diffusion weighted imaging (DWI)– Apparent diffusion coefficient (ADC) 3. Diffusion tensor imaging (DTI) and diffusion kurtosis imaging (DKI) – Fractional anisotropy (FA) | 1. Fibrosis | 1. Detection of interstitial fibrosis, early kidney damage and may provide the information on DKD progression (317,318). |
| 3 | Kidney haemodynamic 1. Phase contrast (PC) | 1. Blood flow velocity and volume of renal artery during cardiac cycle by angiogram | 1. Haemodynamic parameters such as end diastolic velocity (EDV), peak systolic velocity (PSV), and the Renal Arterial Resistive Index (RARI) can provide insights into pathophysiology of DKD in addition to renal perfusion (317). |

| | | | |
|---|---|---|---|
| | <p>2. Arterial spin labelling (ASL)</p> <p>3. Dynamic contrast enhanced (DCE) MRI</p> | <p>2. Renal perfusion by using magnetically labelled arterial blood water protons as endogenous tracer</p> <p>3. Functional parameters such as renal blood flow, GFR, intra-renal volume and mean transit time (MTT) using contrast agent</p> | <p>2. Mainly limited to research and used for assessment of cortical perfusion in different stages of DKD (286).</p> <p>3. Assessment of each kidney function using gadolinium contrast; cortical perfusion (mL/min/100 mL), filtration fraction (%), tubular volume fraction (%), and blood volume fraction (%) (247).</p> |
| 4 | Kidney Oxygenation – Blood oxygen dependent imaging (BOLD) | 1. Non-invasive assessment of deoxyhaemoglobin concentration in tissue by using paramagnetic properties of deoxyhaemoglobin as an endogenous agent | 1. Detection of renal hypoxia in DKD which is contributed by chronic hyperglycaemia and increased renal oxygen consumption (319). |
| 5 | Magnetic resonance elastography (MRE) | 1. Tissue stiffness and fibrosis | 1. Possible detection of fibrosis and renal parenchymal stiffness in DKD, although the role of MRE is still limited (320,321). |
| 6 | Fat content | 1. Perirenal, sinus and renal parenchymal fat | 1. Increased fat content in perirenal and renal parenchyma has been shown to be associated increased risk of DKD (322,323). |

Understanding which MRI parameters can detect early kidney injury, identify the underlying pathology, predict kidney function decline, track disease progression, and monitor treatment response is crucial (324). Despite advancements in the pathophysiological understanding of DKD, clinical translation remains constrained, primarily due to the absence of non-invasive methods for assessing renal microcirculation, oxygenation, inflammation, and fibrosis (325). While renal biopsy remains the gold standard for analysing renal microstructure, its application in DKD is often limited to atypical clinical presentations. Emerging renal MRI techniques can provide non-invasive assessment of renal details, and possible use of these parameters as biomarker which have significant potential to explore the heterogenous and complex pathogenesis of DKD.

Table 3.2 provides a non-exhaustive overview of recent studies in DKD. The predominant MRI techniques utilised in these studies are blood oxygen level dependent (BOLD) MRI, diffusion weighted Imaging (DWI) MRI, diffusion tensor imaging (DTI) MRI with comparatively limited data available on magnetic resonance elastography (MRE), PC-MRI, and ASL-MRI.

3.5.1 Kidney volume

In recent years, the focus of MRI studies in kidney research has shifted significantly from assessing morphometric features, such as kidney volume, to investigating more microscopic features. However, one of the recent studies by Notohamiprodjo et al. (326) demonstrated that renal volume increased progressively from normoglycemic controls to individuals with prediabetes and diabetes (280.3 ± 64.7 ml vs 303.7 ± 67.4 ml vs 320.6 ± 77.7 ml, respectively, $p < 0.001$) even after adjustment for age and sex, suggesting the possibility of hyperfiltration in diabetes group. Renal volume is also shown to have significant association with GFR ($p < 0.05$), which is supported by another study (327) where kidney volume positively correlates with eGFR ($p < 0.003$) but not with UACR. Although fewer studies are now focusing on macroscopic structure of kidney, renal volume findings remain consistent with no significant discrepancy.

3.5.2 Apparent diffusion coefficient (ADC) and fractional anisotropy (FA)

Several studies (n=10) have demonstrated the utility of DWI-MRI and DTI-MRI in DKD. The study by Razek et al. (328) reported increased mean FA and decreased ADC of the renal cortex in diabetic group (0.36 ± 0.10 and $1.74 \pm 0.16 \times 10^{-3} \text{ mm}^2/\text{s}$) compared to healthy volunteers (0.26 ± 0.02 and $1.88 \pm 0.03 \times 10^{-3} \text{ mm}^2/\text{s}$; $p = 0.001$). Similar findings were observed in comparison between macroalbuminuria (0.43 ± 0.10 and $1.63 \pm 0.19 \times 10^{-3} \text{ mm}^2/\text{s}$) and micro/normoalbuminuria groups (0.35 ± 0.12 and $1.80 \pm 0.18 \times 10^{-3} \text{ mm}^2/\text{s}$ ($p=0.001$) in the same study. FA and ADC correlated with urinary albumin ($r = 0.530$; $p = 0.001$, $r = -0.421$; $p = 0.006$) and serum creatinine ($r = 0.381$; $p = 0.013$, $r = -0.349$; $p = 0.023$).

However, opposite results were presented in the studies by Ye et al. (329) and Wang et al. (330). The former study showed reduced FA values in the renal cortex and medulla of the DM group compared to controls (cortical FA, $Z=-2.834$, $p=0.005$; medullary FA, $t=2.768$, $p=0.007$). The latter study described the similar findings in overall 95 subjects (cortex: 0.243 ± 0.038 ; medulla: 0.378 ± 0.068 ; $p < 0.001$) as well as when FA values were compared between microalbuminuria versus normoalbuminuria or healthy volunteer group (0.22 ± 0.04 vs. 0.25 ± 0.03 , $p = 0.032$). Both studies show no significant difference in ADC for all groups.

Similarly, Feng et al. (331) reported lower medullary FA values in micro-albuminuric group compared to controls ($p < 0.01$) and a decreasing trend from control to normoalbuminuric and macroalbuminuric groups. Zheng et al. (332) demonstrated lower ADC values in the renal parenchyma of hyperglycaemic diabetic patients compared to controls ($p = 0.002$), with a negative correlation between ADC and glucose levels. Osman et al. (333) found that ADC values were significantly lower in advanced stages of DKD compared to healthy controls ($2.1 \pm 0.3 \times 10^{-3} \text{ mm}^2/\text{s}$ vs $2.4 \pm 0.1 \times 10^{-3} \text{ mm}^2/\text{s}$, $p < 0.001$). Seah et al. (334) observed reduced cortical FA ($p=0.02$) and ADC in type 1 diabetes, reflecting reduced water diffusion in non-hyper filtering [2.40 ($2.29, 2.53$) ($103 \text{ mm}^2/\text{s}$)] versus hyper filtering [2.61 ($2.53, 2.74$) ($103 \text{ mm}^2/\text{s}$)]. Wei et al. (335) noted significant differences in medullary FA

values among DM subgroups, with negative associations with serum creatinine ($p < 0.001$) and positive associations with eGFR ($p = 0.01$).

Zhao et al. (327) found that cortical ADC has positive correlation with eGFR ($p < 0.001$, negative correlation with UACR ($p < 0.001$) and performed well in discriminating DKD with different eGFR levels (AUC = 0.904). Cortical ADC is also a predictor of renal outcomes (doubling of serum creatinine or ESRD) (hazard ratio = 3.4, 95% CI: 1.1-10.2, $p < 0.05$), independent of baseline eGFR and proteinuria. Duan et al. (336) reported that Δ ADC decreased with increasing CKD stages and was lower in DKD than in non-DKD and mixed groups. Δ ADC was independently associated with eGFR ($p = 0.042$) and UACR ($p = 0.031$), and baseline value was predictive of higher ESRF risk 1.232 -fold (95% CI 1.086, 1.398). Apart from the earlier study by Razek et al. (328), all other studies show consistent results for FA and ADC including their correlation with renal parameters. But challenges remain as many studies were conducted in early stages of DKD, only one study (336) had participants with biopsy-proven DKD and limited numbers of study with long term follow up.

Table 3.2: Recent MRI studies in diabetic kidney disease.

| | Study | Population | KV | ADC | FA | PC | ASL | DCE | BOLD | MRE | Fat | Findings |
|----|-----------------------------------|--|----|-----|----|----|-----|-----|------|-----|-----|--|
| 1. | Razek et al. (328) (2017) | 42 DM Vs 17 HV | | √ | √ | | | | | | | Increased FA and reduced ADC in renal cortex in DM with macroalbuminuria Vs microalbuminuria (p=0.001). FA has positive correlation with UACR and serum creatinine. ADC has negative correlation with UACR and serum creatinine. |
| 2. | Mora-Gutierrez et al.(286) (2017) | 45 T2DM Vs 46 HV | | | | | √ | | | | | Reduction in cortical blood flow seen in DM group compared to HV even with no difference in eGFR or UACR. (p<0.001) Reduced cortical blood flow with decrease in eGFR (p<0.001) |
| 3. | Wang et al. (330) (2018) | 61 T2DM Vs 34 HV (40 normoalbuminuria and 21 microalbuminuria in DM group) | | √ | √ | | | | | | √ | Reduced cortical FA (p=0.032) and reduced medullary FA (p<0.001) in microalbuminuria group. No difference in ADC. Renal fat fraction higher in microalbuminuria group compared to HV and normoalbuminuria (p< 0.001) |
| 4. | Ye et al.(329) (2019) | 36 DM Vs 26 HV | | √ | √ | | | | | | | Reduced FA in cortex and medulla of DM group (p=0.005) No difference in ADC. Positive correlation between cortical ADC and eGFR (p=0.02), cortical FA and eGFR (P=0.034) , medullary FA and eGFR (p= 0.043) |
| 5. | Notohamiprodjo et al.(326) (2020) | 230 normo-glycaemic, 87 pre-DM, 49 DM | √ | | | | | | | | √ | Pre-DM and DM were significantly associated to increased RV (p< 0.01), RSV (p<0.01) and RSF (p<0.001). |

| | | | | | | | | | | | |
|-----|----------------------------------|---|--|---|---|--|---|--|---|---|---|
| 6. | Spit et al.(337) (2020) | 51 T2DM | | | | | | | | √ | RSF correlated negatively with GFR ($p = 0.006$) and positively with effective renal vascular resistance ($p = 0.001$) |
| 7. | Feng et al.(331) (2020) | 30 DM (15 normo or micro and 15 macroalbuminuria) Vs 15 HV | | √ | √ | | | | √ | | Medullary R2* in normoalbuminuria group was higher than control group ($p < 0.01$). Medullary R2* macroalbuminuria group was lower than that in the control ($p = 0.009$) . |
| 8. | Vinovskis et al. (338) (2020) | 50 T1DM Vs 20 HV (Adolescents 12-21 years) | | | | | | | √ | | Whole-kidney RO2: GFR was 25% lower in T1DM versus control ($P < 0.0001$). Whole-kidney RO2:GFR was negatively associated with higher UACR ($P = 0.03$) and RPF ($P = 0.0009$). |
| 9. | Brown et al. (339) (2020) | 30 DM Vs 13 HV | | | | | √ | | | √ | Decreased cortical stiffness with worsening DKD. MRE shear stiffness was positively correlated with eGFR strongly at 90 Hz ($r = 0.41$, $P \leq 0.001$). ASL RBF positively correlated with eGFR levels ($P \leq 0.001$), as well as with MRE shear stiffness at 90 Hz ($P \leq 0.001$). |
| 10. | Lin et al.(340) (2021) | 95 T2DM Vs 51 HV | | | | | | | | √ | Increased RSF, Renal parenchymal volume in DM group ($p < 0.001$) RSF positively associated with UACR ($p = 0.016$) |
| 11. | Zheng et al. (332) (2021) | 57 T2DM Vs 14 HV | | √ | | | | | √ | | Hyperglycaemic diabetes groups have significantly lower ADC values in the renal parenchyma ($P = 0.048$, 0.002) and significantly higher MR2* and MCR values ($P < 0.000$, $P = 0.001$, 0.001 , and 0.005 , respectively) than normo-glycaemic group. |
| 12. | Osman et al. (333) (2021) | 40 DM Vs 20 HV | | √ | | | | | | | ADC lower in DKD compared to HV ($p < 0.001$). |

| | | | | | | | | | | | | |
|-----|------------------------------|-----------------------------|---|---|---|---|---|--|---|--|--|--|
| | | | | | | | | | | | | Negative correlation between increased stage of DKD and ADC (p<0.001). |
| 13. | Seah et al. (334) (2022) | 32 T1DM Vs 10 HV | | √ | √ | | | | √ | | | Reduced cortical and medullary R2* in DM compared to control group (p<0.001). Reduced cortical FA in DM (p = 0.02) compared to control. Reduced cortical ADC in non-hyper-filtering compared to hyper-filtering (p=0.001) |
| 14. | Makvandi et al. (317) (2022) | 38 T2DM Vs 20 HV | √ | √ | | √ | √ | | √ | | | Mean arterial flow (MAF) was the strongest predictor to differentiate diabetes Vs HV (sensitivity 0.94 and 1.0, specificity 1.00 and 0.69; P = 0.04 and 0.004, respectively) |
| 15. | Laursen et al. (341) (2022) | 15 T1DM Vs 15 HV | | | | √ | √ | | √ | | | MR2* was lower in T1DM (P < 0.01) and CR2* was not different compared to control group. Cortical perfusion was lower in T1DM (P < 0.001). Renal artery blood flow was lower in T1DM than in control (P =0 .05). In T1DM, lower cortical oxygenation and renal artery blood flow were both associated with higher UACR and lower eGFR (P < .05). |
| 16. | Wei et al. (335) (2022) | 72 T2DM Vs 20 HV | | √ | √ | | | | √ | | | MR2* and MFA were negatively associated with serum creatinine (SCr) (p< 0.001 and <0.001) and and positively associated with eGFR (p< 0.001 and 0.01). |
| 17. | Sorensen et al. (342) (2023) | 20 T2DM Vs 20 HV | | | | | | | √ | | | No difference in oxygenation between two groups (p=0.05) |
| 18. | Zhao et al. (327) (2023) | 67 DKD 8 years follow up | √ | √ | | | | | | | | Cortical ADC has positive correlation with eGFR (p<0.001) and negative correlation with UACR (p<0.001). |

| | | | | | | | | | | | |
|-----|--------------------------|--|--|---|--|--|--|--|--|--|--|
| | | | | | | | | | | | <p>Cortical ADC is a predictor of renal outcomes (doubling of serum creatinine or ESRD) with HR of 3.4 (95% CI: 1.1-10.2, P<0.05) independent of baseline eGFR and proteinuria.</p> <p>KV has positive correlation with eGFR (p<0.003) but no significant correlation with UACR.</p> |
| 19. | Duan et al. (336) (2024) | 119 T2DM with DKD (89 had biopsy – 38 biopsy-proven DKD, 51 biopsy-proven non-DKD) | | √ | | | | | | | <p>ΔADC was associated with eGFR (p=0.042) and UACR (p=0.031) in DKD.</p> <p>Baseline ΔADC was predictive of higher ESKD risk 1.232 -fold (95% CI 1.086, 1.398), independently of significant clinical confounding.</p> |

KV, kidney volume; ADC, apparent diffusion coefficient; FA, fractional anisotropy; PC, phase contrast MRI; ASL, arterial spin labelling MRI; DCE, dynamic contrast enhanced MRI; BOLD, blood oxygenation level dependent MRI; MRE, magnetic resonance elastography.

3.5.3 Phase contrast (PC) and arterial spin labelling (ASL)

Vascular pathophysiology plays a significant role in pathogenesis and progression of diabetic kidney disease. Following the previous study in 2017 which showed a reduction in cortical perfusion of 28% in patients with DM compared to healthy controls (286), Makvandi et al. (317) demonstrated that mean arterial flow (MAF) emerged as the strongest predictor to differentiate diabetes and healthy volunteer, with a sensitivity of 0.94 and 1.0, and a specificity of 1.00 and 0.69 ($P = 0.04$ and 0.004 , respectively).

Meanwhile, Laursen et al. (341) reported lower cortical perfusion was in diabetes compared to control (163 ± 40 vs. 224 ± 49 mL/100 g/min; $P < 0.001$) and reduced renal artery blood flow (360 ± 130 vs. 430 ± 113 mL/min; $P = 0.05$). Moreover, lower cortical oxygenation and renal artery blood flow correlated with higher UACR and lower eGFR ($P < 0.05$) in DM group. Despite these encouraging data, larger studies incorporating definitive renal outcomes are necessary (and currently ongoing) to validate the potential of PC-MRI and ASL-MRI in predicting renal outcomes.

3.5.4 Blood oxygen level dependent MRI (BOLD-MRI)

Sustained hyperglycaemia in DM results in mitochondrial dysfunction and impaired electrolyte transport in the renal tubules, leading to tissue hypoxia, which has long been recognised as a critical mechanism in the pathogenesis of DKD. Consequently, BOLD-MRI has been widely employed to assess renal oxygenation in DKD patients, although the findings have been inconsistent. The study by Feng et al. (331) found that the $R2^*$ value of the medulla was higher in the normoalbuminuric group compared to controls ($p < 0.01$) and lower in the macroalbuminuric group compared to controls ($p = 0.009$). Vinovskis et al. (338) reported that whole-kidney $RO2: GFR$ (the ratio of renal oxygen availability to glomerular filtration rate) was 25% lower in adolescents with T1DM compared to controls ($P < 0.0001$). In adolescents with T1DM, lower ratio was associated with higher UACR ($r = -0.31$, $P = 0.03$) and renal plasma flow ($r = -0.52$, $P = 0.0009$), suggesting that renal hypoxia in adolescents

with T1DM is associated with albuminuria and increased RPF, indicating a potential role in the development of DKD.

Zheng et al. (332) found significantly higher medullary $R2^*$ ($MR2^*$) and the $R2^*$ ratio between the medulla and cortex (MCR) values in hyperglycaemic DM group compared to the control group ($P = 0.001$ and 0.005 , respectively). Seah et al. (334) reported reduced cortical $R2^*$ [14.7 (13.7, 15.8) (1/s) vs. 15.7 (15.1, 16.6) (1/s), $p < 0.001$] and medullary $R2^*$ [24.8 (21.8, 28.2) (1/s) vs. 29.3 (24.3, 32.4) (1/s), $p < 0.001$] in patients with T1DM compared to controls, indicating more oxygenated parenchyma. Similarly, Laursen et al. (341) described lower mean medullary $R2^*$ in patients with T1DM compared to healthy volunteers ($34 \pm 6/s$ vs. $38 \pm 5/s$; $P < 0.01$), indicating higher oxygenation. No significant difference in cortical $R2^*$ was found.

Wei et al. (335) reported negative association between medullary $R2^*$ and serum creatinine ($p < 0.001$) and positive association with eGFR ($p < 0.001$). Sorensen et al. (342) identified a significant reduction in renal oxygenation from the cortex to medulla in both DM and HV groups ($P < 0.01$), although but no intergroup differences were detected ($P = 0.16$).

Despite inconsistent findings, these studies underscore the potential of BOLD-MRI, both as a standalone modality and in conjunction with other imaging techniques, to significantly benefit the assessment and management of patients DKD.

3.5.5 Magnetic resonance elastography (MRE)

MRE allows for the assessment of tissue stiffness and is particularly valuable for studying fibrotic conditions such as DKD. While being non-invasive, a successful MRE examination can provide a comprehensive overview of how the stiffness is distributed throughout the whole kidney (324). The study by Brown et al. (339) revealed that MRE cortical shear stiffness at 90 Hz was significantly reduced compared to controls across all CKD stages of diabetic nephropathy ($p < 0.001$). In addition, MRE shear stiffness was positively correlated with eGFR at 90 Hz ($r = 0.41$, $P \leq 0.001$).

Unlike observations in hepatic pathologies (343), MRE shear stiffness in the kidneys exhibits a surprising decrease with the progression of CKD (344,345). This counterintuitive finding is likely attributable to the reduced tissue turgor resulting from diminished RBF as CKD advances, subsequently affecting the mechanical properties of the renal parenchyma. This phenomenon underscores the complex pathophysiological mechanisms underlying renal fibrosis and highlights the need for further research to elucidate the intricate relationship between renal haemodynamic and tissue stiffness in DKD.

3.5.6 Renal fat

Renal fat comprises perirenal, sinus, and renal parenchymal fat deposits. High-resolution MRI techniques can effectively measure perirenal and sinus fat volumes, allowing for precise visualisation of the renal fascia that delineates perirenal fat from pararenal adipose tissue (337,346). Renal sinus fat (RSF), which extends from the perirenal fat, is closely associated with the renal pelvis and calyces, highlighting its anatomical and functional relevance in the context of renal physiology and pathology (324).

The study by Wang et al. (330) found that renal fat fraction (FF) in the micro-albuminuric group was significantly higher than in the normoalbuminuric and control groups ($5.6\% \pm 1.3\%$, $4.7\% \pm 1.1\%$, and $4.3\% \pm 0.5\%$, respectively; $p < 0.001$). Notohamiprodjo et al. (326) demonstrated that renal sinus volume (RSV) and RSF progressively increased from normoglycemic controls to individuals with pre-DM and DM. After adjusting for age and sex, both pre-DM and DM were significantly associated with increased RSV ($p < 0.01$) and RSF ($p < 0.001$). Hypertension was significantly associated with increased RSV ($p < 0.05$) and absolute RSF volume ($p < 0.05$).

Spit et al. (337) described that RSF correlated negatively with GFR ($r = -0.38$; $p = 0.006$) and effective RPF ($r = -0.38$; $p = 0.006$), and positively with mean arterial pressure (MAP) ($r = 0.29$; $p = 0.039$) and effective renal vascular resistance ($r = 0.45$, $p = 0.001$), which may mediate hypertension and DKD development. These correlations persisted after adjustment

for visceral adipose tissue (VAT), mean arterial pressure, sex, and body mass index.

Meanwhile, the study by Lin et al. (340) demonstrated that patients with DM had larger RSF volumes ($15.4 \pm 7.5 \text{ cm}^3$ vs. $10.3 \pm 7.1 \text{ cm}^3$, $p < 0.001$) and a higher sinus fat-parenchyma ratio compared to controls. RSF was positively associated with UACR, HbA1c, abdominal VAT, cholesterol, and triglycerides after adjustment for age, sex, ethnicity, and T2DM.

These studies collectively suggest that increased renal fat, particularly RSF, is associated with various metabolic risk factors and impaired renal function in diabetes. The findings indicate a potential role for RSF as an early biomarker for diabetic nephropathy, warranting further investigation to confirm its utility in early detection and management.

3.6 Summary

This chapter provides an overview of the kidney's anatomy, emphasising the blood supply and the various factors influencing RBF. The chapter also explores the basic principles of MRI methods for measuring RBF, including DCE-MRI, PC-MRI, and ASL-MRI. Each method offers unique advantages and limitations, contributing to their specific applications in both research and clinical settings. DCE-MRI is praised for its high resolution but requires contrast agents, PC-MRI and ASL are beneficial for its non-invasive nature and contrast-free alternative although not very widely used in clinical nephrology. These imaging techniques enhance our ability to investigate renal perfusion, advancing both scientific understanding and clinical practice in nephrology. Additionally, the role of imaging biomarkers, with a particular focus on MRI biomarkers for DKD was discussed. This includes an analysis of various MRI studies employing different MRI parameters to evaluate their efficacy and potential as biomarkers in the context of DKD.

Chapter 4

A review on impact of cardiac autonomic neuropathy on diabetic kidney disease

This literature review aims to elaborate the correlation between DKD and CAN by examining evidence from studies on T1 and T2DM over the past three decades. We will summarise different evidence and hypotheses to determine whether the relationship between CAN and DKD is causative or if both conditions are consequences of diabetes.

Abstract

DKD is the leading cause of CKD and ESKD worldwide, with one-third of patients with DM developing kidney disease over the course of their lifetime. With no cure for DKD, its management is mainly conservative. Despite advancement in treatments, the rate of DKD progression to ESKD is unpredictable, varying from months to years in different individuals. Therefore, researchers have been extensively investigating novel risk factors and biomarkers associated with advancement of DKD.

One such emerging factor is CAN which is widespread among diabetic population. It has become imperative to assess whether a causal relationship exists between CAN and DKD. This literature review aims to: (1) summarise current evidence for the correlation between DKD and CAN in T1 and T2DM, and (2) outline hypotheses for a possible causal relationship between CAN and DKD.

The review covers 27 studies (of which 10 are in people with T1DM) over the last 3 decades, including well-designed cohort and case-control analytic studies, which have clearly demonstrated an association between CAN and the progression of DKD by using renal parameters such as eGFR and UACR .

4.1 Introduction

4.1.1 Diagnosis of CAN

There are several different methods used for assessing CAN ranging from relatively simple bedside tests e.g., heart rate variation (HRV) in the time- and frequency-domain (144), cardiovascular reflex testing at rest, deep breathing, standing, and when performing the Valsalva manoeuvre (347) using the O'Brien's (348) or Ewing's (349) protocol to laboratory based assessments such as baroreceptor sensitivity testing. Although multiple abnormalities in different cardiovascular reflex tests are more preferable for the diagnosis of CAN, no single test for CAN is superior to the other (144). The different methods used over the years to diagnose CAN in clinical and research settings were summarised in table 4.1.

For cardiovascular reflex tests, one abnormal test is defined as early CAN; at least two abnormal tests are defined as definite CAN and orthostatic hypotension, and two abnormal tests are defined as advanced or severe CAN. In addition, it is worth noting that tests of sympathetic cholinergic function such as quantitative sudomotor axon reflex test (QSART), thermoregulatory sweat testing (TST), sympathetic skin response (SSR) and pupillary autonomic function testing by the use of pupillometry are used for research purposes in the diagnosis of DAN rather than CAN.

Table 4.1: Different tests for diagnosis of CAN (134)

| Test | Component of autonomic nervous system assessed | Clinical interpretation |
|---|--|---|
| <p>Cardiovascular reflex tests (Ewing's protocol)(350)</p> <ol style="list-style-type: none"> 1. HR response to deep breathing 2. HR response to standing 3. HR response to Valsalva manoeuvre 4. Systolic blood pressure response to standing 5. Diastolic blood pressure response to sustained handgrip <p>(O'Brien protocol) (348)</p> <ol style="list-style-type: none"> 1. HR responses to standing 2. Valsalva manoeuvre 3. Deep breath are compared with age-adjusted reference ranges | <p>Assesses parasympathetic ANS components by testing the ability of the vagal nerve to slow the HR (tests 1,2,3);</p> <p>Assesses sympathetic ANS components of sympathetic plexus by assessing ability to increase HR and BP in response to stimuli (tests 4,5)</p> <p>Parasympathetic and sympathetic components adjusted for age range reference values</p> | <p>Practical to perform in clinic. simple to replicate; classifies number of abnormal HR and BP responses.</p> <p>Classifies number of abnormal HR responses adjusted for age reference values</p> |
| <p>Heart rate variability tests (5 minutes ECG recording)(351)</p> | | |

| | | |
|--|--|---|
| <p>HRV time domain analysis</p> <ol style="list-style-type: none">1. mean heart rate2. root mean squared difference of successive RR intervals (RMSSD)3. standard deviation of the averaged normal RR intervals for all 5-minute segments (SDANN)4. standard deviation of the R-R interval (SDNN)5. SDNN index6. coefficient of variation of the R-R interval (CVRR). | <p>HRV time parameters (between RR intervals); parasympathetic</p> | <p>Classifies abnormal HRV responses adjusted for age range</p> |
| <p>HRV frequency domain analysis</p> | <p>Parasympathetic and sympathetic</p> | <p>Classifies abnormal HRV responses adjusted for age range</p> |
| <p>HRV power spectral analysis</p> | <p>Combined sympathetic and parasympathetic represented by different frequency bands</p> <p>VLF component representing sympathetic</p> | <p>Classifies abnormal HRV responses and clarifies parasympathetic and/or sympathetic damage according to type of abnormal HRV responses (VLF/LF/HF) adjusted for age range</p> |

| | | |
|---|---|--|
| | LF band representing a combination Parasympathetic and sympathetic HF band corresponding to parasympathetic | |
| Spontaneous baroreflex sensitivity | Parasympathetic and sympathetic; requires continuous blood pressure monitoring | Expensive and less available; used for research purposes |
| Cardiac radionucleotide imaging (MIBG scan) | Measures sympathetic innervation of the heart (decreased in CAN) | Expensive and less available; used for research purposes |

ANS = autonomic nervous system; BP = blood pressure; CAN = cardiac autonomic neuropathy; HF = high frequency; HR = heart rate; HRV = heart rate variability; LF = low frequency; MIBG = metaiodobenzylguanidine; VLF = very low frequency.

4.1.2 Renal autonomic nerve supply

A comprehensive understanding of renal autonomic nerve anatomy and physiology is essential for discerning the influence of CAN on DKD. The renal autonomic innervation includes afferent and efferent fibres of the renal plexus, with the efferent fibres being exclusively sympathetic. This plexus consists of fibres from the celiac plexus, intermesenteric plexus, and lumbar splanchnic nerves, which enter the kidney hilum along with the renal artery and vein (352) (Figure 4.1). Parasympathetic innervation via the vagus nerve induces vasodilation and increases blood flow to the afferent arterioles (176), while sympathetic activation stimulates beta-1-adrenergic receptors in juxtaglomerular cells, activating the RAAS. RAAS activation results in renal tubular sodium reabsorption, reduced urinary sodium excretion, and decreased renal blood flow due to vasoconstriction (347,353).

The impact of CAN on DKD may be due to an imbalance between sympathetic and parasympathetic functions. Several studies have explored this relationship, proposing various hypotheses (Table 4.1). This narrative review will examine the existing evidence to outline the relationship between CAN and DKD, its impact on albuminuria and renal function decline, and identify the possible pathophysiological mechanisms involved.

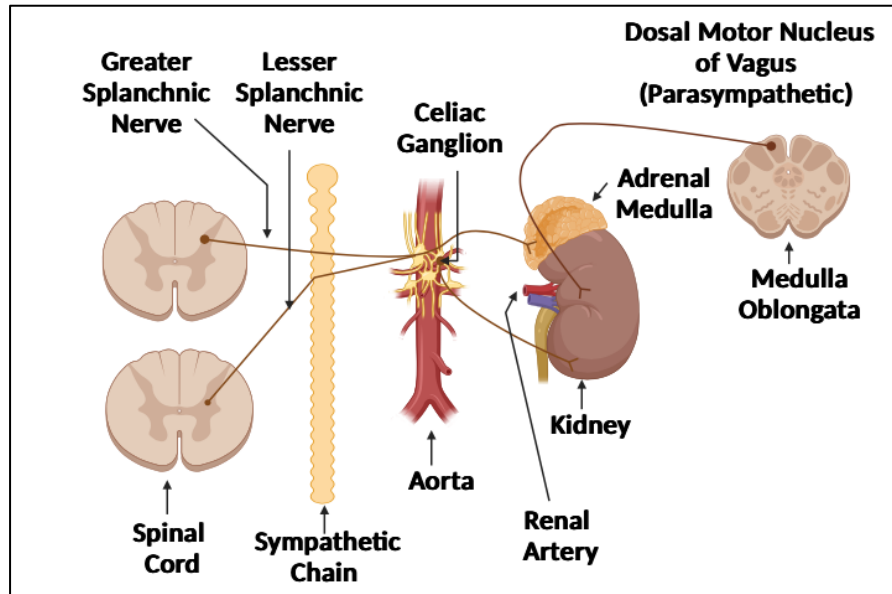


Figure 4.1: Kidney nerve supply

Adapted From: [Anatomy, Abdomen and Pelvis, Kidney Nerves](#) (354)

4.2 Search strategy

A literature search was conducted for studies from January 1993 and December 2023 using the search terms 'diabetic nephropathy', 'diabetic kidney disease', 'diabetic autonomic neuropathy', and 'cardiac autonomic neuropathy' on PubMed, Google Scholar. Full-length original articles and their references were examined to gather recent studies on CAN and DKD. Additional articles were identified through reference lists. Studies on CAN in children and adolescents, non-translated non-English journals and publications were excluded.

Figure 4.2 summarises the PRISMA flow diagram for article screening.

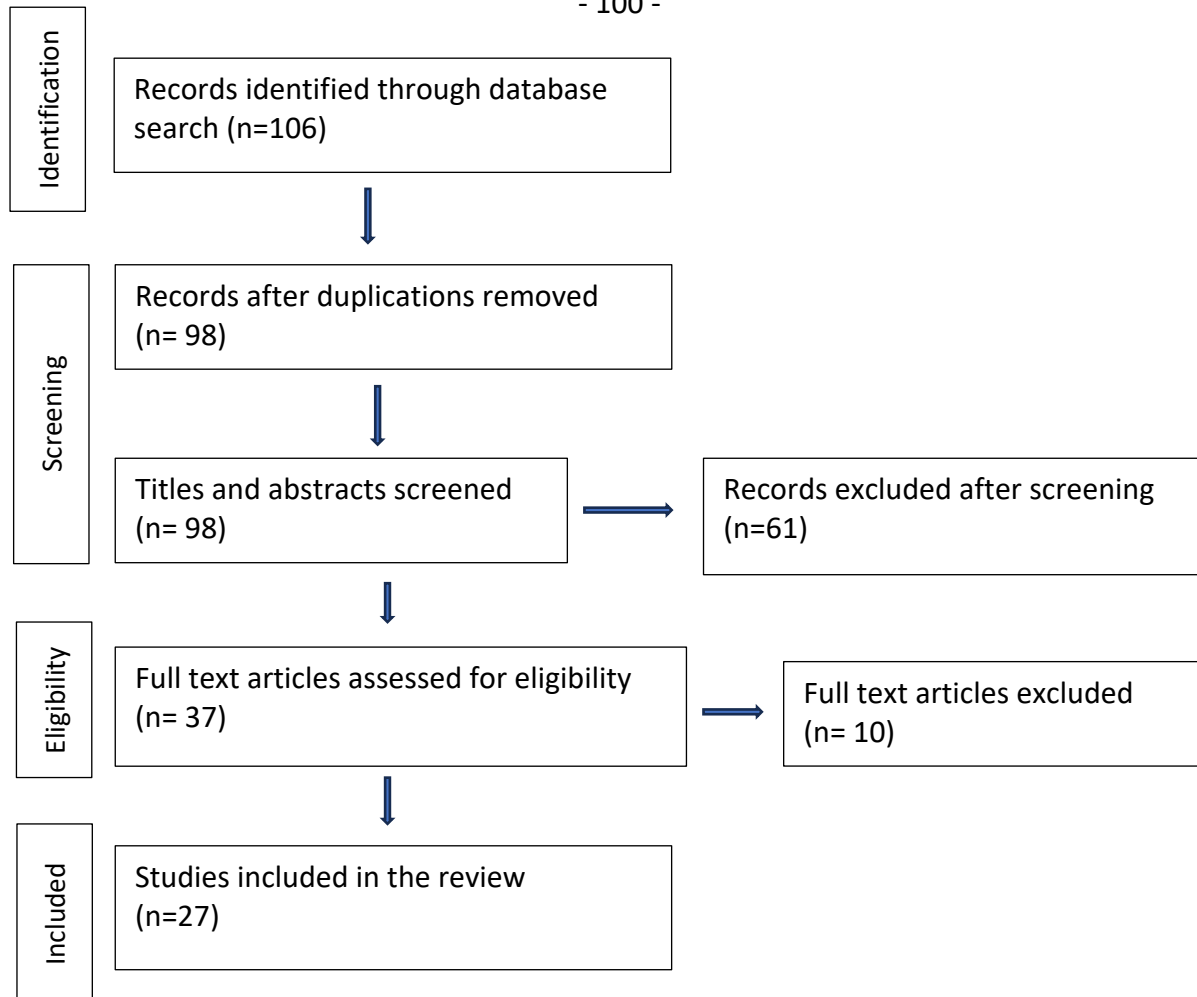


Figure 4.2: PRISMA flow diagram for screening of articles.

4.3 Relationship between CAN and DKD

Table 4.2 presents a summary of 27 studies investigating the association between CAN and DKD in T1 and T2DM. The table includes 6 prospective studies, 3 cross-sectional studies and 1 retrospective study for T1DM and 3 prospective studies, 7 cross-sectional studies and 7 retrospective studies for T2DM.

Table 4.2: Studies describing association between CAN and DKD

| No. | Study | No & Type of DM Type of study | CAN testing | Follow up years | Kidney function outcomes |
|-----|-----------------------------|--|-----------------------------|--------------------|---|
| 1. | (Sundkvist G, 1993)(355) | 35 T1DM Prospective study | DB, Tilt Test | 10 | CAN associated with decline in eGFR. (4.46 ± 0.98 vs. 0.48 ± 0.73 , $p < 0.005$) |
| 2. | (Spallone V, 1994) (356) | 30 normotensive T1DM | DB, LS, VM, OH 24hr ABPM | | CAN associated with increased mean night UAE. (61.4 ± 104.6 [mean \pm SD] vs. 16 ± 25.2 micrograms/min, $p < 0.04$). |
| 3. | (Monteagudo P, 1996) (357) | 38 T1DM | DB, LS, VM, OH 24hr APBM | | CAN associated with reduced nocturnal fall in BP ($r = 0.44$; $p < 0.01$) and increased UAE ($r = 0.69$; $p < 0.0001$). |
| 4. | (Weinrauch LA, 1998)(358) | 26 T1DM with proteinuria Prospective study | DB, LS, VM | 1 | CAN associated with increase in serum creatinine over 12 months compared to baseline ($p < 0.001$). |
| 5. | (Rutter M, 1998) (359) | 43 T2DM with microalbuminuria and 43 T2DM with normoalbuminuria Cross-sectional study | DB, LS, VM, HG, OH, HRV | | CAN and reduced HRV associated with microalbuminuria ($p < 0.05$). |
| 6. | (Smulders Y, 2000) (360) | 536 subjects in total 256 with normal glucose tolerance (NGT), 143 with impaired glucose tolerance (IGT), and 137 T2DM Cross-sectional study | DB, LS, OH | | CAN associated with microalbuminuria in IGT and T2DM. (Odds ratio (95% CI) of 1.19 (1.02-1.39) per point increase in CAN score). |
| 7. | (Burger AJ, 2002)(361) | 23 T1DM with macroalbuminuria Prospective study | DB, LS, VM, HRV | 1 | HRV indexes and CAN associated with decline in eGFR. (creatinine clearance reduction ≥ 8 ml/min, $r = 0.30$, $p = 0.01$). |

| | | | | | |
|-----|-----------------------------|---|-------------------------|------|---|
| 8. | (Forsén A, 2004)(362) | 58 T1DM Prospective study | DB, Tilt test, OH | 7-14 | CAN associated with increased albuminuria (p = 0.0016) and greater fall in eGFR [29 (16.5) ml/min/1.72 m ² vs. 11 (9) ml/min/1.72 m ² ; p = 0.0074]. |
| 9. | (Moran A, 2004) (363) | 132 T2DM Cross-sectional study | DB, VM, LS 24hr ABPM | | CAN associated with increased microalbuminuria. (p < 0.0001). |
| 10. | (Takebayashi K, 2006) (364) | 185 T2DM Prospective study | HRV | 3 | CAN showed a significant correlation only in macroalbuminuric group (p = 0.0064). |
| 11. | (Maguire AM, 2007)(365) | 137 T1DM with normoalbuminuria Prospective study | Pupillary light test | 12 | Small pupil size (impaired pupillometry test) predictor of microalbuminuria. (Odds ratio 4.36 [95% CI 1.32-14.42], P = 0.016) |
| 12. | (Bilal N, 2008) (366) | 53 T2DM Cross-sectional study | DB, LS, VM, OH, HG | | Increased severity of CAN associated with increased prevalence of DKD. (p = 0.046). |
| 13. | (Kim YK, 2009)(347) | 156 T2DM with normoalbuminuria Retrospective longitudinal study | DB, LS, VM, OH | 9 | Definite or severe CAN associated with greater decline in eGFR (mean change, -10.28%; p=0.047) compared to normal or early CAN (mean changes, 4.50% and 0.77%, respectively). |
| 14. | (Tahrani AA, 2014)(367) | 204 T2DM without ESRD Cohort study | DB, LS, VM, OH | 2.5 | CAN predictor of eGFR decline. (-9.0 ± 17.8% vs -3.3 ± 10.3%, p = 0.009). |
| 15. | (Orlov S, 2015)(368) | 204 T1DM with normoalbuminuria 166 T1DM with microalbuminuria Prospective study | MCR during DB | 14 | CAN is a strong independent predictor of early progressive renal decline (p < 0.001). |
| 16. | (Yun JS, 2015)(369) | 755 T2DM without CKD Prospective study | DB, LS, VM, OH | 9.6 | Annual decline in eGFR in the normal, early, and definite CAN group (1.61 ± 2.54, 2.61 ± 3.22, and 4.64 ± 5.06 ml/min/1.73 m ² , respectively, p < 0.001). |

| | | | | | |
|-----|------------------------------------|---|--|-----|---|
| 17. | (Wheelock KM, 2016)(370) | 63 T2DM Cohort study Kidney biopsies | DB, HRV | 9.2 | Increased stage of CAN associates with advanced DN lesions. |
| 18. | (Padmini S, 2017)(371) | 199 T2DM Cross-sectional study | CAN activity measured by ANSiscope | 2 | Strong linear correlation between CAN and albuminuria. |
| 19. | (Bjerre-Christensen T, 2021) (372) | 329 T1DM Cross-sectional study | DB, LS, VM, | 6.1 | CAN associates with 7.8% higher albuminuria increase per year (95% CI:0.50% to 15.63%, p=0.036) than those without CAN. |
| 20. | (Laursen J, 2021)(373) | 24 T2DM Post-hoc analysis of cohort study | DB, LS, VM, HRV | 6 | Decline in eGFR was associated with CAN in unadjusted model (β per 1 SD = 0.37 ml min ⁻¹ 1.73 m ⁻² increase per year; p=0.04), but not after adjustment (p=0.12). No association between CAN and albuminuria. |
| 21. | (Kadoya M, 2021) (374) | 8 T1DM 223 T2M | HRV | | Low HRV associates with increased risk of renal decline in diabetes population. (HR 2.40, 95% CI 1.02–5.60, $p = 0.043$) |
| 22. | (Chen Y, 2021) (375) | 225 T2DM | DB, LS, VM, OH, HG | | CAN positively correlated with albuminuria and left ventricular diastolic dysfunction (P<0.001). |
| 23. | (Eun Jun J, 2022) (376) | 2,033 T2DM Retrospective longitudinal study | DB, LS, VM, OH | 2.9 | CAN associated with significantly higher risk of DKD (HR 1.56, 95% CI 1.15 - 2.12; $p = 0.005$). |
| 24. | (Muramatsu T, 2022)(377) | 831 T2DM Retrospective observational cohort study | HRV | 5.3 | CAN strongly increased the risk of a 40% eGFR decline in patients with macroalbuminuria. (hazard ratio 2.42, 95% confidence interval 1.54-3.80). |
| 26. | (Zeng H, 2022) (378) | 747 T2DM Retrospective cohort study | HRV | 5 | CAN and reduced HRV associated with DKD progression. (β =-19.5, 95% CI: -30.0 to -10.0, $p < 0.01$) |

| | | | | | |
|-----|-------------------------|---|-----|--|---|
| 27. | (Tang Y, 2023) (379) | 469 T1DM 7973 T2DM Retrospective cohort study | HRV | 3.2 for T1DM 4.9 for T2DM | CAN associated with more negative eGFR slopes (-1.15ml/min/1.73m ² year), increased odds of rapid kidney function decline (+111%), and increased hazards of experiencing ≥40% eGFR loss (+150%) independent of known DKD risk factors. CAN was associated with more negative eGFR slopes (-0.34 ml/min/1.73m ² year), increased odds of rapid kidney function decline (+39%), and increased hazards of experiencing ≥40% eGFR loss (+54%). |
|-----|-------------------------|---|-----|--|---|

CAN, cardiovascular autonomic neuropathy; T1DM, type 1 diabetes mellitus; T2DM, type 2 diabetes mellitus; DKD, diabetic kidney disease; NGT, normal glucose tolerance; IGT, impaired glucose tolerance; DB, deep breathing; HRV, heart rate variability; LS, lying to standing; OH, orthostatic hypotension; RR, coefficient of variation; VM, Valsalva manoeuvre; MCR, mean circular resultant; DBP, diastolic blood pressure; ABPM, ambulatory blood pressure monitoring; UAE, urinary albumin excretion; eGFR, estimated glomerular filtration rate

4.3.1 CAN and renal function decline in type 1 and type 2 diabetes mellitus

Many studies have examined the association between CAN and DKD in T1 and T2DM. The most commonly used test to assess CAN was heart rate variability and cardiovascular reflex tests as these are relatively quick and simple to perform.

Renal parameters such as creatinine and eGFR were used to assess the potential mechanisms underlying the progressive renal function decline in individuals with CAN.

In a prospective 10-year follow-up study (355) involving 35 patients with T1DM, those with CAN showed a greater eGFR decline compared to those without CAN. Similar findings were observed in two other studies (358,361) which included intensive glucose and blood pressure control. A 14-year study (368) with 370 patients with T1DM linked baseline DAN to early GFR loss and advanced CKD, independent of various confounding factors including sex, diabetes duration, SBP, DBP, HbA1c, triglycerides, eGFR, and the presence of microalbuminuria. The PERL study (379) (N=469) over 3.2 years also associated CAN with accelerated decline in kidney function, defined as $\geq 40\%$ fall in eGFR. Despite variations in sample size, follow-up duration and the tests used to diagnose CAN, these studies in T1DM indicate that individuals with CAN experienced greater renal function decline.

Similarly, studies in T2DM demonstrate a significant and independent association between CAN and rapid decline in renal function. A 9-year retrospective study (347) with 156 participants showed greater eGFR decline in those with severe CAN. Another study (369) followed 755 T2DM patients for 9.6 years and found early and definite CAN to be linked to higher CKD risks. A cohort study (367) identified CAN as an independent predictor of eGFR decline over a 2.5-year follow-up. Kadoya et al. (374) found CAN to be independently associated with renal function decline, while Muramatsu et al. (377) observed a strong link between CAN and eGFR decline, especially in patients with macroproteinuria. Zeng et al. (378) used KDIGO risk stratification and identified reduced HRV as a risk factor for DKD progression. The ACCORD study (379) with 7973 participants over 4.9 years also found associations between CAN and rapid kidney function decline.

In summary, these studies, which encompass a wide age range (with T2DM cohorts naturally being older than T1DM cohorts) and either match or adjust for key confounding factors such as age, duration of diabetes, HbA1C levels, and blood pressure, demonstrate an association between CAN and renal function decline. However, it is important to note that most of these studies were conducted in the early stages of DKD, raising questions about the role of CAN across different stages of disease severity. Additionally, it remains unclear whether the impact of CAN is consistent across different ethnicities, in younger patients (<40) with T2DM, different stages of CAN severity or in the context of medication use.

4.3.2 CAN and Albuminuria in type 1 and type 2 diabetes

Research in both T1 and T2DM populations has explored the association between CAN and albuminuria using various methods, such as 24-hour urine collection, early morning urine, and random urine tests.

Early studies (357,380) in 1990s for T1DM used 24-hour blood pressure monitoring and cardiovascular reflex tests to assess CAN and day and night UACR measurements for albuminuria. One study (380) demonstrated that mean nocturnal albuminuria was significantly higher in patients with CAN than in those without CAN. Another study (357) found that urinary albuminuria correlated with greater autonomic function abnormality. Similarly, a 14-year prospective study (362) revealed higher rates of albuminuria and greater declines in eGFR in patients with CAN at baseline compared to those without. Another study (372) reported associations with ESRF, all-cause mortality, and significant eGFR decline over 6.1 years, independent of traditional risk factors such as HbA1c, UACR, eGFR, and blood pressure. Additionally, a study (365) that assessed CAN using pupillometry reflex tests found that abnormal results were independently associated with the development of microalbuminuria and retinopathy over a 12-year follow-up.

In T2DM, numerous studies over several years have described similar associations between CAN and albuminuria. An early study by Rutter et al. (359) in the 1998 suggested that CAN was an associated factor rather than an independent predictor, due to links with diabetic

retinopathy, higher BMI, claudication, alcohol use, and calcium channel blocker usage. However, subsequent studies by Smulders et al. (360) and Moran et al. (363) demonstrated independent associations with albuminuria, with an odds ratio of 1.19 per point increase in CAN score. Conversely, a study by Takebayashi et al. (364) found a correlation between CAN and macroalbuminuria, but not with normal or microalbuminuria, in a 3-year follow-up. Other studies (366,376) reported that increased CAN severity was associated with higher prevalence of microvascular complications such as retinopathy and nephropathy, detected by microalbuminuria in 24-hour urine collections or eGFR decline.

Strengths of these studies include the use of diverse measurement methods for assessing albuminuria, such as 24-hour urine collection and early morning urine tests, providing comprehensive data. Longitudinal follow-up, including a 14-year prospective study (362) and a 6.1-year follow-up study (372), enhances the reliability of findings. Adjustments for confounding factors like HbA1c, eGFR, and blood pressure strengthen the validity of conclusions. Investigation of various endpoints beyond albuminuria, including eGFR decline, ESRF, and microvascular complications, offers a holistic view of CAN's impact on renal health. Moreover, the use of different diagnostic tests for CAN, such as pupillometry reflex tests and HRV, captures different aspects of autonomic neuropathy.

However, limitations exist within these studies. Variability in whether CAN is an independent predictor, or an associated factor leads to inconsistent conclusions and reflects the complexity of the relationships. Differences in study populations, including age ranges, and sample sizes, impact generalisability. Limited consideration of ethnic diversity restricts the applicability of results to broader populations. Moreover, most studies focus on the early stages of DKD, raising questions about CAN's role across all disease stages. These findings underscore the importance of CAN in renal function decline and its association with albuminuria. However, further research is needed to clarify the causal relationship between CAN and DKD, especially across different stages of disease severity and among diverse populations.

4.4 Potential mechanisms for impact of CAN on progressive renal function decline in DKD

Several mechanisms have been proposed to explain the pathophysiological impact of CAN on DKD (Figure 4.3).

Parasympathetic dysfunction

In the early stages of CAN, the parasympathetic system is affected, particularly the vagus nerve. This results in relative sympathetic dominance, causing systolic hypertension, resting tachycardia, and increased cardiac output, which promote glomerular membrane injury with excessive filtration of sodium and albumin (347,358,363,376,381).

Sympathetic overactivity

Excessive sympathetic drive leads to a lack of nocturnal blood pressure drop, resulting in higher intraglomerular pressure at night. This leads to glomerular injury and increased sodium and albumin excretion (355,357,360,380,382).

Renin-Angiotensin-Aldosterone System (RAAS) activation

Early compensatory increases in sympathetic tone in response to subclinical parasympathetic denervation activate the intrarenal RAAS, causing renal dysfunction through increased glomerular basement membrane (GBM) thickness and mesangial matrix expansion due to renal vasoconstriction and ischemia (368,383).

Inflammation and oxidative Stress

Sympathetic nervous system impairment affects the regulation of inflammatory cytokines and chemokines (379,384), which are potential therapeutic targets and biomarkers for DKD (379,385). Additionally, reduced renal function is associated with decreased antioxidant scavenging enzymes and increased production of reactive oxygen species, leading to oxidative stress and DKD progression (378,386).

Sympathetic Neuropathy in Late CAN

In the later stages of CAN, sympathetic neuropathy results in diminished renal sodium excretion, reduced RBF, and decreased eGFR due to renal vasoconstriction (347,377).

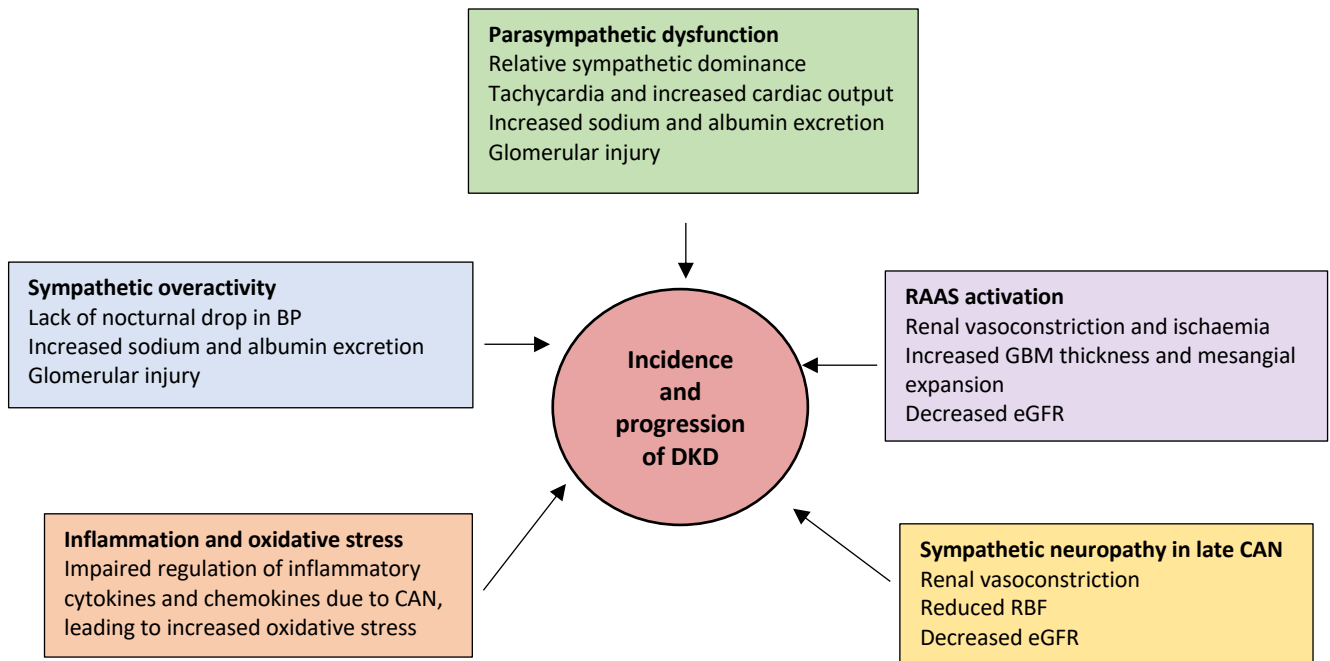


Figure 4.3: Potential mechanisms for the impact of CAN on incidence and progression of DKD

Among these mechanisms, the non-dipping in both SBP and DBP has been the most thoroughly investigated (357,360,380,387–390). A recent study (391) investigated renal hemodynamics (GFR and effective renal plasma flow), using inulin and para-amino Hippurate clearance via the plasma disappearance technique. In individuals with T1DM, a higher modified Toronto Clinical Neuropathy score (a clinical assessment tool for peripheral neuropathy) was associated with lower RBF and greater efferent renal arteriolar resistance, even after adjusting for age, sex, HbA1c, SBP, LDL cholesterol, and 24-hour urine albumin to creatinine ratio. Interestingly, the study did not identify any association between CAN and RBF. Based on the proposed mechanisms and the limited mechanistic studies conducted, it is possible that hemodynamic factors are primarily responsible for the increased renal decline associated with CAN. More robust and better-designed studies utilising novel imaging techniques are needed to accurately measure RBF and hemodynamic.

CAN and renal biopsy

The sole study to date investigating the relationship between CAN and DKD through renal biopsy was conducted by Wheelock et al. (370). They conducted a cross-sectional sub-study involving kidney biopsies of 63 patients with T2DM as part of a 6-year clinical trial assessing the reno-protective effects of losartan. Findings revealed that patients with more advanced renal structural lesions, characterised by greater GBM width, higher cortical interstitial fractional volume, a higher proportion of globally sclerotic glomeruli, and lower glomerular filtration surface density and total filtration surface per glomerulus, exhibited more severe indices of CAN (lower E/I ratio and lower indices of HRV). While causation was not established, the study indicated an association between DKD histopathology and CAN, suggesting the necessity for follow-up renal biopsies to validate this hypothesis.

4.5 Summary

The comprehensive review of 27 studies spanning three decades underscores the significant impact of CAN on both the incidence and progression of DKD in individuals with T1 and T2DM. These studies consistently demonstrate that individuals with CAN face heightened risks of DKD, characterised by declining eGFR and increasing UACR. Mechanisms proposed to elucidate this relationship include sympathetic overactivity-induced renal hemodynamic imbalance (347,358,368,377,383), lack of nocturnal blood pressure dipping leading to increased glomerular pressure and injury (355,357,360,380,382), and elevated oxidative stress and proinflammatory cytokine levels associated with CAN (384) leading to DKD progression (378,386).

Moreover, the relative dominance of sympathetic activity due to impaired parasympathetic function may contribute to systolic hypertension, resting tachycardia, and increased cardiac output, further exacerbating GBM injury and albumin filtration. Persistent systemic hypertension, whether due to inadequate antihypertensive therapy or abnormal physiological responses, can perpetuate end-organ damage and fibrosis within the kidneys, hastening DKD progression (358).

Despite variations in diagnostic approaches, existing evidence points to a significant role of CAN in DKD progression. The underlying mechanisms may serve as novel targets for future drug development. Early detection and management of CAN could aid in identifying high-risk DKD patients and complement conventional medical therapies. To address knowledge gaps, future research should focus on evaluating and comparing renal hemodynamic, with advancements in imaging technologies offering promising avenues for analysing renal perfusion and structural abnormalities in individuals with or without CAN.

Chapter 5

Cardiac autonomic neuropathy severity and its impact on renal decline in T1DM: A 15-year follow up study

This chapter examines the association between CAN, as diagnosed by the gold-standard cardiovascular autonomic reflex tests (CARTs), and DKD, classified according to the KDIGO prognostic risk categories. This analysis is based on a 15-year longitudinal follow-up study.

Abstract

Aim

We investigated the relationship between CAN, diagnosed by gold standard CARTs, and DKD categorised by KDIGO prognostic risk classification over 15-years follow-up period to assess the impact of CAN severity on DKD progression.

Methods

Data from 87 participants with T1DM and $\text{eGFR} > 30\text{ml/min/1.73m}^2$ were analysed. Participants underwent assessment for CAN using CARTs based on O'Brien's criteria. CAN diagnosis required two or more abnormal CARTs out of five. Stratification of participants into KDIGO CKD progression prognostic risk was done by using eGFR (G1-G3) and UACR (A1-A3) stages.

Results

Baseline renal function data revealed that most participants (88.5%) were categorised as KDIGO low risk, followed by (8%) in the moderate-risk group, and (3.5%) in the high-risk group for DKD progression. Higher risk category correlated with increased severity of CAN ($r=0.38$, $p<0.001$) and significant increase in UACR ($p<0.001$) compared to lower risk group over 15 years. Participants with early and confirmed CAN at baseline visit exhibited a mean eGFR decline of $3.1(7.3)$ and $14.8(21.6)$ ml/min/1.73m^2 respectively, compared to $3.3(7.4)$ ml/min/1.73m^2 in those without CAN ($p=0.004$). Meanwhile, mean increases in UACR were

0.4(0.9), 11.3(30.4) and 4(8.9) mg/mmol respectively for no CAN, early CAN and confirmed CAN respectively ($p=0.032$).

Conclusion

Increased severity of CAN is associated with higher KDIGO CKD risk and is an independent risk factor for renal function decline in DKD by our 15 years follow up study data.

5.1 Introduction

DKD is the leading cause of ESKD (392) with no effective means to prevent or cure it (392). The current treatments focus improving glycaemic control, blood pressure, lifestyle modification and using reno protective agents such as ACEi/ARB and more recently SGLT2i (34,393), GLP-1RA (394) and mineralocorticoid receptor antagonists (MRAs) to slow down the progression of DKD in T2DM. However, apart from RAAS inhibition, no new therapies have emerged for T1DM.

CAN is often associated with DKD, sharing common risk factors and mechanisms (355,358,361,368,379). Impairment of renal autonomic function is also implicated in the progression of DKD (347,358,368,377,395). In the early stages of CAN, imbalance in sympathetic and parasympathetic renal innervation may increase intraglomerular pressure resulting in increased sodium and albumin excretion. As CAN progresses, increased RAAS activation further exacerbates glomerular injury and accelerate DKD progression (368,395).

Few prospective studies (355,358,361,368) in T1DM have examined the association between CAN and DKD with differences in study population, age ranges, sample sizes, and methods to assess autonomic neuropathy, limiting overall generalisability of findings. One notable exception is the study by Bjerre-Christensen et al (372) which included the largest cohort of patients with T1DM ($n=329$) with autonomic neuropathy assessed using internationally recognised indices over the longest follow-up period (mean 6.1 years). They found that sympathetic dysfunction was associated with increased albuminuria suggesting a potential marker for DKD progression. However, a major limitation of this study was the

non-random selection of participants with controls having longstanding normoalbuminuria and cases having established DKD with significant albuminuria, introducing a selection bias that may have carried over throughout the follow up period.

This cohort study aims to explore the relationship between CAN severity and progression of DKD in an unselected population with T1DM. The hypothesis is that greater severity of CAN is linked to an accelerated decline in renal function.

5.2 Materials and methods

A retrospective analysis of a prospectively maintained database of 120 unselected participants with T1DM enrolled between 2007 and 2010 at the Royal Hallamshire Hospital, Sheffield, UK, was conducted. Participants were aged 18 – 75 years with eGFR > 30 ml/min/1.73m² (KDIGO G1-G3) and UACR < 30 mg/mmol (A1 or A2) at baseline. At follow-up in 2023-2024, 110 were alive (see CONSORT diagram Figure 5.1). After excluding those with newly diagnosed non-diabetic kidney disease or significant medical comorbidities (e.g., cancer, vasculitis, severe heart failure), 87 participants were included in the analysis. Demographic and clinical data were initially collected at baseline and updated information were collected from hospital, primary healthcare registries and local medical records. All participants provided written informed consent and the study which had prior ethics approval.

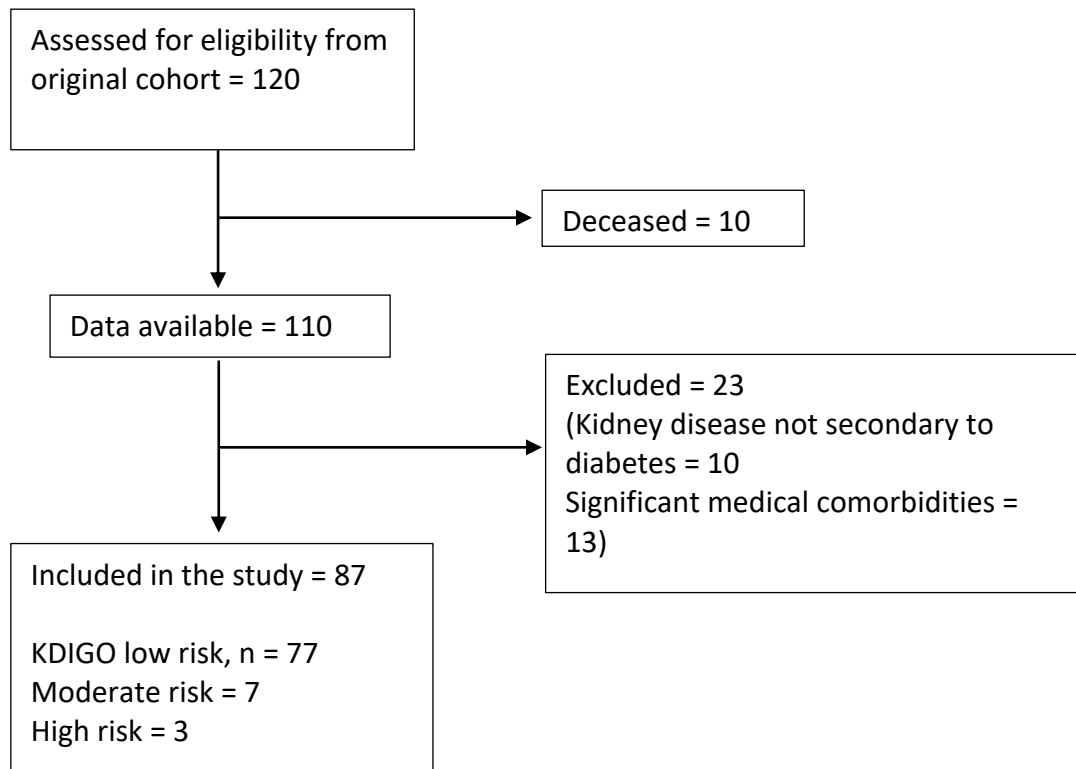


Figure 5.1: CONSORT diagram of participant data collection

5.2.1 Baseline assessments

Cardiac Autonomic Neuropathy (CAN)

At baseline visit, autonomic neuropathy was assessed using CARTs according to the O’Brien’s protocol (348). Participants were instructed to rest lying down for 5 minutes in a quiet room at a controlled temperature (18°C–23°C) before the examination was performed. All participants were also requested to avoid caffeinated drinks, nicotine, or alcohol 3 hours prior to testing.

The standardised CARTs included assessment of; heart rate response to deep breathing (E/I Ratio), Valsalva manoeuvre, lying to standing test (30:15 ratio and blood pressure response). Participants were divided into three groups (348)(Table 5.1).

1. No CAN: All tests normal
2. Early CAN: 1 abnormal test
3. Established CAN: 2 or more abnormal tests

1. Heart Rate Response to Deep Breathing (E/I Ratio):

Procedure: The participant breathes deeply at a rate of six breaths per minute (5 seconds in, 5 seconds out) while heart rate is monitored.

Assessment: The E/I ratio is calculated by dividing the longest R-R interval (heart rate during expiration) by the shortest R-R interval (heart rate during inspiration). A lower E/I ratio indicates autonomic dysfunction.

2. Heart Rate Response to the Valsalva Manoeuvre:

Procedure: The participant forcefully exhales into a mouthpiece while maintaining a closed airway (like trying to blow up a balloon with a blocked nose) for 15 seconds, then breathes normally.

Assessment: The Valsalva ratio is determined by dividing the longest R-R interval shortly after the manoeuvre by the shortest R-R interval during the manoeuvre. A reduced Valsalva ratio suggests autonomic impairment.

3. Heart Rate Response to Standing (30:15 Ratio):

Procedure: The participant lies down and then stands up quickly while their heart rate is recorded.

Assessment: The 30:15 ratio is the ratio of the R-R interval around the 30th beat after standing to the R-R interval around the 15th beat. A lower ratio may indicate CAN.

4. Blood Pressure Response to Standing:

Procedure: Blood pressure is measured while the participant is lying down and then again after standing for 1 and 3 minutes.

Assessment: A significant drop in SBP upon standing (orthostatic hypotension) is indicative of autonomic dysfunction.

5. Blood Pressure Response to Sustained Handgrip:

Procedure: The participant maintains a handgrip at 30% of their maximum strength for 5 minutes.

Assessment: The change in DBP from baseline to the end of the handgrip period is measured. A smaller increase suggests autonomic impairment.

Table 5.1: Evaluation of Cardiovascular reflex tests by O'Brien protocol

| Autonomic function test | Measured parameter | Normal value (score 0) | Limit value (score 1) | Abnormal value (score 2) |
|---|----------------------|------------------------|-----------------------|--------------------------|
| <u>Parasympathetic function analysis</u> Heart Rate Response to Deep Breathing | E/I ratio | ≥ 1.21 | 1.10-1.20 | < 1.10 |
| Heart Rate Response to the Valsalva Manoeuvre | Valsalva ratio | ≥ 1.21 | 1.11-1.20 | < 1.10 |
| Heart Rate Response to Standing (30:15 Ratio): | 30:15 ratio | ≥ 1.04 | 1.01-1.03 | < 1.00 |
| <u>Sympathetic function analysis</u> Blood Pressure Response to Standing | SBP drop (mmHg) | < 10 | 10-20 | > 20 |
| Blood Pressure Response to Sustained Handgrip | DBP elevation (mmHg) | ≥ 16 | 11-15 | < 10 |

Diabetic kidney disease

Participants were stratified at baseline into low, moderate and high-risk prognostic groups according to the 2024 Kidney Disease: Improving Global Outcomes (KDIGO) 2024 guideline for CKD (396) by using eGFR and UACR (Figure 5.2). Due to the limited numbers of participants, the 'high risk' and 'very high risk' categories were combined into a single 'high risk' group. The eGFR was calculated by chronic kidney disease epidemiology collaboration

(CKD-EPI) equation (397) and UACR levels were measured from early morning urine sample (398).

| KDIGO: Prognosis of CKD by GFR and albuminuria categories | | | | Persistent albuminuria categories | | |
|---|-----|----------------------------------|-------|--|---|--|
| | | | | Description and range | | |
| | | | | A1 | A2 | A3 |
| | | | | Normal to mildly increased <30 mg/g <3 mg/mmol | Moderately increased 30–300 mg/g 3–30 mg/mmol | Severely increased >300 mg/g >30 mg/mmol |
| GFR categories (ml/min/1.73 m ²) Description and range | G1 | Normal or high | ≥90 | | | |
| | G2 | Mildly decreased | 60–89 | | | |
| | G3a | Mildly to moderately decreased | 45–59 | | | |
| | G3b | Moderately to severely decreased | 30–44 | | | |
| | G4 | Severely decreased | 15–29 | | | |
| | G5 | Kidney failure | <15 | | | |

Green: low risk (if no other markers of kidney disease, no CKD); Yellow: moderately increased risk; Orange: high risk; Red: very high risk. GFR, glomerular filtration rate.

Figure 5.2: KDIGO CKD prognostic risk classification (399)

5.2.2 Follow up assessments

Healthcare registries containing outcomes of the DM annual screening programme were used to collect endpoint data. Over the 15 years follow-up period, eGFR and UACR values were recorded at four-year intervals at 2007-2010, 2011-2014, 2015-2018 and 2019-2023. A composite kidney outcome was assessed at each time point including development of macroalbuminuria (A3), change in KDIGO risk category, doubling of serum creatinine or at least 30% decline in eGFR, initiation of kidney replacement therapy, or death due to kidney disease (400).

5.2.3 Statistical analysis

Clinical and demographic data were summarised as means with standard deviations (SD) for continuous variables or as counts with percentages (%) for categorical variables. Data distribution was assessed using histograms. Continuous variables were compared using either Student's t-test or the Mann-Whitney U test, depending on normality. Pearson's correlation was used to analyse correlation between continuous variables.

CAN stages and KDIGO risk groups were treated as categorical variables. Chi-square tests assessed the association between CAN stages and KDIGO risk groups and examined differences in categorical variables across CAN stages at baseline. Analysis of variance (ANOVA) was used to compare the mean values of continuous variables across CAN stages and KDIGO risk groups, with multiple linear regression adjusting for potential confounders (Model 1-3). The decline in eGFR and the increase in UACR were compared between CAN and no CAN groups, adjusting for covariates.

Covariates included: age, sex, diabetes duration, HbA1c, SBP, and ACEi/ARB use.

Model 1: Unadjusted.

Model 2: Adjusted for age and sex.

Model 3: Adjusted for age, sex, diabetes duration, HbA1C, ACEi/ARB use, and SBP.

Similar analyses were conducted to assess participants with normal eGFR ($> 90\text{ml/min/1.73m}^2$, G1) and normoalbuminuria ($\text{UACR} < 3\text{mg/mmol}$, A1). The goal was to determine whether the presence of CA significantly impacts this subset of participants who had normal renal function at baseline. Given their optimal renal function and absence of albuminuria, the aim was to explore whether CAN could be associated with a similar detrimental effect on renal outcomes as seen in participants with poorer baseline function.

Time to event for the renal composite outcome was performed using Kaplan-Meier analysis, with censoring at the last follow-up for those free from the outcome. Cox proportional hazards model assessed the impact of covariates on the risk of developing the renal

composite outcome. Binary logistic regression analysis was used to evaluate the survival status at 15 years post-baseline visit. The dependent variable was survival status (free from or composite renal outcome present or absent), with independent variables including CAN status and baseline characteristics (diabetes duration, HbA1c, SBP, and ACEi/ARB use). Backward conditional variable selection ($p > 0.05$) method was used to create a parsimonious final model with odds ratios (ORs) and 95% confidence intervals was calculated, with $OR > 1$ indicating higher odds of survival. All analyses were performed using SPSS (version 29.0) and significance set at $p < 0.05$.

5.3 Results

5.3.1 Baseline demographics

Complete baseline visits and follow up data were available for 87 participants (Table 2). At baseline, 49.4% ($n=43$) were men, with a mean (SD) age 38.1(10.6) years and diabetes duration of 19.8(11.5) years. Mean eGFR 88.4(8.7) ml/min/1.73m² [87.3% G1, 9.1% G2, 3.4% G3] and mean UACR was 1.8(4.3) mg/mmol [90.8% A1, 8% A2, 1.1% A3]. Additionally, 19.5% of participants had hypertension. Participants with established CAN were older (ANOVA $p=0.005$) and had a longer duration of diabetes (ANOVA $p=0.06$). Baseline eGFR was significantly lower in established CAN (ANOVA $p<0.001$). Other parameters, including HbA1C, systolic and diastolic blood pressure, cholesterol, triglycerides, and medication use, showed no statistically significant differences among the groups. While the presence of retinopathy prevalence and history of hypertension were higher in the established CAN group, though these differences were not statistically significant.

Table 5.2: Baseline demographic data of participants with different CAN stages

| | Overall data (n=87) | Normal/ No CAN (N=51) | Early CAN (N=26) | Established CAN (N=10) | P value |
|---|--------------------------------|----------------------------------|-----------------------------|-----------------------------------|----------------|
| Age at baseline (years) | 38.1(10.6) | 38.8(8.1) | 33.6(12.8) | 46(11) | 0.005 |
| Men, n (%) | 43/87(49.4%) | 27/51(52.9%) | 12/26(46.1%) | 4/10(40%) | 0.70 |
| Diabetes duration (years) | 19.8(11.5) | 18.1(9.9) | 19.9(13.5) | 27.6(11.4) | 0.06 |
| eGFR at baseline (ml/min/1.73m ²) | 88.4(8.7) | 90.2(2.7) | 88.6(8.8) | 78.8(18.7) | <0.001 |
| eGFR decline (ml/min/1.73m ²) | 4.6(10.5) | 3.3(7.4) | 3.1(7.3) | 14.8(21.6) | 0.004 |
| eGFR at 15 years (ml/min/1.73m ²) | 84 (14.4) | 87.2 (7.8) | 85.4 (15.1) | 64.8 (22.8) | < 0.001 |
| UACR at baseline (mg/mmol) | 1.8(4.3) | 1.4(4.6) | 1.5(2) | 4.9(6.3) | 0.06 |
| UACR increase (mg/mmol) | 4.1(17.4) | 0.4(0.9) | 11.3(30.4) | 4(8.9) | 0.032 |
| UACR at 15 years (mg/mmol) | 5.9 (19.6) | 1.4 (3.2) | 15.3 (35.9) | 8.6 (11.4) | 0.020 |
| HbA1C (mmol/mol) | 69.69(14.7) | 67.9(14.5) | 70.7(12.5) | 77(19.7) | 0.2 |
| Systolic blood pressure (mmHg) | 125.9(14.9) | 122.8(12.5) | 129.1(16.2) | 133.4(19.2) | 0.05 |
| Diastolic blood pressure (mmHg) | 73.68(7.7) | 73(7.2) | 75.5(9.2) | 72(5.7) | 0.32 |
| Total cholesterol (mmol/L) | 4.4(0.86) | 4.4(0.87) | 4.5(0.81) | 4.3(0.99) | 0.77 |
| Triglyceride (mmol/L) | 1.2(0.63) | 1.17(0.63) | 1.29(0.69) | 1.32(0.51) | 0.70 |

| | | | | | |
|-----------------------------|--------------|---------------|---------------|------------|--------|
| Use of ACEi/ARB (%) | 31/87(35.6%) | 15/51 (29.4%) | 10/26 (38.5%) | 6/10 (60%) | *0.89 |
| Use of beta blocker (%) | 5/82(5.7%) | 1/51(2%) | 3/26(11.5%) | 1/10(10%) | *0.193 |
| Use of statin (%) | 64/87(73.6%) | 39/51(76.4%) | 16/26(61.5%) | 9/10(90%) | *0.17 |
| Diabetic retinopathy (%) | 66/87(75.9%) | 36/51 (70.5%) | 21/26 (80.7%) | 9/10 (90%) | *0.67 |
| History of hypertension (%) | 17/87(19.5%) | 7/51 (13.7%) | 5/26 (19.2%) | 5/10 (50%) | *0.15 |

eGFR, estimated glomerular filtration rate; UACR, urinary albumin creatinine ratio; HbA1C, glycosylated haemoglobin A1C; ACEi, angiotensin converting enzyme inhibitor; ARB, angiotensin receptor blocker; CAN, cardiac autonomic neuropathy; * chi-square test

5.3.2 15-year follow up data in different CAN stages

In the 15-year follow-up data, eGFR values were lowest in the established CAN group [64.8 (22.8) ml/min/1.73m²] compared to the normal [87.2 (7.8) ml/min/1.73m²] and early CAN [85.4 (15.1) ml/min/1.73m², ANOVA $p < 0.001$). A more pronounced decline in eGFR was associated with increased severity of CAN ($p = 0.004$). A similar trend was observed in the progression of UACR ($p = 0.032$), with participants in the early and confirmed CAN groups exhibiting higher baseline and follow-up UACR values (Table 5.2).

5.3.3 CAN and DKD progression

The results of multiple regression analysis examining the relationship between presence of CAN and decline in eGFR decline or increase in UACR increase across different adjusted models are presented table 5.3. CAN is significantly associated with an increase in UACR in both unadjusted (Model 1, $p=0.02$), and age- and sex-adjusted models (Model 2, $p=0.01$) as well as after adjusting for a range of potential confounders (Model 3, $p=0.03$). However, the association with eGFR decline remains insignificant across all 3 models.

Table 5.3: Multiple regression analysis of cardiac autonomic neuropathy (CAN) and its association with estimated glomerular filtration (eGFR) decline and urinary albumin creatinine ratio (UACR) increase across adjusted models

| | Covariates | Outcomes | p value | 95% CI |
|---------|--|---------------|---------|----------|
| Model 1 | Unadjusted | eGFR decline | 0.19 | -1.5:7.6 |
| | | UACR increase | 0.02 | 1.6:16.2 |
| Model 2 | Adjusted for age and sex | eGFR decline | 0.07 | -0.4:8.0 |
| | | UACR increase | 0.01 | 1.8:16.2 |
| Model 3 | Adjusted for age, sex, diabetes duration, HbA1C, ACEi/ARB, and SBP | eGFR decline | 0.43 | -2.5:5.9 |
| | | UACR increase | 0.03 | 1.2:17.6 |

HbA1C, glycosylated haemoglobin A1C; ACEi, angiotensin converting enzyme inhibitor; ARB,

5.3.4 CAN and renal function decline in G1A1 cohort

A more detailed analysis was conducted to assess the extent of decline in eGFR and increase in UACR among participants who initially had an eGFR ≥ 90 ml/min/1.73m² and normoalbuminuria (classified as G1A1). The analysis showed that the CAN group had a mean UACR increase of 7.0 (20.0) mg/mmol, compared to 0.4 (0.9) mg/mmol in the No CAN group in unadjusted model (Model 1, p=0.03, 95%CI 0.7:12.4) (Table 5.4). However, this was no longer significant after adjusting for age and sex (Model 2, p=0.09, 95% CI -0.8:12.5). The correlation regained significance when additional factors such as DM duration, HbA1c, SBP, and use of ACEi or ARB were included into the model (Model 3, p=0.026, 95% CI 1.0:15.5). In contrast, for eGFR, no significant correlation for eGFR was observed across all three models, and the extent of eGFR decline remained comparable between the groups.

Table 5.4: Comparison of estimated glomerular filtration rate (eGFR, ml/min/1.73m²) and urinary albumin creatinine ratio (UACR, mg/mmol) changes in cardiac autonomic neuropathy (CAN) and no CAN in participants with normal eGFR (≥ 90 ml/min/1.73m², G1) and normoalbuminuria (UACR < 3mg/mmol, A1) using multiple regression analysis (p-value and 95% confidence intervals)

| | No CAN (n=46) | CAN (n=23) | Model 1 | Model 2 | Model 3 |
|------------------|--------------------------|-----------------------|-----------------|------------------|-----------------|
| eGFR decline | 3.3 (7.7) | 3.2 (12.2) | 0.96 (-4.9:4.7) | 0.45 (-3.3:7.4) | 0.64 (-6.3:3.9) |
| UACR increase | 0.4 (0.9) | 7.0 (20.0) | 0.03 (0.7:12.4) | 0.09 (-0.8:12.5) | 0.03 (1.0:15.5) |

5.3.5 KDIGO risk classification and CAN

The distribution of KDIGO risk categories among patients with varying stages of CAN shows a clear concentration of low-risk individuals in the No CAN group, with a progressive shift toward higher risk categories as the CAN severity increases ($r=0.38$, $p<0.001$) (Figure 5.3). Notably, the confirmed CAN group has a higher proportion of moderate-risk individuals compared to the other groups, indicating a correlation between increased CAN severity and greater risk classification.

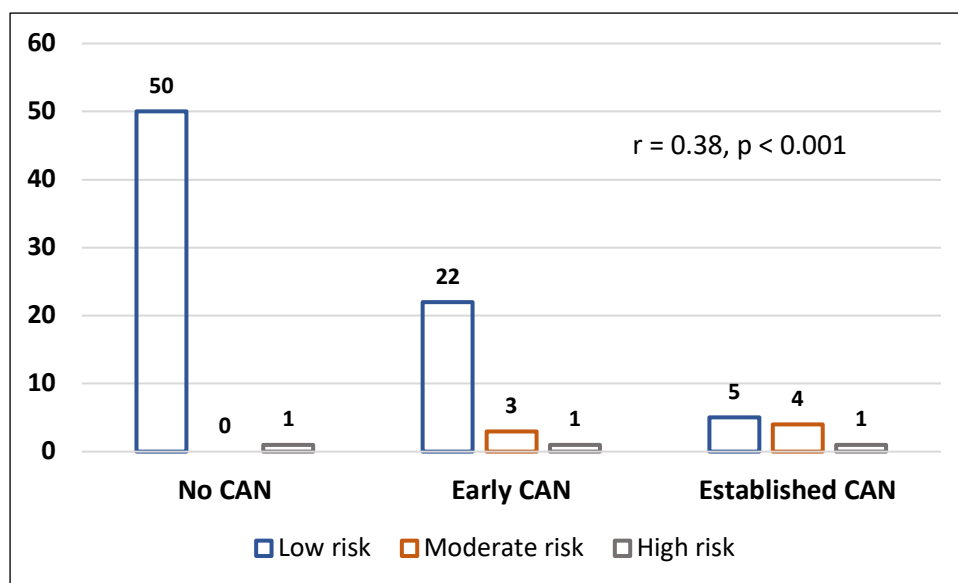


Figure 5.3: The numbers of participants with different KDIGO risk classification in each stage of CAN

In the KDIGO risk assessment, a high proportion of participants were classified as low prognostic risk (88.5%), followed by moderate risk (8%) and high risk (3.5%) for CKD progression (Table 5.5). The analysis showed no significant difference in eGFR decline across KDIGO risk groups ($p=0.30$). However, UACR increased significantly in the high/very high-risk group ($p<0.001$).

Table 5.5: Summary of follow up estimated glomerular filtration rate (eGFR, ml/min/1.73m²) and urinary albumin creatinine ratio (UACR, mg/mmol) changes in different KDIGO risk groups

| | Low Risk (N=77) | Moderate Risk (N=7) | High/Very High Risk (N=3) | P value |
|---|--------------------|------------------------|---------------------------------|------------|
| eGFR decline (ml/min/1.73m ²) | 4.1(9.6) | 10.2(17.8) | 6.7(11.5) | 0.30 |
| UACR increase (mg/mmol) | 2.8(11.5) | 1.8(3.9) | 42.9(74.3) | <0.001 |

5.3.6 Renal end point assessment and CAN

A significantly greater proportion of participants with CAN [11(30.6%)] who reached the composite renal outcome at 15 years compared to No-CAN [6(11.8%); $p=0.03$, Chi-square 4.7]. After conducting the backward conditional variable selection, CAN status emerged as the sole only predictor in the final model [B(SE) 1.26(0.57); Wald Chi-square 4.86; $p=0.03$]. Compared to No-CAN, participants with CAN had a 3.5-fold increased risk of developing the composite renal outcome after 15 years [OR (95%CI): 3.5(1.1:10.7); $p=0.03$].

5.4 Discussion

In this unselected cohort of 87 participants with T1DM, the prevalence of CAN (41%) was consistent with the reported literature (17-66% in T1DM) (134). Participants with established CAN were older and had the longest duration of DM, along with significantly lower eGFR compared to those in the No CAN and Early CAN groups. However, no significant differences were observed in other clinical parameters, including HbA1c, SBP and DBP, retinopathy prevalence, hypertension prevalence, cholesterol levels, and medication use.

In the 15-year follow-up data, CAN severity was associated with a significant decline in eGFR and an increase in UACR. The relationship between CAN and UACR remained statistically significant even after adjusting for relevant covariates. However, no significant association with eGFR decline was observed in either adjusted or unadjusted models. Further analysis of

participants with G1A1 showed that CAN did not significantly affect eGFR decline. However, the association with changes in UACR remained significant after adjusting for all relevant covariates. These findings align with previous studies linking CAN to higher levels of albuminuria (357,362,365,372,388).

This study found that the presence of CAN was associated with a higher KDIGO CKD risk category at baseline and significantly predicted the development of the composite renal outcomes, including macroalbuminuria development, change in KDIGO risk category, doubling of serum creatinine or at least 30% decline in eGFR, kidney replacement therapy, or death due to kidney disease. Individuals with greater severity of CAN exhibited a higher proportion in elevated KDIGO CKD risk categories. However, this association may be coincidental, as diabetes-related complications, such as neuropathy and nephropathy, often co-occur due to shared microvascular damage mechanisms.

Proposed mechanisms for effect of CAN on DKD include early parasympathetic dysfunction leading to relative sympathetic dominance, causing systolic hypertension, resting tachycardia, and increased cardiac output, which promote GBM injury with excessive filtration of sodium and albumin (347,358,363,376,381). With parasympathetic dysfunction leading to relative sympathetic overactivity leads to a lack of nocturnal blood pressure drop, resulting in higher intraglomerular pressure at night. This leads to glomerular injury and increased sodium and albumin excretion (355,357,360,380,382). Another mechanism is activation of RAAS. Early compensatory increases in sympathetic tone in response to subclinical parasympathetic denervation activate the intrarenal RAAS, causing renal dysfunction through increased GBM thickness and mesangial matrix expansion due to renal vasoconstriction and ischemia (368,383).

Presence of increased inflammation and oxidative stress due to autonomic impairment was also mentioned in the literature. Sympathetic nervous system impairment affects the regulation of inflammatory cytokines and chemokines (379,384), which are also described as potential therapeutic targets and biomarkers for DKD (379,385). Additionally, reduced renal function is associated with decreased antioxidant scavenging enzymes and increased production of reactive oxygen species, leading to oxidative stress and DKD progression

(378,386). Effect of sympathetic neuropathy in the late stage of CAN was also demonstrated. In the later stages of CAN, sympathetic neuropathy results in diminished renal sodium excretion, reduced renal blood flow, and decreased eGFR due to renal vasoconstriction (347,377).

The lack of nocturnal drop in both SBP and DBP in CAN group was documented in various studies (357,360,380,387,389,390) over the years, mostly by the use of ambulatory 24-hour BP monitoring. Other neuropathic mechanisms associated with renal vascular haemodynamic have limited evidence. Future studies utilising advanced imaging (e.g. MRI) biomarkers are needed to better assess renal haemodynamic (308).

Based on our findings, we hypothesise that the impact of CAN on DKD may depend on the timing of disease onset. Specifically, the development of CAN prior to DKD appears to have minimal influence on the subsequent rate of renal decline. Conversely, the presence of CAN in patients with more advanced DKD may accelerate the progression of kidney disease. However, due to the relatively small number of patients with advanced DKD in our study, we were unable to test this hypothesis. Further investigation into the temporal and causal relationships between CAN and DKD could provide valuable insights into their interactions and inform potential therapeutic interventions.

The substantial net benefits associated with early identification and intervention of risk factors in individuals already diagnosed with DM and those at high risk of developing DM and cardiovascular events was described in the ADDITION study (401). The study demonstrated that the optimisation of risk factors within the DM population could significantly contribute to a notable decrease in all-cause mortality, underscoring the importance of comprehensive risk management in mitigating the long-term complications associated with DM. The same principle can be applied to the association between CAN and DKD. Recognising CAN as a potential risk factor for DKD suggests that early screening and diagnosis of CAN in patients with DM may offer significant advantages in the proactive management of DKD risk. This approach could enable targeted interventions aimed at mitigating the progression of renal dysfunction, ultimately improving clinical outcomes through more timely and effective risk management strategies.

Strengths of our study include the recruitment of participants with an eGFR above 30 ml/min/1.73m², with the majority demonstrating eGFR levels exceeding 90 ml/min/1.73m² and normoalbuminuria, ensuring a cohort with relatively stable renal function, a comprehensive assessment of renal function decline over a 15-year follow-up period, facilitating a more robust and reliable comparative analysis of long-term renal outcomes. Longitudinal data collection at four-year intervals allowed for robust analyses of renal endpoints, and the low dropout rate enhanced the validity of our findings. Crucially, all participants underwent gold-standard, standardised assessments for CAN, ensuring consistent assessment of autonomic function.

Limitations include a single-centre cohort study, the limited number of participants with lower eGFR or higher UACR precluded a comparison of the impact of CAN on moderate and high-risk groups. Finally, blood data were collected at four-year intervals over a 15-year follow-up period, annual data would provide a more comprehensive assessment of the exact point of deterioration in eGFR or UACR.

Despite its limitations, our study highlights the possible importance of CAN as a novel risk factor for accelerated renal decline. To our knowledge, this is one of the first studies to examine the relationship between CAN and KDIGO prognostic risk in DKD. We demonstrated that increased severity of CAN shows statistically significant association with higher KDIGO risk and CAN acts as an independent risk factor for decline in renal function in DKD. These findings provide mechanistic insight into the possible haemodynamic changes associated with autonomic neuropathy on progression of DKD. This could potentially lead to novel therapeutic strategies to prevent DKD incidence and progression.

5.5 Conclusion

This study demonstrated that CAN is significantly associated with a higher KDIGO CKD risk category and contributes to the progression of DKD in individuals with T1DM. The findings support the study's aims by showing that greater CAN severity correlates with increased

UACR and renal dysfunction, even after adjusting for relevant covariates. Although eGFR decline was not consistently significant across models, the association between CAN and UACR highlights its potential as an independent risk factor for DKD progression, describing the importance of early CAN screening for targeted interventions to prevent renal decline.

Chapter 6

Kidney shape: a potential novel magnetic resonance imaging biomarker for diabetic kidney disease

In this chapter, the three-dimensional shape of the kidneys measured with MRI were evaluated for the possibility of using these parameters as biomarkers for DKD progression by correlating these imaging-derived metrics with kidney function parameters. The aim is to explore the utility of kidney shape factors in MRI and reference values were derived that can act as a point of comparison for future studies.

Abstract

Background/ Aim

The progression of DKD entails significant morphological alterations within the renal structures, notably characterised by kidney hypertrophy and hyperfiltration in early stage of DKD and reductions in both length and cortical thickness during the advanced stages of the disease. Nevertheless, the quantitative assessment of the relationship between these morphological changes and GFR remains insufficiently explored. In this study, we aimed to interpret this relationship by evaluating the three-dimensional size and shape of the kidneys measured with MRI as biomarkers for DKD progression and correlating these imaging-derived metrics with kidney function parameters.

Methods

Data were extracted for the first 134 participants of three sites with the same scanner model in the ongoing iBEAt study, recruiting participants with T2DM with eGFR >30 ml/min/1.73 m². MRI data was acquired on 3T Siemens MAGNETOM Prisma. Shape factors were derived from DIXON data acquired in a single breath hold, 7 minutes after injection of a quarter-dose of a macrocyclic agent. For MRI post-processing, 268 individual kidneys were segmented semi-automatically in 3D with in-house software, using region growing on masks derived from DIXON fat and water images. Following pairwise correlation analysis, the

correlation matrix was clustered to identify groups of biomarkers correlating with volume and most likely to inform on DKD heterogeneity. All analyses were performed in SPSS (version 29.0) and correlations were considered significant if $p < 0.01$.

Results

All shape factors correlate with volume except 2 factors (compactness, and extent) and they have the weakest correlation with volume ($r=0.033$ and -0.017). All features, with the exception of compactness and short axis length, exhibited a statistically significant correlation with eGFR. Conversely, only convex hull volume, surface area, and short axis length demonstrated a significant correlation with UACR.

Conclusion

Dimensionless kidney shape factors measuring compactness and extent are independent of kidney volume and may indicate disease progression and increased risk of future renal decline. Case studies suggest that a reduction in compactness indicates an irregular kidney shape potentially by ageing, cortical thinning, and compression by surrounding structures. This study is the first to explore the utility of kidney shape factors in MRI and has derived reference values that can act as a point of comparison for future studies.

6.1 Introduction

The progression of DKD entails significant morphological alterations within the renal structures, notably characterised by kidney hypertrophy and hyperfiltration in early DKD stage (314) and reductions in both length and cortical thickness during advanced stages. Nevertheless, quantitative assessment of the relationship between these morphological changes and GFR remains insufficiently explored.

MRI has been suggested as a potential source of biomarkers for managing CKD (311–313), such as recognition by the Food and Drug Administration (FDA) and the European Medicines Agency (EMA) of total kidney volume as a prognostic biomarker for Autosomal Dominant Polycystic Kidney Disease (ADPKD) (308,402,403). Recent advancements in MRI techniques

have enabled sensitive assessments of structural and functional tissue characteristics. These characteristics can be measured for left and right kidneys, as well as for cortex and medulla, thereby enabling the mapping of functional and structural heterogeneity within these regions.

Specifically, MRI-based assessments of kidney enlargement have been associated with poorer outcomes in DKD, despite the paradoxically higher GFR observed in larger kidneys (314,315,404). However, these studies have been limited to assessment of renal volume and do not explore changes in shape or architecture. Moreover, advancements in automated segmentation and measurement of structural tissue characteristics allows for the rapid acquisition/analysis of detailed anatomical information. Unlike routine biomarkers which do not reflect the clinical and histological heterogeneity of DKD, advanced MRI has the potential to be a more sensitive diagnostic biomarker of DKD.

The aim of this study was to investigate the relationship between novel MRI derived three-dimensional kidney shape factors with routine clinical markers of DKD (eGFR and UACR). We also want to determine whether renal imaging biomarkers provide additional information on DKD heterogeneity in comparison to routine blood and urine markers used in clinical practice. The hypothesis is that renal imaging-based assessment of structural characteristics of DKD can detect signatures of disease progression that are not related to current routine biomarkers.

6.2 Materials and methods

6.2.1 Participants recruitment

This study is part of the iBEAt study, which is embedded within the larger BEAt-DKD project (Biomarker Enterprise to Attack Diabetic Kidney Disease). Further details on the study protocols for Beat-DKD and iBEAT studies have been published previously (308). In brief, the project involves six centres (Bari, Bordeaux, Exeter, Leeds, Sheffield, and Turku), each recruited participants with T1 and T2DM aged between 18-80 years. Exclusion criteria includes; eGFR less than 30ml/min/1.73m², those receiving renal replacement therapy (haemodialysis, peritoneal dialysis, renal transplantation) or with ESKD under conservative

management, individuals with active renal disease, acute kidney injury, or obstructive uropathy (including hydronephrosis, significant renal cysts, single kidney, bladder, or prostate obstruction) affecting renal function, individuals with active cancer or active liver disease, and claustrophobia or contraindications for MRI.

Following the written informed consent at the screening visit, all participants attended a baseline study and underwent health assessments including medical history with demographic data, past medical history, family medical history, blood and urine tests, and renal MRI. The eGFR was calculated from serum creatinine using the CKD-EPI (Chronic Kidney Disease Epidemiology Collaboration) Creatinine Equation (2021) (397). The UACR was obtained from early morning urine sample collected by the participants before the visit (398).

The study had formal ethical approval and registered with ClinicalTrials.gov, identifier NCT03716401. The study receives funding from the Innovative Medicines Initiative 2 Joint Undertaking under grant agreement No. 115974. This Joint Undertaking receives support from the European Union's Horizon 2020 research and innovation programme, the Juvenile Diabetes Research Foundation (JDRF) and the European Federation of Pharmaceutical Industries and Association (EFPIA).

6.2.2 Magnetic resonance Image pre-processing and features extraction

Renal MR imaging

Renal MRI scans from three study sites (Leeds, Bari, and Exeter) with the same MRI scanner model, 3T Siemens MAGNETOM Prisma (Siemens Healthcare, Erlangen, Germany) were examined. Participants were scanned in the supine position with the body coil placed on the abdomen and the centre of the coil and the coronal-oblique slices were positioned over the kidneys over 1 hour 15 minutes. Renal MRI was acquired using an 18-channel phased array body coil combined with inbuilt spine coil for signal reception. Structural images were derived from DIXON data acquired in a single breath hold, 7 minutes after injection of a quarter-dose of a macrocyclic agent, with FOV 400 mm, 1.5 mm isotropic resolution, TR

4.01ms, TE 1.34/2.57 ms, FA 9 deg, 7/8 partial Fourier, 3D parallel imaging factor 6. Dotarem (Gd-DOTA) was injected intravenously with a dose of 0.05 ml/kg at a rate of 2 ml/s followed by 20 ml saline flush. The injection was given 20 seconds after MRI sequence acquisition started using an automatic power injector.

MRI post-processing

After excluding participants with incomplete MRI datasets or poor-quality imaging, 268 individual kidneys were segmented semi-automatically in 3D with in-house software, using region growing on masks derived from DIXON fat and water images. Initial segmentation process involved applying K-means (Km) clustering on the original Dixon MRI images, into different clusters, to derive a mask that differentiates fat from surrounding tissues. A region-growing algorithm was applied to further segment the tissue mask, followed by an erosion process on the mask, for more precise identification of the kidney. The resulting kidney mask was then manually edited to remove any extra-renal pixels or misclassified regions. All resulting masks, including the final kidney segmentation, were visually inspected and verified through independent analysis. The entire segmentation process, including the visual verification, was overseen and analysed by a nephrologist with experience in MRI imaging to ensure that the kidney mask was consistent with clinical expectations and renal morphology as seen on MRI scans.

Single-kidney volumes were extracted along with 15 shape factors for each kidney, using python package skimage. Altogether, we quantified 15 different morphological features from renal MRI datasets including volume, bounding box volume, convex hull volume, surface area, three measurements of inertia, short and long axis length, maximum depth, extent, solidity, and compactness (Details in appendix figure 1). The values of each feature for the right and left kidneys were analysed and reported individually, treating each kidney as a distinct entity rather than averaging the values between the two.

6.2.3 Statistical analysis

The demographic characteristics of participants were summarised as means and standard deviations (SD) for continuous variables, and as counts and percentages (%) for categorical variables. Kidney parameters, obtained from MRI dataset analyses, were presented in a table with their minimum, maximum, mean, median, and coefficient of variation (CoV) to evaluate variability relative to the mean. Summary parameters for all proposed shape metrics were extracted to serve as references for future research.

As these parameters were derived from volumetric assessments of kidneys, an initial correlation analysis was conducted to determine the nature of their association with kidney volume. This analysis aimed to identify whether any parameters exhibited significant correlations with kidney volume, as well as to detect those that did not correlate with kidney volume, potentially indicating distinctive characteristics or independent predictive value. The detailed examination of these correlations is performed to understand the relationship between kidney morphology and volume, and to identify outliers that may provide unique insights into kidney function and pathology. In this analysis, correlations among 15 parameters were assessed, resulting in 105 unique pairwise comparisons. To control the increased risk of Type I errors associated with multiple comparisons, the Bonferroni correction was employed. By dividing the standard significance threshold of 0.05 by the number of comparisons (105), the adjusted p-value threshold was set at 0.00048.

Consequently, a correlation was considered statistically significant only if the p-value was less than 0.00048, thereby ensuring that the overall likelihood of a false positive remained within acceptable limits. Following the pairwise correlation analysis, the correlation matrix was clustered to identify groups of biomarkers correlating with volume, which are most likely to provide insights into the heterogeneity of DKD. These correlations were visualised using a heat map with a dendrogram to highlight parameter clustering. Hypotheses on diagnostic utility of shapes were derived by closer inspection of case studies at extreme ends of the spectrum.

Given that kidney volume and length are influenced by body size, standardisation of renal volume was achieved by correlating it with body surface area, adjusting all renal volume measurements as per 1.73 m². To explore the factors affecting kidney volume, Pearson correlation was utilised to analyse the relationships between kidney volume (both unadjusted and adjusted for body surface area) and demographic data (continuous variables), while independent samples t-tests were employed for categorical variables. Additionally, the correlations among 15 kidney shape factors, eGFR, and UACR were examined using Pearson correlation to investigate the potential association of these parameters with routine clinical biomarkers.

Of the 15 parameters, further assessment using Pearson correlation with demographic data was conducted for two specific parameters, compactness, and extent, which demonstrated minimal or negative associations with kidney volume. Depending on the initial results, multiple regression analysis was performed to assess the association between shape factor and eGFR or UACR in unadjusted and adjusted models. Scatter plots were used to visualise the nature of the correlations between these two parameters with both unadjusted and body surface area-adjusted kidney volumes, as well as to illustrate the correlation between compactness and extent.

All analyses were performed in SPSS (version 29.0) and statistical significance is set at p value of < 0.01 for all analysis except for the correlation among 15 parameters which is set at p < 0.00048.

6.3 Results

6.3.1 Patient characteristics and features summary

Participants with incomplete clinical, anthropometric, or biological data, as well as those with unsuccessful MRI, poor-quality MRI images or lacking complete anatomical coverage (n=30), were excluded from the analysis. After exclusion, 134 participants were included for analysis (Table 6.1). The participants had a mean (SD) age of 70.13 (8.43) years, comprising

48 women (35.8%). The mean body mass index (BMI) was 30.03 (4.89) kg/m², the mean eGFR was 76.67 (13.6) ml/min/1.73 m² and the mean urinary albumin-to-creatinine ratio (UACR) was 4.3 (14.4) mg/mmol,

Table 6.1: Baseline characteristics / demographics of participant

| Characteristics | N = 134 |
|---|---------------|
| Age, mean (SD) years | 70.13 (8.43) |
| Women, n (%) | 48 (35.8%) |
| Mean body mass index (SD) kg/m ² | 30.03 (4.89) |
| Mean body surface area (SD) m ² | 1.98 (0.20) |
| Mean HbA1C (SD) mmol/mol | 55.5 (20.2) |
| Diabetic retinopathy, n (%) | 19 (14.2%) |
| Diabetic neuropathy, n (%) | 22 (16.4%) |
| History of coronary artery disease, IHD, n (%) | 17 (12.7%) |
| History of smoking (current or previous), n (%) | 71 (53%) |
| Mean eGFR (SD) ml/min /1.73m ² | 76.67 (13.6) |
| Mean Urine ACR (SD) mg/mmol | 4.3 (14.4) |
| Mean Systolic BP (SD) mmHg | 137.84 (16.2) |
| Mean Diastolic BP (SD) mmHg | 77.36 (11) |

6.3.2 Renal structural characteristics

The shape features of the kidneys are summarised in Table 6.2. It includes the initial data obtained for each kidney's volumetric parameters, providing the minimum, maximum, mean, median, and standard deviation for each parameter. The mean kidney volume, as measured by the local software, was approximately 156 (35) ml. The surface area was 227

(36) cm² while the long and short axis length ranged from 9 to 15.6 cm and the short axis length ranged from 3.5 to 7cm respectively.

Table 6.2: Summary statistics for 15 kidney shape factors

| Parameter | Minimum | Maximum | Median | Mean | St Dev | CoV (%) |
|--|---------|---------|--------|------|--------|---------|
| Extent (%) | 17 | 44 | 32 | 32 | 4 | 1.2 |
| Compactness (%) | 49 | 73 | 62 | 62 | 4 | 6.3 |
| Solidity (%) | 57 | 85 | 73 | 73 | 5 | 6.7 |
| Maximum depth (cm) | 0.8 | 1.6 | 1.2 | 1.2 | 0.1 | 8.3 |
| Long axis length (cm) | 9 | 15.6 | 12 | 12 | 1.2 | 9.7 |
| Short axis length (cm) | 3.5 | 7 | 5.2 | 5.3 | 0.6 | 11 |
| Equivalent diameter (cm) | 5.2 | 8 | 6.6 | 6.6 | 0.5 | 7.5 |
| Longest calliper diameter (cm) | 9 | 14.7 | 12 | 12 | 1 | 8.5 |
| Primary moment of inertia (cm ²) | 6 | 14 | 10 | 10 | 2 | 16 |
| Second moment of inertia (cm ²) | 5 | 14 | 9 | 9 | 2 | 18 |
| Third moment of inertia (cm ²) | 2 | 6 | 4 | 4 | 1 | 17 |
| Surface area (cm ²) | 134 | 332 | 226 | 227 | 36 | 16 |
| Volume (ml) | 76 | 275 | 154 | 156 | 35 | 23 |
| Volume (ml/1.73m ²) | 73 | 243 | 137 | 136 | 25 | 18 |
| Bounding box volume (ml) | 202 | 848 | 488 | 495 | 126 | 26 |
| Convex hull volume (ml) | 103 | 362 | 210 | 212 | 48 | 23 |

Volumetric measures such as volume, convex hull volume, and bounding box volume exhibited the highest coefficients of variation (CoV) ranging from 23-26%, indicating substantial variability. In contrast, dimensionless shape factors like extent and compactness demonstrated the lowest CoV (1.2 and 6.3% respectively) (Table 2).

6.3.3 Correlation analysis

This section outlines four distinct correlation analyses. First, the correlation among 15 MRI-derived volumetric parameters was assessed, with results visualised via a heatmap. Next, the correlation between kidney volume and demographic parameters was analysed to identify factors associated with kidney volume. This is followed by analysing correlations between 15 shape factors and both eGFR and UACR to identify key factors. Finally, correlations between compactness, extent, and baseline demographic factors were explored to assess their impact on these two shape factors.

Correlation analysis among 15 volumetric parameters

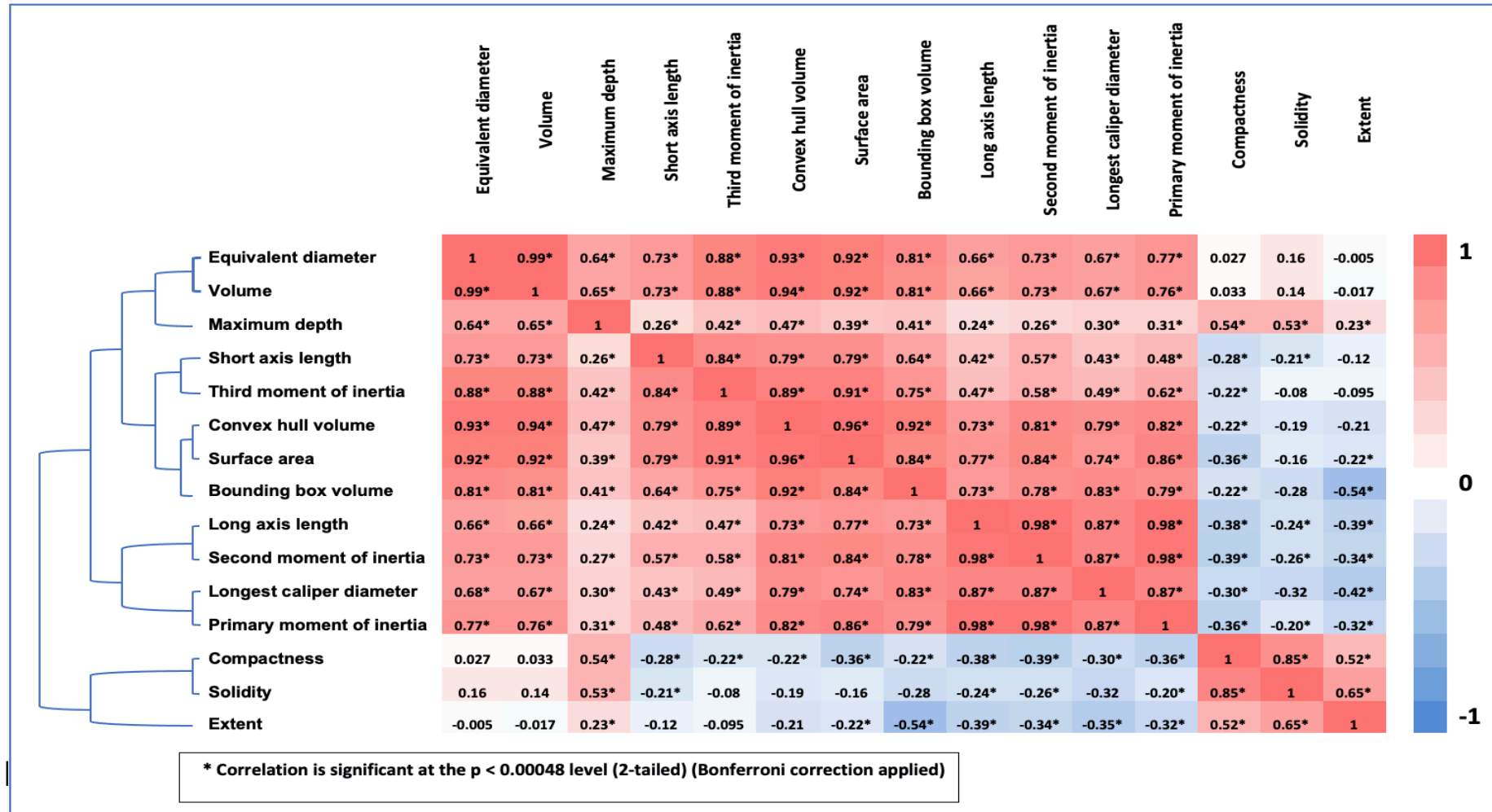


Figure 6.1: Clustered correlation heatmap with dendrogram of different kidney shape features

The heat map (Figure 6.1) highlighted significant correlations between volumetric features and kidney volume showing off-diagonal values ranging from ($r = -0.54$ to 0.99), except for compactness and extent. Compactness and extent showed the weakest correlations with renal volume ($r = 0.033$ and -0.017 , respectively). Conversely, other shape factors, including solidity, exhibited moderate to strong correlations with volume. Further review of heatmap shows that solidity and extent are correlated ($r = 0.65$), providing complementary information. The dendrogram further illustrated the clustering of parameters, demonstrating the association of volumetric and certain shape features.

Correlation analysis between kidney volume and demographic parameters

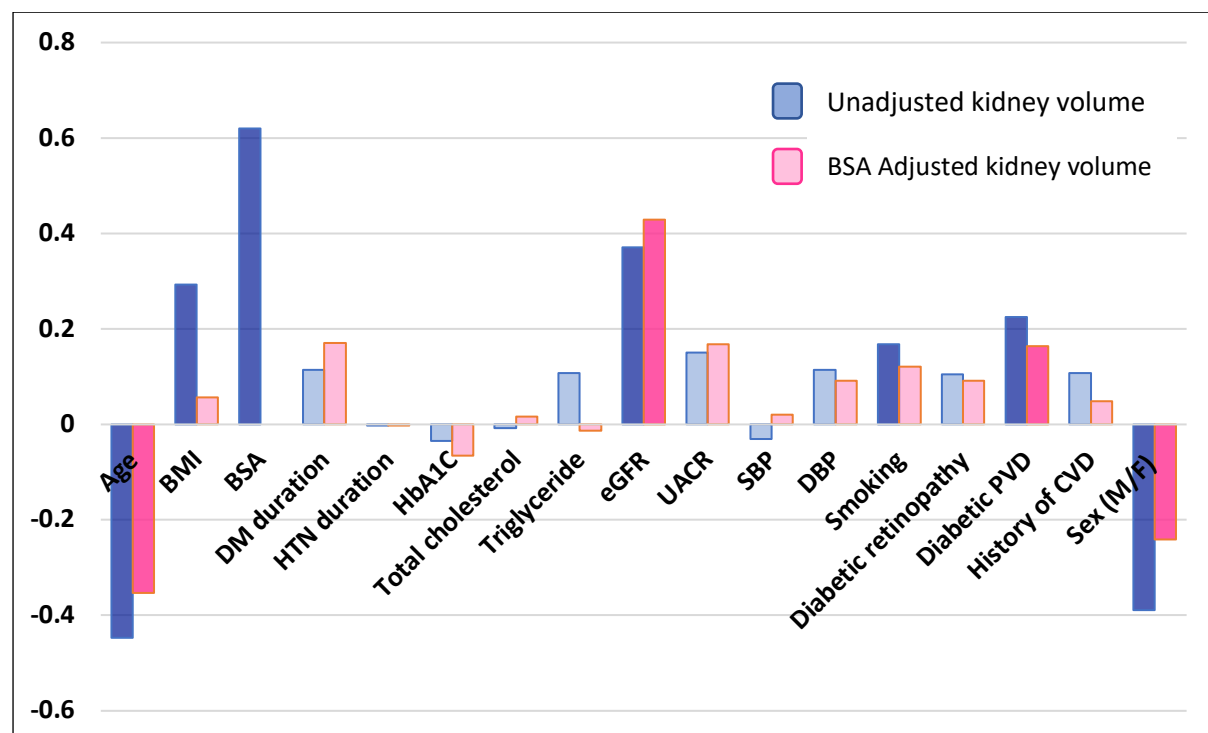


Figure 6.2: Correlation between 2 different kidney volumes (Unadjusted and Body surface area adjusted) with different demographics parameters.

BMI, body mass index; BSA, body surface area; DM, diabetes mellitus; HTN, hypertension; HbA1C, glycated haemoglobin A1C; eGFR, estimated glomerular filtration rate; UACR, urinary albumin creatinine ratio; SBP, systolic blood pressure; DBP, diastolic blood pressure; PVD, peripheral vascular disease.

(r value in left hand side column. Blue represents unadjusted kidney volume and Pink represents body surface area adjusted kidney volume; Darker Blue and Darker Pink represent p value < 0.01 with statistical significance.)

The correlation analysis of kidney volume with various demographic and clinical features was performed to explore the factors affecting kidney volume (Figure 6.2). Unadjusted kidney volume negatively correlated with age ($r = -0.447$, $p < 0.001$) and positively correlated with body mass index ($r = 0.293$, $p < 0.001$), body surface area ($r = 0.620$, $p < 0.001$), and eGFR ($r = 0.371$, $p < 0.001$). Adjusted for body surface area, kidney volume continued to show significant correlations with age ($r = -0.353$, $p < 0.001$) and eGFR ($r = 0.429$, $p < 0.001$). Notably, sex exhibited a highly significant negative correlation with kidney volume in both unadjusted ($r = -0.389$, $p < 0.001$) and adjusted models ($r = -0.241$, $p < 0.001$) in female population. Further analysis indicated significant differences in kidney volume concerning smoking status ($r = 0.168$, $p = 0.006$ unadjusted; $r = 0.121$, $p = 0.049$ adjusted) and diabetic peripheral neuropathy ($r = 0.225$, $p < 0.001$ unadjusted; $r = 0.164$, $p = 0.007$ adjusted).

Correlation analysis between kidney parameter and eGFR, UACR

The analysis of kidney parameters with eGFR and UACR identified several significant associations (Figure 6.3). While most kidney shape parameters are found to be correlated with eGFR, maximum depth ($r = 0.403$, $p < 0.001$), equivalent diameter ($r = 0.374$, $p < 0.001$), volume ($r = 0.371$, $p < 0.001$), and longest caliber diameter ($r = 0.332$, $p < 0.001$) exhibited strong positive correlations. Others, including convex hull volume ($r = 0.286$, $p < 0.001$), primary moment of inertia ($r = 0.290$, $p < 0.001$), solidity ($r = 0.270$, $p < 0.001$) and surface area ($r = 0.291$, $p < 0.001$), also showed significant positive correlations. Meanwhile, dimensionless shape factors such as compactness and extent only showed minimal correlation with eGFR ($r = 0.143$, $p = 0.022$ and $r = 0.166$, $p = 0.008$ respectively).

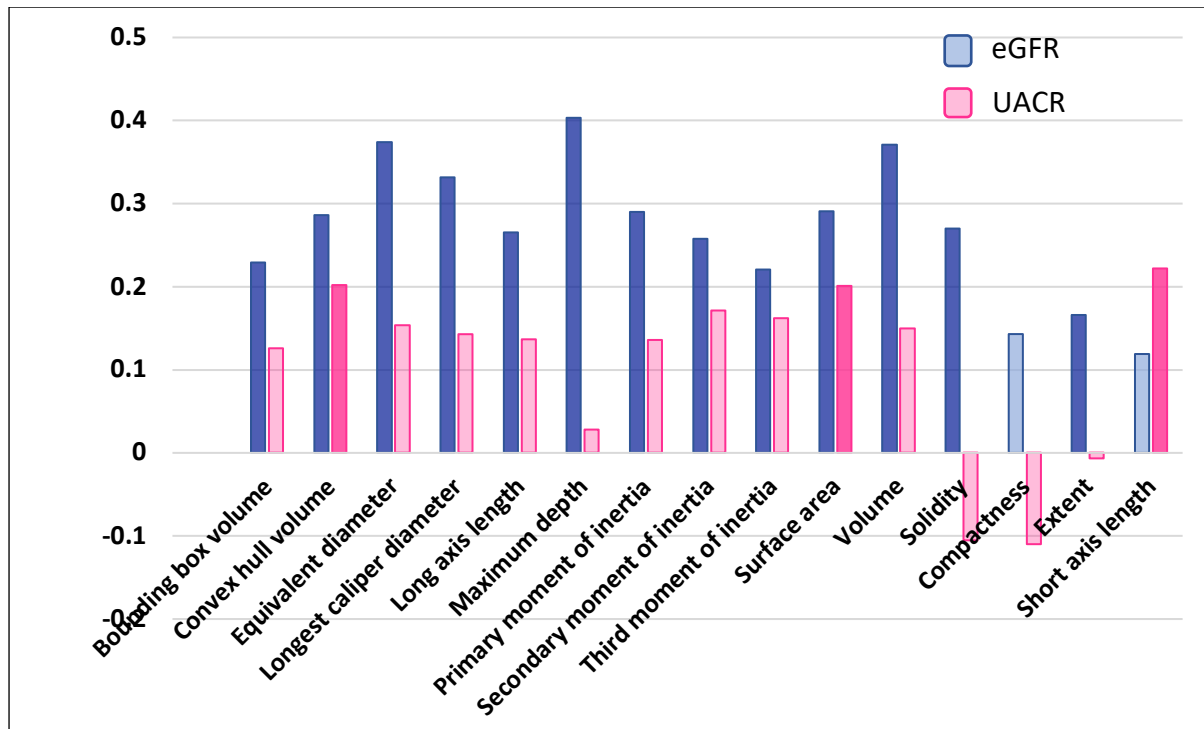


Figure 6.3: Correlation between 15 kidney parameters and estimated glomerular filtration rate (eGFR), urinary albumin creatinine ratio (UACR).

(r value in left hand side column. Blue represents eGFR and Pink represents UACR; Darker Blue and Darker Pink represent p value < 0.01 with statistical significance.)

In contrast, correlations with UACR were generally weaker but still significant, particularly for short axis length ($r = 0.222$, $p < 0.001$), convex hull volume ($r = 0.202$, $p = 0.003$), and surface area ($r = 0.201$, $p = 0.003$). Notably, solidity ($r = -0.105$, $p = 0.122$) and compactness ($r = -0.110$, $p = 0.107$) showed negative or nonsignificant correlations with UACR, highlighting their limited utility in predicting albuminuria.

Correlation analysis between compactness/ extent with baseline demographics

Further analysis was conducted utilising various demographic data to evaluate the potential relationships between these variables and dimensionless shape factors, specifically compactness and extent due to their lack of correlation with kidney volume. The analysis revealed several noteworthy relationships. Compactness showed a negative correlation with age ($r = -0.137$, $p = 0.025$), weight ($r = -0.141$, $p = 0.021$), body surface area (BSA) ($r = -0.155$, $p = 0.011$), and a positive correlation with eGFR ($r = 0.143$, $p = 0.022$) although statistically not significant (Figure 6.4).

Extent demonstrated significant negative correlations with weight ($r = -0.226$, $p < 0.001$), BSA ($r = -0.186$, $p = 0.002$), and BMI ($r = -0.241$, $p < 0.001$), and a positive correlation with eGFR ($r = 0.166$, $p = 0.008$) (Figure 4). However, both compactness and extent showed no significant correlations with UACR, SBP, DBP, duration of diabetes, duration of hypertension, HbA1C, or total cholesterol.

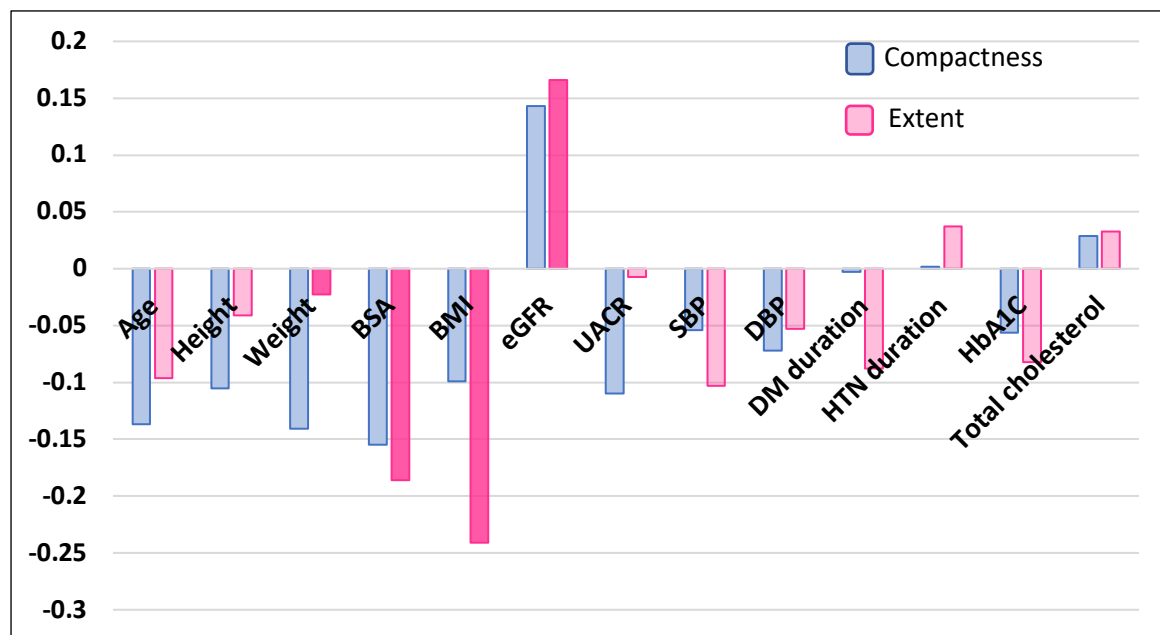


Figure 6.4: Correlation between compactness/ extent and different baseline demographics

(r value in left hand side column. Blue represents compactness and Pink represents extent; Darker Blue and Darker Pink represent p value < 0.01 with statistical significance.)

Multiple regression analysis for compactness

The results of multiple regression analysis examining the relationship between compactness and eGFR or UACR across different adjusted models are presented table 6.3. Compactness is not significantly associated with eGFR or UACR in both unadjusted, and age- and sex-adjusted models as well as after adjusting for a range of potential confounders.

Table 6.3: Multiple regression analysis of compactness and its association with estimated glomerular filtration (eGFR) decline and urinary albumin creatinine ratio (UACR) across adjusted models

| Covariates | Renal function parameters | p value | 95% CI |
|---|---------------------------|---------|---------------|
| Unadjusted | eGFR | 0.02 | 0.02:0.26 |
| | UACR | 0.11 | -0.24:0.02 |
| Adjusted for age and sex | eGFR | 0.09 | -0.01:0.07 |
| | UACR | 0.04 | -0.08: -0.003 |
| Adjusted for age, sex, BMI, SBP, HbA1C. | eGFR | 0.19 | -0.01:0.07 |
| | UACR | 0.02 | -0.09: -0.01 |

BMI, body mass index; SBP, systolic blood pressure; HbA1C, glycated haemoglobin A1C.

6.3.4 Scatter plots and three-dimensional visualisation

This section is divided into four subsections. Scatter plots in first subsection illustrate the relationships between compactness, extent, and kidney volume, followed by 3D visualisations to demonstrate variations in compactness at comparable kidney volumes. A comparison of morphological outlines is conducted across different age groups as well as varying eGFRs with similar compactness.

Scatter plots for correlation between kidney shape factors and kidney volume

Figure 6.5 illustrates the correlation between kidney shape factors (compactness and extent) and kidney volume, both unadjusted and adjusted for body surface area. The scatter plots reveal that the pattern of correlation remains consistent despite the adjustment for body surface area. The final plot in the figure highlights a significant positive correlation between compactness and extent.

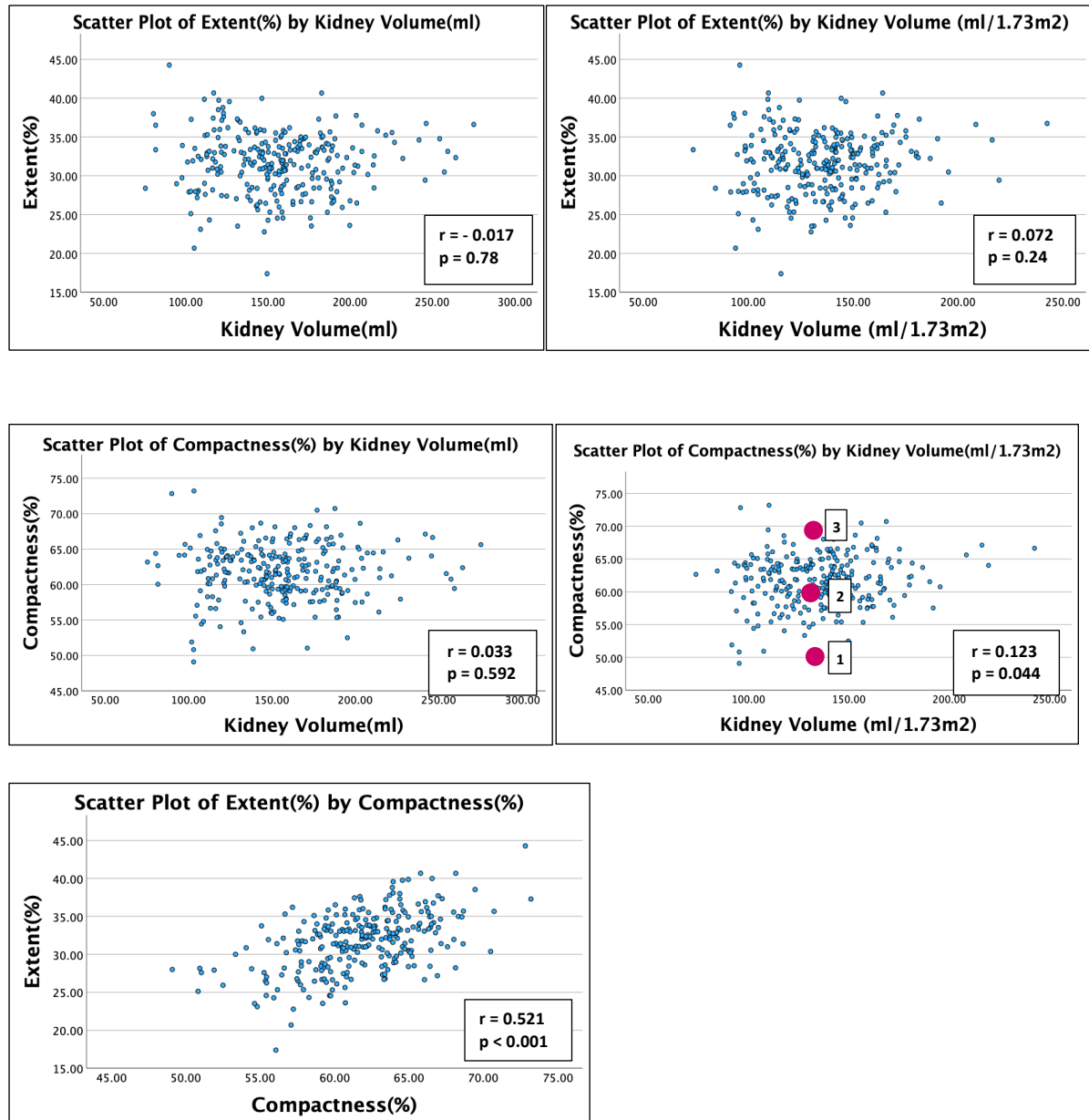


Figure 6.5: Correlation between shape factors (compactness and extent) and kidney volume

(the pattern of scatter plot did not change when correlated with renal volume with and without adjustment to body surface area)

(pink dots demonstrating the different compactness in similar BSA adjusted volume from Figure 3)

Different compactness in similar kidney volumes

Figure 6.6 illustrates three cases with similar kidney volumes but differing levels of compactness. These volumes have been adjusted to body surface area to correct for variations in body size. The parameter of compactness captures significant morphological differences despite similar volumes, allowing for a comparison of kidney shapes.

Despite exhibiting similar eGFRs, kidneys with lower compactness present with more deformed and irregular outlines, as well as more hollowed-out shapes. This suggests a continuum from higher to lower compactness that is not reflected in GFR values. This lack of correlation underscores the potential of compactness as an independent MRI biomarker that warrants further investigation to fully understand its implications and utility in renal assessment.

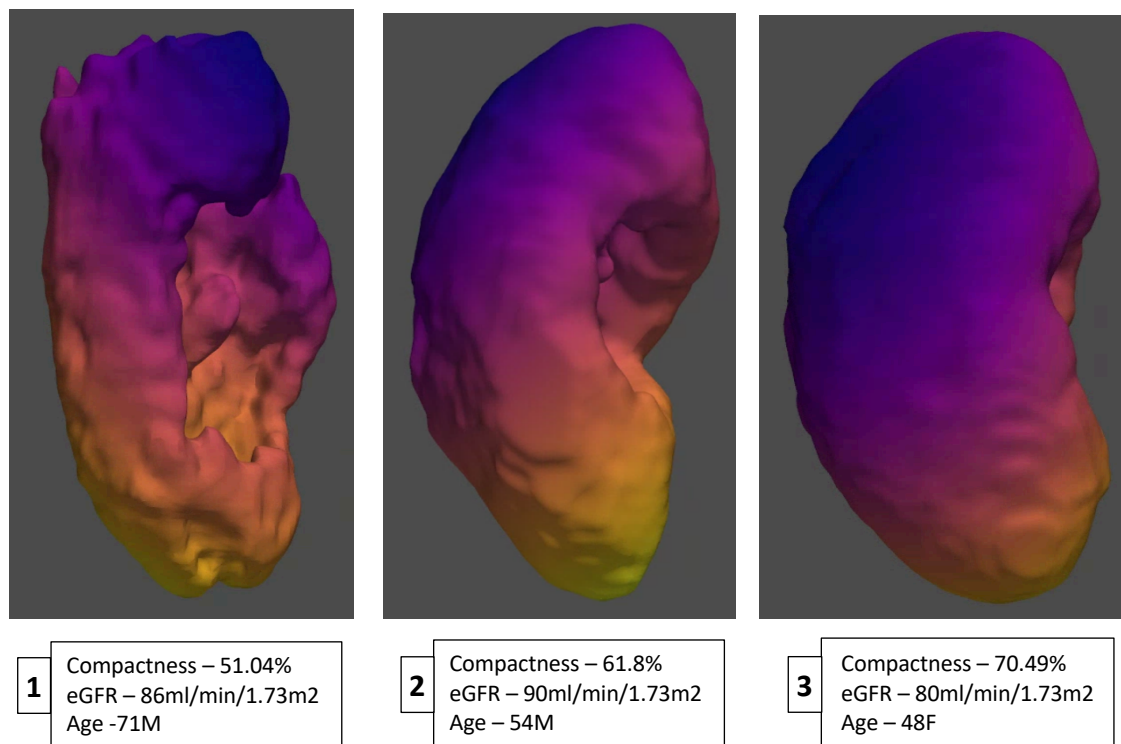


Figure 6.6: Different compactness and kidney shape in similar BSA adjusted kidney volume
(pink dots in figure 5 show three cases on scattered plot)

Similar compactness in different ages

Figure 6.7 illustrates the kidneys of participants across various ages with similar eGFR, demonstrating that despite age differences, kidney with similar compactness remains consistent in their shape, suggesting the limited impact of age on compactness and further proving the correlation analysis result ($r = -0.137$, $p = 0.025$).

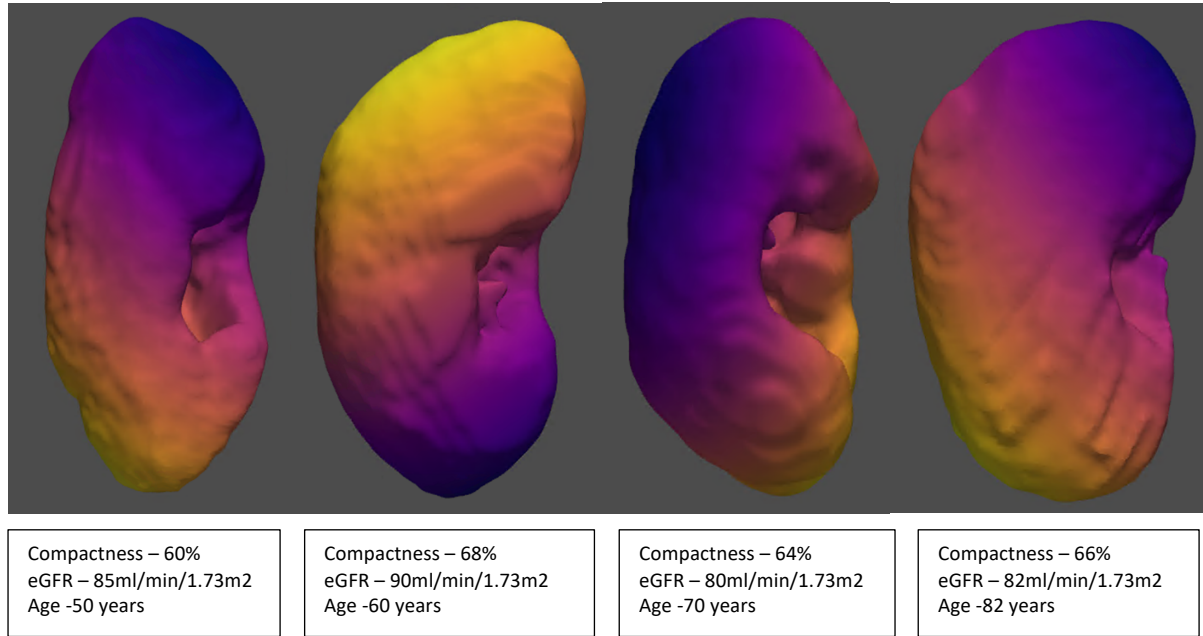


Figure 6.7: Similar compactness and kidney shape in different ages of participants

Similar compactness in different eGFR

The impact of varying eGFR on compactness was investigated through graphical analysis and observation of kidney morphology. Figure 6.8 presents four distinct eGFR levels, all exhibiting similar compactness, which indicates that the kidney shape factor remains consistent across different eGFR levels, provided the compactness does not undergo significant changes. This observation reinforces the findings from the correlation analysis, which demonstrated a lack of significant correlation between kidney compactness and eGFR ($r = 0.143$, $p = 0.022$).

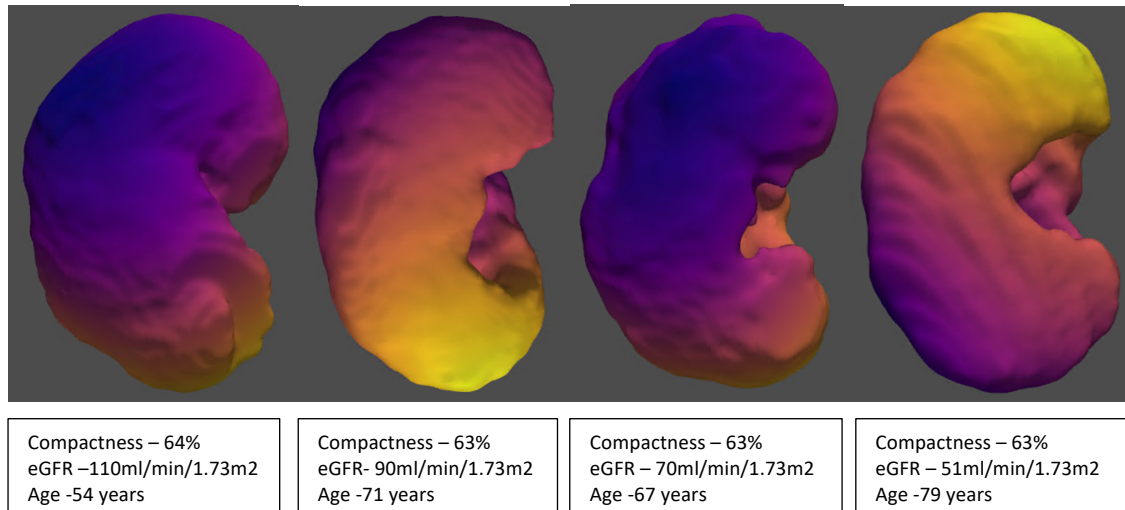


Figure 6.8: Similar compactness and kidney shape in different eGFR

6.4 Discussion

In this study, we evaluated the geometrical alterations in the kidney by analysing three-dimensional, quantitative, and morphological features. We investigated 15 different morphological features derived from MRI scans, including kidney volume, axis length, surface area, solidity, and compactness. The value of kidney volume from this study is comparable to the reference value obtained from the UK Biobank population study (405), which included nearly 38,000 participants. Most parameters, including kidney volume and length, were correlated with kidney function. Notably, among all the morphological features examined, compactness showed no correlation with kidney function and significant impact on kidney morphology.

Case studies suggest that a reduction in compactness indicates an irregular kidney shape despite normal kidney function as demonstrated in figure 6.6, suggesting the possibility of subclinical early DKD changes such as hyperfiltration process in more deformed kidney with reduced compactness. Longitudinal follow-up data would be invaluable in determining whether kidneys exhibiting reduced compactness are more susceptible to a more rapid progression of DKD compared to those with higher compactness. Such data would enhance the understanding of the prognostic significance of kidney compactness and its potential role as a predictive biomarker for DKD progression. Additionally, figures 6.7 and 6.8

illustrate the lack of gross morphological variation in kidney shape as long as the compactness remains stable, despite changes in age and eGFR, although the study with larger population is still required. The strong influence of compactness on kidney shape warrants further exploration into its potential applications in clinical assessments and decision-making processes.

Another factor potentially influencing compactness is the effect of aging and elevated BMI. Compactness correlated negatively with both age and BMI in this study, suggesting that observed changes in kidney morphology might be attributable to cortical thinning due to ageing and increased intra-abdominal fat exerting greater pressure on the kidneys in high BMI individuals. Previous studies (406–409) have indicated that age and BMI influence kidney shape, with kidneys becoming plumper as these variables increase. This plumpness is reflected by a decreased renal shape index (defined as renal length divided by the sum of renal width and renal thickness) or an increased ratio of renal width to renal length (406). One proposed explanation for this phenomenon is the relaxation of the abdominal wall with advancing age, resulting in less compression of the kidneys in older individuals (406). Additionally, a simpler explanation posits that obese patients exhibit larger kidneys (409) due to the increased space created by excess adipose tissue, which accommodates the enlarged organs (406).

The interest in kidney morphology has increased with advancements in imaging technologies. A recent CT-based study (307) in a CKD population examined 17 different renal features and identified the surface area to volume ratio (SVR) as having the highest diagnostic ability for CKD due to its strong association with eGFR ($r = -0.747$, $\beta = -0.001$; $p < 0.0001$), even after adjusting for other variables. Although baseline data for UACR was collected, it was not included in the analysis. The study also investigated other shape features, such as sphericity ($r = 0.435$, $p < 0.0001$), compactness ($r = 0.439$, $p < 0.0001$), and elongation ($r = 0.129$, $p = 0.039$), which showed low to moderate correlations with eGFR and may reflect geometric changes occurring during CKD progression. Our study did not show any association between compactness and eGFR.

Recently, the automated segmentation and measurement of kidney volume using MRI have become increasingly prevalent. This advancement allows for the rapid acquisition of detailed anatomical information. MRI study on kidney morphology by Thanaj et al. (410) investigated the association between kidney shape, defined by surface-to-surface (S2S) distances, through the construction of surface meshes from kidney segmentations derived from abdominal MRI data in 38,868 participants of the UK Biobank. Increased S2S distances signify outward expansion of the subject's vertices relative to the template vertices, while decreased distances indicate inward shrinkage. The study found significant associations of S2S distances with age ($\beta = -0.10$), BMI ($\beta = -0.10$), and waist-to-hip ratio ($\beta = -0.04$). Additionally, S2S distances increased with the presence of type 2 diabetes and decreased with CKD.

In our study, alterations in kidney shape factors may act as indicators of renal stress, potentially elevating the risk of disease progression and susceptibility to injury, even if the overall kidney volume remains unchanged. Among the 15 shape parameters examined, compactness exhibited minimal correlation with volume and no significant correlation with either eGFR or UACR, even after adjusting for other variables. Typically, kidneys with increased compactness are morphologically closer to a perfect sphere, and it was anticipated that compactness would decline with decreased eGFR, as kidneys with advanced CKD deviate from a spherical shape. However, our study did not demonstrate this expected correlation.

As illustrated in Figure 6.6, despite having similar eGFR values, kidneys with low compactness exhibit significant deformity compared to those with high compactness. Although compactness does not correlate with traditional kidney function parameters, it may provide complementary information that these traditional markers (e.g., eGFR, creatinine) miss, potentially capturing aspects of kidney disease, such as early-stage DKD. Given the multifaceted nature of DKD, novel MRI biomarkers like compactness might reflect structural changes or pathological processes that are not detected by conventional blood and urine tests. Our hypothesis is that participants exhibiting low compactness may be predisposed to rapid progression of DKD, despite their eGFR not indicating this potential trajectory. Follow-up data are currently being collected in these participants and will offer

an opportunity to test these hypotheses in the same participants. If confirmed, this may lead to consideration of MRI shape factors in risk assessment for DKD progression – potentially in combination with clinical markers such as renal function (eGFR) and albuminuria.

However, our study has some limitations. Firstly, the absence of previous MRI images precludes the ability to compare current kidney shape changes with past data, thus limiting our understanding of whether these alterations are long-standing or newly developed. Additionally, due to the limited number of young participants included in the initial analysis, we were unable to adequately compare different levels of compactness within this demographic. Compactness has been shown to be negatively correlated with age, it remains unclear whether observed changes in compactness are primarily influenced by advancing age or are predominantly attributable to DKD, although the case study in figure 6.7 did not show any gross difference in kidney shape with increased age in similar eGFR. Moreover, the lack of follow-up data poses a significant constraint, as longitudinal studies are essential to establish whether compactness can serve as a reliable prognostic biomarker in the management of DKD. Without such data, it is challenging to determine the potential of compactness to provide additional prognostic value beyond traditional kidney function markers. The absence of a correlation between compactness and conventional kidney function parameters, such as eGFR and UACR, may reduce its immediate appeal to clinicians, particularly in the absence of longitudinal evidence supporting its prognostic utility. This underscores the necessity for future research to address these gaps. Long-term studies are required to verify the prognostic significance of compactness and to explore its potential role in enhancing the early detection and management of DKD.

6.5 Conclusion

This study explored the relationship between novel MRI-derived kidney shape factors, particularly compactness, and traditional clinical markers of DKD such as eGFR and UACR. We speculate that compactness, while not correlated with conventional kidney function markers, may serve as an indicator of early subclinical kidney changes, potentially providing

insights into DKD progression. This aligns with the study's aims to determine whether renal imaging biomarkers offer additional information on DKD heterogeneity beyond standard blood and urine markers. Although longitudinal data are needed to confirm compactness as a predictive biomarker for DKD, our findings suggest that MRI-based structural assessments could capture disease progression signatures that routine biomarkers may miss, offering potential for improved DKD risk stratification and management.

Chapter 7

Renal perfusion assessment by dynamic contrast enhanced magnetic resonance imaging in patients with cardiac autonomic neuropathy.

This chapter examines the impact of CAN on renal perfusion using DCE-MRI. The findings will focus on the comparison of MRI-derived RBF parameters between participants with and without CAN, providing insights into the effects of CAN on renal perfusion.

Abstract

Background/ Aim

CAN has been described as a potential independent risk factor for the incidence and progression of DKD. Among the various mechanisms proposed, a reduction in renal perfusion caused by over-activation of the sympathetic nervous system and the RAAS is commonly described in the literature. However, despite its prevalence in theoretical discussions, this mechanism has not been extensively studied using imaging techniques. In our study, we aim to fill this gap by assessing renal perfusion using DCE-MRI which allows the non-invasive and precise measurement of RBF, providing valuable insights into the physiological changes associated with CAN.

Methods

Our study included participants from the iBEAt study, which recruited individuals with T1 and T2DM who had eGFR greater than 30 ml/min/1.73 m². Participants (n=81) were stratified into two groups based on the presence or absence CAN. The diagnosis of CAN was established using Ewing's CARTs.

MRI data were acquired in free-breathing using a 2D Turbo-FLASH sequence on a General Electric (GE) MRI scanner. The dynamic dataset consisted of eight coronal-oblique slices covering the kidneys and one axial slice obtained across the abdominal aorta. The contrast

agent Dotarem (Gd-DOTA) was injected intravenously to enhance the visualisation of the kidneys, providing high-resolution images and quantifiable data on renal blood flow. All MRI images underwent pre-processing to correct for motion and other artifacts. Regions of interest (ROIs) were defined for the aorta, renal parenchyma, and renal cortex, followed by the quantification of renal volume, RBF, and perfusion using PMI software.

Correlation analysis was conducted using Spearman's rank and Chi-square tests to compare renal perfusion between the CAN and no-CAN groups. Renal perfusion differences between the groups were compared and analysed by Mann-Whitney U test or Kruskal Wallis test. All statistical analyses were performed using SPSS (version 29), and results were considered statistically significant if the p-value was less than 0.05.

Results

The study did not show any evidence of reduced renal and cortical perfusion in CAN group when compared with no CAN group [(CAN Vs No CAN) (renal perfusion: 286 Vs 297 ml/100ml/min, $p=0.645$) and (cortical perfusion: 315 Vs 310 ml/100ml/min, $p = 0.711$)]. This indifference in renal perfusion parameters remains consistent even when compared in different CAN stages and different eGFR grades. Average renal perfusion decreased with increasing CAN severity as well as increased eGFR grades, but these trends were not statistically significant. Further analysis of renal perfusion in T1 and T2DM separately also did not show any statistically significant difference.

Conclusion

These findings suggest that CAN might not have a significant impact on RBF, contrary to what has been suggested by previous literature. The results demonstrate consistency between T1 and T2DM cohorts, with no variation in renal and cortical perfusion observed in CAN and no CAN groups. These preliminary outcomes highlight the need for future longitudinal studies with larger sample sizes to confirm these findings. Additionally, employing various MRI perfusion methods, such as ASL and PC-MRI, would be beneficial in providing a more comprehensive assessment of the impact of CAN on renal perfusion.

7.1 Introduction

CAN has been identified as a potential independent risk factor for the incidence and progression of DKD over the last few decades (347,367,368). Several studies have demonstrated the role of CAN in DKD using renal parameters such as eGFR (347,361,367,373,379), serum creatinine (358), and UACR (359,360,362,380). These findings have led to the proposal of several mechanisms through which CAN impacts DKD: 1) lack of nocturnal BP drop causes increased glomerular pressure, leading to a decline in renal function (355,357,360,380,382), 2) relative sympathetic overactivity results in renal vasoconstriction and subsequent ischemia, contributing to renal function decline (347,358,363,376,381), 3) RAAS activation increases intraglomerular pressure, causes GBM thickening, and leads to renal vasoconstriction and ischemia (368,383), and 4) endothelial inflammation and interstitial fibrosis caused by impaired regulation of inflammatory cytokines and chemokines due to sympathetic nervous system impairment (379,384).

Among these mechanisms, the lack of nocturnal BP drop has been the only one conclusively proven, using 24-hour ABPM in CAN patients (357,360,380,387,389,390). The mechanism of renal vasoconstriction is frequently mentioned in studies but has not been confirmed through medical imaging.

In this study, we aim to assess the impact of CAN on renal perfusion by using DCE-MRI and to compare between participants with and without CAN. This approach will provide new insights into the physiological changes associated with CAN and their implications for DKD progression.

7.2 Materials and methods

7.2.1 Study

The study is part of the iBEAt study, which is integrated within the broader BEAt-DKD project (Biomarker Enterprise to Attack Diabetic Kidney Disease). BEAt-DKD aims to provide tools and knowledge that will facilitate the development of new, personalised treatments

for DKD. The long-term objective of the project is to determine imaging biomarkers that can improve the differentiation of fast from slow progression in DKD over and above existing and newly discovered panels of serum/plasma and urine biomarkers. Details of the study protocol have been previously published (308). Sheffield is one of six participating centres (Bari, Bordeaux, Exeter, Leeds, Sheffield, and Turku), each recruiting participants with T1 and T2DM, aged between 18-80 years.

The study received formal ethical approval by Health Research Authority (HRA) and Health and Care Research Wales (HCRW) (REC Reference 18/YH/0077) and is registered with ClinicalTrials.gov (identifier NCT03716401). Funding is provided by the Innovative Medicines Initiative 2 Joint Undertaking under grant agreement No. 115974, with support from the European Union's Horizon 2020 research and innovation programme, the Juvenile Diabetes Research Foundation (JDRF), and the European Federation of Pharmaceutical Industries and Associations (EFPIA).

7.2.2 Participants recruitment in Sheffield

Sheffield adhered to standardised recruitment criteria and protocol (308), as outlined in Tables 7.1-7.3. Following the acquisition of ethical and R&D approval, recruitment commenced with the screening of potential participants. NHS Summary Care Record, blood test results from the ICE system and correspondence letters from the outpatient diabetes clinic documented in System One were utilised for screening.

Table 7.1: Inclusion criteria for T1 and T2DM

| Inclusion Criteria for T2DM | Inclusion criteria for T1DM |
|--|--|
| <ol style="list-style-type: none">1. Diagnosed T2DM2. eGFR \geq 30 ml/min/1.73m²3. Able to provide informed consent4. Age between 18 years and 80 years | <ol style="list-style-type: none">1. Diagnosed T1DM2. Duration of diabetes \geq 15 years3. All other inclusion / exclusion criteria will be same as the T2DM cohort |

Table 7.2: Exclusion criteria for T1 and T2DM

| Exclusion Criteria |
|--|
| <ol style="list-style-type: none"> 1. Renal transplantation 2. On permanent dialysis 3. Significant comorbidities with life expectancy of < 1 year 4. Use of investigational drug within 1 month prior to screening 5. Known clinical history of urinary obstruction on renal US: either post-voiding residue over 100 ml, or pyelectasis. 6. Known clinical history of aortic endoprosthesis at the renal level. 7. Current pregnancy 8. History of Hepatitis B or Hepatitis C + 9. Use of antiretroviral medication 10. Known current or clinical history of renal or urinary tract malignancy 11. Biopsy proven non-diabetic primary renal disease 12. Autosomal Dominant Polycystic Kidney Disease (APKD) 13. Renal stones causing CKD 14. Cirrhotic liver disease, or non-cirrhotic chronic liver disease where ALT >2 x upper limit of normal. 15. Current metastatic malignancy 16. Current malignancy with expected survival < study follow up period (4 years) 17. Melanomatous skin cancer < 5 years ago (fully resected melanoma >5 years ago, i.e., surgical cure, can be recruited) 18. Any other significant disease or disorder which, in the opinion of the investigators, may either put the patient at risk because of participation in the study, or may influence the result of the study, or the patient's ability to participate in the study |

Table 7.3: Standard MRI exclusion criteria

| Standard MRI exclusion criteria |
|---|
| <ol style="list-style-type: none"> 1. Cochlear Implant 2. Aneurysm Clips 3. Neurological stimulators |

4. Implanted cardiac devices (ICD, PPM, loop recorders, or any others)
5. Metal heart valve
6. History of metal foreign bodies in orbits
7. Other implanted metal device which prevents MR imaging
8. Known allergy to Gadolinium contrast
9. Claustrophobia
10. Weight exceeding 250 kg

A total of 1,800 potential participants with T2DM and 200 with T1DM were pre-screened, with 180 (10%) and 80 (40%) meeting the study criteria, respectively. After initial contact and further assessment, 77 participants with T2DM and 37 with T1DM were excluded for clinical or study-related reasons (e.g., claustrophobia, lack of interest, work commitments, or contrast-related concerns). Figure 7.1 presents the participant flow.

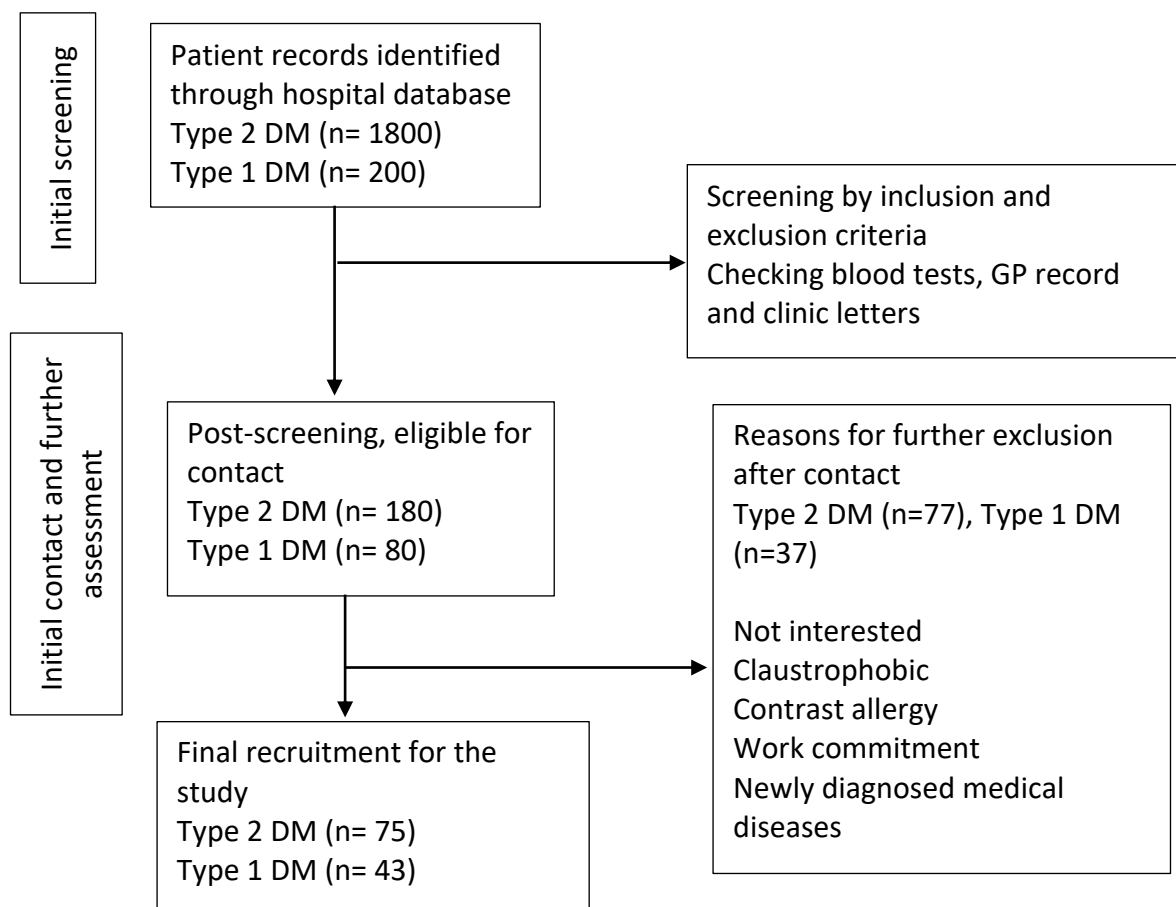


Figure 7.1: Participant recruitment flow chart for T1 and T2DM

Potential participants were contacted by phone, and those expressing interest were sent participant information sheets. Follow-up calls were made within 7-10 days to confirm participation and address any questions. Upon consent, participants were scheduled for a study session lasting four hours in the morning. Appointment letters, study day instructions, and urine bottles for early morning sample collection were then sent to the participants.

7.2.3 Data and sample collection

The baseline visit took place at the Diabetes Research Laboratory, Royal Hallamshire Hospital. Participants were instructed to refrain from smoking, fasting from midnight (at least eight hours), and avoiding strenuous exercise for 24 hours prior. Medication guidelines for fasting were provided (Appendix B). After blood tests and cannulation, participants consumed their regular medications with a standardised breakfast. Detailed preparation instructions were sent to participants (Appendix C).

Upon arrival, participants provided a urine sample and had blood glucose levels checked to prevent hypoglycaemia (glucose <3.5 mmol/L). Insulin users were instructed to monitor blood glucose at home and contact the researcher if levels were <4 mmol/L. Written informed consent was obtained, and baseline data—including demographic, clinical, and medication history, biofluid samples, and MRI images—were collected. Follow-up visits for three years collected the same data, except MRI imaging, which was only performed at baseline. Biofluid samples were processed at local and University of Sheffield laboratories, with eGFR calculated via CKD-EPI Creatinine Equation (2021) and UACR derived from early morning urine samples.

Table 7.4: Outline of data collection, biofluid collection and clinical examination

(BEAt-DKD protocol- amended version April 2022)

| Protocol details | Screening | Baseline/ Consent | Year 2 Follow up | Year 3 Follow up | Year 4 Follow up |
|-----------------------------|-----------|----------------------|-----------------------|-------------------------|-------------------------|
| Window | Day 0 | 0-3 months | 1year +/- 3 months | 2 years +/- 3 months | 3 years +/- 3 months |
| Informed Consent | | X | | | |
| Demographics | | X | | | |
| Clinical information | | X | X | X | X |
| Blood collection | | X | X | X | X |
| Urine collection | | X | X | X | X |
| MRI | | X | | | |
| Autonomic Function Tests | | X | X | X | X |

After blood and urine samples collection, participants were provided with a standardised breakfast (two slices of brown toast and 250 ml of water), followed by face-to-face data collection and administration of questionnaires. The questionnaires included adherence to study instructions, demographic information (gender, age, geographical origin), clinical exam data (height, weight, waist/hip circumference, blood pressure), current and family medical history (e.g., diabetes, cardiovascular disease, renal disease), social history (smoking, alcohol intake), and medication usage (Appendix D). Relevant clinical and laboratory results were also obtained with consent. Table 7.5 outlines the blood and urine tests conducted according to the iBEAt protocol.

Table 7.5: Blood tests and urine tests data collected.

| Blood tests data | Urine tests data |
|---|---|
| 1. Haematocrit 2. HbA1c 3. Haemoglobin 4. Glucose 5. CRP 6. Albumin 7. Urea and electrolytes 8. LDL, HDL, total cholesterol, triglycerides | 1. Urinary albumin 2. Urinary creatinine 3. Urinary albumin creatinine ratio (UACR) |

Portions of biofluids were analysed at the University of Sheffield before being frozen at -80°C and sent to the University of Lund, Sweden, for BEAt-DKD project further analyses. This report focuses on blood and urine test results from the hospital laboratory, excluding Sheffield lab processing details.

Data protection measures include secure storage of physical documents, anonymisation of datasets by removing personal identifiers, and separate storage of consent forms. Digital blood and urine test results are securely stored with encryption and access controls, ensuring compliance with ethical standards and participant confidentiality.

7.2.4 Assessment of cardiac autonomic neuropathy by Ewing's method

At baseline visits, participants were assessed for CAN using CARTs according to Ewing's protocol (349). Participants rested supine for 10 minutes in a temperature-controlled room (18°C–23°C) and were instructed to avoid caffeine for 24 hours prior. The tests were conducted using the MDE device (ESP-01-PA Adult portable system, Measuring Development Engineering Co. Ltd, Budapest, Hungary), which is equipped with software for Ewing's tests. Detailed procedures for each test are outlined in Chapter 7.

R-R intervals, heart rate, and blood pressure were measured. Scores were assigned to each parameter according to the criteria in Table 7.6, with a scoring system of 0 for normal, 1 for borderline, and 2 for abnormal values. The cumulative score was used to assess the severity of autonomic neuropathy, with higher scores indicating greater severity. Based on the total score, a diagnosis of cardiac autonomic neuropathy was established.

No abnormal test: Normal/ No CAN

1 abnormal test: Early CAN

2-3 abnormal tests: Confirmed CAN

≥ 3 or 2 abnormal tests plus postural hypotension: Advanced CAN

Table 7.6: Evaluation of Cardiovascular reflex tests by Ewing's method

| Autonomic function test | Measured parameter | Normal value (score 0) | Limit value (score 1) | Abnormal value (score 2) |
|--|------------------------------------|---------------------------|--------------------------|-----------------------------|
| <u>Parasympathetic function analysis</u> | | | | |
| Heart rate changes during deep inhalation and exhalation | Heart rate changes beats/minute | ≥ 15 | 11-14 | ≤ 10 |
| Valsalva manoeuvre | Valsalva ratio | ≥ 1.21 | 1.11-1.20 | ≤ 1.10 |
| Heart rate changes as result of standing up | 30/15 ratio | ≥ 1.04 | 1.01-1.03 | ≤ 1.00 |
| <u>Sympathetic function analysis</u> | | | | |
| Blood pressure drop as result of standing up | SBP drop (mmHg) | ≤ 10 | 11-29 | ≥ 30 |
| Handgrip test | DBP elevation (mmHg) | ≥ 16 | 11-15 | ≤ 10 |

7.2.5 MRI methodology

MRI examinations were conducted on an outpatient basis at the University of Sheffield MRI department, lasting approximately 1 hour and 15 minutes, with contrast administration to assess renal blood flow. Participants were informed of potential risks, including contrast allergies, loud noise, claustrophobia, and the rare risk of nephrogenic systemic fibrosis in individuals with eGFR < 30 ml/min (411). The following sequences were acquired according to the BEAt-DKD protocol (Table 7.7) (detailed MRI acquisition protocol for the GE scanner in Sheffield is provided in Appendix D & E).

Table 7.7: MRI sequences for iBEAt

| MRI sequences acquired as per protocol |
|---|
| 1. Morphological T2 |
| 2. Morphological T1 |
| 3. Diffusion-weighted imaging |
| 4. Diffusion-Tensor Imaging |
| 5. Relaxometry: T1- T2 and T2* mapping (BOLD) |
| 6. Phase contrast |
| 7. Quarter-dose MR Renography (MRR) |
| 8. Post-contrast morphological T1 (in-phase). |

All MRI data were anonymised and exported in DICOM format to the central imaging management system at the Swiss Institute of Bioinformatics. The radiographer was instructed to notify the research fellow of any incidental findings, which were then reviewed, and if necessary, referred to the central MRI report team for urgent evaluation. Significant findings were communicated to the patient and their GP. RBF for this thesis was assessed using DCE-MRI.

Image pre-processing and features extraction for DCE-MRI

Renal MRI data were acquired on GE 3T Discovery PET/MR scanner (GE Healthcare, Milwaukee, USA) using 18-channel phased array body coil combined with inbuilt spine coil

for signal reception. Participants were scanned in the supine position with the body coil placed on the abdomen and the centre of the coil and the coronal-oblique slices were positioned over the kidneys. Data were acquired in free-breathing using 2D Turbo-FLASH sequence and dynamic dataset consisted of eight coronal-oblique slices that covers the kidneys, and one axial slice obtained across the abdominal aorta.

Images were acquired every 1.5 seconds for 7:07 minutes resulting in total 265 images. DCE sequence parameters were TR 179 ms; TE 0.97 ms; flip angle 10°; TI 85 ms; voxel size 1.0 x 1.0 x 7.5 mm; matrix size 400 x 300; slice spacing = 1.5 mm. Parallel imaging technique GRAPPA was employed with acceleration factor = 2. Dotarem (Gd-DOTA) was injected intravenously with a dose of 0.05 ml/kg at a rate of 2 ml/s followed by 20 ml saline flush. The injection was given 20 seconds after the DCE MRI sequence acquisition started using an automatic power injector.

MRI post-processing

DCE-MRI post-processing was performed using PMI software. A map of maximum signal enhancement was generated on a pixel-by-pixel basis to define the aorta on an axial slice. A lower threshold value (typically 30-35% of maximum signal enhancement) was set to mask out background pixels, followed by manual exclusion of pixels outside the aorta. The arterial input function (AIF) derived from this region of interest (ROI) was used for kinetic modelling. Model-free deconvolution analysis was performed to create maps of extracellular volume. These maps were then used for whole kidney segmentation on coronal-oblique slices. The parenchyma was initially outlined by manually selecting a lower threshold, followed by manual exclusion of voxels in the renal pelvis, collecting system, or outside the kidney. A similar methodology was employed for the segmentation of the renal cortex.

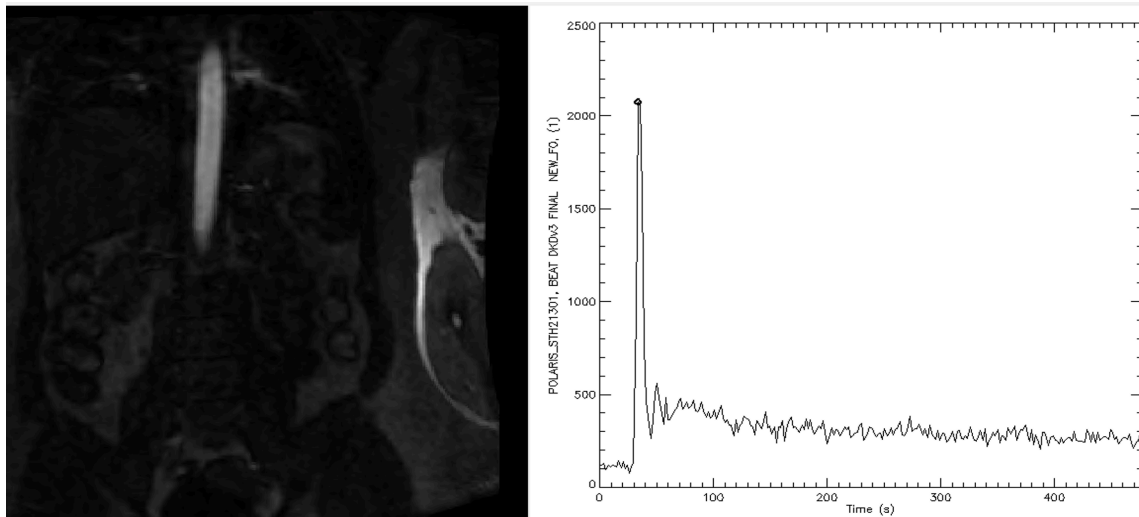


Figure 7.2A: Segmentation of aorta on DCE-derived map of maximal signal enhancement and derived concentration-time curve

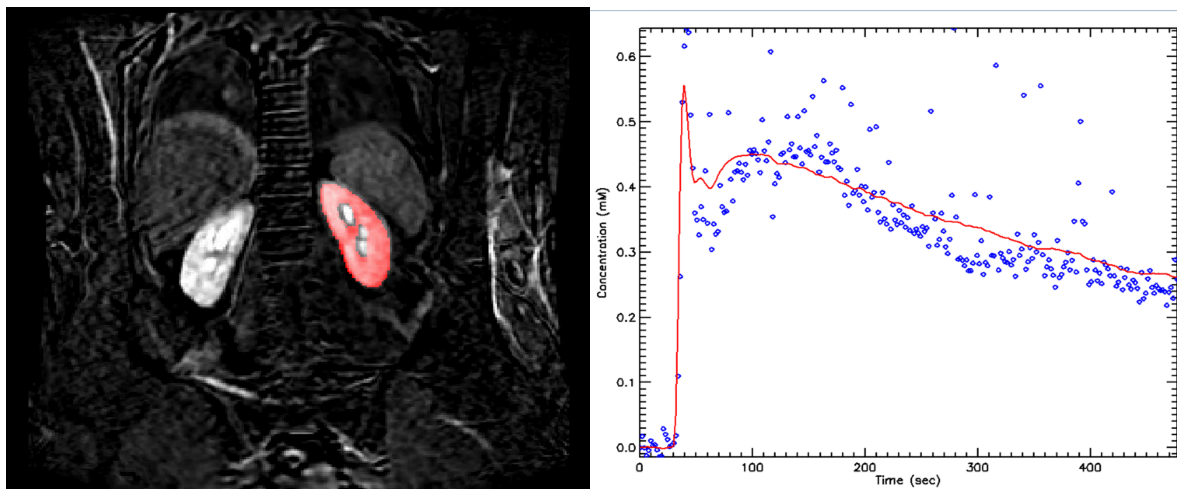


Figure 7.2B: Segmentation of left renal parenchyma on DCE-derived map and derived concentration-time curve

The concentration-time curves for each kidney and the aorta were estimated (Figure 7.2A and 7.2B), assuming a nonlinear relationship between signal intensity and contrast agent concentration. Tracer-kinetic analysis was performed using a two-compartment filtration model, describing the kidney as vascular (pre-glomerular) and tubular (post-glomerular)

spaces. This analysis, implemented in PMI software, enabled the determination of the following physiological parameters:

1. Renal perfusion (mL/min/100 mL): Averaged for the right and left kidneys and cortices.
2. Glomerular filtration rate (GFR; mL/min): Calculated as the product of tubular flow and regional volume.
3. Vascular and tubular mean transit time (MTT): The time blood takes to traverse the vascular and tubular volumes, respectively.
4. Renal tubular flow (ml/min/100ml): The rate of fluid within the kidney's tubular system, originating as renal ultrafiltrate and exiting kidneys as urine in ureter.
5. Kidney extraction fraction (%): The percentage of plasma entering the kidneys which is filtered.
6. Kidney volume (mL): The volume of the renal parenchyma, presented as the total volume of both kidneys.

The reliability of DCE-MRI analysis using PMI software has been previously validated through assessments of inter-observer variability, involving both novice and expert observers. Although these findings have not yet been published, they underscore the robustness of the analysis method, obviating the need for further validation within this study.

7.2.6 Statistical analysis plan

The data management process began with data cleaning, where the dataset was inspected for missing values, outliers, and data entry errors. The results were tested for normality and subsequent statistical comparisons between groups were made. A variety of statistical analysis techniques were used, depending on the distribution of the data. To assess for the distribution of the data, a histogram was drawn. This enabled easy identification of whether the data being analysed was normally distributed or skewed. Descriptive statistics was run to understand the distribution and identify anomalies. Summary statistics such as mean,

standard deviation, minimum, and maximum values for continuous variables were extracted by descriptive statistics. Frequency distributions were used for categorical variables.

The demographic characteristics of the participants were summarised using means and standard deviations (SD) for continuous variables and counts and percentages (%) for categorical variables. The baseline characteristics were presented for the total sample (n=81) and further stratified into type 1 (n=33) and type 2 (n=48) diabetes groups. Kidney parameters, derived from the DCE-MRI dataset analyses, were similarly presented in a table. Standardisation of renal volume was achieved by correlating it with body surface area, as kidney volume and length are influenced by body size, subsequently normalising all measurements to renal volume per 1.73 m².

Correlation analyses were conducted, with the Pearson Correlation Coefficient, and the Spearman Rank Correlation was used if the assumption of normality was violated. A heatmap with correlation analysis was demonstrated to explore the associations between clinical and physiological variables, with a primary focus on identifying factors influencing renal perfusion parameters.

Initial comparisons of renal perfusion between participants with and without CAN, irrespective of diabetes type, were conducted using non-parametric tests such as Mann-Whitney U test to check for statistical significance. The same test was employed for more detailed comparisons of renal perfusion between different eGFR grades and within each type of diabetes (T1 and T2DM). The Chi-square test was utilised to evaluate the statistical significance and correlation of categorical variables within each group. Further analyses included correlation and comparison of perfusion parameters across different stages or severity levels of CAN using a Kruskal-Wallis's test due to the absence of the normality of the distribution and homogeneity of variances across groups.

All statistical analyses were performed using SPSS (SPSS version 29, IBM Corporation, Armonk, New York, United States of America), ensuring comprehensive data management, statistical testing, and result visualisation. Graphical representations like box plots, tables and heatmap were used to visualise the distribution and relationships within the data.

Results were presented in tables and graphs, with accompanying narrative descriptions. Statistical significance was determined at a p-value of less than 0.05, and effect sizes were reported to provide context to the findings. Utilising SPSS, robust and comprehensive statistical analysis was obtained to effectively address the study's objectives and hypotheses.

7.3 Results

7.3.1 Patient characteristics and features summary

The study initially aimed to recruit 100 participants; however, due to 18 failed MRI sessions by factors such as high BMI, claustrophobia, unreported metallic prostheses, and withdrawals, the recruitment was increased to 118. Despite this adjustment, 7 datasets were excluded due to poor image quality or loading errors in the PMI software. Additionally, 12 participants did not undergo DCE-MRI due to refusal of the contrast agent or a change of decision on the study day (Figure 7.3).

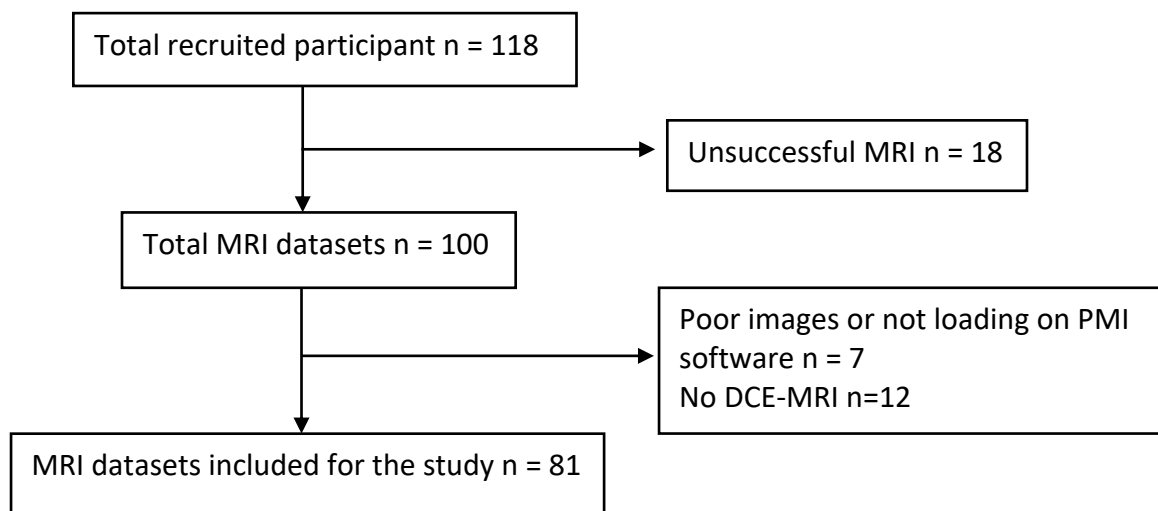


Figure 7.3: CONSORT diagram of participants and MRI data

Table 7.8 summarises the baseline demographic and clinical characteristics of 81 participants. The mean age was 62.3 (10.3) years, with a mean BMI of 29.3 (4.9) kg/m², an

average diabetes duration of 22 (13.7) years, and a mean hypertension duration of 7.5 (10) years. The average HbA1c was 63.5 (13.8) mmol/mol, mean eGFR was 80.7 (18.9) ml/min/1.73m², and mean UACR was 5.5 (27) mg/mmol.

The comparison between participants with T1 and T2DM revealed significant differences between the two groups (Table 7.8). Participants with T1DM were significantly younger, with a mean age of 57.2 (11.1) years, compared to 65.8 (8.1) years in the T2DM group ($P < 0.001$). BMI was also significantly lower in the T1DM group at 27.8 (5) kg/m², compared to 30.4 (4.7) kg/m² in the T2DM group ($P = 0.005$). The duration of diabetes was markedly longer in T1DM, averaging 33.6 (10.8) years, compared to 14.1 (9) years in the T2DM group ($P < 0.001$). eGFR was significantly higher in participants with T1DM at 88 (19) ml/min/1.73m² compared to 76 (17) ml/min/1.73m² in participants with T2DM ($P = 0.006$). However, UACR did not differ significantly between the two groups ($P = 0.070$). Lastly, the mean CAN score of overall group (1.6(0.6)), T1 (1.64 (0.6)) and T2DM (1.58 (0.6)) participants did not differ significantly ($p = 0.654$).

Table 7.8: Baseline demographics of overall, T1 and T2DM participants

| Baseline Characteristics | Total (n=81) | T1DM (n=33) | T2DM (n=48) | P value |
|--------------------------|--------------|--------------|--------------|---------|
| Age (years) | 62.3 (10.3) | 57.2 (11.1) | 65.8 (8.1) | < 0.001 |
| BMI (kg/m ²) | 29.3 (4.9) | 27.8 (5.0) | 30.4 (4.7) | 0.005 |
| Height (cm) | 169.4 (8.4) | 168.1 (9.0) | 170.3 (7.9) | 0.197 |
| Weight (kg) | 85.2 (15.1) | 79.5 (13.5) | 89.2 (15.1) | 0.004 |
| Haematocrit (%) | 43.2 (4.2) | 43.2 (4.1) | 43.1 (4.3) | 0.992 |
| Duration of DM (years) | 22.0 (13.7) | 33.6 (10.8) | 14.1 (9.0) | < 0.001 |
| Duration of HTN (years) | 7.5 (10) | 5.3 (9.6) | 8.9 (10.4) | 0.063 |
| Systolic (mmHg) | 136.3 (17.5) | 138.3 (19.9) | 134.9 (15.6) | 0.433 |

| | | | | |
|-----------------------------------|-------------|------------|------------|---------|
| Diastolic (mmHg) | 80.6 (9.2) | 80.4 (8.6) | 80.7 (9.7) | 0.802 |
| HbA1c (mmol/mol) | 63.5 (13.8) | 64 (13) | 63 (14) | 0.676 |
| eGFR (ml/min/1.73m ²) | 80.7 (18.9) | 88 (19) | 76 (17) | 0.006 |
| UACR (mg/mmol) | 5.5 (27) | 7.7 (39) | 4 (14) | 0.070 |
| Cholesterol (mmol/L) | 4.2 (0.9) | 4.2 (0.9) | 4.2 (1) | 0.779 |
| Triglyceride (mmol/L) | 1.7 (0.9) | 1.1 (0.7) | 2.1 (0.9) | < 0.001 |
| Gender, men, n (%) | 45 (55.6%) | 15 (45.5%) | 30 (62.5%) | |
| CAN score (tests) | 1.6 (0.6) | 1.64 (0.6) | 1.58 (0.6) | 0.654 |

7.3.2 Renal parameters from DCE-MRI

The DCE-MRI data in Table 7.9 demonstrates that renal perfusion, cortical perfusion, renal volume, extraction fraction, and mean transit time are consistent with reference values from the literature (412–415). Average kidney perfusion was 290 (126) ml/100ml/min, with a mean transit time of 8 (4) seconds. Cortical perfusion averaged 313 (104) ml/100ml/min, and the renal extraction fraction was 28 (8) %. The average renal volume was 135 (28) ml, normalized to 121 (26) ml/1.73m². The left kidney GFR was 49 (21) ml/min/1.73m², and the right kidney GFR was 53 (22) ml/min/1.73m². These values provide an overview of renal blood flow and functional parameters in the study participants.

Table 7.9: Summary values of renal blood flow parameters measured by DCE-MRI

| MRI parameters (units) | Mean (SD) (n=81) | Minimum | Maximum |
|---|-----------------------------|----------------|----------------|
| LK perfusion (ml/100ml/min) | 285 (130) | 49 | 700 |
| RK perfusion (ml/100ml/min) | 292 (127) | 70 | 766 |
| Average kidney perfusion (ml/100ml/min) | 290 (126) | 60 | 734 |
| LK blood mean transit time (sec) | 8 (6) | 3.0 | 47 |
| RK blood mean transit time (sec) | 8 (3) | 3.3 | 28 |
| Average kidney blood MTT (sec) | 8 (4) | 3.4 | 29 |
| Left cortical perfusion (ml/100ml/min) | 307 (111) | 81 | 832 |
| Right cortical perfusion (ml/100ml/min) | 319 (104) | 90 | 650 |
| Average cortical perfusion (ml/100ml/min) | 313 (104) | 85 | 711 |
| LK extraction fraction (%) | 27 (9) | 9 | 54 |
| RK extraction fraction (%) | 28 (8) | 12 | 59 |
| Average renal extraction fraction (%) | 28 (8) | 10 | 54 |
| LK volume (ml) | 133 (30) | 65 | 217 |
| LK volume (ml/1.73m ²) | 117 (25) | 63 | 179 |
| RK volume (ml) | 138 (30) | 79 | 219 |
| RK volume (ml/1.73m ²) | 124 (28) | 61 | 187 |
| Average renal volume (ml) | 135 (28) | 78 | 212 |
| Average renal volume (ml/1.73m ²) | 121 (26) | 66 | 184 |
| LK GFR (ml/min/1.73m ²) | 49 (21) | 9.5 | 122 |

| | | | |
|-------------------------------------|---------|------|-----|
| RK GFR (ml/min/1.73m ²) | 53 (22) | 16 | 131 |
| LK tubular flow (ml/100ml/min) | 42 (16) | 7.3 | 86 |
| RK tubular flow (ml/100ml/min) | 43 (15) | 11.2 | 83 |
| Average tubular flow (ml/100ml/min) | 42 (15) | 9.6 | 83 |
| LK tubular MTT (min) | 4 (15) | 0.44 | 136 |
| RK tubular MTT (min) | 3 (14) | 0 | 125 |
| Average tubular MTT (min) | 4 (14) | 0.6 | 131 |

LK = left kidney, RK = right kidney, MTT = mean transit time, GFR = glomerular filtration rate

7.3.3 Correlation analysis

A correlation analysis was performed to investigate the relationships between various clinical and physiological variables, with a particular focus on identifying factors that may influence renal perfusion parameters. This analysis aimed to detect significant correlations, offering insights into how different variables interact. Given the distribution patterns of the data, Spearman's rank correlation was employed due to its non-parametric nature, making it suitable for assessing the strength and direction of monotonic relationships between variables. This method allows for a robust examination of potential associations without the assumption of normality.

The heat map (Figure 7.4) revealed significant correlations between various clinical variables and MRI measures of kidney perfusion, with off-diagonal values ranging from -0.56 to 0.70. Notably, average kidney perfusion (AKP), cortical perfusion (ACP), and tubular flow (ATF) negatively correlated with age ($r = -0.49, -0.54, \text{ and } -0.38$, respectively; $p < 0.001$) and positively correlated with eGFR ($r = 0.33, 0.43, \text{ and } 0.27$; $p < 0.001$). Kidney mean transit time (AKMTT) and extraction fraction (AKEF) showed positive correlations with age ($r = 0.33 \text{ and } 0.26$; $p < 0.05$). Significant positive correlations were also observed between key kidney

parameters (AKP, ACP, and ATF), while these parameters were negatively correlated with AKMTT, ATMTT, and AKEF.

Age exhibited a strong negative correlation with eGFR ($r = -0.32$, $p < 0.001$). UACR had limited significant associations with renal parameters, except for a positive correlation with AKMTT ($r = 0.24$, $p < 0.05$). Duration of diabetes was negatively correlated with BMI ($r = -0.32$, $p < 0.001$), BSA ($r = -0.42$, $p < 0.001$), and triglycerides ($r = -0.56$, $p < 0.001$). Additionally, HbA1c was positively correlated with UACR ($r = 0.25$, $p < 0.05$), and SBP and DBP were strongly correlated with each other ($r = 0.66$, $p < 0.001$). These findings highlight important associations between kidney perfusion metrics and various health parameters, underscoring the potential impact of metabolic factors on renal perfusion.

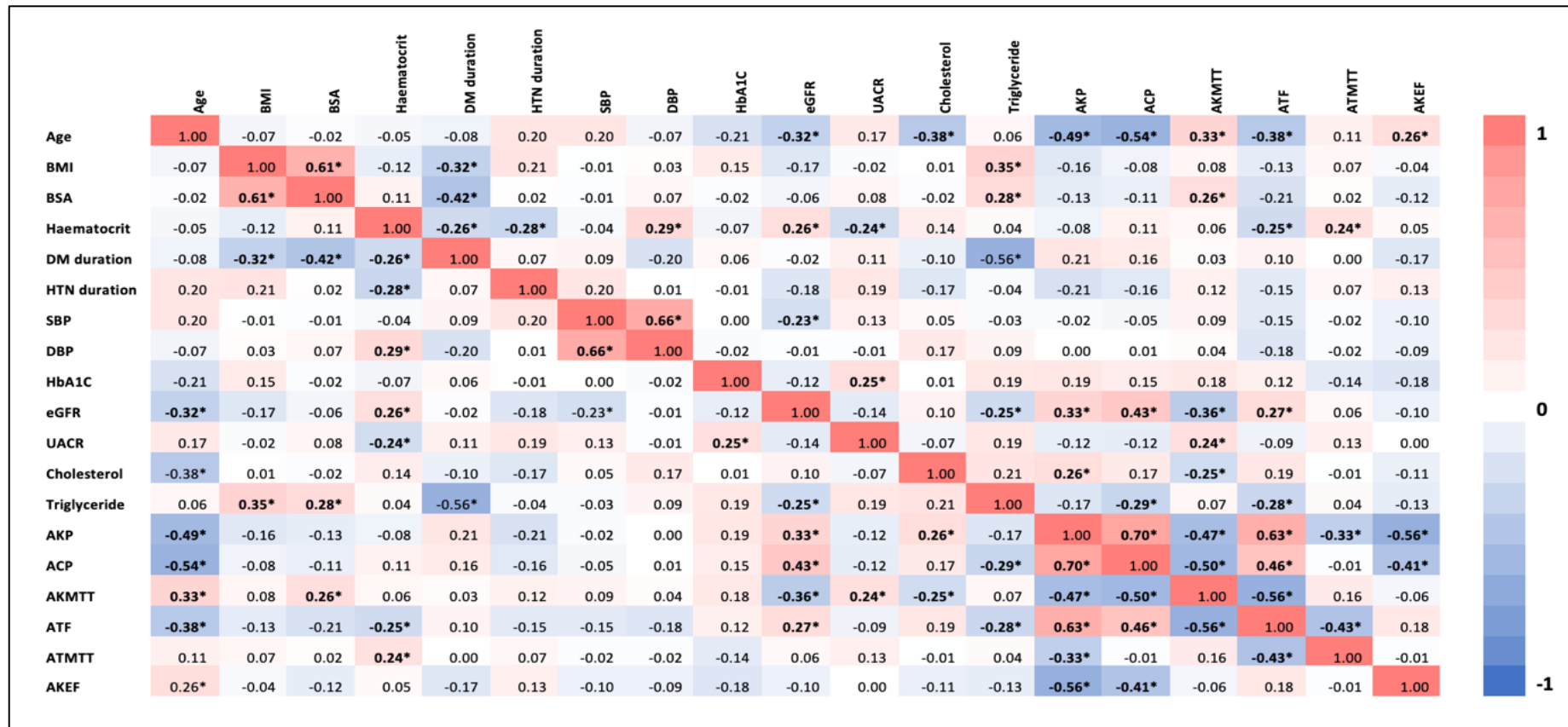


Figure 7.4: Correlation heatmap demonstrating the correlation between renal perfusion parameters with different demographic data.

(Correlations with p value < 0.05 are significant and are in **bold format and marked with *** for easy visualisation)

BMI= body mass index, BSA= body surface area, DM= diabetes mellitus, HTN= hypertension, SBP= systolic blood pressure, DBP= diastolic blood pressure, HbA1C = haemoglobin A1C, eGFR = estimated glomerular filtration rate, UACR = urinary albumin-creatinine-ratio, AKP = average kidney perfusion, ACP = average cortical perfusion, AKMTT = average kidney mean transit time, ATF = average tubular flow, ATMTT = average tubular mean transit time, AKEF = average kidney extraction fraction.

7.3.4 Comparison of participants characteristics in no CAN and CAN groups

No CAN Vs CAN (Overall data)

Table 7.10 compares participant characteristics between groups with (n=54) and without (n=27) CAN. Participants in the CAN group were slightly younger (61.3 (11) vs. 64.2 (8.6) years; $p = 0.328$), with a longer diabetes duration (23.2 (12.8) vs. 19.7 (15.4) years; $p = 0.167$), though these differences were not statistically significant. eGFR was higher in the CAN group (82.8 (20.3) vs. 76.6 (15) ml/min/1.73m²; $p = 0.096$), while UACR was significantly elevated (7.8 (32.9) vs. 0.9 (1.5) mg/mmol; $p = 0.042$). No significant differences were found in lipid profiles, insulin use, ACEI/ARBs, SGLT2i, statin use, or cardiovascular disease events between the groups. Overall, most baseline characteristics did not differ significantly except for UACR, body weight, and SBP.

Table 7.10: Comparison of participants characteristics between no CAN and CAN group (Overall data)

| Baseline Characteristics | No CAN group Mean (SD) (n=27) | CAN group Mean (SD) (n=54) | P value |
|--------------------------|-------------------------------------|----------------------------------|---------|
| Age (years) | 64.2 (8.6) | 61.3 (11) | 0.328 |
| BMI (kg/m ²) | 30.2 (4.2) | 28.9 (5.2) | 0.096 |
| Height (cm) | 171.1 (7.7) | 168.5 (8.6) | 0.174 |
| Weight (kg) | 89.7 (12.5) | 83 (15.9) | 0.032 |

| | | | |
|----------------------------|-------------|-------------|--------|
| Haematocrit (%) | 44 (4.4) | 42.7 (4) | 0.266 |
| Duration of DM (years) | 19.7 (15.4) | 23.2 (12.8) | 0.167 |
| Duration of HTN (years) | 5.7 (8.1) | 8.4 (11) | 0.419 |
| Systolic (mmHg) | 141 (13) | 134 (18.9) | 0.023 |
| Diastolic (mmHg) | 81.4 (8.2) | 80 (9.7) | 0.464 |
| HbA1C(mmol/mol) | 64.3 (11.6) | 63 (14.8) | 0.426 |
| eGFR (ml/min/1.73m2) | 76.6 (15) | 82.8 (20.3) | 0.096 |
| UACR (mg/mmol) | 0.9 (1.5) | 7.8 (32.9) | 0.042 |
| total cholesterol (mmol/L) | 4.1 (0.9) | 4.3 (1) | 0.521 |
| Triglyceride (mmol/L) | 1.8 (1) | 1.7 (0.9) | 0.673 |
| Gender, men, n (%) | 17 (62.9%) | 28 (51.8%) | *0.343 |
| *Chi-square test | | | |
| Retinopathy, n (%) | 16 (59.2%) | 35 (64.8) | *0.625 |
| Smoking status | | | |
| Non-smoker | 13 (48.1%) | 28 (51.8%) | *0.760 |
| Current smoker | 6 (22.2%) | 14 (25.9%) | |
| Ex-smoker | 8 (29.6%) | 12 (22.2%) | |
| Insulin use, n (%) | 12 (44.4%) | 30 (55.5%) | *0.345 |
| ACEi/ ARB use, n (%) | 12 (44.4%) | 25 (46.2%) | *0.875 |
| SGLT2 inhibitor, n (%) | 5 (18.5%) | 12 (22.2%) | *0.70 |
| Statin, n (%) | 24 (88.9%) | 39 (72.2%) | *0.089 |
| CVD events, n (%) | 3 (1.1%) | 5 (9.2%) | *0.792 |

No CAN Vs CAN (T1DM)

Table 7.11 presents key differences in baseline characteristics between participants with and without CAN in T1DM. Participants with CAN were significantly younger, with a mean age of 54.3 (11) years compared to 63.8 (6.8) years in the no CAN group ($P = 0.013$). SBP was also significantly lower in the CAN group, averaging 133.9 (21) mmHg, compared to 148.5 (13.1) mmHg in the no CAN group ($P = 0.018$). Other variables, such as BMI, diabetes duration, hypertension duration, DBP, HbA1c, eGFR, UACR, total cholesterol, and triglyceride levels, did not differ significantly between the groups. However, retinopathy was more prevalent in the CAN group (91%) compared to the no CAN group (90%, $P < 0.001$), and cardiovascular disease events were more common in the CAN group (8.7%) compared to none in the no CAN group ($P < 0.001$). These findings indicate that age, SBP, retinopathy, and CVD are more strongly associated with CAN in T1DM.

Table 7.11: Comparison of characteristics between no CAN and CAN group (T1DM)

| MRI parameters | No CAN (n=10) | CAN (n=23) | P value |
|-----------------------------------|---------------|-------------|---------|
| Age (years) | 63.8 (6.8) | 54.3 (11) | 0.013 |
| BMI (kg/m ²) | 28.6 (3.9) | 27.4 (5.4) | 0.253 |
| Duration of DM (years) | 35.5 (11.6) | 32.8 (10.6) | 0.550 |
| Duration of HTN (years) | 6.2 (8.9) | 4.9 (10) | 0.499 |
| SBP (mmHg) | 148.5 (13.1) | 133.9 (21) | 0.018 |
| DBP (mmHg) | 82.2 (6.9) | 79.5 (9.2) | 0.363 |
| HbA1C (mmol/mol) | 60.8 (11.6) | 65.3 (13.8) | 0.406 |
| eGFR (ml/min/1.73m ²) | 81.4 (14.4) | 90.6 (20) | 0.123 |
| UACR (mg/mmol) | 0.6 (0.6) | 10.8 (46.8) | 0.384 |
| Total cholesterol (mmol/L) | 4.0 (0.6) | 4.3 (0.9) | 0.675 |
| Triglyceride (mmol/L) | 0.9 (0.3) | 1.2 (0.8) | 0.325 |

| | | | |
|-------------------------|------------|--------------|-----------|
| Retinopathy present (%) | 9/10 (90%) | 21/23 (91%) | * < 0.001 |
| *Chi-Square tests | | | |
| CVD events present (%) | 0/10 (0%) | 2/23 (8.7%) | * < 0.001 |
| Use of ACEI/ ARB (%) | 5/10 (50%) | 9/23 (39.1%) | *0.384 |

No CAN Vs CAN (T2DM)

In the T2DM, age and BMI were similar between participants with and without CAN (P = 0.567 and P = 0.169, respectively) (Table 7.12). The CAN group had a significantly longer diabetes duration at 16.1 (9.1) years compared to 10.3 (7.9) years in the no CAN group (P = 0.023). While hypertension duration tended to be longer in the CAN group, this difference was not significant (P = 0.089). BP, HbA1c, eGFR, UACR, and lipid parameters were comparable between the groups. Retinopathy prevalence was similar (P = 0.386), while cardiovascular events were significantly more frequent in the no CAN group (P < 0.001). Use of ACEI/ARBs did not differ significantly between groups.

Table 7.12: Comparison of characteristics between no CAN and CAN group (T2DM)

| MRI parameters | No CAN (n=17) | CAN (n=31) | P value |
|-----------------------------------|---------------|--------------|---------|
| Age (years) | 64.4 (9.7) | 66.5 (7.2) | 0.567 |
| BMI (kg/m ²) | 31.2 (4.2) | 29.9 (4.9) | 0.169 |
| Duration of DM (years) | 10.3 (7.9) | 16.1 (9.1) | 0.023 |
| Duration of HTN (years) | 5.3 (7.9) | 10.9 (11.1) | 0.089 |
| SBP (mmHg) | 137 (12) | 133.8 (17.4) | 0.306 |
| DBP (mmHg) | 81 (9) | 80.5 (10.1) | 0.698 |
| HbA1C (mmol/mol) | 66.4 (11.5) | 61.3 (15.5) | 0.110 |
| eGFR (ml/min/1.73m ²) | 73.8 (15.3) | 77 (18.6) | 0.371 |
| UACR (mg/mmol) | 1.1 (1.8) | 5.5 (17.2) | 0.058 |

| | | | |
|--|--------------|---------------|-----------|
| Total cholesterol (mmol/L) | 4.1 (1.1) | 4.2 (1) | 0.666 |
| Triglyceride (mmol/L) | 2.4 (0.9) | 2.0 (0.9) | 0.120 |
| Retinopathy present (%) * Chi-Square test | 7/17 (41.2%) | 14/31 (45.1%) | * < 0.386 |
| CVD events present (%) | 3/17 (17.6%) | 3/31 (9.7%) | * < 0.001 |
| Use of ACEI/ ARB (%) | 7/17 (41.2%) | 16/31 (51.6%) | * 0.773 |

After detailed comparison of participants characteristics, the next section will compare the renal perfusion parameters from DCE-MRI.

7.3.5 Comparison of renal perfusion and parameters in no CAN and CAN groups

After exploring the potential correlations between various variables and factors affecting renal perfusion through the heat map, data analysis was conducted by stratifying and comparing renal parameters in different groups of participants.

No CAN Vs CAN (Overall cohort)

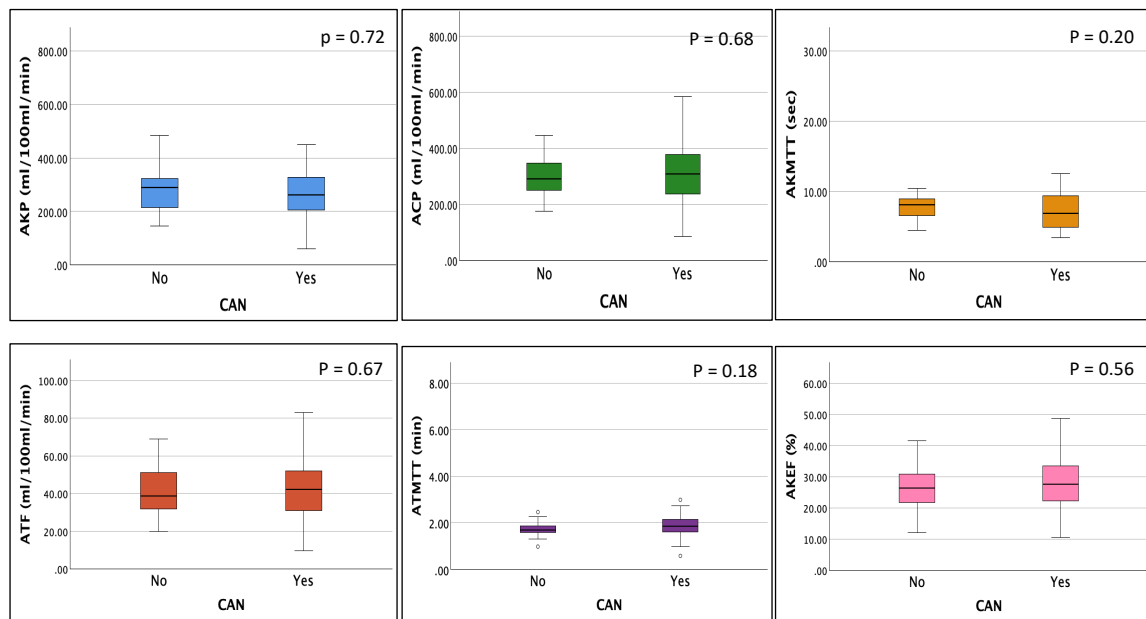


Figure 7.5: Comparison of renal parameters between no CAN and CAN groups (Overall cohort)

AKP, average kidney perfusion; ACP, average cortical perfusion; AKMTT, average kidney mean transit time; ATF, average tubular flow; ATMTT, average tubular mean transit time; AKEF, average kidney extraction fraction.

In a comparison of MRI-derived renal parameters between patients without CAN (n=27) and those with CAN (n=54), no statistically significant differences were observed (Figure 7.5).

The AKP was 293 (123) ml/100ml/min in patients without CAN compared to 286 (129) ml/100ml/min in those with CAN ($p = 0.72$). Similarly, the ACP was 310 (104) ml/100ml/min in the no-CAN group versus 315 (106) ml/100ml/min in the CAN group ($p = 0.68$). The AKMTT was 8.3 (3) seconds in patients without CAN and 8.1 (4.9) seconds in patients with CAN ($p = 0.20$). Furthermore, the ATF was 41 (13) ml/100ml/min in the no-CAN group compared to 43 (16) ml/100ml/min in the CAN group ($p = 0.67$), while the ATMTT was 1.7 (0.4) minutes versus 2.1 (1.8) minutes, respectively ($p = 0.18$). Lastly, the AKEF was 27 (9) % in the no-CAN group and 28 (8) % in the CAN group ($p = 0.56$).

No CAN Vs CAN (G1, eGFR ≥ 90 ml/min/1.73m²)

Given the lack of significant differences in renal MRI parameters between participants with and without CAN, further analysis was conducted focusing on participants with G1, eGFR of 90 ml/min/1.73m² or higher (n=21). This stratification was implemented under the assumption that certain renal parameter values may be influenced by renal function, and to determine whether subtle differences that were not apparent in the overall cohort might be revealed by comparing the renal MRI-derived parameters in the presence or absence of CAN.

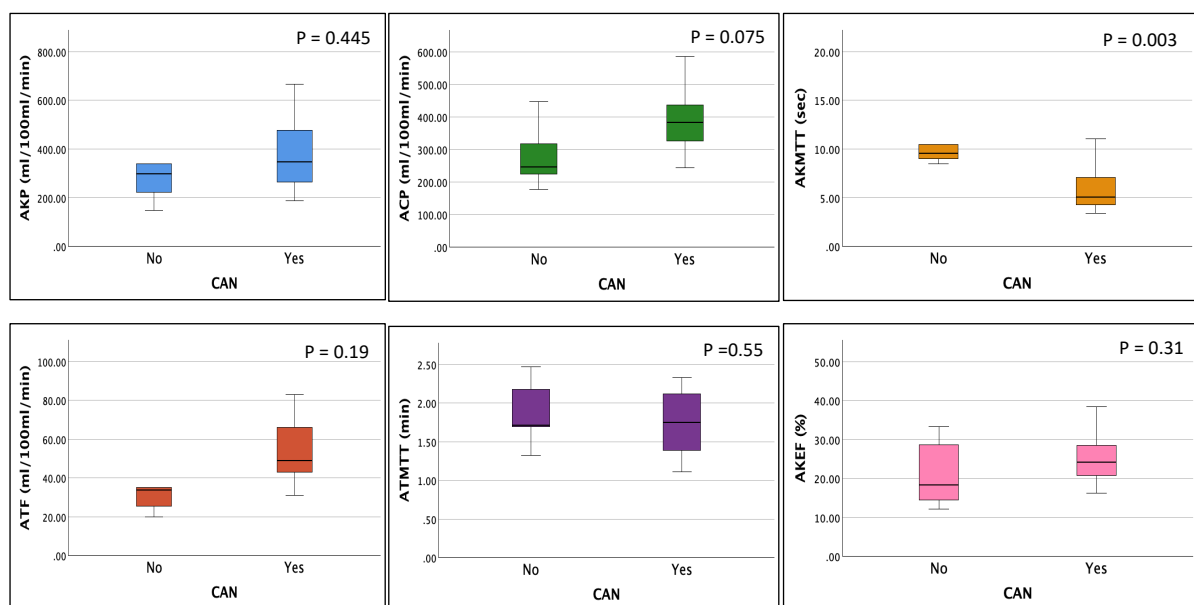


Figure 7.6: Comparison of renal parameters between no CAN and CAN groups (eGFR ≥ 90 ml/min/1.73m²)

AKP, average kidney perfusion; ACP, average cortical perfusion; AKMTT, average kidney mean transit time; ATF, average tubular flow; ATMTT, average tubular mean transit time; AKEF, average kidney extraction fraction.

In a subgroup analysis of participants with eGFR of 90 ml/min/1.73m² or higher, renal MRI parameters were compared between those without CAN (n=5) and those with CAN (n=16) (Figure 7.6). The AKP was 347 (228) ml/100ml/min in the no-CAN group compared to 385 (148) ml/100ml/min in the CAN group, with a p-value of 0.445. The ACP was 282 (105) ml/100ml/min in the no-CAN group and 388 (90) ml/100ml/min in the CAN group (p = 0.075). A significant difference was observed in the AKMTT, which was 10.6 (2.9) seconds in

participants without CAN versus 5.9 (2.1) seconds in those with CAN ($p = 0.003$). The ATF was 33.5 (13) ml/100ml/min in the no-CAN group and 53 (15) ml/100ml/min in the CAN group ($p = 0.19$). The ATMTT was 1.9 (0.4) minutes in the no-CAN group compared to 1.7 (0.4) minutes in the CAN group ($p = 0.55$). Lastly, the AKEF was 21 (9) % in the no-CAN group and 26 (8) % in the CAN group, with a p-value of 0.31.

No CAN Vs CAN (G2, eGFR 60 - 89 ml/min/1.73m²)

Similarly, in a comparative analysis of renal MRI parameters between participants without CAN ($n=20$) and those with CAN ($n=32$) in G2, no statistically significant differences were observed (Figure 7.7). The AKP was 289 (89) ml/100ml/min in the no-CAN group compared to 251 (88) ml/100ml/min in the CAN group ($p = 0.132$). The ACP was 329 (103) ml/100ml/min in participants without CAN and 302 (90) ml/100ml/min in those with CAN ($p = 0.328$). The AKMTT was 7.7 (2.9) seconds in the no-CAN group and 7.6 (3.1) seconds in the CAN group ($p = 0.763$). The ATF was 43 (13) ml/100ml/min in the no-CAN group and 40 (15) ml/100ml/min in the CAN group ($p = 0.486$). The ATMTT was 1.7 (0.4) minutes in participants without CAN compared to 2.1 (1) minute in those with CAN, reaching significance with a p-value of 0.046. Lastly, the AKEF was 27 (8) % in the no-CAN group and 30 (7) % in the CAN group ($p = 0.214$).

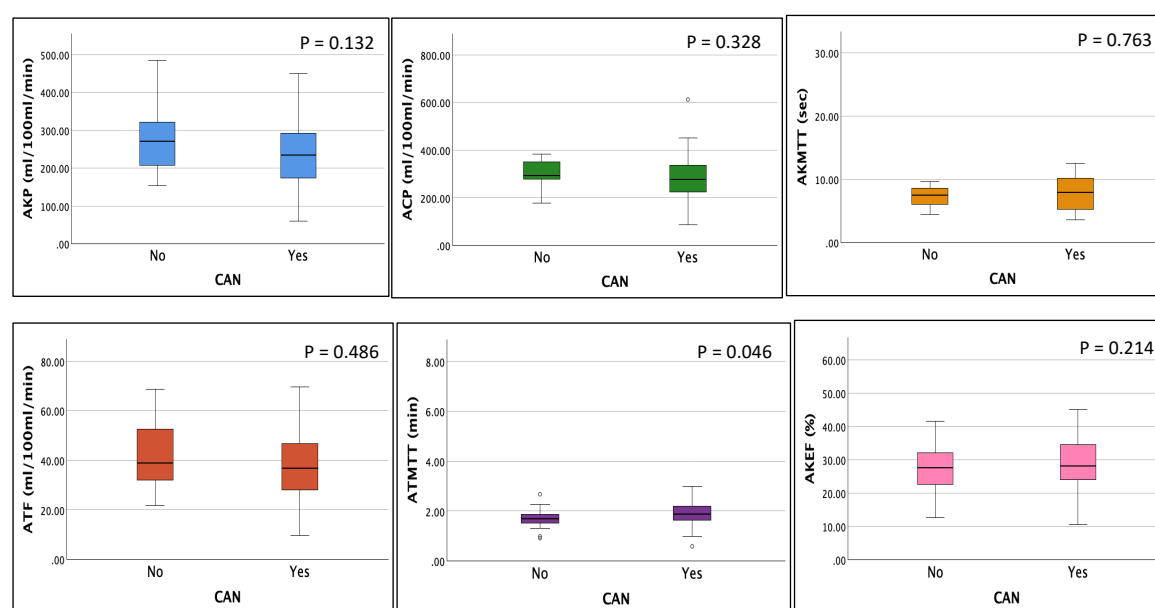


Figure 7.7: Comparison of renal parameters between no CAN and CAN groups (G2, eGFR 60 – 89 ml/min/1.73m²)

AKP, average kidney perfusion; ACP, average cortical perfusion; AKMTT, average kidney mean transit time; ATF, average tubular flow; ATMTT, average tubular mean transit time; AKEF, average kidney extraction fraction.

No CAN Vs CAN (G3, eGFR 30 - 59 ml/min/1.73m²)

The comparison of renal MRI parameters between participants with and without CAN was not performed in the subgroup with stage G3 (eGFR 30-59 ml/min/1.73m²). This decision was made due to the limited number of participants in this category, with only 6 participants in the CAN group and 2 in the no-CAN group.

No CAN Vs CAN (T1DMcohort)

In order to explore potential differences in pathophysiology and to investigate whether CAN has a similar impact on renal perfusion in T1DM, a further analysis was conducted. Renal MRI parameters were compared between those without CAN (n=10) and those with CAN (n=23) (Figure 7.8). The AKP was 291 (57) ml/100ml/min in the no-CAN group compared to 369 (138) ml/100ml/min in the CAN group (p = 0.123). The ACP was 351 (140) ml/100ml/min in participants without CAN and 368 (110) ml/100ml/min in those with CAN (p = 0.363). A statistically significant difference was observed in the AKMTT, which was 9.4 (4.3) seconds in the no-CAN group compared to 6.8 (3.9) seconds in the CAN group (p = 0.018). The ATF was 41 (14) ml/100ml/min in the no-CAN group and 52 (17) ml/100ml/min in the CAN group (p = 0.133). The ATMTT was similar between groups, being 1.8 (0.5) minutes in the no-CAN group and 1.7 (0.5) minutes in the CAN group (p = 0.686). Lastly, the AKEF was 25 (7) % in the no-CAN group and 26 (7) % in the CAN group, with a p-value of 1.

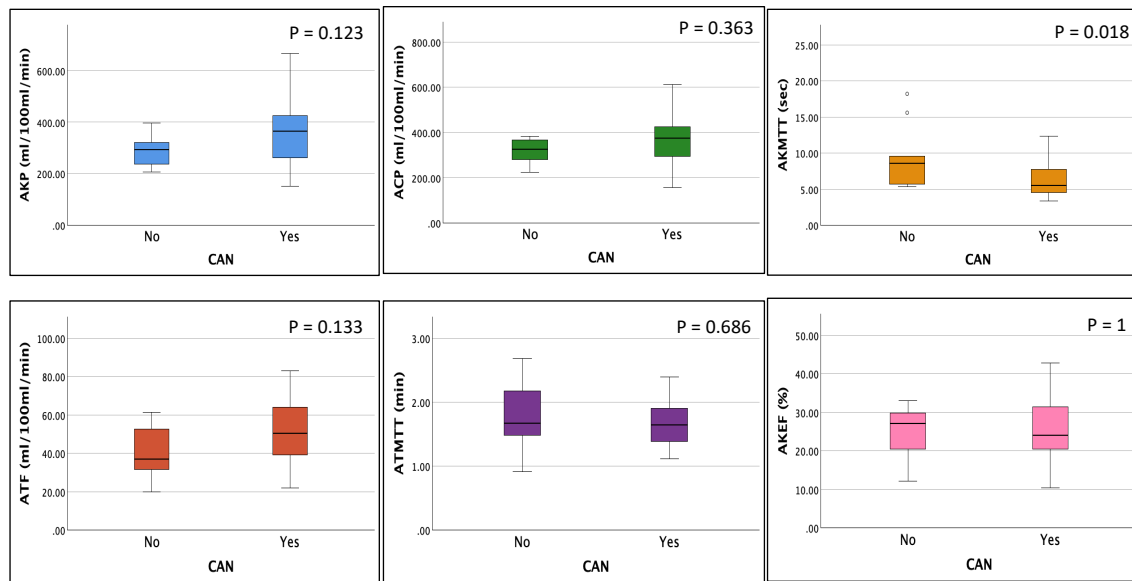


Figure 7.8: Comparison of renal parameters between no CAN and CAN groups (T1DM cohort)

AKP, average kidney perfusion; ACP, average cortical perfusion; AKMTT, average kidney mean transit time; ATF, average tubular flow; ATMTT, average tubular mean transit time; AKEF, average kidney extraction fraction.

No CAN Vs CAN (T2DM cohort)

The comparison of renal perfusion in T2DM cohort between participants with (n=31) or without CAN (n=17) shows similar perfusion findings (Figure 7.9). The AKP was 295 (150) ml/100ml/min in the no-CAN group compared to 224 (78) ml/100ml/min in the CAN group (p = 0.146). The ACP was 286 (71) ml/100ml/min in participants without CAN and 275 (84) ml/100ml/min in those with CAN (p = 0.659). The AKMTT was 7.6 (1.6) seconds in the no-CAN group and 9.2 (5.3) seconds in the CAN group (p = 0.484). The ATF was 41 (13) ml/100ml/min in the no-CAN group compared to 37 (13) ml/100ml/min in the CAN group (p = 0.407). Notably, the ATMTT was significantly different, with 1.7 (0.3) minutes in participants without CAN and 2.2 (1.1) minutes in those with CAN (p = 0.014). The AKEF was 28 (10) % in the no-CAN group and 30 (8) % in the CAN group (p = 0.348).

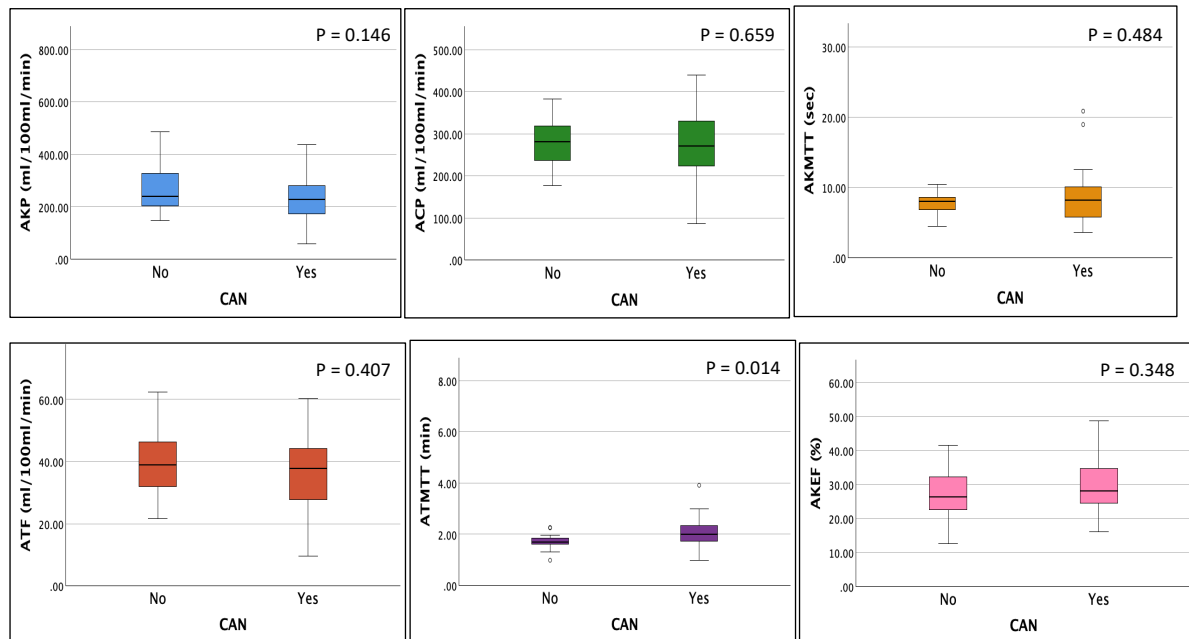


Figure 7.9: Comparison of renal parameters between no CAN and CAN groups (T2DM cohort)

AKP, average kidney perfusion; ACP, average cortical perfusion; AKMTT, average kidney mean transit time; ATF, average tubular flow; ATMTT, average tubular mean transit time; AKEF, average kidney extraction fraction.

No CAN Vs CAN (G2, T1 and T2DM cohort)

Further analysis of renal MRI parameters in the T1 and T2DM cohorts was stratified according to different eGFR categories (G1-G3) to assess whether there was any difference in pathophysiology which could lead to significant differences in renal parameters in CAN group. However, due to the small sample sizes within each eGFR group, analysis was only feasible for participants with stage G2 eGFR (60-89 ml/min/1.73m²), where more balanced numbers were available in each CAN category.

In the T1DM cohort, the distribution of participants across the eGFR grades was as follows: G1 (n=13, No CAN=3, CAN=10), G2 (n=19, No CAN=7, CAN=12), and G3 (n=1, CAN=1). For the T2DM cohort, the corresponding distributions were: G1 (n=8, No CAN=2, CAN=6), G2 (n=33, No CAN=13, CAN=20), and G3 (n=7, No CAN=2, CAN=5). Given the limited participant numbers in G1 and G3 for both cohorts, the statistical analysis focused solely on the G2

group, where participant numbers were sufficiently comparable across CAN categories to yield meaningful insights.

T1DM cohort (G2)

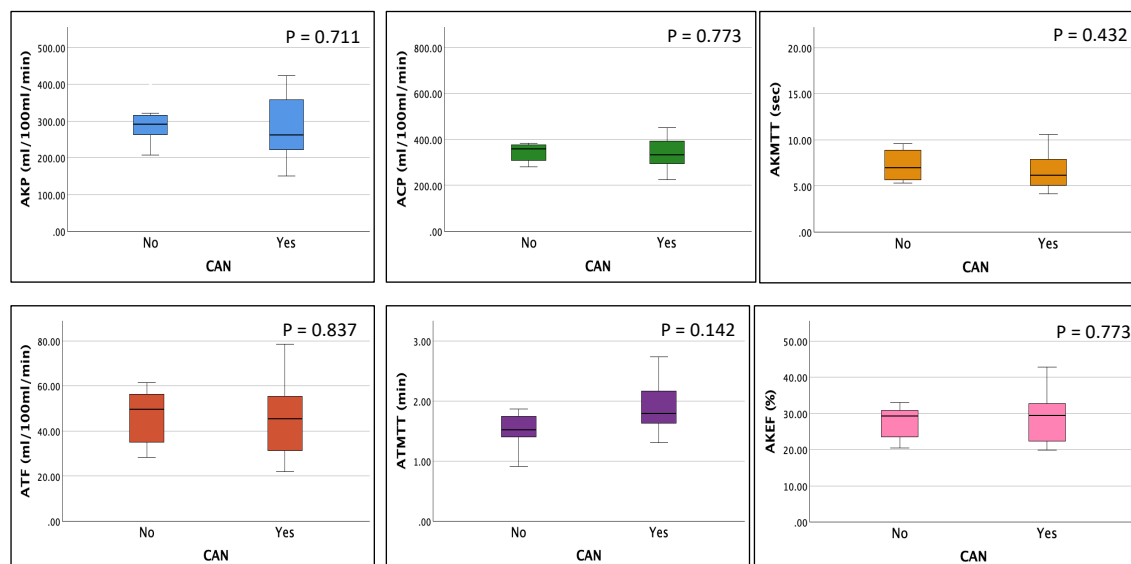


Figure 7.10: Comparison of renal parameters between no CAN and CAN groups (G2, T1DM cohort)

AKP, average kidney perfusion; ACP, average cortical perfusion; AKMTT, average kidney mean transit time; ATF, average tubular flow; ATMTT, average tubular mean transit time; AKEF, average kidney extraction fraction.

In participants with T1DM and G2 eGFR (60-89 ml/min/1.73m²), a comparison of renal MRI parameters between those without CAN (n=7) and those with CAN (n=12) revealed no statistically significant differences (Figure 7.10). AKP was 293 (61) ml/100ml/min in the no-CAN group versus 285 (88) ml/100ml/min in the CAN group (p = 0.711). ACP was 390 (152) ml/100ml/min in the no-CAN group compared to 357 (102) ml/100ml/min in the CAN group (p = 0.773). AKMTT was 8.5 (4.5) seconds in the no-CAN group and 6.9 (2.5) seconds in the CAN group (p = 0.432). ATF was 46 (13) ml/100ml/min in the no-CAN group and 45 (16) ml/100ml/min in the CAN group (p = 0.837). ATMTT was 1.6 (0.5) minutes in the no-CAN group compared to 1.9 (0.4) minutes in the CAN group (p = 0.142). AKEF was 27 (5) % in the no-CAN group and 29 (7)% in the CAN group (p = 0.773).

T2DM (G2)

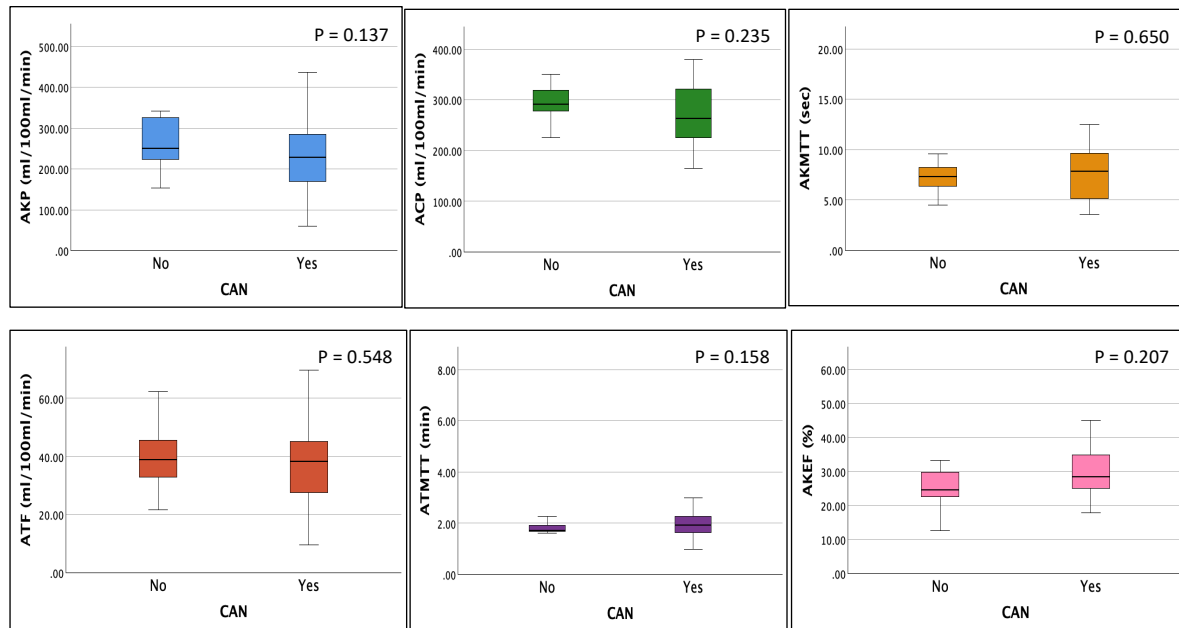


Figure 7.11: Comparison of renal parameters between no CAN and CAN groups (G2, T2DM cohort)

AKP, average kidney perfusion; ACP, average cortical perfusion; AKMTT, average kidney mean transit time; ATF, average tubular flow; ATMTT, average tubular mean transit time; AKEF, average kidney extraction fraction.

In participants with T2DM and G2 eGFR, renal MRI parameters also did not show statistically significant differences between those without CAN (n=13) and those with CAN (n=20) (Figure 7.11). AKP was 287 (103) ml/100ml/min in the no-CAN group compared to 230 (84) ml/100ml/min in the CAN group (p = 0.137). ACP was 296 (45) ml/100ml/min in the no-CAN group and 270 (64) ml/100ml/min in the CAN group (p = 0.235). AKMTT was 7.2 (1.5) seconds in the no-CAN group and 8.0 (3.5) seconds in the CAN group (p = 0.650). ATF was 41 (13) ml/100ml/min in the no-CAN group versus 38 (14) ml/100ml/min in the CAN group (p = 0.548). ATMTT averaged 1.7 (0.3) minutes in the no-CAN group and 2.2 (1.3) minutes in the CAN group (p = 0.158). AKEF was 27 (10) % in the no-CAN group and 30 (7) % in the CAN group (p = 0.207).

Following the comparison of renal MRI parameters between CAN and no-CAN groups, the next section of this chapter will focus on analysing renal parameters, with a particular emphasis on renal perfusion, across the different stages of CAN.

7.3.6 Comparison of renal perfusion in different stages of CAN

Given the documented association between increased progression of renal function decline and CAN in the literature, a comparative analysis of renal perfusion across different stages of CAN was conducted to determine if there is a significant decrease in renal perfusion or changes in renal parameters associated with the progression of the disease.

Different stages of CAN (Overall cohort)

Figure 7.12 presents the analysis of renal parameters across CAN stages among all participants (n=81). The groups were classified as No CAN (n=5), Early CAN (n=22), and Confirmed CAN (n=54). Due to the small number of participants with advanced CAN (n=2), it was added to confirmed CAN group. All parameters of renal perfusion did not show any significant difference across all stages of CAN.

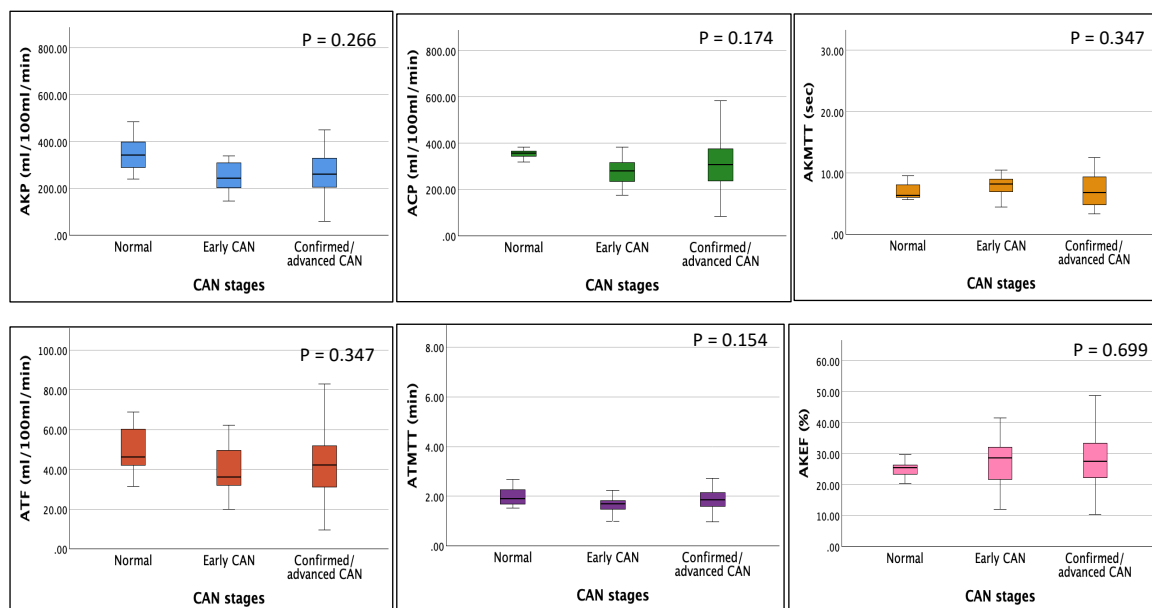


Figure 7.12: Comparison of renal parameters among different stages of CAN (Overall cohort)

AKP, average kidney perfusion; ACP, average cortical perfusion; AKMTT, average kidney mean transit time; ATF, average tubular flow; ATMTT, average tubular mean transit time; AKEF, average kidney extraction fraction.

In a comparison of renal MRI parameters across different stages of CAN, no statistically significant differences were observed in any of the measured parameters. AKP was 350 (95) ml/100ml/min in the no CAN group, 280 (126) ml/100ml/min in early CAN, and 286 (129) ml/100ml/min in confirmed/advanced CAN ($p = 0.266$). ACP was 354 (24) ml/100ml/min in the no CAN group, 300 (113) ml/100ml/min in early CAN, and 315 (106) ml/100ml/min in confirmed/advanced CAN ($p = 0.174$). The AKMTT was 7.1 (1.6) seconds, 8.5 (3.1) seconds, and 8.1 (4.9) seconds across the respective groups ($p = 0.347$). Tubular flow averaged 50 (15) ml/100ml/min in the no CAN group, 39 (12) ml/100ml/min in early CAN, and 43 (16) ml/100ml/min in confirmed/advanced CAN ($p = 0.347$). ATMTT was 2 (0.5) minutes, 1.7 (0.4) minutes, and 2 (0.9) minutes, respectively ($p = 0.154$). Lastly, AKEF was 25 (3) % in the no CAN group, 27 (9) % in early CAN, and 28 (8) % in confirmed/advanced CAN ($p = 0.699$).

Different stages of CAN (T1DM)

Additional analyses to assess renal perfusion across different stages of CAN was conducted to explore whether increased severity of CAN has a progressively greater impact on renal perfusion. Literature has suggested that increased CAN severity correlates with increased albuminuria, and increased extent of renal decline.

The comparison of renal perfusion among different stages of CAN in participants with T1DM; no CAN ($n=2$), early CAN ($n=8$), confirmed CAN ($n=23$) and no advanced CAN, no statistically significant differences were observed (Figure 7.13). AKP was 344 (76) ml/100ml/min in the no CAN group, 278 (49) ml/100ml/min in early CAN, and 369 (138) ml/100ml/min in confirmed CAN ($p = 0.249$). Cortical perfusion averaged 362 (7) ml/100ml/min in the no CAN group, 349 (159) ml/100ml/min in early CAN, and 368 (110) ml/100ml/min in confirmed CAN ($p = 0.551$). The AKMTT was 7.6 (2.7) seconds in the no CAN group, 9.8 (4.7) seconds in early CAN, and 6.8 (3.9) seconds in confirmed CAN ($p = 0.062$). Tubular flow averaged 46 (20) ml/100ml/min in the no CAN group, 40 (14) ml/100ml/min in early CAN, and 51 (17) ml/100ml/min in confirmed CAN ($p = 0.288$). ATMTT was 2.1 (0.8) minutes in the no CAN group, 1.7 (0.5) minutes in early CAN, and 1.7 (0.5) minutes in confirmed CAN ($p = 0.744$). Lastly, AKEF was 23 (3) % in the no CAN group, 26 (7) % in early CAN, and 26 (7) % in confirmed CAN ($p = 0.807$).

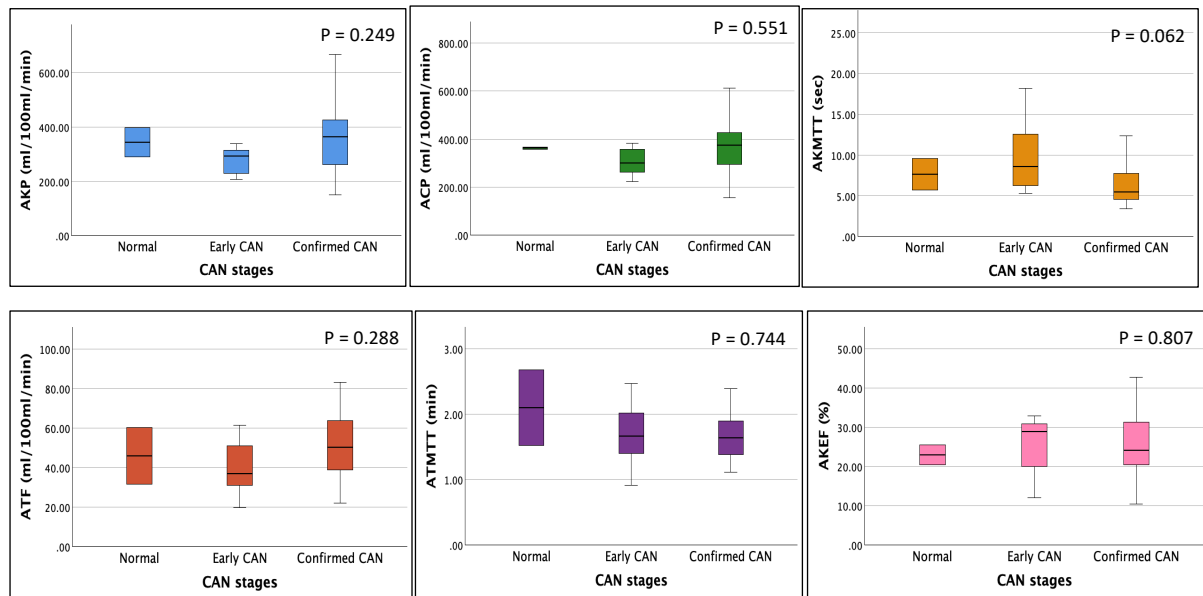


Figure 7.13: Comparison of renal parameters among different stages of CAN (T1DM)

AKP, average kidney perfusion; ACP, average cortical perfusion; AKMTT, average kidney mean transit time; ATF, average tubular flow; ATMTT, average tubular mean transit time; AKEF, average kidney extraction fraction.

Different stages of CAN (T2DM)

In T2DM, a comparison of renal MRI parameters across different stages of CAN)—no CAN (n=3), early CAN (n=14), and confirmed CAN (n=31)—no statistically significant differences were found in most parameters, except for tubular mean transit time (Figure 7.14). AKP was 355 (122) ml/100ml/min in the no CAN group, 282 (156) ml/100ml/min in early CAN, and 224 (78) ml/100ml/min in confirmed CAN ($p = 0.116$). ACP was 349 (32) ml/100ml/min in the no CAN group, 273 (70) ml/100ml/min in early CAN, and 275 (84) ml/100ml/min in confirmed CAN ($p = 0.176$). The AKMTT was 6.8 (1.1) seconds in the no CAN group, 7.8 (1.6) seconds in early CAN, and 9.1 (5.3) seconds in confirmed CAN ($p = 0.523$). Tubular flow (ATF) averaged 52 (14) ml/100ml/min in the no CAN group, 38 (11) ml/100ml/min in early CAN, and 37 (13) ml/100ml/min in confirmed CAN ($p = 0.176$). ATMTT showed a significant difference, being 1.9 (0.3) minutes in the no CAN group, 1.6 (0.3) minutes in early CAN, and 2.2 (1.1) minutes in confirmed CAN ($p = 0.022$). AKEF was 26 (3) % in the no CAN group, 28 (11) % in early CAN, and 30 (8) % in confirmed CAN ($p = 0.635$).

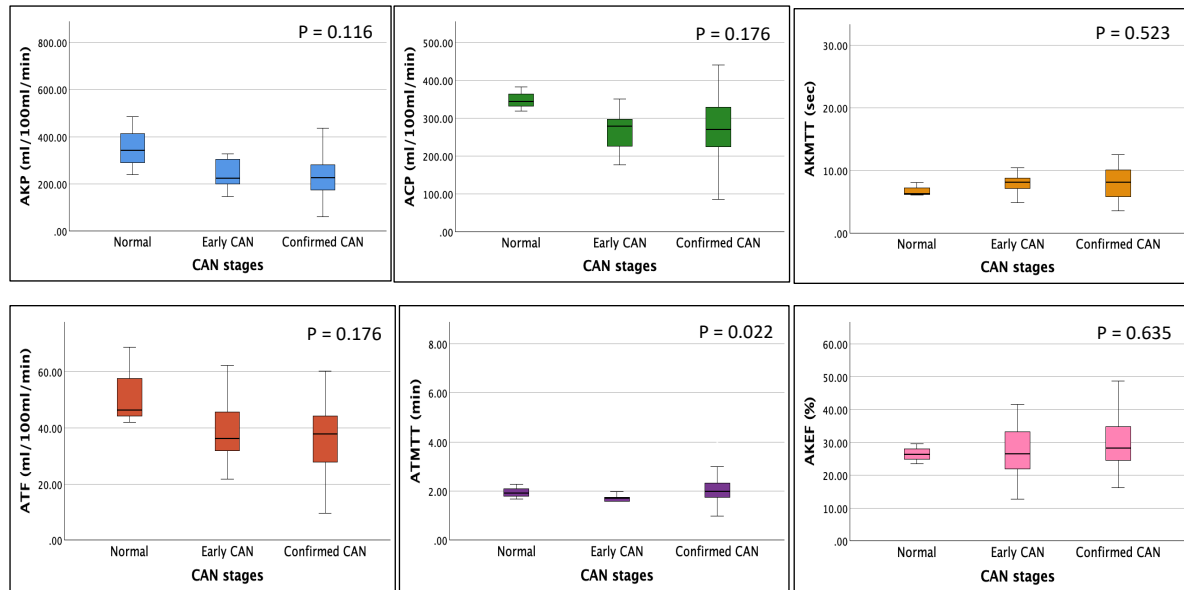


Figure 7.14: Comparison of renal parameters among different stages of CAN (T2DM)

AKP, average kidney perfusion; ACP, average cortical perfusion; AKMTT, average kidney mean transit time; ATF, average tubular flow; ATMTT, average tubular mean transit time; AKEF, average kidney extraction fraction.

The next part of the chapter will describe the exploratory analysis done to explore the impact of CAN on renal parameters.

7.3.7 Exploratory analysis

An exploratory analysis was conducted to investigate whether the observed trend of higher renal perfusion with higher eGFR grades persists when comparing participants with and without CAN. From the overall cohort (n=81), a sufficient number of participants were available in the G1 (n=21, no CAN = 5, CAN = 16) and G2 (n=52, no CAN = 20, CAN = 32) groups, while the G3 group (n=8, no CAN = 2, CAN = 6) had limited representation. Consequently, comparisons focused on G1 and G2 to enhance the robustness of the analysis.

The baseline comparison of renal parameters between the G1 and G2 groups was first conducted, followed by subgroup comparisons within the CAN and no-CAN groups,

respectively, to determine whether the relationship between eGFR and renal perfusion holds true in both conditions.

G1 Vs G2 (Overall)

Baseline analysis in figure 7.15 showed that AKP was notably higher in G1 group at 376 (165) ml/100ml/min compared to 266 (90) ml/100ml/min in the G2 group ($p = 0.006$). Similarly, ACP was significantly greater in G1, measuring 363 (102) ml/100ml/min, compared to 312 (95) ml/100ml/min in G2 ($p = 0.024$). No significant differences were found for AKMTT, which was 7.0 (3) seconds in G1 and 7.6 (3) seconds in G2 ($p = 0.278$), or for ATF with 49 (16) ml/100ml/min in G1 versus 41 (14) ml/100ml/min in G2 ($p = 0.079$). ATMTT remained similar between groups at 1.8 (0.4) minutes in G1 and 1.9 (0.9) minutes in G2 ($p = 0.559$). However, a statistically significant difference was observed in AKEF, which was 25 (8) % in G1 compared to 29 (8) % in G2 ($p = 0.034$). These findings suggest that higher eGFR is associated with better renal perfusion and lower kidney extraction fraction in participants with CAN.

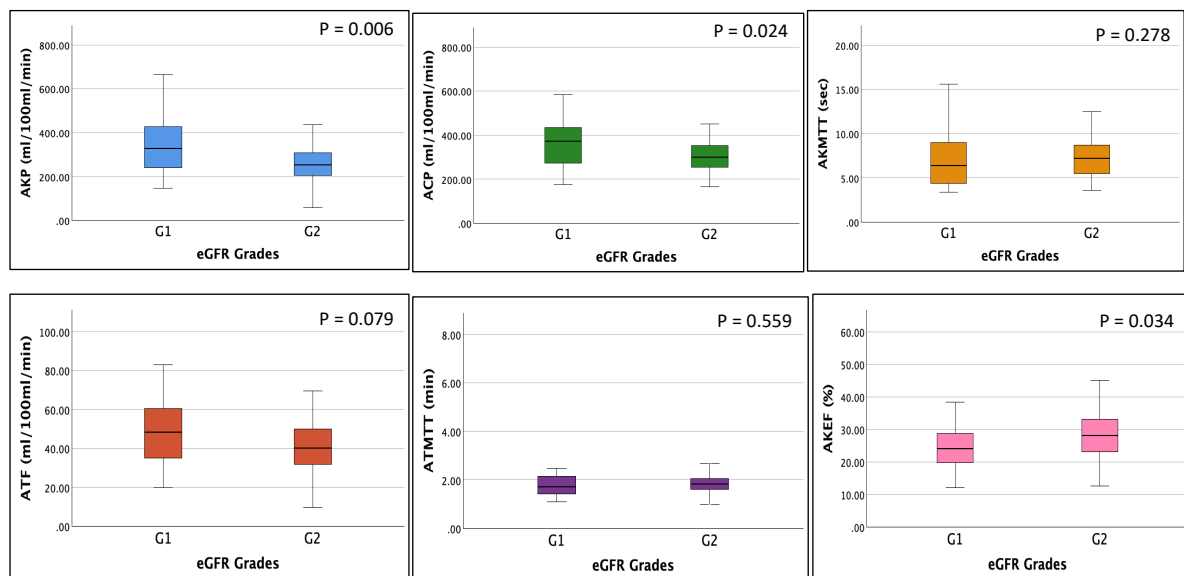


Figure 7.15: Comparison of renal parameters between G1 and G2 (Overall cohort)

AKP, average kidney perfusion; ACP, average cortical perfusion; AKMTT, average kidney mean transit time; ATF, average tubular flow; ATMTT, average tubular mean transit time; AKEF, average kidney extraction fraction.

G1 Vs G2 (No CAN group)

In participants with no CAN, renal MRI parameters were compared between G1 (n=5) and G2 (n=20) (Figure 7.16). The AKP was similar between the two groups, with 347 (228) ml/100ml/min in G1 and 289 (89) ml/100ml/min in G2 ($p = 0.974$). ACP was slightly higher in G2 at 329 (103) ml/100ml/min compared to 282 (105) ml/100ml/min in G1, though the difference was not statistically significant ($p = 0.243$). A significant difference was observed in AKMTT, which was longer in G1 at 10.6 (2.8) seconds compared to 7.7 (2.9) seconds in G2 ($p = 0.010$). ATF was higher in G2, averaging 43 (13) ml/100ml/min compared to 33 (13) ml/100ml/min in G1, although this difference did not reach statistical significance ($p = 0.169$). No significant differences were found in ATMTT, which was 1.9 (0.4) minutes in G1 and 1.7 (0.4) minutes in G2 ($p = 0.488$), or in AKEF, which was 21 (9) % in G1 and 27 (8) % in G2 ($p = 0.216$).

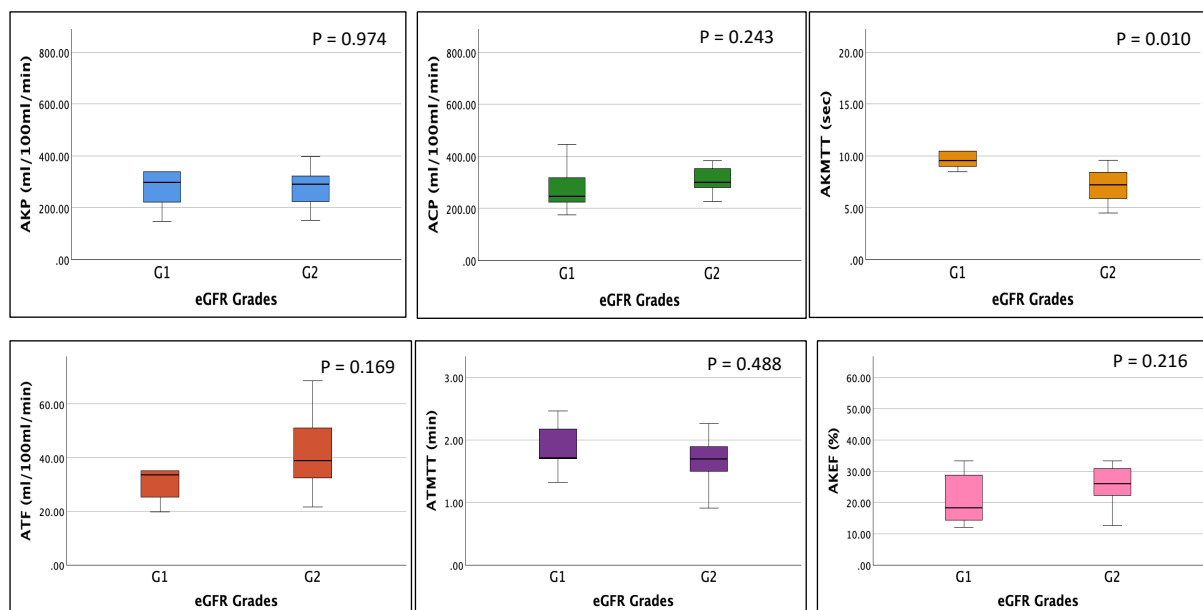


Figure 7.16: Comparison of renal parameters between G1 and G2 (No CAN group)

AKP, average kidney perfusion; ACP, average cortical perfusion; AKMTT, average kidney mean transit time; ATF, average tubular flow; ATMTT, average tubular mean transit time; AKEF, average kidney extraction fraction.

G1 Vs G2 (CAN group)

In participants with CAN, renal MRI parameters in figure 7.17 showed significant differences between G1 (n=16) and G2 (n=32). AKP was significantly higher in the G1 group at 384 (148)

ml/100ml/min compared to 251 (88) ml/100ml/min in the G2 group ($p = 0.002$). Similarly, ACP was greater in the G1 group, averaging 388 (90) ml/100ml/min versus 302 (90) ml/100ml/min in the G2 group ($p = 0.002$). The AKMTT was significantly shorter in G1 at 5.9 (2.1) seconds compared to 7.6 (3.1) seconds in G2 ($p = 0.029$). ATF was also notably higher in the G1 group, averaging 53 (15) ml/100ml/min compared to 41 (15) ml/100ml/min in G2 ($p = 0.009$). There were no significant differences in ATMTT, which was 1.7 (0.4) minutes in G1 and 2.1 (1.1) minutes in G2 ($p = 0.175$), or in AKEF, which was 26 (1) % in G1 and 30 (7) % in G2 ($p = 0.069$).

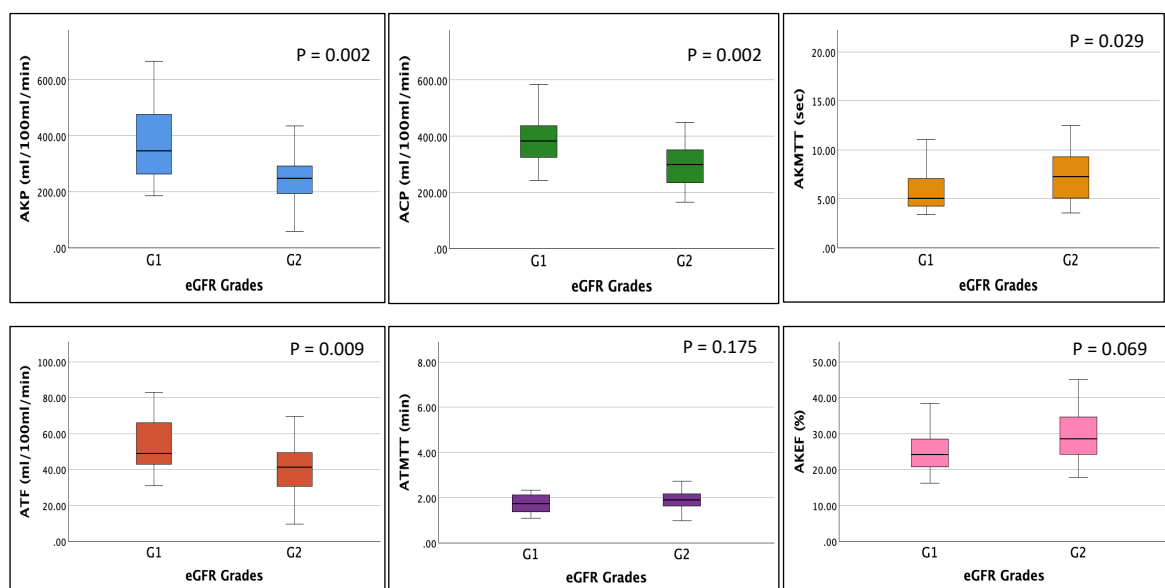


Figure 7.17: Comparison of renal parameters between G1 and G2 (CAN group)

AKP, average kidney perfusion; ACP, average cortical perfusion; AKMTT, average kidney mean transit time; ATF, average tubular flow; ATMTT, average tubular mean transit time; AKEF, average kidney extraction fraction.

7.4 Discussion

This study investigated the impact of CAN on renal perfusion in participants with T1 and T2DM, utilising DCE-MRI to assess renal perfusion related parameters. The findings provide important insights into the relationships between CAN, renal hemodynamic, and other clinical characteristics in diabetic populations.

The comparison of renal MRI parameters between participants with and without CAN revealed largely consistent renal perfusion values between the two groups. In both T1 and T2DM, kidney perfusion (AKP) and cortical perfusion (ACP) did not differ significantly between CAN and no-CAN groups, suggesting that the presence of CAN does not overtly impair renal blood flow.

The analysis also compared CAN and no CAN groups, by eGFR grades, and CAN severity. Interestingly, participants in the CAN group were generally younger and had better eGFR values compared to those without CAN in both types of diabetes. However, despite these differences in age and kidney function, no significant differences were found in renal perfusion, cortical perfusion, tubular flow, or extraction fraction between the CAN and no CAN groups, suggesting that CAN may not have a direct impact on renal blood flow parameters in these populations.

Despite the relatively preserved perfusion, longer renal mean transit times (AKMTT) and tubular mean transit times (ATMTT) were observed in certain subgroups, particularly in participants with confirmed CAN. This finding may indicate subtle vascular or functional changes possibly at the capillary and glomerular level that delay renal transit but do not immediately affect overall perfusion. Individuals with higher eGFR (G1 grade) and no CAN exhibited longer renal transit times, while those with lower eGFR (G2 grade) and CAN demonstrated prolonged tubular transit times. Moreover, increased tubular mean transit time (ATMTT) was observed with greater severity of CAN, suggesting potential microvascular alterations, or underlying DKD pathology. Although longer transit times might appear counterintuitive in individuals with preserved eGFR, this may reflect compensatory mechanisms such as enhanced renal reabsorption, which prolong the duration of blood and filtrate within the nephron. These findings underscore the complexity of renal physiology in diabetes, where compensatory adaptations may mask early signs of renal impairment, complicating the detection of subtle disease progression.

These findings show that CAN might not have a significant impact on RBF, contrary to what has been suggested by previous literature (347,358,363,376,381). This raises the question of whether other mechanisms proposed in the literature might have a more substantial impact

than the renal vasoconstriction caused by increased sympathetic activity and RAAS activation. It is possible that CAN acts as an additional risk factor, contributing to the overall burden of microvascular complications in diabetes, but not significantly impacting DKD through renal perfusion. Nonetheless, other potential mechanisms by which CAN may influence DKD, which have yet to be proven, could not be disregarded.

This study also includes exploratory analysis which examined whether the trend of higher renal perfusion with better eGFR persisted across participants with and without CAN. Baseline comparisons of renal perfusion and other MRI-derived parameters were conducted between G1 and G2, as well as within the CAN and no-CAN subgroups. Given the findings, it is hypothesised that higher eGFR correlates with better renal perfusion and lower extraction fraction and this relationship is more pronounced in the presence of CAN, suggesting that CAN contributes to microvascular dysfunction in the kidneys, particularly in individuals with moderate kidney impairment (G2). This raises the question of whether participants in the G1 group with CAN might be experiencing hyperfiltration associated with early DKD, combined with a late stage of CAN characterised by loss of sympathetic drive and resulting vasodilation. This could explain the paradoxical findings of higher renal perfusion and longer transit times in G1 participants with CAN, suggesting a compensatory hyperfiltration state in the presence of microvascular dysfunction.

Despite advances in understanding DKD pathophysiology, clinical application remains limited due to the lack of non-invasive methods to assess renal microcirculation, oxygenation, inflammation, and fibrosis (325). Renal MRI offers a potential alternative to biopsies, providing comprehensive evaluation of both kidneys and eliminating sampling bias, with its high spatial resolution allowing detailed visualization of the renal cortex and medulla. Vascular pathophysiology plays a key role in DKD progression, as evidenced by studies showing a 28% reduction in cortical perfusion in diabetic patients compared to healthy controls (286). Laursen et al. (341) further reported lower cortical perfusion in diabetes [163 (40) vs. 224 (49) mL/100 g/min; $P < 0.001$] and reduced renal artery blood flow [360 (130) vs. 430 (113) mL/min; $P = 0.05$], with both cortical oxygenation and blood flow inversely correlating with UACR and eGFR ($P < 0.05$).

Renal MRI perfusion in patients with CAN remains an underexplored area. A recent study in type 1 diabetes (391) investigated renal hemodynamic using inulin and para-amino Hippurate clearance but found no significant association between CAN and RBF. The authors attributed this to the limited severity of neuropathy and DKD in the study population, as participants had mean eGFR values comparable to healthy controls [102 (17.1) vs. 105 (18.9) ml/min/1.73m²], potentially obscuring the possible impact of CAN on renal perfusion.

This study has several notable strengths. All participants underwent MRI scans under uniform conditions, strictly adhering to the study protocol. The use of a consistent MRI protocol ensured standardised imaging procedures. Additionally, participants uniformly followed pre-scan guidelines, including the withholding of medications, adherence to fasting, and the avoidance of smoking and caffeine. This controlled environment minimised potential confounding variables, thereby enhancing the reliability and reproducibility of findings.

The study also has some limitations. The small sample size limits the statistical power and generalisability of findings. Additionally, DCE-MRI was used as the sole method for measuring renal perfusion, while other techniques such as ASL and PC-MRI remain unexplored. These methods could potentially validate the findings and provide a more comprehensive assessment of renal perfusion. The study was conducted at a single centre in Sheffield, with a predominantly Caucasian participant cohort, limiting the ethnic diversity of the sample. Future studies should include a more diverse population to assess whether the findings are consistent across different ethnic groups.

Furthermore, the cross-sectional design of the study does not allow for the assessment of causality or longitudinal changes in renal perfusion. Longitudinal studies are needed to determine whether increased severity of CAN is associated with reduced renal blood flow in the same individuals over time. Repeated MRI assessments in follow-up years would provide valuable insights into the temporal relationship between CAN and renal perfusion. Additionally, incorporating other imaging modalities and biomarkers could elucidate the mechanisms by which CAN affects renal function in diabetes.

7.5 Conclusion

This study investigated the impact of CAN on renal perfusion in individuals with T1 and T2DM using DCE-MRI. The findings showed no significant differences in renal perfusion between participants with and without CAN, despite variations in age and kidney function. While renal blood flow appeared largely preserved, certain subgroups with CAN exhibited prolonged renal transit times, suggesting subtle microvascular changes that do not immediately affect overall perfusion. These results indicate that CAN may not have a direct impact on RBF, challenging previous assumptions of its role in DKD progression. However, the prolonged transit times observed in some cases highlight the complexity of renal physiology in diabetes and warrant further exploration. Longitudinal studies with larger, more diverse populations are necessary to fully understand the relationship between CAN and renal perfusion and to assess its potential as a marker for early DKD detection and management.

Chapter 8

Conclusion and future work

8.1 Overview and summary of findings

This thesis investigates the complex interplay between DKD and CAN, with a particular focus on the role of MRI biomarkers.

A critical review of the literature in chapter 4 highlights the intricate relationship between CAN and DKD, evaluating whether the association is causative or if both conditions represent parallel complications of diabetes. Using longitudinal data and established diagnostic tools like CARTs and KDIGO risk classifications, the study in chapter 5 investigates how CAN impacts renal function and progression of DKD over time.

The chapter 6 further explores the potential of three-dimensional kidney shape metrics, derived from MRI, as novel biomarkers for tracking DKD progression. By correlating these imaging parameters with kidney function data, reference values were established, providing a foundation for future research.

Additionally, the chapter 7 focuses on the use of DCE-MRI to assess the impact of CAN on renal perfusion. Comparative analyses between participants with and without CAN reveal insights into how autonomic dysfunction affects RBF and perfusion.

8.2 Implications of research findings

8.2.1 Role of cardiac autonomic neuropathy in diabetic kidney disease

The findings from 15-years follow up study provide significant insights into the relationship between CAN and DKD. CAN severity was associated with increased UACR and a significant

decline in renal function, as reflected in eGFR and composite renal outcomes such as macroalbuminuria and KDIGO risk classification. These findings highlight CAN's role as a predictor of renal decline, suggesting that autonomic dysfunction, particularly sympathetic dominance, may contribute to glomerular injury via mechanisms such as elevated nocturnal blood pressure, activation of the RAAS, and increased inflammation and oxidative stress.

The association between CAN and DKD progression appears to be more pronounced in patients with advanced DKD, indicating that CAN may accelerate renal dysfunction in later disease stages. Overall, these findings suggest that early identification and management of CAN may offer a valuable strategy for mitigating DKD progression, potentially informing novel therapeutic approaches aimed at improving long-term renal outcomes in diabetes.

8.2.2 Role of kidney shape as MRI biomarker in diabetic kidney disease

The volumetric study provides valuable insights into the role of kidney shape metrics, particularly compactness, as potential biomarkers for DKD progression. By analysing three-dimensional morphological features derived from MRI scans, the study explored 15 distinct renal parameters, including kidney volume, surface area, and compactness, and correlated these features with kidney function markers. The findings suggest that most kidney morphological parameters, including volume and length, correlate with kidney function; however, compactness showed no significant association with traditional markers like eGFR and UACR, indicating a potential role as a distinct biomarker for early DKD changes.

The discovery that compactness does not correlate with kidney function but highlights kidney deformation, even in participants with normal eGFR, suggests that compactness may capture subclinical changes related to DKD, such as hyperfiltration, which are missed by conventional assessments. This finding implies that kidney compactness may provide complementary information to traditional measures of kidney function, offering insights into early structural changes not reflected by eGFR or albuminuria.

One significant implication of these findings is the potential for compactness to serve as a predictive biomarker for DKD progression. Longitudinal follow-up studies will be essential to confirm whether kidneys with reduced compactness are more susceptible to accelerated DKD progression. Such studies could provide invaluable prognostic data, particularly in understanding the temporal relationship between kidney shape alterations and DKD severity.

8.2.3 The impact of cardiac autonomic neuropathy on renal perfusion

The renal perfusion study provides valuable insights into the effects of CAN on renal perfusion in individuals with T1 and T2DM, using DCE-MRI. By comparing renal perfusion parameters between participants with and without CAN, the study explored the relationship between CAN, renal hemodynamic, and other clinical characteristics in diabetic populations.

The study found no significant differences in renal perfusion parameters between participants with CAN and those without, in both T1 and T2DM groups. This contradicts previous hypotheses linking CAN to impaired renal perfusion due to increased sympathetic activity and activation of the RAAS. These findings raise the possibility that CAN may contribute to the broader microvascular complications of diabetes but may not directly affect renal perfusion.

Interestingly, the study found that while renal perfusion was preserved, renal transit times were longer in certain subgroups, particularly in those with more severe CAN. This suggests that although overall blood flow remains stable, subtle vascular or functional changes may occur at the capillary or glomerular level, leading to prolonged transit times. This could reflect microvascular alterations, delayed filtrate movement, or compensatory mechanisms such as increased renal reabsorption, which may not immediately affect perfusion but could contribute to disease progression over time.

8.3 Limitations and future work

8.3.2 CAN severity and renal outcomes in longitudinal data

The study included few participants with advanced DKD, limiting the ability to explore the full spectrum of CAN's impact on renal function across different stages of kidney disease. Future studies should incorporate more participants with advanced DKD to better understand CAN's role in late-stage kidney disease progression. Moreover, the study was conducted at a single centre with a relatively small sample size, particularly under-representing younger participants. Expanding the study to multiple centres and including a more diverse and larger population will improve the generalisability of the findings.

8.3.3 Kidney shape factor 'compactness' as biomarkers for diabetic kidney disease progression

The study lacks follow-up data to assess whether compactness can serve as a predictive biomarker for long-term DKD progression. Without longitudinal evidence, the study cannot establish whether reduced compactness is associated with faster disease progression. Future studies should incorporate follow-up data to validate whether compactness predicts DKD progression over time. The absence of earlier MRI scans prevents comparison of kidney shape changes over time, which could clarify whether observed alterations are long-standing or newly developed. Compactness did not correlate with conventional kidney function parameters (eGFR, UACR), which may limit its immediate clinical appeal without further validation. Further studies should explore whether compactness can be linked to clinically relevant outcomes, such as the need for dialysis or kidney failure.

8.3.4 Cardiac autonomic neuropathy and renal perfusion in diabetes

This cross-sectional study prevents the evaluation of how CAN impacts renal perfusion over time. Without longitudinal data, the study cannot establish causality or track renal function

changes in the same participants. Future research should include repeated MRI assessments over time to investigate the long-term impact of CAN on renal perfusion and function. The study relied solely on DCE-MRI to measure renal perfusion. Other imaging techniques, such as ASL and PC-MRI, were not employed, potentially limiting the depth of renal hemodynamic assessment. Employing other non-invasive imaging techniques, such as ASL or PC-MRI, would offer a more comprehensive evaluation of renal perfusion and validate the findings. The study population was predominantly Caucasian, which restricts the generalisability of the findings across different ethnic groups. Including a more ethnically and geographically diverse population will enhance the applicability of the findings across broader demographics.


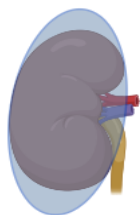
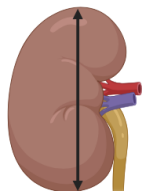
8.4 Overall conclusion


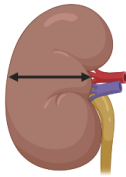
This thesis investigates whether MRI biomarkers can enhance our understanding of the association between CAN and DKD. A comprehensive literature review provided insights into various proposed mechanisms linking CAN with renal dysfunction in diabetes. The longitudinal study demonstrated a significant association between CAN severity and adverse renal outcomes, suggesting CAN as a potential contributor to DKD progression. The morphological study identified kidney compactness as a possible novel MRI biomarker with potential predictive value for DKD, highlighting shape alterations even in the absence of traditional renal dysfunction markers. The renal perfusion study, however, found no direct correlation between CAN and renal blood flow parameters, though subtle microvascular changes were observed.

This thesis describes the complexity of the CAN-DKD relationship, suggesting that while CAN may not overtly affect renal perfusion, it could contribute to disease progression through other mechanisms, such as microvascular dysfunction or delayed renal transit times. The work highlights the importance of advanced imaging modalities for non-invasive assessment of renal function and morphology, setting the stage for future research aimed at refining MRI-based biomarkers and larger, more diverse cohorts, advanced imaging techniques, and longitudinal designs to improve the robustness of these findings and deepen our

understanding of CAN's role in DKD. These efforts will aid in developing more reliable tools for early detection and targeted interventions in diabetic populations at risk of kidney disease.

Appendix A: Summary of definitions of renal MRI volumetric parameters

| Features | Definition |
|--|--|
| Bounding box volume  | Bounding box volume (or bounding region) for a set of objects is a closed region that completely contains the union of the objects in the set. |
| Convex hull volume  | For objects in three dimensions, the convex hull is the smallest possible convex bounding volume of the objects. |
| Equivalent diameter | The diameter of the circle whose area is equal to the contour area is known as the equivalent diameter. The Contour is an outline representing or bounding the shape or form of something. |
| Longest calliper diameter | The longest calliper diameter refers to the greatest internal diameter of a hollow structure or lumen. |
| Long axis length  | Renal length <i>measured along the long axis of the kidney from upper to lower pole – bipolar length.</i> |
| Maximum depth | Thickness of kidney |
| Moment of inertia | The moment of inertia is defined as the product of mass of section and the square of the distance between the reference axis and the centroid of the section. |
| Surface area | Surface area of kidney |

| | |
|---|--|
| Volume | Renal volume is calculated by using the ellipsoid formula: Volume = length × width × thickness × $\pi/6$. |
| Solidity | The solidity of an object as the ratio of the contour area to its convex hull area. |
| Compactness  | Compactness is the surface-to-volume ratio relative to that of an equivalent sphere, which has 100% compactness. |
| Extent | Extent is the ratio of kidney volume to its bounding box volume. |
| Short axis length  | Renal width <i>measured along the short axis of the kidney</i> . |

Appendix B: Summary of medication advice for participants following an overnight fasting

| Medication | Advice following overnight fasting |
|---|--|
| Short acting insulin (e.g., Novorapid, Humalog, Humulin, Actrapid) | Bring insulin pen to the study day and take half normal dose with standardised breakfast. |
| Mixed insulin (e.g., Humulin M3, Novomix 25) | Bring insulin pen to the study day and take half normal dose with standardised breakfast. |
| Long-acting insulin (e.g., Insulatard, Levemir, Detemir, Humulin I, Glargine (lantus), Insuman basal) | Take as normal |
| GLP-1 Analogues (e.g., Exenatide, Dulaglutide) | Omit in the morning, but bring and take afterwards with lunch. |
| Metformin | Omit and bring to take with standardised breakfast |
| Sulphonylureas (e.g., Gliclazide, Glimepiride, Glibenclamide, Tolbutamide) | Omit in the morning |
| Gliptins and Thiazolidinedione (e.g., Vildagliptin, Sitagliptin, pioglitazone) | Omit in the morning |
| Anti-hypertensive medications (e.g., ACEIs, ARBs, CCBs) | Take as normal |
| Statins | Take as normal (the night before) |
| Ezetimibe | Omit in the morning |
| Anti-depressants | Amitriptylline – take as normal SSRI (e.g., Citalopram, mirtazapine) – omit in the morning and bring to take with standardised breakfast. |
| Anti-fungal, corticosteroids | Oral – omit in the morning Topical cream – omit in the morning and night before |
| Nitrates | GTN spray – take as normal Monomax – omit in the morning |
| Medication for IBS – Mebeverine | Omit in the morning |
| Medications for gout – allopurinol | Take as normal |
| Medications for diuretics (e.g., furosemide, Bendroflumethiazide, indapamide) | Omit in the morning of appointment and bring to take at the end of visit |
| Antibiotics | Acute infection – no visit for one week after condition has resolved Prophylaxis – take as normal |

| | |
|--|--|
| Other medications | Pain killers – omit ibuprofen and naproxen on the morning. Other pain killers can be taken as normal |
| Alendronic acid | Omit on the day if due and take as usual the next morning |
| Iron tablets | Omit in the morning |
| Calcichew Forte | Omit in the morning |
| Thyroid (e.g., Levothyroxine) | Take as normal |
| Insomina (e.g., Zolpidem, Nitrazepam) | Take as normal |
| Prostate (e.g., Tamsulosin, Doxazosin, finasteride) | Take as normal |
| Antacid and PPI (e.g., Omeprazole, Lansoprazole, Ranitidine) | Take as normal |
| Anti-platelets (e.g., Clopidogrel, aspirin , dipyridamole) | Take as normal |
| Beta Blockers (e.g., atenolol, bisoprolol) | Take as normal |
| Anti-arrhythmia (e.g., amiodarone) | Take as normal |
| Inhalers | Take as normal |
| Tamoxifen | Take as normal |
| Warfarin and DOAC | Take as normal |

Adapted from Prognostic Imaging Biomarkers for Diabetic Kidney Disease(iBEAt): Manual of procedures

Appendix C: iBEAT letter to participant for the study day

Preparation for the study day

Thank you very much for your participation in the iBEAt study. Please find the following information for the study day.

The night before the study day

- You will need to fast from midnight onwards. It means that nothing to eat or drink apart from clear water (Not fizzy water) from midnight onwards.

Study day morning

- When you wake up in the morning, please collect the first morning void of urine in the bottle provided for the study and bring along with you to the hospital.
- Please bring your regular medications to the hospital including diabetes medications (oral medications / insulin) to take them with standard breakfast provided by the research team. (2 slices of brown toast with butter)
- You may notice that some of your regular medications will need to be omitted in the morning of study day. These medications can be taken after the MRI scan. MRI scan will be done by mid-day. (You can bring along those medications if you want to take them immediately after the scan.)

If you are on insulin

- Please check your sugar level in the morning before you leave the house.
- If sugar level is less than 4, it means that you are having hypoglycaemia, and you will need to eat or drink something immediately.
- It means that we will need to postpone the appointment for another day as it is not safe to do the study day in the presence of low blood sugar level (hypoglycaemia).

Smoking

- All the participants are requested to avoid smoking (Cigarettes, electronic Cigarettes) for at least 4 hours before the start of the study time.
- If your appointment is at 8am, please avoid smoking after 4am.

Strenuous exercise

- All the participants are requested not to do any strenuous exercise at least 24 hours before the study day.

COVID Vaccine / Flu Vaccine

- All the participants should be at least 2 weeks from any vaccine before the study day.
- The study day will need to be rescheduled if the participant had any vaccine within last 2 weeks.

Outline of the study day

1. Arrival - M Floor, Royal Hallamshire Hospital.
2. Please take a seat in front of the main lift. The researcher will come and greet you.
3. Collection of urine bottle.
4. Cannula and blood tests, including blood sugar level.
5. Breakfast.
6. Questionnaires.
7. Height, weight, examination of hands and feet for neuropathy (nerve damage)
8. ECG recording, Blood pressure check.
9. Second urine sample
10. Going down to C Floor MRI department to have MRI scan
11. End of the study day.

Research team will contact you a few days before the study day to go through the letter with you and to answer any questions you may have.

We look forward to seeing you for the iBEAt study day.

Thank you.

Diabetes research team

Appendix D: Case report form for medical and social history

Follow-up Y1 date: _____

Follow-up Y2 date: _____

Follow-up Y3 date: _____

Instructions: Participants should respond to all questions. Shaded areas should be taken from the patient available medical chart data. For baseline, only the 2 columns under “Baseline” are applicable, for follow-up, please use the columns under each respective year.

| MEDICAL HISTORY | | Baseline | | Year 1 FU | | Year 2 FU | | Year 3 FU | |
|-----------------|---|----------------------|------|------------------------|------------------|------------------------|------------------|------------------------|------------------|
| Q | | Response | | | | | | | |
| 1 | Date of diagnosis Type 2 Diabetes (year) | | YYYY | | | | | | |
| 2 | Does the participant take medical therapy for their diabetes? | O Y O N | | O Y O N | | O Y O N | | O Y O N | |
| 3 | Date Type 2 Diabetes medical therapy initiated (year) | | YYYY | O Y O N O No chg | If yes, year: | O Y O N O No chg | If yes, year: | O Y O N O No chg | If yes, year: |
| 4 | Does the participant have a diagnosis of hypertension? | O Y O N O Unknown | | O Y O N O No chg | If yes, year: | O Y O N O No chg | If yes, year: | O Y O N O No chg | If yes, year: |
| 5 | Date of diagnosis for hypertension (year) | | YYYY | O Y O N O No chg | If yes, year: | O Y O N O No chg | If yes, year: | O Y O N O No chg | If yes, year: |
| 6 | Does the participant take hypertensive medication? | O Y O N | | O Y O N O No chg | If yes, year: | O Y O N O No chg | If yes, year: | O Y O N O No chg | If yes, year: |
| 7 | Date hypertensive medical therapy initiated (year) | | YYYY | O Y O N O No chg | If yes, year: | O Y O N O No chg | If yes, year: | O Y O N O No chg | If yes, year: |

| | | | | | |
|---|--|--|--|--|--|
| 8 | Does the patient have diabetic retinopathy? From available medical chart data (If no DR diagnosis is >14 months then record as unknown) | <input type="radio"/> Y <input type="radio"/> N <input type="radio"/> Unknown | <input type="radio"/> Y <input type="radio"/> N <input type="radio"/> Unknown | <input type="radio"/> Y <input type="radio"/> N <input type="radio"/> Unknown | <input type="radio"/> Y <input type="radio"/> N <input type="radio"/> Unknown |
|---|--|--|--|--|--|

| | | Baseline | Year 1 FU | Year 2 FU | Year 3 FU |
|----|--|--|--|--|--|
| 9 | Grade of diabetic retinopathy: From available medical chart data (If DR grade is >14 months record as unknown unless they have documented previous treatment for proliferative DR) | 1 No DR 2 Non-proliferative DR (including background/ microaneurysms only) 3 Proliferative DR 4 Previous Treatment for proliferative DR 5 Unknown | 1 2 3 4 5 | 1 2 3 4 5 | 1 2 3 4 5 |
| 10 | Does the patient have maculopathy? From available medical chart data To be taken from clinical data if available. If data is > 14 months: <ul style="list-style-type: none"> Class no macular oedema as "Unknown" If "Documented macular oedema" (DMO) or previous treatment for DMO then class as 2 and 3, respectively | 1 No macular edema 2 Documented macular edema 3 Previous treatment for macular edema 4 Unknown | 1 2 3 4 | 1 2 3 4 | 1 2 3 4 |
| 11 | Does the patient have diabetic neuropathy? From available medical chart data To be defined on monofilaments if data available. In patients with no neuropathy and no available data within last 14 months, document as "Unknown" | <input type="radio"/> Y <input type="radio"/> N <input type="radio"/> Unknown | <input type="radio"/> Y <input type="radio"/> N <input type="radio"/> Unknown | <input type="radio"/> Y <input type="radio"/> N <input type="radio"/> Unknown | <input type="radio"/> Y <input type="radio"/> N <input type="radio"/> Unknown |
| 12 | If yes, is the diabetic neuropathy painful? | <input type="radio"/> Y <input type="radio"/> N <input type="radio"/> Not applicable | <input type="radio"/> Y <input type="radio"/> N <input type="radio"/> Not applicable | <input type="radio"/> Y <input type="radio"/> N <input type="radio"/> Not applicable | <input type="radio"/> Y <input type="radio"/> N <input type="radio"/> Not applicable |

| | | | | | |
|----|---|--|--|--|--|
| 13 | Does the patient have heart failure stage II or IV? | <input type="radio"/> Y <input type="radio"/> N <input type="radio"/> Unknown | <input type="radio"/> Y <input type="radio"/> N <input type="radio"/> Unknown | <input type="radio"/> Y <input type="radio"/> N <input type="radio"/> Unknown | <input type="radio"/> Y <input type="radio"/> N <input type="radio"/> Unknown |
|----|---|--|--|--|--|

| | | Baseline | Year 1 FU | | Year 2 FU | | Year 3 FU | |
|----|--|--|--|------------------|--|------------------|--|------------------|
| 14 | Does the patient have any macrovascular diseases? (If yes then progress to questions 15, 16, & 17) | <input type="radio"/> Y <input type="radio"/> N <input type="radio"/> Unknown | <input type="radio"/> Y <input type="radio"/> N <input type="radio"/> No chg | If yes, year: | <input type="radio"/> Y <input type="radio"/> N <input type="radio"/> No chg | If yes, year: | <input type="radio"/> Y <input type="radio"/> N <input type="radio"/> No chg | If yes, year: |
| 15 | Does the patient have history or evidence of coronary artery disease (check all that apply): | <input type="checkbox"/> Myocardial infarction <input type="checkbox"/> Angina <input type="checkbox"/> Angioplasty <input type="checkbox"/> Stent <input type="checkbox"/> CABG | <input type="checkbox"/> Myocardial infarction <input type="checkbox"/> Angina <input type="checkbox"/> Angioplasty <input type="checkbox"/> Stent <input type="checkbox"/> CABG | | <input type="checkbox"/> Myocardial infarction <input type="checkbox"/> Angina <input type="checkbox"/> Angioplasty <input type="checkbox"/> Stent <input type="checkbox"/> CABG | | <input type="checkbox"/> Myocardial infarction <input type="checkbox"/> Angina <input type="checkbox"/> Angioplasty <input type="checkbox"/> Stent <input type="checkbox"/> CABG | |
| 16 | If yes to history or evidence of coronary artery disease, is there evidence or history of peripheral artery disease? | <input type="radio"/> Y <input type="radio"/> N | <input type="radio"/> Y <input type="radio"/> N | | <input type="radio"/> Y <input type="radio"/> N | | <input type="radio"/> Y <input type="radio"/> N | |
| 17 | Does the patient have any history or evidence of cerebrovascular disease? (Ischemic stroke and TIA confirmed by specialist (excluding TIA not confirmed by specialist, hemorrhagic stroke, and stroke associated with blood disease, tumors, trauma or surgical procedures)) | <input type="radio"/> Y <input type="radio"/> N <input type="radio"/> Not applicable <input type="radio"/> Unknown | <input type="radio"/> Y <input type="radio"/> N <input type="radio"/> Not applicable <input type="radio"/> Unknown | | <input type="radio"/> Y <input type="radio"/> N <input type="radio"/> Not applicable <input type="radio"/> Unknown | | <input type="radio"/> Y <input type="radio"/> N <input type="radio"/> Not applicable <input type="radio"/> Unknown | |
| 18 | Does the patient have a history of malignancy? | <input type="radio"/> Y <input type="radio"/> N <input type="radio"/> Unknown | <input type="radio"/> Y <input type="radio"/> N <input type="radio"/> No chg | If yes, year: | <input type="radio"/> Y <input type="radio"/> N <input type="radio"/> No chg | If yes, year: | <input type="radio"/> Y <input type="radio"/> N <input type="radio"/> No chg | If yes, year: |
| 19 | When? (year) | | YYYY | | | | | |

| SOCIAL HISTORY | | Baseline | Year 1 FU | Year 2 FU | Year 3 FU |
|----------------|---|---|---|---|---|
| 20 | Current or previous tobacco use? (check all that apply) | <input type="checkbox"/> Cigarettes <input type="checkbox"/> Pipe <input type="checkbox"/> Cigars, cigarillos, or little cigars <input type="checkbox"/> E-cigs <input type="checkbox"/> Smokeless tobacco <input type="checkbox"/> Never used tobacco | <input type="checkbox"/> Cigarettes <input type="checkbox"/> Pipe <input type="checkbox"/> Cigars, cigarillos, or little cigars E-cigs <input type="checkbox"/> Smokeless tobacco <input type="checkbox"/> Never used tobacco | <input type="checkbox"/> Cigarettes <input type="checkbox"/> Pipe <input type="checkbox"/> Cigars, cigarillos, or little cigars E-cigs <input type="checkbox"/> Smokeless tobacco <input type="checkbox"/> Never used tobacco | <input type="checkbox"/> Cigarettes <input type="checkbox"/> Pipe <input type="checkbox"/> Cigars, cigarillos, or little cigars E-cigs <input type="checkbox"/> Smokeless tobacco <input type="checkbox"/> Never used tobacco |
| 21 | If current or previous smoker, number of cigarettes smoked a day: | <input type="radio"/> Not applicable | <input type="radio"/> Not applicable | <input type="radio"/> Not applicable | <input type="radio"/> Not applicable |
| 22 | If current or previous smoker, number of years smoking: | <input type="radio"/> Not applicable | <input type="radio"/> Not applicable | <input type="radio"/> Not applicable | <input type="radio"/> Not applicable |
| 23 | If previous tobacco user, number of years tobacco-free: | <input type="radio"/> Not applicable | <input type="radio"/> Not applicable | <input type="radio"/> Not applicable | <input type="radio"/> Not applicable |
| FAMILY HISTORY | | | | | |
| 24 | Does patient have a family history of renal disease? | <input type="radio"/> Y <input type="radio"/> N <input type="radio"/> Unknown | <input type="radio"/> Y <input type="radio"/> N <input type="radio"/> Unknown | <input type="radio"/> Y <input type="radio"/> N <input type="radio"/> Unknown | <input type="radio"/> Y <input type="radio"/> N <input type="radio"/> Unknown |
| 25 | Does patient have a family history of hypertension? | <input type="radio"/> Y <input type="radio"/> N <input type="radio"/> Unknown | <input type="radio"/> Y <input type="radio"/> N <input type="radio"/> Unknown | <input type="radio"/> Y <input type="radio"/> N <input type="radio"/> Unknown | <input type="radio"/> Y <input type="radio"/> N <input type="radio"/> Unknown |
| 26 | Does patient have a family history of Type 2 diabetes? | <input type="radio"/> Y <input type="radio"/> N <input type="radio"/> Unknown | <input type="radio"/> Y <input type="radio"/> N <input type="radio"/> Unknown | <input type="radio"/> Y <input type="radio"/> N <input type="radio"/> Unknown | <input type="radio"/> Y <input type="radio"/> N <input type="radio"/> Unknown |
| 27 | Does patient have a family history of cardiovascular disease? | <input type="radio"/> Y <input type="radio"/> N <input type="radio"/> Unknown | <input type="radio"/> Y <input type="radio"/> N <input type="radio"/> Unknown | <input type="radio"/> Y <input type="radio"/> N <input type="radio"/> Unknown | <input type="radio"/> Y <input type="radio"/> N <input type="radio"/> Unknown |
| 28 | Does patient have a family history of malignancy? | <input type="radio"/> Y <input type="radio"/> N <input type="radio"/> Unknown | <input type="radio"/> Y <input type="radio"/> N <input type="radio"/> Unknown | <input type="radio"/> Y <input type="radio"/> N <input type="radio"/> Unknown | <input type="radio"/> Y <input type="radio"/> N <input type="radio"/> Unknown |

| | | | | | |
|----|--|--|--|--|--|
| 29 | Does patient have a family history of Type I Diabetes? | <input type="radio"/> Y <input type="radio"/> N <input type="radio"/> Unknown | <input type="radio"/> Y <input type="radio"/> N <input type="radio"/> Unknown | <input type="radio"/> Y <input type="radio"/> N <input type="radio"/> Unknown | <input type="radio"/> Y <input type="radio"/> N <input type="radio"/> Unknown |
|----|--|--|--|--|--|

Appendix E: iBEAt MRI protocol for GE MRI scanner in the University of Sheffield

Before scanning

Patients with contraindications to or interference with MRI (ferromagnetic metal prosthesis, aneurysm clips, MRI incompatible pacemakers, severe claustrophobia, large abdominal/back tattoos, subjects too large to fit safely in the magnet bore, etc.) and/or imaging contrast agent (dotarem or gadovist) are excluded from participation.

Patient preparation

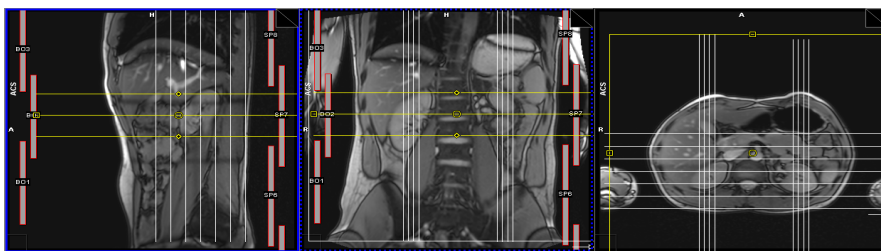
1. The patient must enter the magnet bore feet first and lie in supine position. In case of coil element placement issues or patient discomfort, the patient may be allowed to enter the bore head first.
2. ECG triggering elements need to be used (for the *Phase Contrast Imaging Sequence*) within this MRI protocol.
3. Phased array surface or body coil should be placed to cover the abdominal cavity with the center of the coil positioned over the kidneys (L3 on the spine). In case of insufficient coverage, use 2 body coils.
4. The breath-hold sequences in this study need to be carried out in *expiration mode* only. Please ensure that the patient is provided with breathing instructions prior to the actual imaging. Go through 1 breath-hold practice run with the patient. If problem with breath-hold in expiration then allow breath-hold in inspiration.
5. The patient must be informed about the approximate duration of the MRI scan.

Performing the scan

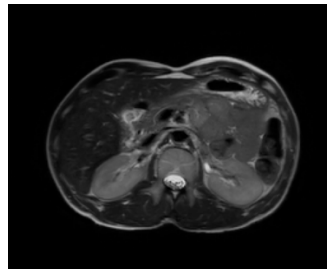
1. Register the patient on the scanner: Include patient specific iBEAt study ID and please retain the height and weight.
2. Ensure that the spine coil elements are active for full abdomen coverage.
3. **Localizers**: The localizers should ideally be scanned in breath-hold mode. Acquire all 3 planes (i.e. sagittal, coronal, and transverse view). See image below:

Example Localizer Planning: Sagittal, Coronal, and Transverse view.

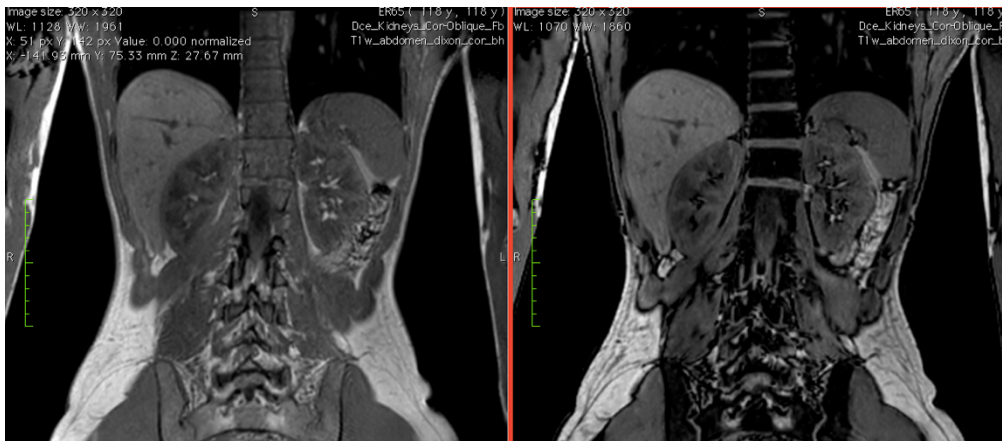
4. in



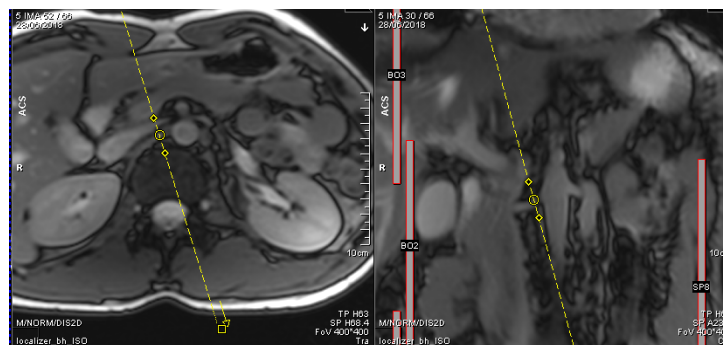
5. **T2w abdomen haste tra mbh**: Breath-hold sequence in transverse view. Centre slice on the kidneys. This sequence should cover both kidneys entirely. See example image below.



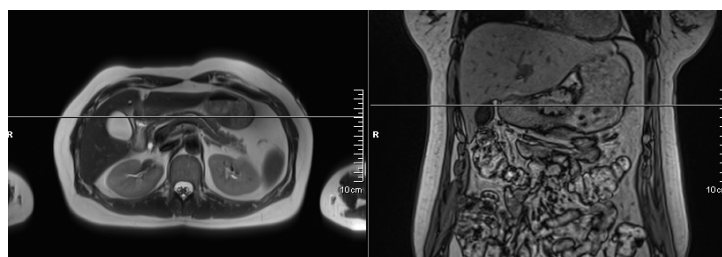
6. **T1w abdomen dixon cor bh**: Breath-hold sequence in coronal plane. Sequence should acquire entire abdomen in the coronal view (ensure both kidneys are included). Centre the field of view (FOV) on the kidneys (for front-to-back coverage). See example image below for ideal top-to-bottom FOV coverage.



7. **Phase Contrast Sequence Planning:** Use the localizer to plan the phase contrast (PC) sequence. Utilize the HASTE sequence to position the acquisition plane perpendicular to the renal artery (as shown below, left panel). Simultaneously, use the coronal view from localizer to aid positioning the PC plane.

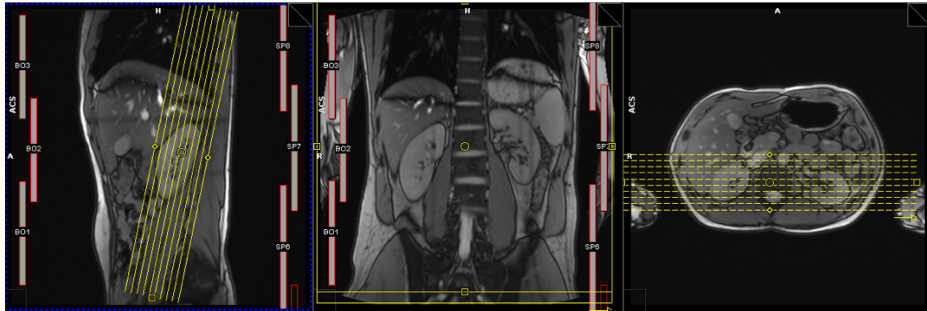


8. **Phase Contrast Renal Artery Right/Left:** Both sequences should be acquired with ECG-triggering (retro-ECG mode on scanner, if available) in free breathing mode. Ensure both right and left artery sequence is acquired with same number of cardiac phases. If aliasing issue present – increase velocity encoding for both arteries from 120cm/sec to 150cm/sec.
9. **T2star map pancreas tra mbh:** Breath-hold sequence acquired in transverse view. This sequence should be acquired centered at the body of the pancreas (*look for pancreatic duct: see image below*). Sequence can be planned off the T2w_abdomen_HASTE_tra_mbh sequence for easily locating the pancreas.

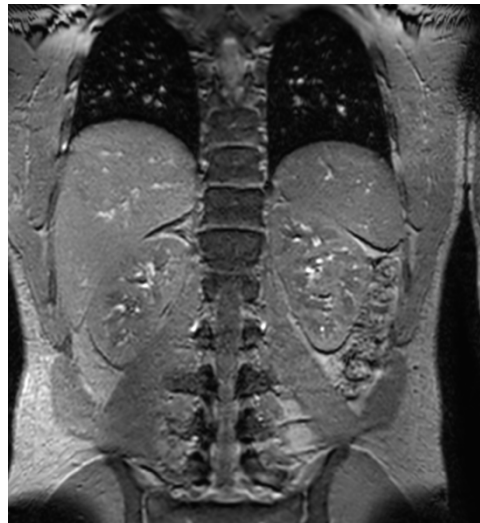


Transverse view centre slice (coronal view, right) overlaid on pancreas in Transverse view.

10. **T1w kidneys cor-oblique mbh**: Breath-hold sequence acquired in *coronal-oblique* view (see below). Centre FOV on the kidneys and ensure full coverage of kidneys (i.e. anterior to posterior in coronal view). Example images below:



Coronal-Oblique planning



Centre sliced FOV on the kidneys

11. **T1map kidneys cor-oblique mbh**: Breath-hold sequence acquired in coronal-oblique view with simulated ECG (see instructions below). Switch on the simulator right before to acquiring this sequence (Note: do not switch on simulator while scanning previous sequence). Copy the image slice location from previous sequence (*T1w_kidneys_cor-oblique_mbh*). **NOTE: Manually reduce the number of slices to 5.**

How to switch on the simulator:

Turn on cardiac gating if not already switched on. You should see an ECG waveform tab.

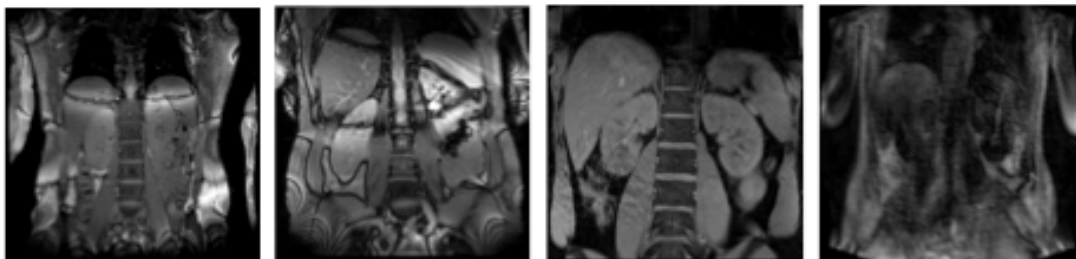
- Tools->command window
- Type in the command window: **ECGsimulator135**
- Return to console and run the T1-mapping sequence
- Do not switch off simulator until end of iBEAt protocol

12. **T2map kidneys cor-oblique mbh**: Breath-hold sequence acquired in coronal-oblique view with simulated ECG (simulator instructions same as T1-mapping). Copy the image slice location from previous sequence (*T1w_kidneys_cor-oblique_mbh*). **NOTE: Manually reduce the number of slices to 5.**
13. **T2star map kidneys cor-oblique bh**: Breath-hold sequence acquired in coronal-oblique view. Copy the image slice location from previous sequence (*T1w_kidneys_cor-oblique_mbh*). **NOTE: Manually reduce the number of slices to 5.**
14. **DTI kidney cor-obliqua fb**: Free breathing sequence acquired in coronal-oblique view. Copy the image location from previous sequence (*T1w_kidneys_cor-oblique_mbh*).
15. **IVIM kidneys cor-oblique fb**: Free-breathing sequence acquired in coronal-oblique view. Copy the image slice location from previous sequence (*T1w_kidneys_cor-oblique_mbh*).
16. **MT OFF kidneys cor-oblique bh**: Breath-hold sequence acquired in coronal-oblique view. Copy the image location from previous sequence (*T1w_kidneys_cor-oblique_mbh*). **NOTE: Manually reduce the number of slices to 16.**
17. **MT ON kidneys cor-oblique bh**: Breath-hold sequence acquired in coronal-oblique view. Copy the image location from previous sequence (*T1w_kidneys_cor-oblique_mbh*). **NOTE: Manually reduce the number of slices to 16.**
18. **ASL**: License not available in Sheffield. Do not acquire. In progress.
19. **3D DISCO Dyn kidneys cor-oblique fb**: Free breathing sequence. Start contrast agent administration 20 seconds AFTER starting the DCE MRI sequence. The *coronal-oblique* slices centered to the kidneys. Make sure that the aorta is always inside the scan slab (ensure while planning in sagittal view). Please check *attached document* for DOTAREM/GADOVIST dosage (based on patient weight) and injection rate.
20. **T1w abdomen post contrast dixon cor bh**: Breath-hold sequence with same positioning as *T1w_abdomen_dixon_cor_bh* sequence.

Switch off simulator (TPS RESET)

Additional Considerations

1. ***Specific Absorption Rate (SAR) level issues:*** In case of SAR level issues, change the scan mode from Normal to 1st level. In case of required further changes, select suggested new flip angle.
2. ***Image Quality Control:*** Please ensure a quick visual check on the acquired images is made right after each acquired sequence to avoid potential artifacts that may require repeating the scan. See below for unacceptable artifacts in the images that necessarily require scan repetition.
3. ***Insufficient Kidney Coverage:*** Increase the slice slab by first increasing the slice spacing and then by increasing the number of slices (if required).
4. ***Imaging Artifacts to be Avoided:*** Check acquired image for following artifacts and repeat if any of the below is true:



Appendix F: iBEAT MR acquisition protocol (GE MRI scanner)

MRI data were acquired on GE MRI scanner using 18-channel phased array body coil combined with inbuilt spine coil for signal reception. The following MR sequences are part of the iBEAT study (308).

Phase contrast MRI

PC-MRI was acquired with ECG-triggering 2D gradient echo (GRE) pulse sequence. Renal arteries were depicted off a combination of a coronal survey scan and an axial HASTE sequence. The imaging plane of PC was positioned perpendicular to the renal artery close to its origin from the descending aorta. The free-breathing PC acquisition was performed with retrospective gating using the following parameters: TR 40.48 ms; TE 2.74 ms; matrix 350x238; flip angle 25°; slice thickness 6mm, velocity encoding 120 cm/sec. At a typical R-R interval, 20 temporal frames during the heart cycle were acquired, with 1.40 minutes total scan time for each renal artery.

Arterial spin labelling

ASL was performed using pseudo-continuous labelling (pCASL) and 3D turbo gradient spin-echo readout (TGSE) in free-breathing mode. ASL was acquired in a coronal-oblique orientation using the following parameters: FOV 300mm; slice thickness 5mm; Number of slices 16; TR 5000ms; TE 19.28ms; flip angle 28°, labelling duration 1500ms, post-labelling delay 3000ms. Sequence acquisition results in multiple sets of MR images: label image, control image, and proton density weighted image (M0).

RBF maps were reconstructed online, preceded by retrospective 2D motion correction that is applied to the acquired MR datasets. (WEASEL software)

Dynamic contrast enhanced MRI

MRI data were acquired in free-breathing using 2D Turbo-FLASH sequence. The dynamic dataset consisted of 8 coronal-oblique slices that covers the kidneys and 1 axial slice obtained across the abdominal aorta, images were acquired every 1.5 s for 7:07 min resulting in a total of 265 images. DCE sequence parameters were: TR 179 ms; TE 0.97 ms; flip angle 10°; TI 85

ms; voxel size 1.0×1.0×7.5 mm; matrix size 400×300; slice spacing= 1.5 mm. Parallel imaging technique GRAPPA was employed with acceleration factor=2.

Dotarem (Gd-DOTA) was injected intravenously with a dose of 0.05 ml/kg at a rate of 2mL/s followed by a 20 mL saline flush. The injection was given 20 seconds after the acquisition started using an automatic power injector.

References

1. Hole B, Gilg J, Casula A, Methven S, Castledine C. UK renal registry 20th annual report: Chapter 1 UK renal replacement therapy adult incidence in 2016: National and centre-specific analyses. *Nephron*. 2018;139.
2. Burgos LG, Ebert TJ, Asiddao C, Turner LA, Pattison CZ, Wang-Cheng R, et al. Increased intraoperative cardiovascular morbidity in diabetics with autonomic neuropathy. *Anesthesiology*. 1989;70(4).
3. Astrup AS, Tarnow L, Rossing P, Hansen B V., Hilsted J, Parving HH. Cardiac autonomic neuropathy predicts cardiovascular morbidity and mortality in type 1 diabetic patients with diabetic nephropathy. *Diabetes Care*. 2006;29(2).
4. Copur S, Onal EM, Afsar B, Ortiz A, van Raalte DH, Cherney DZ, et al. Diabetes mellitus in chronic kidney disease: Biomarkers beyond HbA1c to estimate glycemic control and diabetes-dependent morbidity and mortality. Vol. 34, *Journal of Diabetes and its Complications*. 2020.
5. Sapra A, Bhandari P. Diabetes Mellitus [Internet]. StatPearls. 2021. Available from: <http://www.ncbi.nlm.nih.gov/pubmed/31855345>
6. Owen K, Turner H, Wass J. Oxford handbook of endocrinology and diabetes . 4th ed. 2022. 837–978 p.
7. IDF. International Diabetes Federation Atlas [Internet]. 2024 [cited 2024 Jun 1]. Available from: <https://diabetesatlas.org/>
8. World Health Organisation. World Health Organisation-Health Topic-Diabetes [Internet]. 2024 [cited 2024 Jun 1]. Available from: https://www.who.int/health-topics/diabetes#tab=tab_1
9. Diabetes UK. Diabetes Statistics [Internet]. 2024 [cited 2024 Jun 1]. Available from: <https://www.diabetes.org.uk/professionals/position-statements-reports/statistics>
10. Diabetes UK. Guide to diabetes [Internet]. 2024 [cited 2024 Jun 1]. Available from: <https://www.diabetes.org.uk/guide-to-diabetes/complications>
11. NICE UK. Type 2 Diabetes in adults: management. NICE guideline. NICE guideline. 2015;(December).
12. Diabetes.co.uk. Cost of diabetes. 2023 Oct [cited 2024 Jun 1]; Available from: <https://www.diabetes.co.uk/cost-of->

- diabetes.html#:~:text=This%20equates%20to%20over%20£,to%204%20million%20by%202025.
13. Zimmerman RS. Diabetes mellitus: management of microvascular and macrovascular complications. J Cleveland Clinic: Centers for Continuing Education. 2016.
 14. Thomas M, BM, SK et al. Diabetic kidney disease . Nature Review Disease Primers. 2015 Jul;
 15. Sugahara M, Pak WLW, Tanaka T, Tang SCW, Nangaku M. Update on diagnosis, pathophysiology, and management of diabetic kidney disease. Nephrology [Internet]. 2021 Jun 17;26(6):491–500. Available from: <https://onlinelibrary.wiley.com/doi/10.1111/nep.13860>
 16. Redon J. Measurement of microalbuminuria - What the nephrologist should know. Vol. 21, Nephrology Dialysis Transplantation. 2006. p. 573–6.
 17. Brotman DJ, Bash LD, Qayyum R, Crews D, Whitsel EA, Astor BC, et al. Heart rate variability predicts ESRD and CKD-related hospitalization. Journal of the American Society of Nephrology. 2010;21(9).
 18. Noble R, Taal MW. Epidemiology and causes of chronic kidney disease. Vol. 47, Medicine (United Kingdom). 2019.
 19. Steddon S, Chesser A, Cunningham J, Ashman N. Oxford Handbook of Nephrology and Hypertension. The Kidney in systemic disease, Chapter 8; Diabetic Nephropathy. second edition. Oxford Handbook of Nephrology and Hypertension. Oxford, UK: Oxford University Press; 2014.
 20. 11. Microvascular Complications and Foot Care: *Standards of Medical Care in Diabetes—2021*. Diabetes Care [Internet]. 2021 Jan 1;44(Supplement_1):S151–67. Available from: https://diabetesjournals.org/care/article/44/Supplement_1/S151/30492/11-Microvascular-Complications-and-Foot-Care
 21. Department of health: Republic of South Africa. Type 2 diabetes Management of in adults [Internet]. 2019. Available from: <https://www.nice.org.uk/guidance/ng28>
 22. 2019 ESC Guidelines on diabetes, pre-diabetes, and cardiovascular diseases developed in collaboration with the EASD: The Task Force for diabetes, pre-diabetes, and cardiovascular diseases of the European Society of Cardiology (ESC) and the

- European Association for the Study of Diabetes (EASD). *Revista Española de Cardiología* (English Edition). 2020;73(5).
23. Selby NM, Taal MW. An updated overview of diabetic nephropathy: Diagnosis, prognosis, treatment goals and latest guidelines. *Diabetes Obes Metab* [Internet]. 2020 Apr 8;22(S1):3–15. Available from:
<https://onlinelibrary.wiley.com/doi/10.1111/dom.14007>
 24. Persson F, Rossing P. Diagnosis of diabetic kidney disease: state of the art and future perspective. Vol. 8, *Kidney International Supplements*. 2018.
 25. Parving HH, Gall MA, Skøtt P, Jørgensen HE, Løkkegaard H, Jørgensen F, et al. Prevalence and causes of albuminuria in non-insulin-dependent diabetic patients. *Kidney Int*. 1992;41(4).
 26. Gambará V, Mecca G, Remuzzi G, Bertani T. Heterogeneous nature of renal lesions in type II diabetes. *Journal of the American Society of Nephrology*. 1993;3(8).
 27. Fioretto P, Mauer M, Brocco E, Velussi M, Frigato F, Muollo B, et al. Patterns of renal injury in NIDDM patients with microalbuminuria. In: *Diabetologia*. 1996.
 28. Bermejo S, Pascual J, Soler MJ. The current role of renal biopsy in diabetic patients. Vol. 109, *Minerva Medica*. 2018.
 29. Alicic RZ, Rooney MT, Tuttle KR. Diabetic kidney disease: Challenges, progress, and possibilities. *Clinical Journal of the American Society of Nephrology*. 2017;12(12).
 30. Sinha SK, Nicholas SB. Pathomechanisms of Diabetic Kidney Disease. Vol. 12, *Journal of Clinical Medicine*. 2023.
 31. Qazi M, Sawaf H, Ismail J, Qazi H, Vachharajani T. Pathophysiology of Diabetic Kidney Disease Key Points. Citation: *EMJ Nephrol*. 2022;10(1).
 32. Bonner R, Albajrami O, Hudspeth J, Upadhyay A. Diabetic Kidney Disease. Primary Care: Clinics in Office Practice [Internet]. 2020 Dec 1;47(4):645–59. Available from:
<https://linkinghub.elsevier.com/retrieve/pii/S0095454320300580>
 33. Hesp AC, Schaub JA, Prasad P V., Vallon V, Laverman GD, Bjornstad P, et al. The role of renal hypoxia in the pathogenesis of diabetic kidney disease: a promising target for newer renoprotective agents including SGLT2 inhibitors? Vol. 98, *Kidney International*. 2020.

34. DeFronzo RA, Reeves WB, Awad AS. Pathophysiology of diabetic kidney disease: impact of SGLT2 inhibitors. Vol. 17, *Nature Reviews Nephrology*. Nature Research; 2021. p. 319–34.
35. Maric-Bilkan C. Obesity and Diabetic Kidney Disease. Vol. 97, *Medical Clinics of North America*. 2013.
36. Pichler RH, De Boer IH. Dual renin-angiotensin-aldosterone system blockade for diabetic kidney disease. Vol. 10, *Current Diabetes Reports*. 2010.
37. Benigni A, Cassis P, Remuzzi G. Angiotensin II revisited: New roles in inflammation, immunology and aging. Vol. 2, *EMBO Molecular Medicine*. 2010.
38. Chen D, Chen Z, Park C, Centrella M, McCarthy T, Chen L, et al. Aldosterone stimulates fibronectin synthesis in renal fibroblasts through mineralocorticoid receptor-dependent and independent mechanisms. *Gene*. 2013;531(1).
39. Raina R, Chauvin A, Chakraborty R, Nair N, Shah H, Krishnappa V, et al. The role of endothelin and endothelin antagonists in chronic kidney disease. Vol. 6, *Kidney Diseases*. 2020.
40. Susztak K, Raff AC, Schiffer M, Böttinger EP. Glucose-induced reactive oxygen species cause apoptosis of podocytes and podocyte depletion at the onset of diabetic nephropathy. *Diabetes*. 2006;55(1).
41. Jha JC, Banal C, Chow BSM, Cooper ME, Jandeleit-Dahm K. Diabetes and Kidney Disease: Role of Oxidative Stress. Vol. 25, *Antioxidants and Redox Signaling*. 2016.
42. Hensley K, Robinson KA, Gabbita SP, Salsman S, Floyd RA. Reactive oxygen species, cell signaling, and cell injury. In: *Free Radical Biology and Medicine*. 2000.
43. Bernhardt WM, Schmitt R, Rosenberger C, Münchenhagen PM, Gröne HJ, Frei U, et al. Expression of hypoxia-inducible transcription factors in developing human and rat kidneys. *Kidney Int*. 2006;69(1).
44. Advani A, Gilbert RE. The Endothelium in Diabetic Nephropathy. *Semin Nephrol*. 2012;32(2).
45. Araújo LS, Torquato BGS, Da Silva CA, Dos Reis Monteiro MLG, Dos Santos Martins ALM, Da Silva MV, et al. Renal expression of cytokines and chemokines in diabetic nephropathy. *BMC Nephrol*. 2020;21(1).
46. Flyvbjerg A. The role of the complement system in diabetic nephropathy. Vol. 13, *Nature Reviews Nephrology*. 2017.

47. Gu HF. Genetic and epigenetic studies in diabetic kidney disease. *Front Genet.* 2019;10(JUN).
48. Freedman BI, Bostrom M, Daeihagh P, Bowden DW. Genetic factors in diabetic nephropathy. Vol. 2, *Clinical Journal of the American Society of Nephrology.* 2007.
49. Kato M, Natarajan R. Diabetic nephropathy-emerging epigenetic mechanisms. Vol. 10, *Nature Reviews Nephrology.* 2014.
50. Fyhrquist F, Tiitu A, Saijonmaa O, Forsblom C, Groop PH. Telomere length and progression of diabetic nephropathy in patients with type 1 diabetes. *J Intern Med.* 2010;267(3).
51. Sutanto SSI, McLennan SV, Keech AC, Twigg SM. Shortening of telomere length by metabolic factors in diabetes: protective effects of fenofibrate. *J Cell Commun Signal.* 2019;13(4).
52. Wang X, Liu J, Zhen J, Zhang C, Wan Q, Liu G, et al. Histone deacetylase 4 selectively contributes to podocyte injury in diabetic nephropathy. *Kidney Int.* 2014;86(4).
53. Miao F, Wu X, Zhang L, Yuan YC, Riggs AD, Natarajan R. Genome-wide analysis of histone lysine methylation variations caused by diabetic conditions in human monocytes. *Journal of Biological Chemistry.* 2007;282(18).
54. Kato M, Natarajan R. Epigenetics and epigenomics in diabetic kidney disease and metabolic memory. Vol. 15, *Nature Reviews Nephrology.* 2019.
55. Yuan H, Reddy MA, Deshpande S, Jia Y, Park JT, Lanting LL, et al. Epigenetic histone modifications involved in profibrotic gene regulation by 12/15-lipoxygenase and its oxidized lipid products in diabetic nephropathy. *Antioxid Redox Signal.* 2016;24(7).
56. Zhang L, Chen L, Gao C, Chen E, Lightle AR, Foulke L, et al. Loss of histone H3 K79 methyltransferase dot1l facilitates kidney fibrosis by upregulating endothelin 1 through histone deacetylase 2. *Journal of the American Society of Nephrology.* 2020;31(2).
57. Mimura I. Epigenetic memory in kidney diseases. Vol. 89, *Kidney International.* 2016.
58. Vestra MD, Saller A, Bortoloso E, Mauer M, Fioretto P. Structural involvement in type 1 and type 2 diabetic nephropathy. In: *Diabetes and Metabolism.* 2000.
59. Lewko B, Stepinski J. Hyperglycemia and mechanical stress: Targeting the renal podocyte. Vol. 221, *Journal of Cellular Physiology.* 2009.

60. Qian Y, Feldman E, Pennathur S, Kretzler M, Brosius FC. From fibrosis to sclerosis: Mechanisms of glomerulosclerosis in diabetic nephropathy. Vol. 57, Diabetes. 2008.
61. Lemley K v., Abdullah I, Myers BD, Meyer TW, Blouch K, Smith WE, et al. Evolution of incipient nephropathy in type 2 diabetes mellitus. *Kidney Int.* 2000;58(3).
62. Gil CL, Hooker E, Larrivée B. Diabetic Kidney Disease, Endothelial Damage, and Podocyte-Endothelial Crosstalk. *Kidney Med [Internet]*. 2021 Jan;3(1):105–15. Available from: <https://linkinghub.elsevier.com/retrieve/pii/S2590059520302624>
63. Kato H, Gruenwald A, Suh JH, Miner JH, Barisoni-Thomas L, Taketo MM, et al. Wnt/ β -catenin pathway in podocytes integrates cell adhesion, differentiation, and survival. *Journal of Biological Chemistry.* 2011;286(29).
64. Herman-Edelstein M, Thomas MC, Thallas-Bonke V, Saleem M, Cooper ME, Kantharidis P. Dedifferentiation of immortalized human podocytes in response to transforming growth factor- β : A model for diabetic podocytopathy. *Diabetes.* 2011;60(6).
65. Bohle A, Mackensen-Haen S, von Gise H, Grund KE, Wehrmann M, Batz C, et al. The Consequences of Tubulo-Interstitial Changes for Renal Function in Glomerulopathies: A Morphometric and Cytological Analysis. *Pathol Res Pract.* 1990;186(1).
66. Mogensen CE, Christensen CK, Vittinghus E. The stages in diabetic renal disease. With emphasis on the stage of incipient diabetic nephropathy. Vol. 32, Diabetes. 1983.
67. Mogensen CE. Renal function changes in diabetes. *Diabetes.* 1976;25(SUP.2).
68. Ayodele OE, Alebiosu CO, Salako BL. Diabetic nephropathy - A review of the natural history, burden, risk factors and treatment. Vol. 96, *Journal of the National Medical Association.* 2004.
69. Altemtam N, Russell J, El Nahas M. A study of the natural history of diabetic kidney disease (DKD). *Nephrol Dial Transplant.* 2012;27(5).
70. Haneda M, Utsunomiya K, Koya D, Babazono T, Moriya T, Makino H, et al. A new Classification of Diabetic Nephropathy 2014: A report from Joint Committee on Diabetic Nephropathy. *J Diabetes Investig.* 2015;6(2).
71. Bilous Rudy. Microvascular disease: what does the UKPDS tell us about diabetic nephropathy? *Diabetic Medicine.* 2008 Jul 18;25(2):25–9.
72. KDIGO 2020 Clinical Practice Guideline for Diabetes Management in Chronic Kidney Disease. *Kidney Int.* 2020;98(4).

73. McGrath K, Edi R. Diabetic Kidney Disease: Diagnosis, Treatment, and Prevention. Am Fam Physician [Internet]. 2019 Jun 15;99(12):751–9. Available from: <http://www.ncbi.nlm.nih.gov/pubmed/31194487>
74. Roberts CK, Barnard RJ. Effects of exercise and diet on chronic disease. Vol. 98, Journal of Applied Physiology. 2005.
75. Allison RL. Back to Basics: The Effect of Healthy Diet and Exercise on Chronic Disease Management. South Dakota medicine : the journal of the South Dakota State Medical Association. 2017.
76. Zemchenkov A, Vishnevsky K, Rumyantsev A, Zakharova E. KDIGO 2022 CLINICAL PRACTICE GUIDELINE FOR DIABETES MANAGEMENT IN CHRONIC KIDNEY DISEASE. Nephrology and Dialysis. 2023;25(2).
77. Shamoon H, others. The effect of intensive treatment of diabetes on the development and progression of long-term complications in insulin-dependent diabetes mellitus. The Diabetes Control and Complications Trial Research Group. N Engl J Med. 1993;329.
78. Garrick R. Intensive Diabetes Therapy and Glomerular Filtration Rate in Type 1 Diabetes. Yearbook of Medicine. 2012;2012.
79. Nunnelee JD. Review of an article: The ADVANCE Collaborative Group. (2008). Intensive Blood Glucose Control and Vascular Outcomes in Patients with Type 2 Diabetes. NEJM 2008;358:2560-2572. Journal of Vascular Nursing. 2008;26(4).
80. Saphner T, Wolff AC, Sledge GW, Wood WC, Davidson NE, Tu D, et al. Effects of Intensive Glucose Lowering in Type 2 Diabetes. The Action to Control Cardiovascular Risk in Diabetes Study Group. October. 2008;358(24).
81. Perkovic V, Jardine MJ, Neal B, Bompont S, Heerspink HJL, Charytan DM, et al. Canagliflozin and Renal Outcomes in Type 2 Diabetes and Nephropathy. New England Journal of Medicine. 2019;380(24).
82. Baigent C, Landray MJ, Reith C, Emberson J, Wheeler DC, Tomson C, et al. The effects of lowering LDL cholesterol with simvastatin plus ezetimibe in patients with chronic kidney disease (Study of Heart and Renal Protection): A randomised placebo-controlled trial. The Lancet. 2011;377(9784).
83. McGarry JD. Dysregulation of Fatty Acid Metabolism in the Etiology of Type 2 Diabetes. Diabetes. 2002;51(1).

84. Sandhu S, Wiebe N, Fried LF, Tonelli M. Statins for improving renal outcomes: A meta-Analysis. *Journal of the American Society of Nephrology*. 2006;17(7).
85. Chung YH, Lee YC, Chang CH, Lin MS, Lin JW, Lai MS. Statins of high versus low cholesterol-lowering efficacy and the development of severe renal failure. *Pharmacoepidemiol Drug Saf*. 2013;22(6).
86. Haynes R, Lewis D, Emberson J, Reith C, Agodoa L, Cass A, et al. Effects of lowering LDL cholesterol on progression of kidney disease. *Journal of the American Society of Nephrology*. 2014;25(8).
87. Ansquer JC, Foucher C, Rattier S, Taskinen MR, Steiner G. Fenofibrate reduces progression to microalbuminuria over 3 years in a placebo-controlled study in type 2 diabetes: Results from the Diabetes Atherosclerosis Intervention Study (DAIS). *American Journal of Kidney Diseases*. 2005;45(3).
88. Tonolo G, Velussi M, Brocco E, Abaterusso C, Carraro A, Morgia G, et al. Simvastatin maintains steady patterns of GFR and improves AER and expression of slit diaphragm proteins in type II diabetes. *Kidney Int*. 2006;70(1).
89. Tonelli MA, Wanner C, Cass A, Garg AX, Holdaas H, Jardine AG, et al. Kidney Disease: Improving Global Outcomes (KDIGO) lipid work group. KDIGO clinical practice guideline for lipid management in chronic kidney disease. *Kidney Int Suppl* (2011). 2013;3(3).
90. Hsiao CC, Yeh JK, Li YR, Sun WC, Fan PY, Yen CL, et al. Statin uses in adults with non-dialysis advanced chronic kidney disease: Focus on clinical outcomes of infectious and cardiovascular diseases. *Front Pharmacol*. 2022;13.
91. Hitzeman N. Statins for non-dialysis chronic kidney disease. Vol. 81, *American Family Physician*. 2010.
92. Group TMCS. Captopril reduces the risk of nephropathy in IDDM patients with microalbuminuria. *Diabetologia*. 1996;39(5).
93. Viberti G, Mogensen CE, Groop LC, Pauls JF, Boner G, van Dyk DJ, et al. Effect of Captopril on Progression to Clinical Proteinuria in Patients With Insulin-Dependent Diabetes Mellitus and Microalbuminuria. *JAMA: The Journal of the American Medical Association*. 1994;271(4).

94. Lewis EJ, Hunsicker LG, Bain RP, Rohde RD. The effect of angiotensin-converting-enzyme inhibition on diabetic nephropathy. The Collaborative Study Group. New England Journal of Medicine. 1993;329(20).
95. Lewis EJ, Hunsicker LG, Clarke WR, Berl T, Pohl MA, Lewis JB, et al. Renoprotective Effect of the Angiotensin-Receptor Antagonist Irbesartan in Patients with Nephropathy Due to Type 2 Diabetes. New England Journal of Medicine. 2001;345(12).
96. Brenner BM, Cooper ME, de Zeeuw D, Keane WF, Mitch WE, Parving HH, et al. Effects of Losartan on Renal and Cardiovascular Outcomes in Patients with Type 2 Diabetes and Nephropathy. New England Journal of Medicine. 2001;345(12).
97. Viberti G, Wheeldon NM. Microalbuminuria reduction with valsartan in patients with type 2 diabetes mellitus: A blood pressure-independent effect. Circulation. 2002;106(6).
98. Parving HH, Lehnert H, Bröchner-Mortensen J, Gomis R, Andersen S, Arner P. The Effect of Irbesartan on the Development of Diabetic Nephropathy in Patients with Type 2 Diabetes. New England Journal of Medicine. 2001;345(12).
99. Sica DA, Bakris GL. Type 2 diabetes: RENAAL and IDNT - The emergence of new treatment options. J Clin Hypertens. 2002;4(1).
100. Ruggenenti P, Cravedi P, Remuzzi G. The RAAS in the pathogenesis and treatment of diabetic nephropathy. Nat Rev Nephrol. 2010;6(6).
101. Emdin CA, Rahimi K, Neal B, Callender T, Perkovic V, Patel A. Blood pressure lowering in type 2 diabetes : A systematic review and meta-analysis. Vol. 313, JAMA - Journal of the American Medical Association. 2015.
102. Cheung AK, Chang TI, Cushman WC, Furth SL, Hou FF, Ix JH, et al. Executive summary of the KDIGO 2021 Clinical Practice Guideline for the Management of Blood Pressure in Chronic Kidney Disease. Kidney Int. 2021;99(3).
103. Heerspink HJL, Stefánsson B V., Correa-Rotter R, Chertow GM, Greene T, Hou FF, et al. Dapagliflozin in Patients with Chronic Kidney Disease. New England Journal of Medicine. 2020;383(15).
104. Empagliflozin in Patients with Chronic Kidney Disease. New England Journal of Medicine. 2023;388(24).

105. Merovci A, Solis-Herrera C, Daniele G, Eldor R, Vanessa Fiorentino T, Tripathy D, et al. Dapagliflozin improves muscle insulin sensitivity but enhances endogenous glucose production. *Journal of Clinical Investigation*. 2014;124(2).
106. DeFronzo RA, Hompesch M, Kasichayanula S, Liu X, Hong Y, Pfister M, et al. Characterization of renal glucose reabsorption in response to dapagliflozin in healthy subjects and subjects with type 2 diabetes. *Diabetes Care*. 2013;36(10).
107. Ye N, Jardine MJ, Oshima M, Hockham C, Heerspink HJL, Agarwal R, et al. Blood Pressure Effects of Canagliflozin and Clinical Outcomes in Type 2 Diabetes and Chronic Kidney Disease: Insights From the CREDENCE Trial. *Circulation*. 2021;143(18).
108. Mazidi M, Rezaie P, Gao HK, Kengne AP. Effect of sodium-glucose cotransport-2 inhibitors on blood pressure in people with type 2 diabetes mellitus: A systematic review and meta-analysis of 43 randomized control trials with 22 528 patients. *J Am Heart Assoc*. 2017;6(6).
109. Beal B, Schutte AE, Neuen BL. Blood Pressure Effects of SGLT2 Inhibitors: Mechanisms and Clinical Evidence in Different Populations. Vol. 25, *Current Hypertension Reports*. 2023.
110. Packer M. Mechanisms of enhanced renal and hepatic erythropoietin synthesis by sodium-glucose cotransporter 2 inhibitors. Vol. 44, *European Heart Journal*. 2023.
111. Berman C, Vidmar AP, Chao LC. Glucagon-like peptide-1 receptor agonists for the treatment of type 2 diabetes in youth. Vol. 19, *touchREVIEWS in Endocrinology*. 2023.
112. Sattar N, Lee MMY, Kristensen SL, Branch KRH, Del Prato S, Khurmi NS, et al. Cardiovascular, mortality, and kidney outcomes with GLP-1 receptor agonists in patients with type 2 diabetes: a systematic review and meta-analysis of randomised trials. *Lancet Diabetes Endocrinol*. 2021;9(10).
113. Perkovic V, Tuttle KR, Rossing P, Mahaffey KW, Mann JFE, Bakris G, et al. Effects of Semaglutide on Chronic Kidney Disease in Patients with Type 2 Diabetes. *N Engl J Med* [Internet]. 2024 May 24; Available from: <http://www.ncbi.nlm.nih.gov/pubmed/38785209>
114. Agarwal R, Kolkhof P, Bakris G, Bauersachs J, Haller H, Wada T, et al. Steroidal and non-steroidal mineralocorticoid receptor antagonists in cardiorenal medicine. Vol. 42, *European Heart Journal*. 2021.

115. Bakris GL, Agarwal R, Anker SD, Pitt B, Ruilope LM, Rossing P, et al. Effect of Finerenone on Chronic Kidney Disease Outcomes in Type 2 Diabetes. *New England Journal of Medicine*. 2020;383(23).
116. Pitt B, Filippatos G, Agarwal R, Anker SD, Bakris GL, Rossing P, et al. Cardiovascular Events with Finerenone in Kidney Disease and Type 2 Diabetes. *New England Journal of Medicine*. 2021;385(24).
117. Ito S, Kashiwara N, Shikata K, Nangaku M, Wada T, Okuda Y, et al. Esaxerenone (CS-3150) in patients with type 2 diabetes and microalbuminuria (ESAX-DN): Phase 3 randomized controlled clinical trial. *Clinical Journal of the American Society of Nephrology*. 2020;15(12).
118. Ito S, Shikata K, Nangaku M, Okuda Y, Sawanobori T. Efficacy and safety of esaxerenone (CS-3150) for the treatment of type 2 diabetes with microalbuminuria A randomized, double-blind, placebo-controlled, phase ii trial. *Clinical Journal of the American Society of Nephrology*. 2019;14(8).
119. Sharma JK, Rohatgi A, Sharma D. Diabetic autonomic neuropathy: a clinical update. *Journal of the Royal College of Physicians of Edinburgh [Internet]*. 2020 Sep;50(3):269–73. Available from: <https://www.rcpe.ac.uk/college/journal/diabetic-autonomic-neuropathy-clinical-update>
120. Vinik AI, Maser RE, Mitchell BD, Freeman R. Diabetic autonomic neuropathy. Vol. 26, *Diabetes Care*. 2003.
121. Tracy JA, Dyck PJB. The Spectrum of Diabetic Neuropathies. Vol. 19, *Physical Medicine and Rehabilitation Clinics of North America*. 2008.
122. Ziegler D. Autonome diabetische Neuropathie. *Der Diabetologe [Internet]*. 2020 May 12;16(3):315–26. Available from: <http://link.springer.com/10.1007/s11428-020-00596-w>
123. Spallone V, Ziegler D, Freeman R, Bernardi L, Frontoni S, Pop-Busui R, et al. Cardiovascular autonomic neuropathy in diabetes: Clinical impact, assessment, diagnosis, and management. Vol. 27, *Diabetes/Metabolism Research and Reviews*. 2011.
124. Ewing DJ, Boland O, Neilson JMM, Cho CG, Clarke BF. Autonomic neuropathy, QT interval lengthening, and unexpected deaths in male diabetic patients. *Diabetologia*. 1991;34(3).

125. Fisher VL, Tahrani AA. Cardiac autonomic neuropathy in patients with diabetes mellitus: Current perspectives. Vol. 10, Diabetes, Metabolic Syndrome and Obesity: Targets and Therapy. 2017.
126. The effect of intensive diabetes therapy on measures of autonomic nervous system function in the Diabetes Control and Complications Trial (DCCT). Diabetologia. 1998;41(4).
127. Yan LJ. Pathogenesis of chronic hyperglycemia: From reductive stress to oxidative stress. Vol. 2014, Journal of Diabetes Research. 2014.
128. Pang L, Lian X, Liu H, Zhang Y, Li Q, Cai Y, et al. Understanding diabetic neuropathy: Focus on oxidative stress. Oxid Med Cell Longev. 2020;2020.
129. Goldin A, Beckman JA, Schmidt AM, Creager MA. Advanced glycation end products: Sparking the development of diabetic vascular injury. Vol. 114, Circulation. 2006.
130. Østergaard L, Finnerup NB, Terkelsen AJ, Olesen RA, Drasbek KR, Knudsen L, et al. The effects of capillary dysfunction on oxygen and glucose extraction in diabetic neuropathy. Vol. 58, Diabetologia. 2015.
131. Pennathur S, Jaiswal M, Vivekanandan-Giri A, White EA, Ang L, Raffel DM, et al. Structured lifestyle intervention in patients with the metabolic syndrome mitigates oxidative stress but fails to improve measures of cardiovascular autonomic neuropathy. J Diabetes Complications. 2017;31(9).
132. Yagihashi S, Mizukami H, Sugimoto K. Mechanism of diabetic neuropathy: Where are we now and where to go? Vol. 2, Journal of Diabetes Investigation. 2011.
133. Ormazabal V, Nair S, Elfeky O, Aguayo C, Salomon C, Zuñiga FA. Association between insulin resistance and the development of cardiovascular disease. Vol. 17, Cardiovascular Diabetology. 2018.
134. Williams S RSKMRUKPZSMABEAU. Cardiac Autonomic Neuropathy in Type 1 and 2 Diabetes: Epidemiology, Pathophysiology, and Management. Clin Ther. 2022 Oct;
135. Politi C, Ciccacci C, D'Amato C, Novelli G, Borgiani P, Spallone V. Recent advances in exploring the genetic susceptibility to diabetic neuropathy. Vol. 120, Diabetes Research and Clinical Practice. 2016.
136. Ciccacci C, Latini A, Greco C, Politi C, D'Amato C, Lauro D, et al. Association between a MIR499A polymorphism and diabetic neuropathy in type 2 diabetes. J Diabetes Complications. 2018;32(1).

137. Osztoivits J, Horváth T, Littvay L, Steinbach R, Jermendy Á, Tárnoki Á, et al. Effects of genetic vs. environmental factors on cardiovascular autonomic function: A twin study. *Diabetic Medicine*. 2011;28(10).
138. Serhiyenko VA, Serhiyenko AA. Cardiac autonomic neuropathy: Risk factors, diagnosis and treatment. *World J Diabetes*. 2018;9(1).
139. Pop-Busui R, Kirkwood I, Schmid H, Marinescu V, Schroeder J, Larkin D, et al. Sympathetic dysfunction in type 1 diabetes: Association with impaired myocardial blood flow reserve and diastolic dysfunction. *J Am Coll Cardiol*. 2004;44(12).
140. Taskiran M, Rasmussen V, Rasmussen B, Fritz-Hansen T, Larsson HBW, Jensen GB, et al. Left ventricular dysfunction in normotensive Type 1 diabetic patients: The impact of autonomic neuropathy. *Diabetic Medicine*. 2004;21(6).
141. Kuehl M, Stevens MJ. Cardiovascular autonomic neuropathies as complications of diabetes mellitus. Vol. 8, *Nature Reviews Endocrinology*. 2012.
142. Pop-Busui R, Boulton AJM, Feldman EL, Bril V, Freeman R, Malik RA, et al. Diabetic neuropathy: A position statement by the American diabetes association. *Diabetes Care*. 2017;40(1).
143. Gibbons CH, Schmidt P, Biaggioni I, Frazier-Mills C, Freeman R, Isaacson S, et al. The recommendations of a consensus panel for the screening, diagnosis, and treatment of neurogenic orthostatic hypotension and associated supine hypertension. Vol. 264, *Journal of Neurology*. 2017.
144. Spallone V. Update on the impact, diagnosis and management of cardiovascular autonomic neuropathy in diabetes: What is defined, what is new, and what is unmet. Vol. 43, *Diabetes and Metabolism Journal*. 2019.
145. Didangelos TP, Arsos GA, Karamitsos DT, Athyros VG, Georga SD, Karatzas ND. Effect of quinapril or losartan alone and in combination on left ventricular systolic and diastolic functions in asymptomatic patients with diabetic autonomic neuropathy. *J Diabetes Complications*. 2006;20(1).
146. Upd D, the and. Effect of Chronic Quinapril Administration on Heart Rate Variability in Patients With Diabetic Autonomic Neuropathy From the Divisions of Cardiology (. [cited 2023 Jul 30]; Available from: <http://diabetesjournals.org/care/article-pdf/20/3/355/583960/20-3-355.pdf>

147. Hjortkjaer HØ, Jensen T, Kofoed KF, Mogensen UM, Sigvardsen PE, Køber L, et al. Nocturnal antihypertensive treatment in patients with type 1 diabetes with autonomic neuropathy and non-dipping: A randomised, placebo-controlled, double-blind cross-over trial. *BMJ Open*. 2016;6(12).
148. Ebbenhøj E, Poulsen P, Hansen K, Knudsen S, Mølgaard H, Mogensen C. Effects on heart rate variability of metoprolol supplementary to ongoing ACE-inhibitor treatment in type I diabetic patients with abnormal albuminuria. *Diabetologia*. 2002;45(7).
149. Manzella D, Barbieri M, Ragno E, Paolisso G. Chronic administration of pharmacologic doses of vitamin E improves the cardiac autonomic nervous system in patients with type 2 diabetes. *American Journal of Clinical Nutrition*. 2001;73(6).
150. Serhiyenko VA, Mankovsky BN, Serhiyenko LM, Serhiyenko AA. The effect of omega-3 polyunsaturated fatty acids on ambulatory blood pressure monitoring parameters in patients with type 2 diabetes mellitus and cardiovascular autonomic neuropathy. *Diabetes Mellitus*. 2019;22(1).
151. Serhiyenko VA, Segin VB, Serhiyenko AA. Effects of omega-3 polyunsaturated fatty acids on the circadian rhythm of heart rate variability parameters in patients with type 2 diabetes mellitus and cardiovascular autonomic neuropathy. *Russian Journal of Cardiology*. 2018;(5).
152. Akbari M, Ostadmohammadi V, Lankarani KB, Tabrizi R, Kolahdooz F, Khatibi SR, et al. The effects of alpha-lipoic acid supplementation on glucose control and lipid profiles among patients with metabolic diseases: A systematic review and meta-analysis of randomized controlled trials. Vol. 87, *Metabolism: Clinical and Experimental*. 2018.
153. Tankova T, Koev D, Dakovska L. Alpha-lipoic acid in the treatment of autonomic diabetic neuropathy (controlled, randomized, open-label study). *Rom J Intern Med*. 2004;42(2).
154. Didangelos T, Karlafti E, Kotzakioulafi E, Kontoninas Z, Margaritidis C, Giannoulaki P, et al. Efficacy and safety of the combination of superoxide dismutase, alpha lipoic acid, Vitamin B12, and carnitine for 12 months in patients with diabetic neuropathy. *Nutrients*. 2020;12(11).
155. Capilupi MJ, Kerath SM, Becker LB. Vagus nerve stimulation and the cardiovascular system. *Cold Spring Harb Perspect Med*. 2020;10(2).

156. Shankar R, Olotu VO, Cole N, Sullivan H, Jory C. Case report: Vagal nerve stimulation and late onset asystole. *Seizure*. 2013;22(4).
157. Pascual FT. Vagus nerve stimulation and late-onset bradycardia and asystole: Case report. Vol. 26, *Seizure*. 2015.
158. Ben-Menachem E. Vagus nerve stimulation, side effects, and long-term safety. Vol. 18, *Journal of Clinical Neurophysiology*. 2001.
159. Chalouhy CharbelGT, Gest T. Kidney anatomy [Internet]. 2017 [cited 2024 Jul 9]. Available from: <https://emedicine.medscape.com/article/1948775-overview>
160. Oliver Jones. The kidneys [Internet]. 2024 [cited 2024 Jul 9]. Available from: <https://teachmeanatomy.info/abdomen/viscera/kidney/>
161. Gopalan C, Kirk E. Chapter 7 - Renal physiology. In: *Biology of Cardiovascular and Metabolic Diseases*. 2022.
162. Theodorou C, Leatherby R, Dhanda R. Function of the nephron and the formation of urine. Vol. 22, *Anaesthesia and Intensive Care Medicine*. 2021.
163. U.S. Department of Health and Human Services. The Kidneys and How They Work. National Institutes of Health. 2009;
164. Filonova S. Blood supply of kidney [Internet]. 2023 [cited 2024 Jul 9]. Available from: <https://www.wikilectures.eu/w/WikiLectures:Contacts>
165. Ritz E, Wolf G. Pathogenesis, Clinical Manifestations, and Natural History of Diabetic Nephropathy. In: *Comprehensive Clinical Nephrology*. 2010.
166. Mashitani T, Hayashino Y, Okamura S, Kitatani M, Furuya M, Iburi T, et al. Association between dipstick hematuria and decline in estimated glomerular filtration rate among Japanese patients with type 2 diabetes: A prospective cohort study [Diabetes Distress and Care Registry at Tenri (DDCRT 14)]. *J Diabetes Complications*. 2017;31(7).
167. Dalal R, Bruss ZS, Sehdev JS. Physiology, Renal Blood Flow and Filtration. *StatPearls*. 2021;
168. Botti RE, Razzak MA, Macintyre WJ, Pritchard WH. The relationship of renal blood flow to cardiac output in normal individuals as determined by concomitant radioisotopic measurements. Vol. 2, *Cardiovascular Research*. 1968.
169. Prasad P v., Li LP, Thacker JM, Li W, Hack B, Kohn O, et al. Cortical perfusion and tubular function as evaluated by magnetic resonance imaging correlates with annual loss in renal function in moderate chronic kidney disease. *Am J Nephrol*. 2019;49(2).

170. DiBartola SP. Applied Renal Physiology. In: Fluid, Electrolyte, and Acid-Base Disorders in Small Animal Practice, Fourth Edition. 2011.
171. Williamson GA, Loutzenhiser R, Wang X, Griffin K, Bidani AK. Systolic and mean blood pressures and afferent arteriolar myogenic response dynamics: A modeling approach. *Am J Physiol Regul Integr Comp Physiol*. 2008;295(5).
172. Staplin N, Herrington WG, Murgia F, Ibrahim M, Bull KR, Judge PK, et al. Determining the Relationship Between Blood Pressure, Kidney Function, and Chronic Kidney Disease: Insights From Genetic Epidemiology. *Hypertension*. 2022;79(12).
173. Beloncle F, Piquilloud L, Asfar P. Renal Blood Flow and Perfusion Pressure. In: *Critical Care Nephrology: Third Edition*. 2019.
174. Post EH, Vincent JL. Renal autoregulation and blood pressure management in circulatory shock. Vol. 22, *Critical Care*. 2018.
175. Pallone TL, Silldorff EP. Pericyte regulation of renal medullary blood flow. Vol. 9, *Experimental Nephrology*. 2001.
176. Supply of Blood and Nerves to the Kidneys. *MedLibretexts.org*. 2020 Aug;
177. Ito S, Carretero OA, Abe K. Nitric oxide in the regulation of renal blood flow. Vol. 3, *New Horizons: Science and Practice of Acute Medicine*. 1995.
178. Malpas SC, Leonard BL. Neural regulation of renal blood flow: A re-examination. Vol. 27, *Clinical and Experimental Pharmacology and Physiology*. 2000.
179. Johns EJ, Kopp UC, DiBona GF. Neural control of renal function. *Compr Physiol*. 2011;1(2).
180. Harrison-Bernard LM. The renal renin-angiotensin system. *American Journal of Physiology - Advances in Physiology Education*. 2009;33(4).
181. Bankir L, Bichet DG, Morgenthaler NG. Vasopressin: physiology, assessment and osmosensation. In: *Journal of Internal Medicine*. 2017.
182. Choi MR, Fernández BE. Protective Renal Effects of Atrial Natriuretic Peptide: Where Are We Now? Vol. 12, *Frontiers in Physiology*. 2021.
183. Rotunno R, Oppo I, Saetta G, Aveta P, Bruno S. NSAIDs and heart failure: A dangerous relationship. *Monaldi Archives for Chest Disease*. 2018;88(2).
184. Imamura H, Hata J, Iida A, Manabe N, Haruma K. Evaluating the effects of diclofenac sodium and etodolac on renal hemodynamics with contrast-enhanced ultrasonography: A pilot study. *Eur J Clin Pharmacol*. 2013;69(2).

185. Hellms S, Gueler F, Gutberlet M, Schebb NH, Rund K, Kielstein JT, et al. Single-dose diclofenac in healthy volunteers can cause decrease in renal perfusion measured by functional magnetic resonance imaging. *Journal of Pharmacy and Pharmacology*. 2019;71(8).
186. Lubas A, Kade G, Saracyn M, Niemczyk S, Dyrła P. Dynamic tissue perfusion assessment reflects associations between antihypertensive treatment and renal cortical perfusion in patients with chronic kidney disease and hypertension. *Int Urol Nephrol*. 2018;50(3).
187. van der Bel R, Coolen BF, Nederveen AJ, Potters W v., Verberne HJ, Vogt L, et al. Magnetic resonance imaging-derived renal oxygenation and perfusion during continuous, steady-state angiotensin-II infusion in healthy humans. *J Am Heart Assoc*. 2015;5(3).
188. Wilkinson R. β -Blockers and Renal Function. Vol. 23, *Drugs*. 1982.
189. Epstein M, Oster JR. Beta blockers and renal function: a reappraisal. Vol. 1, *Journal of clinical hypertension*. 1985.
190. Sasaki H, Saiki A, Endo K, Ban N, Yamaguchi T, Kawana H, et al. Protective effects of efonidipine, a T- and L-type calcium channel blocker, on renal function and arterial stiffness in type 2 diabetic patients with hypertension and nephropathy. *J Atheroscler Thromb*. 2009;16(5).
191. Benstein JA, Dworkin LD. Renal vascular effects of calcium channel blockers in hypertension. *Am J Hypertens*. 1990;3(10).
192. Schrier RW, Burke TJ. Role of calcium-channel blockers in preventing acute and chronic renal injury. *J Cardiovasc Pharmacol*. 1991;18.
193. Richard E. Klabunde. *Cardiovascular Pharmacology Concepts*. Cardiovascular Pharmacology Concepts. 2022;
194. Lannemyr L, Ricksten SE, Rundqvist B, Andersson B, Bartfay SE, Ljungman C, et al. Differential effects of levosimendan and dobutamine on glomerular filtration rate in patients with heart failure and renal impairment: A randomized double-blind controlled trial. *J Am Heart Assoc*. 2018;7(16).
195. Sarna MA, Hollenberg NK, Seely EW, Ahmed SB. Oral contraceptive progestins and angiotensin-dependent control of the renal circulation in humans. *J Hum Hypertens*. 2009;23(6).

196. Hollenberg NK, Williams GH, Burger B, Chenitz W, Hoosmand I, Adams DF. Renal blood flow and its response to angiotensin II. An interaction between oral contraceptive agents, sodium intake, and the renin angiotensin system in healthy young women. *Circ Res.* 1976;38(1).
197. Kang AK, Duncan JA, Cattran DC, Floras JS, Lai V, Scholey JW, et al. Effect of oral contraceptives on the renin angiotensin system and renal function. *Am J Physiol Regul Integr Comp Physiol.* 2001;280(3 49-3).
198. Cherney DZI, Scholey JW, Cattran DC, Kang AK, Zimpelmann J, Kennedy C, et al. The effect of oral contraceptives on the nitric oxide system and renal function. *Am J Physiol Renal Physiol.* 2007;293(5).
199. Ribstein J, Halimi JM, du Cailar G, Mimran A. Renal Characteristics and Effect of Angiotensin Suppression in Oral Contraceptive Users. *Hypertension.* 1999;33(1).
200. Bongers CCWG, Alsady M, Nijenhuis T, Tulp ADM, Eijsvogels TMH, Deen PMT, et al. Impact of acute versus prolonged exercise and dehydration on kidney function and injury. *Physiol Rep.* 2018;6(11).
201. Sawka MN. Adverse functional outcomes associated with body water deficits. *Nutr Hosp.* 2015;32 Suppl 2.
202. Perney P, Taourel P, Gallix B, Dauzat M, Joomaye Z, Djafari M, et al. Changes in renal artery resistance after meal-induced splanchnic vasodilatation in cirrhotic patients. *Journal of Clinical Ultrasound.* 2001;29(9).
203. Kishino T, Harashima K, Hashimoto S, Fukuta N, Seki M, Ohnishi H, et al. Meal Ingestion and Hemodynamic Interactions Regarding Renal Blood Flow on Duplex Sonography: Potential Diagnostic Implications. *Ultrasound Med Biol.* 2018;44(9).
204. Normand G, Lemoine S, Villien M, le Bars D, Merida I, Irace Z, et al. AGE content of a protein load is responsible for renal performances: A pilot study. *Diabetes Care.* 2018;41(6).
205. Kalantarinia K, Belcik JT, Patrie JT, Wei K. Real-time measurement of renal blood flow in healthy subjects using contrast-enhanced ultrasound. *Am J Physiol Renal Physiol.* 2009;297(4).
206. Hauser JA, Muthurangu V, Steeden JA, Taylor AM, Jones A. Comprehensive assessment of the global and regional vascular responses to food ingestion in humans using novel rapid MRI. *Am J Physiol Regul Integr Comp Physiol.* 2016;310(6).

207. Samnegård B, Brundin T. Renal extraction of insulin and C-peptide in man before and after a glucose meal. *Clinical Physiology*. 2001;21(2).
208. Fellner RC, Cook AK, O'Connor PM, Zhang S, Pollock DM, Inscho EW. High-salt diet blunts renal autoregulation by a reactive oxygen species-dependent mechanism. *Am J Physiol Renal Physiol*. 2014;307(1).
209. Yanagisawa H, Miyazaki T, Nodera M, Miyajima Y, Suzuki T, Kido T, et al. Zinc-excess intake causes the deterioration of renal function accompanied by an elevation in systemic blood pressure primarily through superoxide radical-induced oxidative stress. *Int J Toxicol*. 2014;33(4).
210. Poortmans JR. Exercise and renal function. *Sports Med*. 1984 Mar;125–53.
211. Kotoku K, Yasuno T, Kawakami S, Fujimi K, Matsuda T, Nakashima S, et al. Effect of exercise intensity on renal blood flow in patients with chronic kidney disease stage 2. *Clin Exp Nephrol*. 2019;23(5).
212. Kawakami S, Yasuno T, Matsuda T, Fujimi K, Ito A, Yoshimura S, et al. Association between exercise intensity and renal blood flow evaluated using ultrasound echo. *Clin Exp Nephrol*. 2018;22(5).
213. Suzuki M. Physical exercise and renal function. *J Phys Fit Sports Med*. 2015;4(1).
214. Liu J, Varghese BM, Hansen A, Borg MA, Zhang Y, Driscoll T, et al. Hot weather as a risk factor for kidney disease outcomes: A systematic review and meta-analysis of epidemiological evidence. Vol. 801, *Science of the Total Environment*. 2021.
215. Lee WS, Kim WS, Lim YH, Hong YC. High temperatures and kidney disease morbidity: A Systematic Review and Meta-analysis. Vol. 52, *Journal of Preventive Medicine and Public Health*. 2019.
216. Chapman CL, Johnson BD, Parker MD, Hostler D, Pryor RR, Schlader Z. Kidney physiology and pathophysiology during heat stress and the modification by exercise, dehydration, heat acclimation and aging. Vol. 8, *Temperature*. 2021.
217. Weinstein JR, Anderson S. The Aging Kidney: Physiological Changes. Vol. 17, *Advances in Chronic Kidney Disease*. 2010.
218. Hollenberg NK, Adams DF, Solomon HS, Rashid A, Abrams HL, Merrill JP. Senescence and the renal vasculature in normal man. *Circ Res*. 1974;34(3).
219. DAVIES DF, SHOCK NW. Age changes in glomerular filtration rate, effective renal plasma flow, and tubular excretory capacity in adult males. *J Clin Invest*. 1950;29(5).

220. Gava AL, Freitas FPS, Meyrelles SS, Silva I V., Graceli JB. Gender-dependent effects of aging on the kidney. Vol. 44, Brazilian Journal of Medical and Biological Research. 2011.
221. Miller JA, Anacta LA, Cattran DC. Impact of gender on the renal response to angiotensin II. Kidney Int. 1999;55(1).
222. Alhummiyany B, Sharma K, Buckley DL, Soe KK, Sourbron SP. Physiological confounders of renal blood flow measurement. Magnetic Resonance Materials in Physics, Biology and Medicine. 2023.
223. Toering TJ, Van Der Graaf AM, Visser FW, Buikema H, Navis G, Faas MM, et al. Gender differences in response to acute and chronic angiotensin II infusion: A translational approach. Physiol Rep. 2015;3(7).
224. Stasi A, Cosola C, Caggiano G, Cimmarusti MT, Palieri R, Acquaviva PM, et al. Obesity-Related Chronic Kidney Disease: Principal Mechanisms and New Approaches in Nutritional Management. Vol. 9, Frontiers in Nutrition. 2022.
225. Basolo A, Salvetti G, Giannese D, Genzano SB, Ceccarini G, Giannini R, et al. Obesity, Hyperfiltration, and Early Kidney Damage: A New Formula for the Estimation of Creatinine Clearance. Journal of Clinical Endocrinology and Metabolism. 2023;108(12).
226. Chagnac A, Weinstein T, Herman M, Hirsh J, Gafter U, Ori Y. The effects of weight loss on renal function in patients with severe obesity. Journal of the American Society of Nephrology. 2003;14(6).
227. Conrad KP, Davison JM. The renal circulation in normal pregnancy and preeclampsia: Is there a place for relaxin? Vol. 306, American Journal of Physiology - Renal Physiology. 2014.
228. Cheung KL, Lafayette RA. Renal Physiology of Pregnancy. Vol. 20, Advances in Chronic Kidney Disease. 2013.
229. Mandic Markovic V, Mikovic Z, Djukic M, Simic Ogrizovic S, Vasiljevic M. Doppler parameters of maternal renal blood flow in normal pregnancy. Clin Exp Obstet Gynecol. 2013;40(1).
230. Moe Eggebø T, Leknes Jensen EJ, Deibele KU, Scholbach T. Venous blood flow in maternal kidneys in third trimester of pregnancy. Journal of Maternal-Fetal and Neonatal Medicine. 2020;33(13).

231. Van Beek E, Houben AJHM, Van Es PN, Willekes C, Korten ECCM, De Leeuw PW, et al. Peripheral haemodynamics and renal function in relation to the menstrual cycle. *Clin Sci*. 1996;91(2).
232. Krejza J, Ustymowicz A, Szylak A, Tomaszewski M, Hryniewicz A, Jawad A. Assessment of variability of renal blood flow Doppler parameters during the menstrual cycle in women. *Ultrasound in Obstetrics and Gynecology*. 2005;25(1).
233. Brøchner-Mortensen J, Paaby P, Fjeldborg P, Raffn K, Larsen CE, Møller-Petersen J. Renal haemodynamics and extracellular homeostasis during the menstrual cycle. *Scand J Clin Lab Invest*. 1987;47(8).
234. Mohandas R, Douma LG, Scindia Y, Gumz ML. Circadian rhythms and renal pathophysiology. Vol. 132, *Journal of Clinical Investigation*. 2022.
235. WESSON LG. ELECTROLYTE EXCRETION IN RELATION TO DIURNAL CYCLES OF RENAL FUNCTION. *Medicine*. 1964;43(5).
236. Eckerbom P, Hansell P, Cox E, Buchanan C, Weis J, Palm F, et al. Circadian variation in renal blood flow and kidney function in healthy volunteers monitored with noninvasive magnetic resonance imaging. *Am J Physiol Renal Physiol*. 2020;319(6).
237. PFEIFFER JB, WOLFF HG, WINTER OS. Studies in renal circulation during periods of life stress and accompanying emotional reactions in subjects with and without essential hypertension; observations on the role of neural activity in regulation of renal blood flow. *J Clin Invest*. 1950;29(9).
238. Ducher M, Bertram D, Pozet N, Laville M, Fauvel JP. Stress-induced renal alterations in normotensives offspring of hypertensives and in hypertensives. *Am J Hypertens*. 2002;15(4 I).
239. Castellani S, Ungar A, Cantini C, La Cava G, Di Serio C, Altobelli A, et al. Excessive vasoconstriction after stress by the aging kidney: Inadequate prostaglandin modulation of increased endothelin activity. *Journal of Laboratory and Clinical Medicine*. 1998;132(3).
240. Orth S. Cigarette smoking: an important renal risk factor – far beyond carcinogenesis. *Tob Induc Dis*. 2003;1(2).
241. Halimi JM, Philippon C, Mimran A. Contrasting renal effects of nicotine in smokers and non-smokers. *Nephrology Dialysis Transplantation*. 1998;13(4).

242. Eid HA, Moazen EM, Elhussini M, Shoman H, Hassan A, Elsheikh A, et al. The Influence of Smoking on Renal Functions Among Apparently Healthy Smokers. *J Multidiscip Healthc.* 2022;15.
243. Yoon HJ, Park M, Yoon H, Son KY, Cho BL, Kim S. The differential effect of cigarette smoking on glomerular filtration rate and proteinuria in an apparently healthy population. *Hypertension Research.* 2009;32(3).
244. Palubiski LM, O'Halloran KD, O'Neill J. Renal Physiological Adaptation to High Altitude: A Systematic Review. *Front Physiol.* 2020;11.
245. Ge RL, Witkowski S, Zhang Y, Alfrey C, Sivieri M, Karlsen T, et al. Determinants of erythropoietin release in response to short-term hypobaric hypoxia. *J Appl Physiol.* 2002;92(6).
246. Tonneijck L, Muskiet MHA, Smits MM, Van Bommel EJ, Heerspink HJL, Van Raalte DH, et al. Glomerular hyperfiltration in diabetes: Mechanisms, clinical significance, and treatment. Vol. 28, *Journal of the American Society of Nephrology.* 2017.
247. Pedersen M, Irrera P, Dastrù W, Zöllner FG, Bennett KM, Beeman SC, et al. Dynamic contrast enhancement (dce) mri-derived renal perfusion and filtration: Basic concepts. In: *Methods in Molecular Biology.* 2021.
248. Bokacheva L, Rusinek H, Chen Q, Oesingmann N, Prince C, Kaur M, et al. Quantitative determination of Gd-DTPA concentration in T 1-weighted MR renography studies. *Magn Reson Med.* 2007;57(6).
249. Kannenkeril D, Janka R, Bosch A, Jung S, Kolwelter J, Striepe K, et al. Detection of Changes in Renal Blood Flow Using Arterial Spin Labeling MRI. *Am J Nephrol.* 2021;52(1).
250. Alhummiyany BA, Shelley D, Saysell M, Olaru MA, Kühn B, Buckley DL, et al. Bias and Precision in Magnetic Resonance Imaging-Based Estimates of Renal Blood Flow: Assessment by Triangulation. *Journal of Magnetic Resonance Imaging.* 2022;55(4).
251. Guyader JM, Huizinga W, Poot DHJ, van Kranenburg M, Uitterdijk A, Niessen WJ, et al. Groupwise image registration based on a total correlation dissimilarity measure for quantitative MRI and dynamic imaging data. *Sci Rep.* 2018;8(1).
252. Johansson A, Balter J, Cao Y. Rigid-body motion correction of the liver in image reconstruction for golden-angle stack-of-stars DCE MRI. *Magn Reson Med.* 2018;79(3).

253. Zöllner FG, Daab M, Sourbron SP, Schad LR, Schoenberg SO, Weisser G. An open source software for analysis of dynamic contrast enhanced magnetic resonance images: UMMPerfusion revisited. *BMC Med Imaging*. 2016;16(1).
254. Sourbron SP, Michaely HJ, Reiser MF, Schoenberg SO. MRI-measurement of perfusion and glomerular filtration in the human kidney with a separable compartment model. *Invest Radiol*. 2008;43(1).
255. Royal College of Radiologists. Guidance on gadolinium-based contrast agent administration to adult patients Contents [Internet]. 2019. Available from: www.rcr.ac.uk
256. Prince MR, Zhang H, Zou Z, Staron RB, Brill PW. Incidence of immediate gadolinium contrast media reactions. *American Journal of Roentgenology*. 2011;196(2).
257. Behzadi AH, Zhao Y, Farooq Z, Prince MR. Immediate allergic reactions to gadolinium-based contrast agents: A systematic review and meta-analysis. Vol. 286, *Radiology*. 2018.
258. Schieda N, Maralani PJ, Hurrell C, Tsampalieros AK, Hiremath S. Updated Clinical Practice Guideline on Use of Gadolinium-Based Contrast Agents in Kidney Disease Issued by the Canadian Association of Radiologists. Vol. 70, *Canadian Association of Radiologists Journal*. 2019.
259. Rogosnitzky M, Branch S. Gadolinium-based contrast agent toxicity: a review of known and proposed mechanisms. Vol. 29, *BioMetals*. 2016.
260. Ibrahim MA, Hazhirkarzar B, Dublin AB. Gadolinium magnetic resonance imaging. *NCBI Bookshelf*. 2023.
261. Thomson LK, Thomson PC, Kingsmore DB, Blessing K, Daly CD, Cowper SE, et al. Diagnosing nephrogenic systemic fibrosis in the post-FDA restriction era. *Journal of Magnetic Resonance Imaging*. 2015;41(5).
262. Girardi M, Kay J, Elston DM, Leboit PE, Abu-Alfa A, Cowper SE. Nephrogenic systemic fibrosis: Clinicopathological definition and workup recommendations. *J Am Acad Dermatol*. 2011;65(6).
263. Do JG, Kim YB, Lee DG, Hwang JH. A case of delayed onset nephrogenic systemic fibrosis after gadolinium based contrast injection. *Ann Rehabil Med*. 2012;36(6).
264. Nakai K, Takeda K, Kimura H, Miura S, Maeda A. Nephrogenic systemic fibrosis in a patient on long-term hemodialysis. *Clin Nephrol*. 2009;71(2).

265. N. B, J.M. H, P. M, L. S. Nephrogenic systemic fibrosis symptoms alleviated by renal transplantation. Vol. 40, Dialysis and Transplantation. 2011.
266. Di Girolamo M, Grossi A. Contrast agents for MRI and side effects. In: Nuclear Medicine and Molecular Imaging: Volume 1-4. 2022.
267. Rosen MA, Schnall MD. Dynamic Contrast-Enhanced Magnetic Resonance Imaging for Assessing Tumor Vascularity and Vascular Effects of Targeted Therapies in Renal Cell Carcinoma. *Clinical Cancer Research*. 2007;13(2).
268. Su MYM, Huang KH, Chang CC, Wu VC, Wu WC, Liu KL, et al. MRI evaluation of the adaptive response of the contralateral kidney following nephrectomy in patients with renal cell carcinoma. *Journal of Magnetic Resonance Imaging*. 2015;41(3).
269. Lim SW, Chrysochou C, Buckley DL, Kalra PA, Sourbron SP. Prediction and assessment of responses to renal artery revascularization with dynamic contrast-enhanced magnetic resonance imaging: A pilot study. *Am J Physiol Renal Physiol*. 2013;305(5).
270. Michaely HJ, Schoenberg SO, Oesingmann N, Ittrich C, Buhlig C, Friedrich D, et al. Renal artery stenosis: Functional assessment with dynamic MR perfusion measurements-feasibility study. In: *Radiology*. 2006.
271. Eikefjord E AEHESELARJ. Quantification of Single-Kidney Function and Volume in Living Kidney Donors Using Dynamic Contrast-Enhanced MRI. *AJR Am J Roentgenol*. 2016;207(5):1022–30.
272. Sade R, Kantarci M, Karaca L, Okur A, Ogul H, Keles M, et al. Value of dynamic MRI using the Ktrans technique for assessment of native kidneys in pre-emptive renal transplantation. *Acta radiol*. 2017;58(8).
273. Boss A, Martirosian P, Fuchs J, Obermayer F, Tsiflikas I, Schick F, et al. Dynamic MR urography in children with uropathic disease with a combined 2D and 3D acquisition protocol-comparison with MAG3 scintigraphy. *British Journal of Radiology*. 2014;87(1044).
274. Ku MC, Fernández-Seara MA, Kober F, Niendorf T. Noninvasive renal perfusion measurement using arterial spin labeling (asl) mri: Basic concept. In: *Methods in Molecular Biology*. 2021.
275. Iutaka T, de Freitas MB, Omar SS, Scortegagna FA, Nael K, Nunes RH, et al. Arterial Spin Labeling: Techniques, Clinical Applications, and Interpretation. *Radiographics*. 2023;43(1).

276. Rock P, Gaillard F. Arterial spin labelling MR perfusion. In: Radiopaedia.org. 2016.
277. Odudu A, Nery F, Harteveld AA, Evans RG, Pendse D, Buchanan CE, et al. Arterial spin labelling MRI to measure renal perfusion: a systematic review and statement paper. Vol. 33, Nephrology Dialysis Transplantation. 2018.
278. Nery F, Buchanan CE, Harteveld AA, Odudu A, Bane O, Cox EF, et al. Consensus-based technical recommendations for clinical translation of renal ASL MRI. *Magnetic Resonance Materials in Physics, Biology and Medicine*. 2020;33(1).
279. Nery F, Gordon I, Thomas D. Non-Invasive Renal Perfusion Imaging Using Arterial Spin Labeling MRI: Challenges and Opportunities. *Diagnostics*. 2018;8(1).
280. Taso M, Aramendía-Vidaurreta V, Englund EK, Francis S, Franklin S, Madhuranthakam AJ, et al. Update on state-of-the-art for arterial spin labeling (ASL) human perfusion imaging outside of the brain. Vol. 89, *Magnetic Resonance in Medicine*. 2023.
281. Wang DJJ, Chen Y, Fernández-Seara MA, Detre JA. Potentials and challenges for arterial spin labeling in pharmacological magnetic resonance imaging. *Journal of Pharmacology and Experimental Therapeutics*. 2011;337(2).
282. Cai YZ, Li ZC, Zuo PL, Pfeuffer J, Li YM, Liu F, et al. Diagnostic value of renal perfusion in patients with chronic kidney disease using 3D arterial spin labeling. *Journal of Magnetic Resonance Imaging*. 2017;46(2).
283. Dong J, Yang L, Su T, Yang XD, Chen B, Zhang J, et al. Quantitative assessment of acute kidney injury by noninvasive arterial spin labeling perfusion MRI: A pilot study. *Sci China Life Sci*. 2013;56(8).
284. Rapacchi S, Smith RX, Wang Y, Yan L, Sigalov V, Krasileva KE, et al. Towards the identification of multi-parametric quantitative MRI biomarkers in lupus nephritis. *Magn Reson Imaging*. 2015;33(9).
285. Hueper K, Gueler F, Bräsen JH, Gutberlet M, Jang MS, Lehner F, et al. Functional MRI detects perfusion impairment in renal allografts with delayed graft function. *Am J Physiol Renal Physiol*. 2015;308(12).
286. Mora-Gutiérrez JM, Garcia-Fernandez N, Slon Roblero MF, Páramo JA, Escalada FJ, Wang DJJ, et al. Arterial spin labeling MRI is able to detect early hemodynamic changes in diabetic nephropathy. *Journal of Magnetic Resonance Imaging*. 2017;46(6).

287. Villa G, Ringgaard S, Hermann I, Noble R, Brambilla P, Khatir DS, et al. Phase-contrast magnetic resonance imaging to assess renal perfusion: a systematic review and statement paper. Vol. 33, Magnetic Resonance Materials in Physics, Biology and Medicine. 2020.
288. Wymer DT, Patel KP, Burke WF, Bhatia VK. Phase-contrast MRI: Physics, techniques, and clinical applications. Radiographics. 2020;40(1).
289. Ballinger J, BD. Phase contrast imaging. Reference article. Radiopaedia.org. 2021;
290. Nayak KS, Nielsen JF, Bernstein MA, Markl M, Gatehouse PD, Botnar RM, et al. Cardiovascular magnetic resonance phase contrast imaging. Vol. 17, Journal of Cardiovascular Magnetic Resonance. 2015.
291. Khatir DS, Pedersen M, Jespersen B, Buus NH. Evaluation of Renal Blood Flow and Oxygenation in CKD Using Magnetic Resonance Imaging. American Journal of Kidney Diseases. 2015;66(3).
292. Cortsen M, Petersen LJ, Ståhlberg F, Thomsen C, Søndergaard L, Petersen JR, et al. MR velocity mapping measurement of renal artery blood flow in patients with impaired kidney function. Acta radiol. 1996;37(1).
293. Khatir DS, Pedersen M, Jespersen B, Buus NH. Reproducibility of MRI renal artery blood flow and BOLD measurements in patients with chronic kidney disease and healthy controls. Journal of Magnetic Resonance Imaging. 2014;40(5).
294. Prowle JR, Molan MP, Hornsey E, Bellomo R. Measurement of renal blood flow by phase-contrast magnetic resonance imaging during septic acute kidney injury: A pilot investigation. Crit Care Med. 2012;40(6).
295. Prowle JR, Molan MP, Hornsey E, Bellomo R. Ciné phase-contrast magnetic resonance imaging for the measurement of renal blood flow. Contrib Nephrol. 2010;165.
296. Schoenberg SO, Knopp M v., Londy F, Krishnan S, Zuna I, Lang N, et al. Morphologic and functional magnetic resonance imaging of renal artery stenosis: A multireader tricenter study. Journal of the American Society of Nephrology. 2002;13(1).
297. Oyen R. W.C. O'Neill: Atlas of renal ultrasonography. Eur Radiol. 2002;12(8).
298. Gupta P, Chatterjee S, Debnath J, Nayan N, Gupta SD. Ultrasonographic predictors in chronic kidney disease: A hospital based case control study. Journal of Clinical Ultrasound. 2021;49(7).

299. Mankuzhy SSG, Balasubramaniam P, Reddy KS. Role of Ultrasound and Colour Doppler in Diabetic Nephropathy-Correlation with Biochemical Parameters. *International Journal of Anatomy, Radiology and Surgery*. 2019;8(3).
300. Ke L, Guo Y, Geng X. Value of Color Doppler Ultrasonography for Diagnosing Early Diabetic Nephropathy. *Iran J Kidney Dis*. 2022;16(5).
301. Nickavar A, Safaeian B, Zaeri H, Gharib MH, Chaharnaei T. Usefulness of Doppler ultrasound for the early diagnosis of diabetic nephropathy in type 1 diabetes mellitus. *J Ultrasound*. 2022;25(1).
302. Venables HK, Wiafe YA, Adu-Bredu TK. Value of Doppler ultrasound in early detection of diabetic kidney disease: A systematic review and meta-analysis. Vol. 29, *Ultrasound*. 2021.
303. Ham YR, Lee EJ, Kim HR, Jeon JW, Na KR, Lee KW, et al. Ultrasound Renal Score to Predict the Renal Disease Prognosis in Patients with Diabetic Kidney Disease: An Investigative Study. *Diagnostics*. 2023;13(3).
304. Huang X HYZYZQ. Two-Dimensional Ultrasound-Based Radiomics Nomogram for Diabetic Kidney Disease: A Pilot Study. *Int J Gen Med*. 2024 May;
305. Sahbaee P, Abadi E, Segars WP, Marin D, Nelson RC, Samei E. The effect of contrast Material on radiation Dose at CT: Part II. A Systematic Evaluation across 58 Patient Models1. *Radiology*. 2017;283(3).
306. Tuna IS, Tatli S. Contrast-enhanced CT and MR imaging of renal vessels. *Abdom Imaging*. 2014;39(4).
307. Choi YH, Jo S, Lee RW, Kim JE, Paek JH, Kim B, et al. Changes in CT-Based Morphological Features of the Kidney with Declining Glomerular Filtration Rate in Chronic Kidney Disease. *Diagnostics*. 2023;13(3).
308. Gooding KM, Lienczewski C, Papale M, Koivuviita N, Maziarz M, Dutius Andersson AM, et al. Prognostic imaging biomarkers for diabetic kidney disease (iBEAt): Study protocol. *BMC Nephrol*. 2020;21(1).
309. Alam A, Dahl NK, Lipschutz JH, Rossetti S, Smith P, Sapir D, et al. Total kidney volume in autosomal dominant polycystic kidney disease: A biomarker of disease progression and therapeutic efficacy. *American Journal of Kidney Diseases*. 2015;66(4).

310. Tangri N, Hougen I, Alam A, Perrone R, McFarlane P, Pei Y. Total kidney volume as a biomarker of disease progression in autosomal dominant polycystic kidney disease. *Can J Kidney Health Dis.* 2017;4.
311. Andersen UB, Haddock B, Asmar A. Multiparametric magnetic resonance imaging: A robust tool to test pathogenesis and pathophysiology behind nephropathy in humans. Vol. 43, *Clinical Physiology and Functional Imaging.* 2023.
312. Selby NM, Blankestijn PJ, Boor P, Combe C, Eckardt KU, Eikefjord E, et al. Magnetic resonance imaging biomarkers for chronic kidney disease: a position paper from the European Cooperation in Science and Technology Action PARENCHIMA. *Nephrol Dial Transplant.* 2018;33(2).
313. Buchanan CE, Mahmoud H, Cox EF, McCulloch T, Prestwich BL, Taal MW, et al. Quantitative assessment of renal structural and functional changes in chronic kidney disease using multi-parametric magnetic resonance imaging. *Nephrology Dialysis Transplantation.* 2020 Jun 1;35(6):955–64.
314. Zerbini G, Bonfanti R, Meschi F, Boggetti E, Paesano PL, Gianolli L, et al. Persistent renal hypertrophy and faster decline of glomerular filtration rate precede the development of microalbuminuria in type 1 diabetes. *Diabetes.* 2006;55(9).
315. Rigalleau V, Garcia M, Lasseur C, Laurent F, Montaudon M, Raffaitin C, et al. Large kidneys predict poor renal outcome in subjects with diabetes and chronic kidney disease. *BMC Nephrol.* 2010;11(1).
316. Chawla R, Zala S, Punyani H, Dhingra J. Correlation between cortical renal thickness and estimated glomerular filtration rate in diabetic nephropathy patients. *Journal of Diabetology.* 2020;11(3).
317. Makvandi K, Hockings PD, Jensen G, Unnerstall T, Leonhardt H, Jarl L V., et al. Multiparametric magnetic resonance imaging allows non-invasive functional and structural evaluation of diabetic kidney disease. *Clin Kidney J.* 2022;15(7).
318. Cox EF, Buchanan CE, Bradley CR, Prestwich B, Mahmoud H, Taal M, et al. Multiparametric renal magnetic resonance imaging: Validation, interventions, and alterations in chronic kidney disease. *Front Physiol.* 2017;8(SEP).
319. Hansell P, Welch WJ, Blantz RC, Palm F. Determinants of kidney oxygen consumption and their relationship to tissue oxygen tension in diabetes and hypertension. Vol. 40, *Clinical and Experimental Pharmacology and Physiology.* 2013.

320. Han JH, Ahn JH, Kim JS. Magnetic resonance elastography for evaluation of renal parenchyma in chronic kidney disease: a pilot study. *Radiologia Medica*. 2020;125(12).
321. Shatil AS, Kirpalani A, Younus E, Tyrrell PN, Krizova A, Yuen DA. Magnetic Resonance Elastography-derived Stiffness Predicts Renal Function Loss and Is Associated with Microvascular Inflammation in Kidney Transplant Recipients. *Transplant Direct*. 2022;8(6).
322. Shen Y, Xie L, Chen X, Mao L, Qin Y, Lan R, et al. Renal fat fraction is significantly associated with the risk of chronic kidney disease in patients with type 2 diabetes. *Front Endocrinol (Lausanne)*. 2022;13.
323. Chen X, Mao Y, Hu J, Han S, Gong L, Luo T, et al. Perirenal Fat Thickness Is Significantly Associated With the Risk for Development of Chronic Kidney Disease in Patients With Diabetes. *Diabetes*. 2021;70(10).
324. Friedli I BASURMAJLHPD. Magnetic Resonance Imaging in Clinical Trials of Diabetic Kidney Disease. *J Clin Med*. 2023 Jul;
325. Mora-Gutiérrez JM, Fernández-Seara MA, Echeverría-Chasco R, García-Fernández N. Perspectives on the role of magnetic resonance imaging (Mri) for noninvasive evaluation of diabetic kidney disease. Vol. 10, *Journal of Clinical Medicine*. 2021.
326. Notohamiprodjo M, Goepfert M, Will S, Lorbeer R, Schick F, Rathmann W, et al. Renal and renal sinus fat volumes as quantified by magnetic resonance imaging in subjects with prediabetes, diabetes, and normal glucose tolerance. *PLoS One*. 2020;15(2).
327. Zhao K, Li S, Liu Y, Li Q, Lin H, Wu Z, et al. Diagnostic and prognostic performance of renal compartment volume and the apparent diffusion coefficient obtained from magnetic resonance imaging in mild, moderate and severe diabetic kidney disease. *Quant Imaging Med Surg*. 2023;13(6).
328. Razek AAKA, Al-Adlany MAAA, Alhadidy AM, Atwa MA, Abdou NEA. Diffusion tensor imaging of the renal cortex in diabetic patients: correlation with urinary and serum biomarkers. *Abdominal Radiology*. 2017;42(5).
329. Ye XJ, Cui SH, Song JW, Liu K, Huang XY, Wang L, et al. Using magnetic resonance diffusion tensor imaging to evaluate renal function changes in diabetic patients with early-stage chronic kidney disease. *Clin Radiol*. 2019;74(2).

330. Wang YC, Feng Y, Lu CQ, Ju S. Renal fat fraction and diffusion tensor imaging in patients with early-stage diabetic nephropathy. *Eur Radiol.* 2018;28(8).
331. Feng YZ, Ye YJ, Cheng ZY, Hu JJ, Zhang CB, Qian L, et al. Non-invasive assessment of early stage diabetic nephropathy by DTI and BOLD MRI. *British Journal of Radiology.* 2020;93(1105).
332. Zheng SS, He YM, Lu J. Noninvasive evaluation of diabetic patients with high fasting blood glucose using DWI and BOLD MRI. *Abdominal Radiology.* 2021;46(4).
333. Osman NMM, Kader MA, Nasr TAEA, Sharawy MA, Keryakos HKH. The role of diffusion-weighted mri and apparent diffusion coefficient in assessment of diabetic kidney disease: Preliminary experience study. *Int J Nephrol Renovasc Dis.* 2021;14.
334. Seah J mine, Botterill E, MacIsaac RJ, Milne M, Ekinici EI, Lim RP. Functional MRI in assessment of diabetic kidney disease in people with type 1 diabetes. *J Diabetes Complications.* 2022;36(1).
335. Wei X, Hu R, Zhou X, Ni L, Zha D, Feng H, et al. Alterations of Renal Function in Patients with Diabetic Kidney Disease: A BOLD and DTI Study. *Comput Intell Neurosci.* 2022;2022.
336. Duan S, Geng L, Lu F, Chen C, Jiang L, Chen S, et al. Utilization of the corticomedullary difference in magnetic resonance imaging-derived apparent diffusion coefficient for noninvasive assessment of chronic kidney disease in type 2 diabetes. *Diabetes and Metabolic Syndrome: Clinical Research and Reviews.* 2024;18(2).
337. Spit KA, Muskiet MHA, Tonneijck L, Smits MM, Kramer MHH, Joles JA, et al. Renal sinus fat and renal hemodynamics: a cross-sectional analysis. *Magnetic Resonance Materials in Physics, Biology and Medicine.* 2020;33(1).
338. Vinovskis C, Li LP, Prasad P, Tommerdahl K, Pyle L, Nelson RG, et al. Relative hypoxia and early diabetic kidney disease in type 1 diabetes. *Diabetes.* 2020;69(12).
339. Brown RS, Sun MRM, Stillman IE, Russell TL, Rosas SE, Wei JL. The utility of magnetic resonance imaging for noninvasive evaluation of diabetic nephropathy. *Nephrology Dialysis Transplantation.* 2020;35(6).
340. Lin L, Dekkers IA, Huang L, Tao Q, Paiman EHM, Bizino MB, et al. Renal sinus fat volume in type 2 diabetes mellitus is associated with glycated hemoglobin and metabolic risk factors. *J Diabetes Complications.* 2021;35(9).

341. Laursen JC, Søndergaard-Heinrich N, Haddock B, Rasmussen IKB, Hansen CS, Larsson HBW, et al. Kidney oxygenation, perfusion and blood flow in people with and without type 1 diabetes. *Clin Kidney J.* 2022;15(11).
342. Sørensen SS, Gullaksen S, Vernstrøm L, Ringgaard S, Laustsen C, Funck KL, et al. Evaluation of renal oxygenation by BOLD-MRI in high-risk patients with type 2 diabetes and matched controls. *Nephrology Dialysis Transplantation.* 2023;38(3).
343. Li J, Venkatesh SK, Yin M. *Advances in Magnetic Resonance Elastography of Liver.* Vol. 28, *Magnetic Resonance Imaging Clinics of North America.* 2020.
344. Güven AT, Idilman IS, Cebayilov C, Önal C, Kibar MÜ, Sağlam A, et al. Evaluation of renal fibrosis in various causes of glomerulonephritis by MR elastography: a clinicopathologic comparative analysis. *Abdominal Radiology.* 2022;47(1).
345. Chauveau B, Merville P, Soulabaille B, Taton B, Kaminski H, Visentin J, et al. Magnetic Resonance Elastography as Surrogate Marker of Interstitial Fibrosis in Kidney Transplantation: A Prospective Study. *Kidney360.* 2022;3(11).
346. De Vries APJ, Ruggenenti P, Ruan XZ, Praga M, Cruzado JM, Bajema IM, et al. Fatty kidney: Emerging role of ectopic lipid in obesity-related renal disease. Vol. 2, *The Lancet Diabetes and Endocrinology.* 2014.
347. Kim YK, Lee JE, Kim YG, Kim DJ, Oh HY, Yang CW, et al. Cardiac Autonomic Neuropathy as a Predictor of Deterioration of the Renal Function in Normoalbuminuric, Normotensive Patients with Type 2 Diabetes Mellitus. *J Korean Med Sci [Internet].* 2009;24(Suppl 1):S69. Available from: <https://jkms.org/DOIx.php?id=10.3346/jkms.2009.24.S1.S69>
348. O'Brien IA, O'Hare P, Corral RJM. Heart rate variability in healthy subjects: Effect of age and the derivation of normal ranges for tests of autonomic function. *Br Heart J.* 1986;55(4).
349. Ewing DJ, Martyn CN, Young RJ, Clarke BF. The value of cardiovascular autonomic function tests: 10 years experience in diabetes. *Diabetes Care.* 1985;8(5).
350. Ewing DJ, Campbell IW, Clarke BF. The natural history of diabetic autonomic neuropathy. *QJM.* 1980;49(1).
351. Agelink MW, Malessa R, Baumann B, Majewski T, Akila F, Zeit T, et al. Standardized tests of heart rate variability: Normal ranges obtained from 309 healthy humans, and effects of age, gender, and heart rate. *Clinical Autonomic Research.* 2001;11(2).

352. Kopp UC, DiBona GF. Neural Control of Renal Function*. In: Reflex Control of the Circulation. 2020.
353. DiBona GF. Physiology in perspective: The Wisdom of the Body. Neural control of the kidney. In: American Journal of Physiology - Regulatory Integrative and Comparative Physiology. 2005.
354. Kirkpatrick JJ, Foutz S, Leslie SW. Anatomy, Abdomen and Pelvis, Kidney Nerves. StatPearls Publishing. 2020;01.
355. Sundkvist G, Lilja B. Autonomic neuropathy predicts deterioration in glomerular filtration Rate in patients with IDDM. Diabetes Care. 1993;16(5).
356. Spallone V, Gambardella S, Maiello MR, Barini A, Frontoni S, Menzinger G. Relationship between autonomic neuropathy, 24-h blood pressure profile, and nephropathy in normotensive IDDM patients. Diabetes Care. 1994;17(6).
357. Monteagudo PT, Nóbrega JC, Cezarini PR, Ferreira SRG, Kohlmann O, Ribeiro AB, et al. Altered blood pressure profile, autonomic neuropathy and nephropathy in insulin-dependent diabetic patients. Eur J Endocrinol. 1996;135(6).
358. Weinrauch LA, Kennedy FP, Gleason RE, Keough J, D'Elia JA. Relationship between autonomic function and progression of renal disease in diabetic proteinuria: Clinical correlations and implications for blood pressure control. Am J Hypertens. 1998;11(3 I).
359. Rutter MK, McComb JM, Brady S, Marshall SM. Autonomic neuropathy in asymptomatic subjects with non-insulin-dependent diabetes mellitus and microalbuminuria. Clinical Autonomic Research. 1998;8(5).
360. Y M Smulders AJGJMDGNRJHLMBCDS. Cardiovascular autonomic function is associated with (micro-)albuminuria in elderly Caucasian subjects with impaired glucose tolerance or type 2 diabetes- the Hoorn Study. Diabetes Care. 2000;
361. Burger AJ, D'Elia JA, Weinrauch LA, Lerman I, Gaur A. Marked abnormalities in heart rate variability are associated with progressive deterioration of renal function in type I diabetic patients with overt nephropathy. Int J Cardiol. 2002;86(2-3).
362. Forsén A, Kangro M, Sterner G, Norrgren K, Thorsson O, Wollmer P, et al. A 14-year prospective study of autonomic nerve function in Type 1 diabetic patients: Association with nephropathy. Diabetic Medicine. 2004;21(8).

363. Moran A, Palmas W, Field L, Bhattarai J, Schwartz JE, Weinstock RS, et al. Cardiovascular Autonomic Neuropathy Is Associated with Microalbuminuria in Older Patients with Type 2 Diabetes. *Diabetes Care*. 2004;27(4).
364. Takebayashi K, Matsutomo R, Matsumoto S, Suetsugu M, Wakabayashi S, Aso Y, et al. Relationships between heart rate variability and urinary albumin excretion in patients with type 2 diabetes. *American Journal of the Medical Sciences*. 2006;331(2).
365. Maguire AM, Craig ME, Craighead A, Chan AKF, Cusumano JM, Hing SJ, et al. Autonomic nerve testing predicts the development of complications: A 12-year follow-up study. *Diabetes Care*. 2007;30(1).
366. Bilal N, Erdogan M, Özbek M, Çetinkalp Ş, Karadeniz M, Özgen AG, et al. Increasing severity of cardiac autonomic neuropathy is associated with increasing prevalence of nephropathy, retinopathy, and peripheral neuropathy in Turkish type 2 diabetics. *J Diabetes Complications*. 2008;22(3).
367. Tahrani AA, Dubb K, Raymond NT, Begum S, Altaf QA, Sadiqi H, et al. Cardiac autonomic neuropathy predicts renal function decline in patients with type 2 diabetes: a cohort study. *Diabetologia* [Internet]. 2014 Jun 13;57(6):1249–56. Available from: <http://link.springer.com/10.1007/s00125-014-3211-2>
368. Orlov S, Cherney DZI, Pop-Busui R, Lovblom LE, Ficociello LH, Smiles AM, et al. Cardiac autonomic neuropathy and early progressive renal decline in patients with nonmacroalbuminuric type 1 diabetes. *Clinical Journal of the American Society of Nephrology*. 2015;10(7).
369. Yun JS, Ahn YB, Song KH, Yoo KD, Kim HW, Park YM, et al. The association between abnormal heart rate variability and new onset of chronic kidney disease in patients with type 2 diabetes: A ten-year follow-up study. *Diabetes Res Clin Pract*. 2015;108(1).
370. Wheelock KM, Jaiswal M, Martin CL, Fufaa GD, Weil EJ, Lemley K V., et al. Cardiovascular autonomic neuropathy associates with nephropathy lesions in American Indians with type 2 diabetes. In: *Journal of Diabetes and its Complications*. 2016.
371. Padmini S, Pulichikkat R, Menon SV, Abbas R. CARDIAC AUTONOMIC NEUROPATHY AND MICROALBUMINURIA IN TYPE 2 DIABETES MELLITUS- A CROSS-SECTIONAL ANALYSIS. *Journal of Evidence Based Medicine and Healthcare*. 2017;4(14).

372. Bjerre-Christensen T, Winther SA, Tofte N, Theilade S, Ahluwalia TS, Lajer M, et al. Cardiovascular autonomic neuropathy and the impact on progression of diabetic kidney disease in type 1 diabetes. *BMJ Open Diabetes Res Care*. 2021;9(1).
373. Laursen JC, Rasmussen IKB, Zobel EH, Hasbak P, von Scholten BJ, Holmvang L, et al. The Association Between Cardiovascular Autonomic Function and Changes in Kidney and Myocardial Function in Type 2 Diabetes and Healthy Controls. *Front Endocrinol (Lausanne)*. 2021;12.
374. Kadoya M, Morimoto A, Miyoshi A, Kakutani-Hatayama M, Kosaka-Hamamoto K, Konishi K, et al. Sleep quality, autonomic dysfunction and renal function in diabetic patients with pre-CKD phase. *Sci Rep*. 2021;11(1).
375. Chen Y, Gong Y, Cai K. Correlations of cardiovascular autonomic neuropathy with urinary albumin excretion rate and cardiac function in patients with type 2 diabetes mellitus. *Minerva Endocrinology*. 2021;
376. Eun Jun J, Sun Choi M, Hyeon Kim J. Cardiovascular autonomic neuropathy and incident diabetic kidney disease in patients with type 2 diabetes. *Diabetes Res Clin Pract*. 2022;184.
377. Muramatsu T, Takahashi M, Kakinuma R, Sato T, Yamamoto M, Akazawa M, et al. Decline in renal function associated with cardiovascular autonomic neuropathy positively coordinated with proteinuria in patients with type 2 diabetes. *J Diabetes Investig*. 2022;13(1).
378. Zeng H, Liu J, Chen Z, Yu P, Liu J. Cardiac Autonomic Dysfunction Is Associated With Risk of Diabetic Kidney Disease Progression in Type 2 Diabetes Mellitus. *Front Endocrinol (Lausanne)*. 2022 Jul 1;13.
379. Tang Y, Ang L, Jaiswal M, Dillon BR, Esfandiari NH, Shah HS, et al. ONLINE-ONLY SUPPLEMENTAL MATERIAL Cardiovascular autonomic neuropathy and risk of kidney function decline in type 1 and type 2 diabetes: findings from the PERL and ACCORD cohorts Short Title: Cardiovascular autonomic neuropathy and diabetic kidney disease. 2023 Jul.
380. Spallone V, Gambardella S, Maiello MR, Barini A, Frontoni S, Menzinger G. Relationship Between Autonomic Neuropathy, 24-h Blood Pressure Profile, and Nephropathy in Normotensive IDDM Patients. *Endocrinology [Internet]*. [cited 2023

- Jul 26]; Available from: <http://diabetesjournals.org/care/article-pdf/17/6/578/442668/17-6-578.pdf>
381. G. D, A.A. T. Cardiac autonomic neuropathy in patients with diabetes mellitus [Internet]. Vol. 5, World Journal of Diabetes. A.A. Tahrani, Centre of Endocrinology, Diabetes and Metabolism, School of Clinical and Experimental Medicine, University of Birmingham, Edgbaston, B15 2TT Birmingham, United Kingdom. E-mail: a.a.tahrani@bham.ac.uk: Baishideng Publishing Group Co (Room 1701, 17/F, Henan Bulding, No.90 Jaffe Road, Wanchai,Hong Kong, China, China); 2014. p. 17–39. Available from: <http://www.wjgnet.com/1948-9358/pdf/v5/i1/17.pdf>
 382. Winocour PH, Dhar H, Anderson DC. The Relationship Between Autonomic Neuropathy and Urinary Sodium and Albumin Excretion in Insulin-Treated Diabetics. *Diabetic Medicine*. 1986;3(5).
 383. Pop-Busui R. What do we know and we do not know about cardiovascular autonomic neuropathy in diabetes. *J Cardiovasc Transl Res*. 2012;5(4).
 384. Fadaee SB, Beetham KS, Howden EJ, Stanton T, Isbel NM, Coombes JS. Oxidative stress is associated with decreased heart rate variability in patients with chronic kidney disease. *Redox Report*. 2017;22(5).
 385. Niewczas MA, Pavkov ME, Skupien J, Smiles A, Md Dom ZI, Wilson JM, et al. A signature of circulating inflammatory proteins and development of end-stage renal disease in diabetes. *Nat Med*. 2019;25(5).
 386. Salman IM. Cardiovascular Autonomic Dysfunction in Chronic Kidney Disease: a Comprehensive Review. Vol. 17, *Current Hypertension Reports*. 2015.
 387. Wiegmann TB, Herron KG, Chonko AM, Macdougall ML, Moore W V. Recognition of hypertension and abnormal blood pressure burden with ambulatory blood pressure recordings in type I diabetes mellitus. *Diabetes*. 1990;39(12).
 388. Spallone V, Maiello MR, Cicconetti E, Pannone A, Barini A, Gambardella S, et al. Factors determining the 24-h blood pressure profile in normotensive patients with type 1 and type 2 diabetes. *J Hum Hypertens*. 2001;15(4).
 389. Dauphinot V, Gosse P, Kossovsky MP, Schott AM, Rouch I, Pichot V, et al. Autonomic nervous system activity is independently associated with the risk of shift in the non-dipper blood pressure pattern. *Hypertension Research*. 2010;33(10).

390. Chiriaco M, Sacchetta L, Forotti G, Leonetti S, Nesti L, Taddei S, et al. Prognostic value of 24-hour ambulatory blood pressure patterns in diabetes: A 21-year longitudinal study. *Diabetes Obes Metab.* 2022;24(11).
391. Lytvyn Y, Albakr R, Bjornstad P, Lovblom LE, Liu H, Lovshin JA, et al. Renal hemodynamic dysfunction and neuropathy in longstanding type 1 diabetes: Results from the Canadian study of longevity in type 1 diabetes. *J Diabetes Complications.* 2022;36(11).
392. Varghese RT, Jialal I, Doerr C. Diabetic Nephropathy (Nursing). *StatPearls.* 2022.
393. Patoulas D, Katsimardou A, Fragakis N, Christodoulos Papadopoulos ·, Doumas · Michael. Effect of SGLT-2 inhibitors on cardiac autonomic function in type 2 diabetes mellitus: a meta-analysis of randomized controlled trials. *Acta Diabetol [Internet].* 1958 [cited 2023 Jul 26];60:1–8. Available from: <https://doi.org/10.1007/s00592-022-01958-0>
394. Yarlagadda C, Abutineh M, Reddy AJ, Landau AB, Travis LM, Perrone CG, et al. An Investigation on the Efficacy of Glucagon-Like Peptide 1 Receptor Agonists Drugs in Reducing Urine Albumin-to-Creatinine Ratio in Patients With Type 2 Diabetes: A Potential Treatment for Diabetic Nephropathy. *Cureus.* 2023;
395. Pop-Busui R. Cardiac autonomic neuropathy in diabetes: A clinical perspective. Vol. 33, *Diabetes Care.* 2010.
396. Stevens et al. The Kidney Disease: Improving Global Outcomes (KDIGO) 2024 Clinical Practice Guideline for the Evaluation and Management of Chronic Kidney Disease (CKD). *Kidney Int.* 2024 Apr;105(4):A1.
397. Levey AS, Stevens LA. Estimating GFR Using the CKD Epidemiology Collaboration (CKD-EPI) Creatinine Equation: More Accurate GFR Estimates, Lower CKD Prevalence Estimates, and Better Risk Predictions. Vol. 55, *American Journal of Kidney Diseases.* 2010.
398. Witte EC, Heerspink HJL, De Zeeuw D, Bakker SJL, De Jong PE, Gansevoort R. First morning voids are more reliable than spot urine samples to assess microalbuminuria. *Journal of the American Society of Nephrology.* 2009;20(2).
399. Levin A, Ahmed SB, Carrero JJ, Foster B, Francis A, Hall RK, et al. Executive summary of the KDIGO 2024 Clinical Practice Guideline for the Evaluation and Management of

- Chronic Kidney Disease: known knowns and known unknowns. *Kidney Int.* 2024;105(4).
400. Inker LA, Lambers Heerspink HJ, Mondal H, Schmid CH, Tighiouart H, Noubary F, et al. GFR Decline as an Alternative End Point to Kidney Failure in Clinical Trials: A Meta-analysis of Treatment Effects from 37 Randomized Trials. *American Journal of Kidney Diseases.* 2014;64(6).
401. Lauritzen T, Borch-Johnsen K, Davies MJ, Khunti K, Rutten GE, Sandbæk A, et al. Screening for diabetes: what do the results of the ADDITION trial mean for clinical practice? *Diabetes Management.* 2013;3(5).
402. CDER-BiomarkerQualificationProgram. List of Qualified Biomarkers [Internet]. [cited 2024 Jun 30]. Available from: <https://www.fda.gov/drugs/biomarker-qualification-program/status-biomarker-qualification-submissions>
403. Perrone RD, Mouksassi MS, Romero K, Czerwiec FS, Chapman AB, Gitomer BY, et al. Total Kidney Volume Is a Prognostic Biomarker of Renal Function Decline and Progression to End-Stage Renal Disease in Patients With Autosomal Dominant Polycystic Kidney Disease. *Kidney Int Rep.* 2017;2(3).
404. Mancini M, Masulli M, Liuzzi R, Mainenti PP, Ragucci M, Maurea S, et al. Renal duplex sonographic evaluation of type 2 diabetic patients. *Journal of Ultrasound in Medicine.* 2013;32(6).
405. Cho JM, Koh JH, Kim SG, Lee S, Kim Y, Cho S, et al. Associations of MRI-derived kidney volume, kidney function, body composition and physical performance in ≈38 000 UK Biobank participants: a population-based observational study. *Clin Kidney J.* 2024;17(4).
406. Nakazato T, Ikehira H, Imasawa T. Determinants of renal shape in chronic kidney disease patients. *Clin Exp Nephrol.* 2016;20(5).
407. Emamian SA, Nielsen MB, Pedersen JF, Ytte L. Kidney dimensions at sonography: Correlation with age, sex, and habitus in 665 adult volunteers. *American Journal of Roentgenology.* 1993;160(1).
408. Gong IH, Hwang J, Choi DK, Lee SR, Hong YK, Hong JY, et al. Relationship among total kidney volume, renal function and age. *Journal of Urology.* 2012;187(1).

409. Paul L, Talhar S, Sontakke B, Shende M, Waghmare J. Relation between Renal Length and Renal Volume with Patient's BMI: A Critical Appraisal. *Anatomy & Physiology*. 2016;06(06).
410. Thanaj M, Basti N, Cule M, Sorokin EP, Whitcher B, Srinivasan R, et al. Kidney shape statistical analysis: associations with disease and anthropometric factors. *BMC Nephrol*. 2023;24(1).
411. Woolen SA, Shankar PR, Gagnier JJ, MacEachern MP, Singer L, Davenport MS. Risk of Nephrogenic Systemic Fibrosis in Patients with Stage 4 or 5 Chronic Kidney Disease Receiving a Group II Gadolinium-Based Contrast Agent: A Systematic Review and Meta-analysis. *JAMA Intern Med*. 2020;180(2).
412. Bokacheva L, Rusinek H, Zhang JL, Lee VS. Assessment of Renal Function with Dynamic Contrast-Enhanced MR Imaging. Vol. 16, *Magnetic Resonance Imaging Clinics of North America*. 2008.
413. Winter JD, St. Lawrence KS, Margaret Cheng HL. Quantification of renal perfusion: Comparison of arterial spin labeling and dynamic contrast-enhanced MRI. *Journal of Magnetic Resonance Imaging*. 2011;34(3).
414. Eckerbom P, Hansell P, Cox E, Buchanan C, Weis J, Palm F, et al. Multiparametric assessment of renal physiology in healthy volunteers using noninvasive magnetic resonance imaging. *Am J Physiol Renal Physiol*. 2019;316(4).
415. Wu WC, Su MY, Chang CC, Tseng WYI, Liu KL. Renal perfusion 3-T MR imaging: A comparative study of arterial spin labeling and dynamic contrast-enhanced techniques. *Radiology*. 2011;261(3).